

Enantioselective Synthesis of (-)-Paeonilide

Dissertation

Zur Erlangung des Doktorgrades

Dr. rer. nat.

an der Fakultät für Chemie und Pharmazie

der Universität Regensburg



vorgelegt von

Klaus Harrar

aus Straubing

Regensburg 2011

Die Arbeit wurde angeleitet von: Prof. Dr. Oliver Reiser

Promotionsgesuch eingereicht am: 15.11.2011

Promotionskolloquium am: 13.12.2011

Prüfungsausschuss:	Vorsitz: Prof. Dr. Axel Jacobi von Wangelin
	1. Gutachter: Prof. Dr. Oliver Reiser
	2. Gutachter: Priv. Doz. Dr. Kirsten Zeitler
	3. Prüfer: Prof. Dr. Henri Brunner

Der experimentelle Teil der vorliegenden Arbeit wurde in der Zeit von Oktober 2007 bis August 2011 unter der Leitung von Prof. Dr. Oliver Reiser am Institut für Organische Chemie der Universität Regensburg angefertigt.

Herrn Prof. Dr. Oliver Reiser möchte ich herzlich für die Überlassung des äußerst interessanten Themas, die anregenden Diskussionen und seine stete Unterstützung während der Durchführung dieser Arbeit danken.

Meiner Familie

„Wissen ist Nacht.“

Prof. Dr. Abdul Nachtigaller

Table of contents

A. Introduction	1
B. Main Part.....	11
1. Preparatory work for the asymmetric cyclopropanation	13
2. Cyclopropanation	16
2.1 General information.....	16
2.2 Furan cyclopropanation.....	19
3. Toward the furo-lactone formation	26
4. Side chain introduction by C-H insertion	40
4.1 General information.....	40
4.2 Preparatory work for the C-H insertion reaction	45
4.3 C-H insertion experiments.....	48
5. Side chain introduction by established chemistry.....	53
6. Final steps toward (-)-Paeonilide	57
7. Characterization and biological evaluation of (-)-Paeonilide	65
C. Summary & Schematic Overview.....	67
1. Summary.....	67
2. Schematic overview of synthesized compounds.....	72
D. Experimental	74
1. General comments.....	74
2. Synthesis of literature-known compounds and reagents.....	76
3. Syntheses	77
E. Appendix	114
1. NMR spectra	114
2. X-ray crystallography data	151
3. List of publications.....	197
4. Poster presentations and scientific meetings	197
5. Curriculum vitae	198
F. References	200
G. Acknowledgement	208

Abbreviations

abs	absolute	M	molar
acac	acetylacetonate	Me	methyl
AIBN	aza- <i>isobutyronitrile</i>	min	minute
Bn	benzyl	mp	melting point
bp	boiling point	MS	mass spectroscopy
brine	saturated NaCl solution	NBS	<i>N</i> -bromosuccinimide
brsm	based on recovered starting material	NMR	nuclear magnetic resonance
BTS	bis(trimethylsilyl)sulfate	NOE	nuclear Overhauser effect
Bu	butyl	OTf	triflate
Bz	benzoyl	<i>p</i>	<i>para</i>
CAN	cerium(IV) ammonium nitrate	PE	hexanes
cat	catalytic	PPTS	pyridinium <i>p</i> -toluenesulfate
conc	concentrated	Pr	propyl
d	day	<i>p</i> -TSA	<i>para</i> -toluenesulfonic acid
DBU	1,8-diazabicyclo[5.4.0]undec-7-ene	py	pyridine
DCM	dichloromethane	ref	reference
DMA	dimethylacetamide	r.t.	room temperature
DMAP	<i>N,N</i> -dimethyl-4-aminopyridine	<i>t</i>	<i>tert</i>
DME	dimethoxyethane	TBAF	tetrabutylammonium fluoride
DMF	dimethyl formamide	TBDMS	<i>tert</i> -butyldimethylsilyl
DMPU	1,3-dimethyl-3,4,5,6-tetrahydro-2(1H)-pyrimidinone	TFA	trifluoroacetic acid
<i>dr</i>	diastereomeric ratio	THF	tetrahydrofuran
EA	ethyl acetate	TLC	thin layer chromatography
<i>ee</i>	enantiomeric excess	TMS	trimethylsilyl
eq	equivalent	Ts	tosyl
Et	ethyl	vol%	volume %
<i>fl</i>	fluid	wt%	weight %
h	hour		
HMBC	heteronuclear multiple-bond correlation		
HPLC	high-pressure liquid chromatography		
HSQC	heteronuclear single-quantum correlation		
<i>i</i>	<i>iso</i>		
<i>m</i>	<i>meta</i>		

A. Introduction

Traditional herbal prescriptions attracted worldwide attention within the last years, due to their effectiveness against many afflictions and their low toxicity. In some instances they provide an even more effective way to heal diseases where western therapies failed or were insufficient to provide a palliative cure.¹⁻⁴

Natural products of herbal origin had an indisputable impact in modern medicinal chemistry and still break ground for new drugs. Peony root bark (chinese: “mu-dan-pi” or “dan-pi”) containing prescriptions like the multiherbal formula GuiZhiFuLing-Wan are employed in China, Japan and Korea to alleviate the syndromes of blood stasis and stiffness of abdominal muscles.⁵⁻⁷ Since Peony roots are under phytochemical investigation for many years, several new monoterpenoids could be isolated, characterized and pharmacologically analyzed (Figure 1):⁸⁻⁹

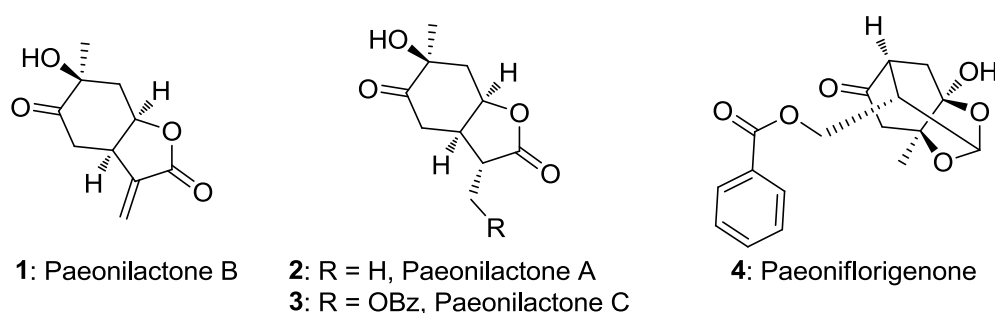


Figure 1: Examples of natural products isolated from peony roots.

For example, Paeonilactone C (**3**) suppresses both directly and indirectly stimulated muscle twitching of sciatic nerve-sartorius muscle preparations from frogs,¹⁰ while Paeoniflorigenone (**4**) has a blocking effect on the neuromuscular junction in phrenic nerve diaphragm preparations of mice.⁵

The highly oxygenated monoterpenoid (+)-Paeonilide (+)-(**5**) was isolated from *Paeonia delavayi* in 2000 (Figure 2),¹¹ which is endemic to the chinese provinces Likiang and Yunnan.¹² 1.13 kg of *Paeonia delavayi* roots were necessary to obtain 8 mg of pure (+)-Paeonilide (+)-(**5**). Its new monoterpenoid skeleton could be confirmed by the combination of spectroscopic and crystallographic analyses.¹¹

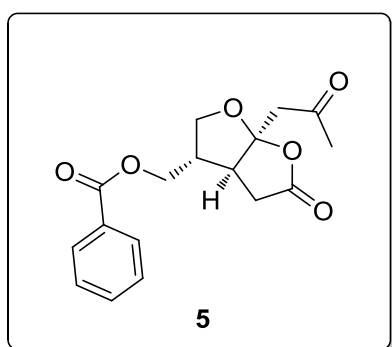
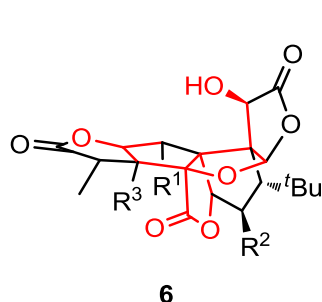


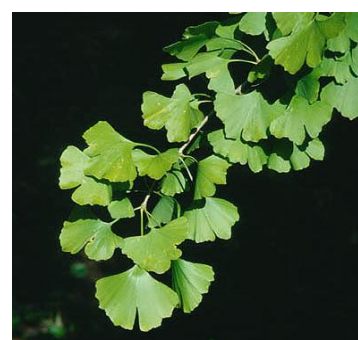
Figure 2: Structure of (-)-Paeonilide (**5**) and photo of *Paeonia delavayi* (photo by courtesy of Walter Good).¹³

(+)-**5** bears a sub-structural unit of the privileged class of ginkgolides **6** (Table 1), which themselves have very interesting properties. Ginkgolides **6** are diterpenoids derived from the dioecious “living fossil” *Ginkgo biloba* L., the last living member of a family of trees that appeared more than 250 million years ago.¹⁴ Due to the medicinal interest in the *Ginkgo biloba* extracts over 8000 tons of dried leaves are produced each year.¹⁵

Table 1: Ginkgolide structure and photo of *Ginkgo biloba* L.; Paeonilide substructure marked in red (photo by courtesy of Armin Jagel, Bochumer Botanischer Verein).¹⁶



Ginkgolide	R ¹	R ²	R ³
A	H	H	OH
B	OH	H	OH
C	OH	OH	OH
J	H	OH	OH
M	OH	OH	H



These extracts are used in the treatment of cardiac and cerebral vascular and peripheral circulatory disorders,¹⁷ diverse neurological disorders¹⁸ (e.g. cerebrovascular insufficiency with symptoms of vertigo, tinnitus, short term memory loss, headache, hearing loss and depression) and early senile dementia (Alzheimer’s disease).¹⁹ Ginkgolides are inhibiting the human platelet aggregation by inhibition of the binding of (3H)-PAF-acether to its membrane platelet receptor.

The pharmacological properties are, inter alia, antagonism on PAF induced thrombosis, lung anaphylaxis, cardiac anaphylaxis and inhibition of transplant rejection.²⁰

Due to the structural similarity between Ginkgolides and Paeonilide (+)-(5), it was tested in bioassays.¹¹ The results showed a selective inhibition of the platelet aggregation induced by the phospholipide PAF (7) (platelet activating factor, 1-O-alkyl-2-acetyl-*sn*-glycero-3-phosphocholine) with an IC₅₀ value of 25 μ M (8 μ g/mL), but no effect on the platelet aggregation induced by adenoside diphosphate (ADP) (8) or arachidonic acid (AA) (9) (Figure 3).

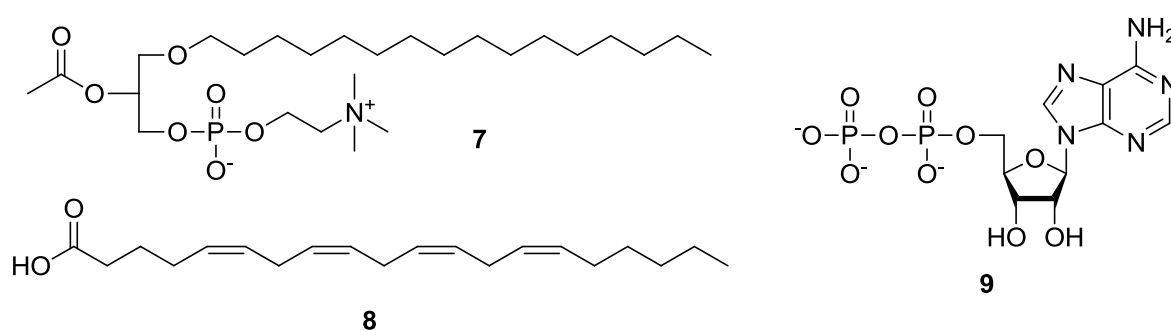


Figure 3: Structure of PAF (7), AA (8) and ADP (9).

The PAF receptor is a 7-transmembrane G protein receptor belonging to the rhodopsin family.²¹ A feature of this family is that critical residues, which are in charge of binding ligands, are located in the membrane spanning helices within the lipid double-layer and not exclusively on the surface. When PAF is binding to the PAF-receptor it starts a transduction cascade that facilitates the conformational change of glycoprotein (GP) IIb and IIIa (50000-80000 copies of this receptor on platelet surface), which is necessary to enable the binding of the receptor to fibrinogen (Figure 4). This is by far the most important ligand for GP IIb and IIIa. In this way fibrinogen cross-links two separate platelets which is critical for their aggregation.²²

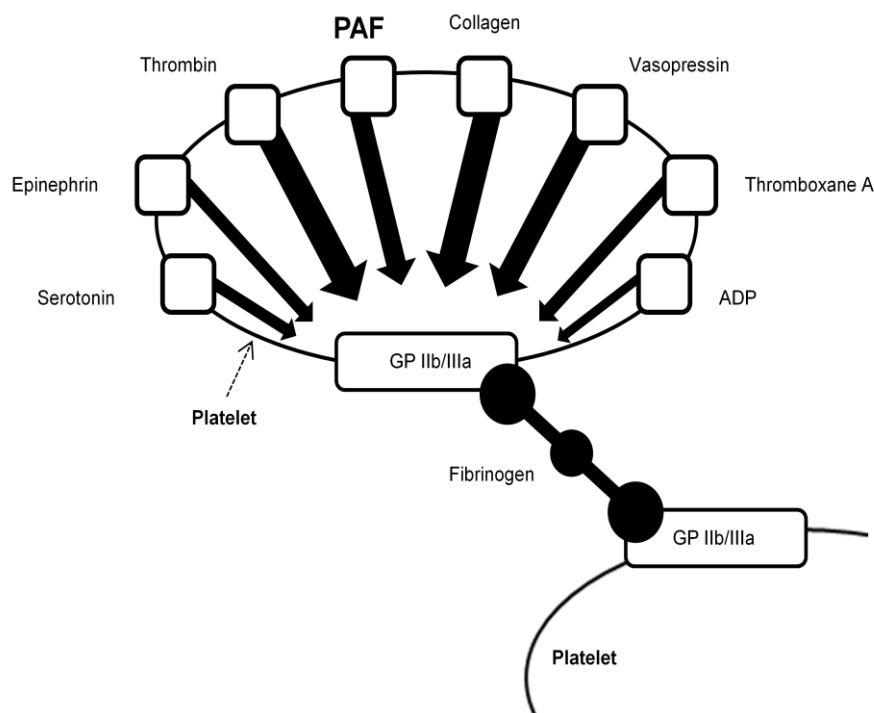
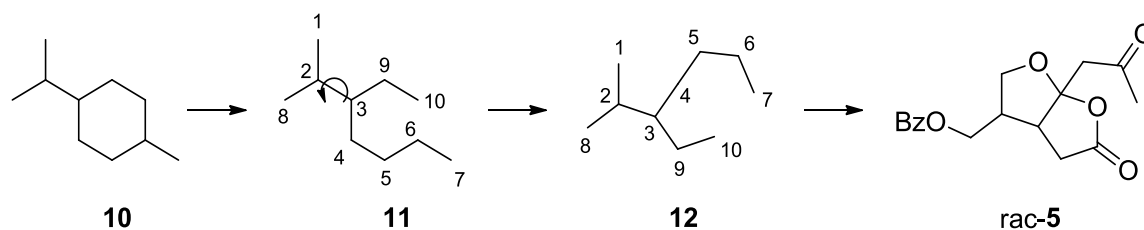


Figure 4: Pathway of platelet activation (the thickness of arrows indicates the strength of the activator).²³

So far, the bio-synthetic pathway of Paeonilide is still not clarified. It belongs to a group of irregular acyclic monoterpeneoids which seems to descend from re-arrangements of isoprene units via cleavage of the cyclic monoterpeneoid *p*-menthan (**10**). A subsequent ring formation between C1, C4 and C10 would give rise to the core structure of Paeonilide (Scheme 1).

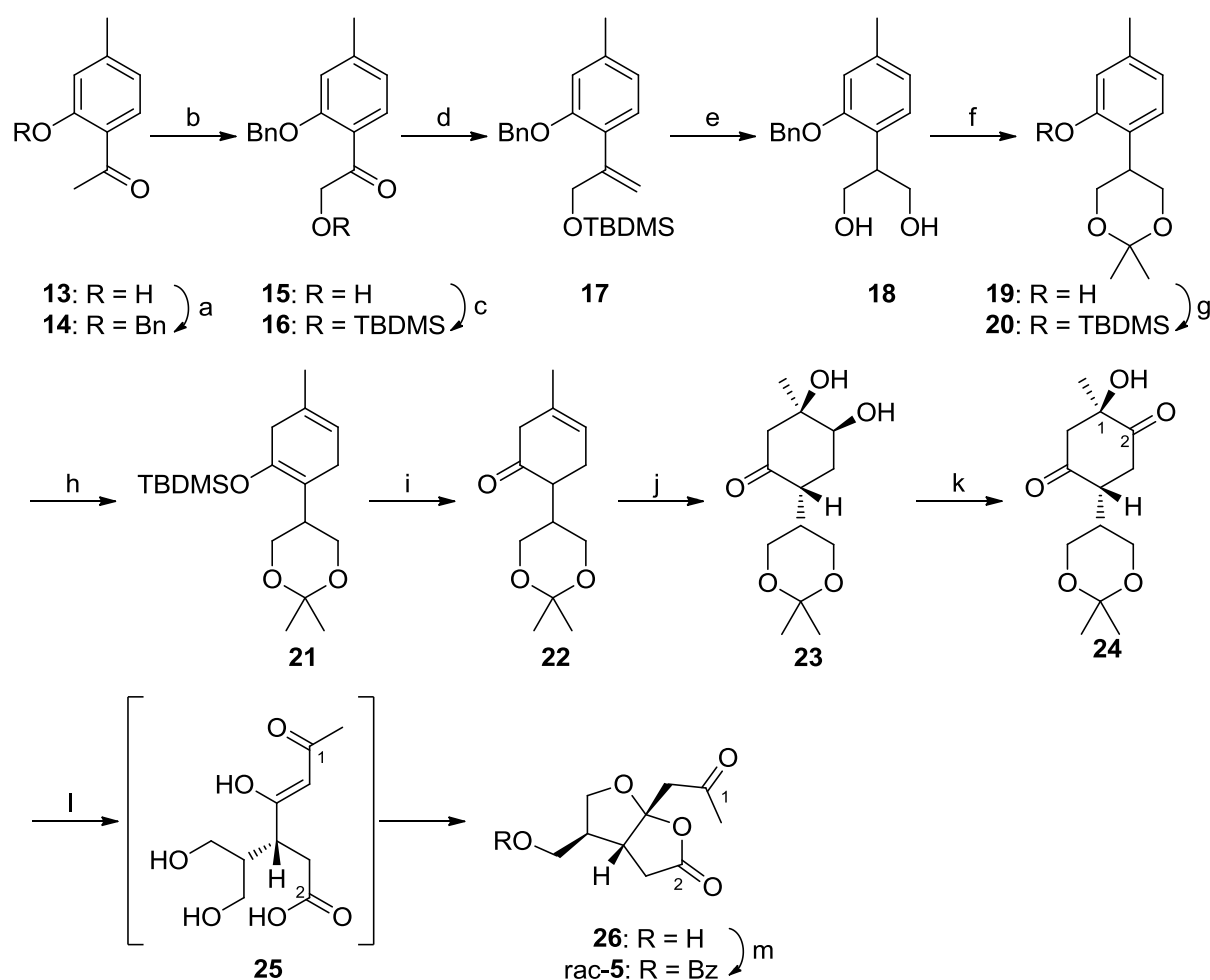
Scheme 1: Proposed biosynthetic route to Paeonilide rac-(**5**).¹¹



Up to now three syntheses of Paeonilide are published, two delivering the racemic product²⁴⁻²⁵ and one diastereoselective.²⁶

The first total synthesis was accomplished by Zhang *et al.* in 2006, consisting of 16 steps and an overall yield of 15%.²⁴ The synthesis started from commercially available 2-hydroxy-4-methylacetophenone (**13**) (Scheme 2), benzyl protection and Rubottom oxidation²⁷ lead to α -hydroxy ketone **15**. A further conversion of the intermediate via Wittig olefination, hydroboration of the resulting C-C double bond and a deprotection-protection step of the hydroxyl groups afforded the TBDMS protected acetal **20**.

Scheme 2: Zhang's racemic synthesis of rac-5.

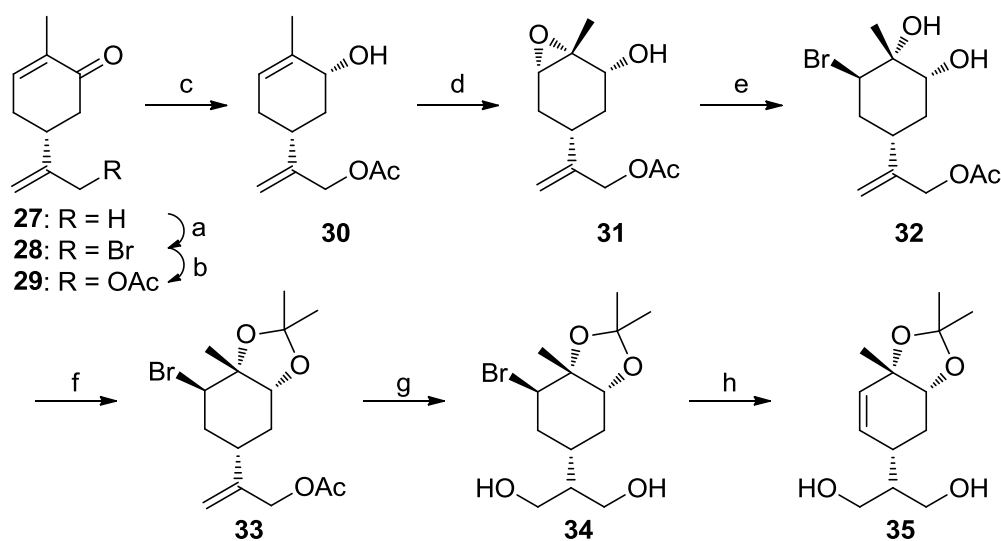


Reagents and Conditions: a) K_2CO_3 , KI, BnCl, MeCN, 95%; b) i. LDA, THF, TMSCl; ii. *m*CPBA, DCM, $NaHCO_3$; iii. HCl, 95%; c) TBDMSCl, Imidazole, DMF, quant.; d) Ph_3PCH_3I , *t*BuOK, THF, 95%; e) i. $BH_3 \cdot THF$; ii. H_2O_2 , NaOH, 90%; f) i. Pd/C, H_2 ; ii. DMP, PPTS; 94% over two steps based on **18**; g) TBDMSCl, NEt_3 , DCM, quant; h) Li, NH_3 (*f*), THF/EtOH, 90%; i) H_3BO_3 , TBAF, THF/ H_2O , 87%; j) OsO_4 , NMO, THF, *t*BuOH, H_2O , 92%; k) IBX, EA, 94%; l) H_5IO_6 , EA; m) BzCl, py, DCM, 46% over four steps based on **24**.

Acetal **20** was subjected to a Birch reduction and the resulting enol ether **21** was hydrolyzed to ketone **22**. The subsequent Osmium mediated *syn*-dihydroxylation of the remaining C-C double bond afforded selectively **23**, since the six-membered acetal ring shielded the back side of **22**. Afterwards the secondary alcohol was oxidized by IBX to **24**, which was afterwards cleaved in an oxidative pathway to generate the intermediate **25**. A subsequent intramolecular cyclization delivered the alcohol **26**. Final benzoyl protection of the free hydroxyl group yielded racemic Paeonilide rac-(**5**).

The first diastereoselective synthesis was also established by Zhang *et al.* starting from (*R*)-(-)-Carvone (**27**), which is readily available from the chiral pool, providing (+)-**5** within 16 steps and 6.2% overall yield (Scheme 3).²⁶

Scheme 3: Part one of Zhang's diastereoselective synthesis of (+)-Paeonilide (+)-(**5**).

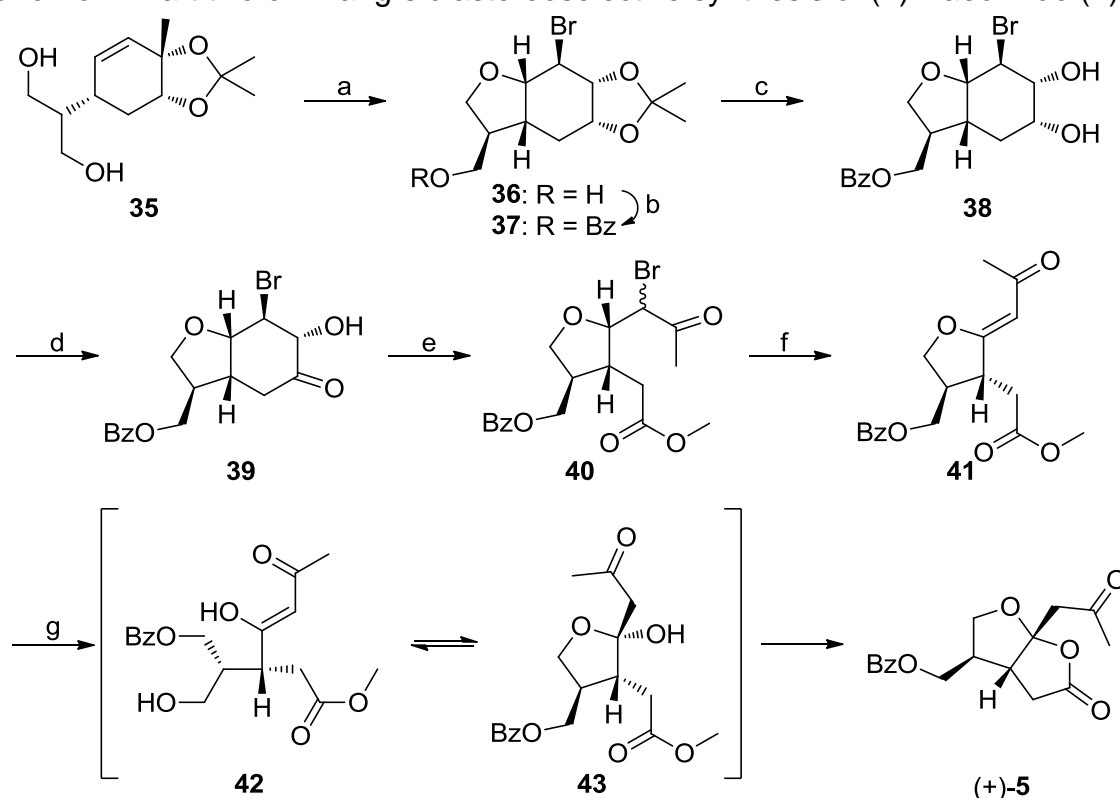


Reagents and Conditions: a) NBS, NaOAc, AcOH, DCM, 35%; b) AgOAc, acetone, 92%; c) NaBH₄, CeCl₃, MeOH, 95%; d) *m*CPBA, DCM, NaHCO₃, 93%; e) LiBr (*in situ*), THF, AcOH, 97%; f) DMP, DCM, TsOH, 95%; g) BH₃·SMe₂, THF, H₂O₂, NaOH, 89%; h) *t*BuOK, DMF, 95%.

Carvone **27** was transformed to acetyl protected **29** by the allyl bromide intermediate **28**, which was further subjected to a Luche-reduction of the carbonyl group and an epoxidation by *m*CPBA. Since the hydroxyl group of **30** exhibits a directing effect, the epoxide is formed chemo- and stereoselectively. Therefore, the resulting oxirane ring is located on the same side as the hydroxyl group in **31**. *In situ* generated LiBr opened the epoxide to the corresponding vicinal *syn*-diol **32**, which was ketal

protected, hydroborated and treated with the strong base *t*BuOK to eliminate HBr and form the diol **35**. The reaction with NBS lead to the formation of the *cis*-fused rings **36** as a single diastereomer, which was subsequently benzoyl protected on the free hydroxyl group to afford **37**, which was deprotected under acidic conditions to yield diol **38** (Scheme 4). The additional treatment with IBX created ketone **39**, which was cleaved oxidatively to furan **40** and subsequent HBr elimination by DBU yielded the key intermediate **41**. Finally **41** was submitted to an acidic furan opening, subsequent cyclization to the hemiacetal **43** and the formation of the lactone afforded (+)-Paeonilide (+)-**5** in a diastereoselective manner.

Scheme 4: Part two of Zhang's diastereoselective synthesis of (+)-Paeonilide (+)-**5**.

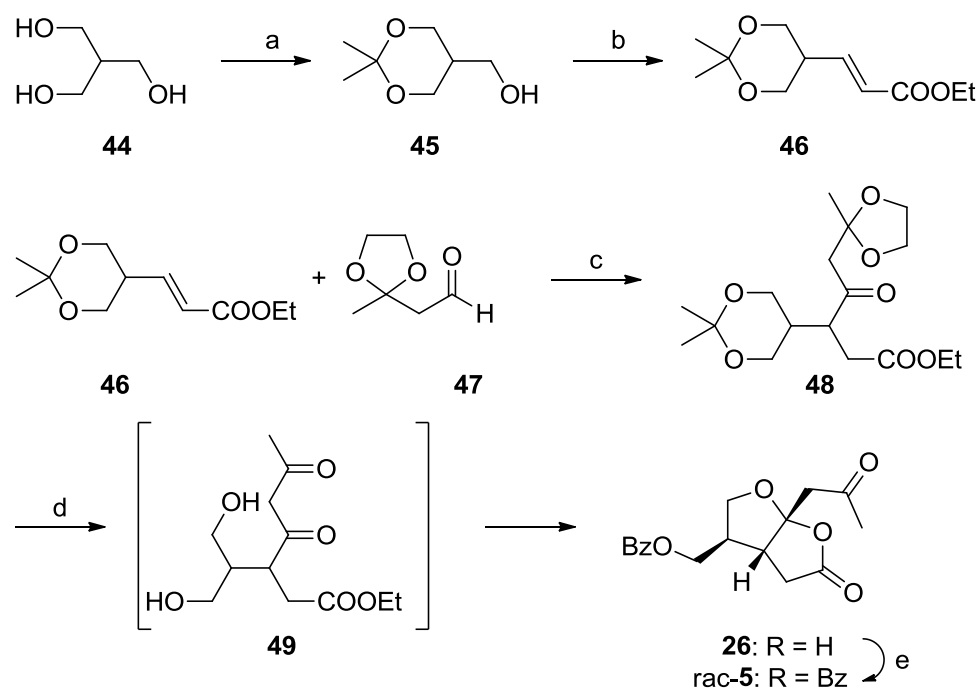


Reagents and conditions: a) NBS, THF, 95%; b) BzCl, py, DCM, 99%; c) HCl, MeOH, 92%; d) IBX, EA, 90%; e) H₅IO₆, EA, CH₂N₂, Et₂O; f) DBU, benzene; g) HCl, EA, 40%.

The latest and so far shortest synthesis of Paeonilide rac-(**5**) was published by Du *et al.* providing racemic rac-**5** in five steps in an overall yield of 59% starting from commercially available tris(hydroxymethyl)methane (**44**) (Scheme 5). This triol **44** was converted to the corresponding acetal **45** and submitted to an one-pot Swern-Wittig-reaction to furnish the desired (*E*)-olefin **46**. Subsequently, **46** and aldehyde **47** were subjected to a benzoyl peroxide promoted radical addition to give

rise to the critical ketone-ester **48**, which undergoes an *in situ* deprotection/hemiacetal-formation/lactonization cascade while treating it with HCl. This three-reaction-one-pot approach delivers **26** which is finally benzoyl protected to the desired racemic Paeonilide rac-(**5**).

Scheme 5: Du's racemic synthesis of Paeonilide rac-(**5**).

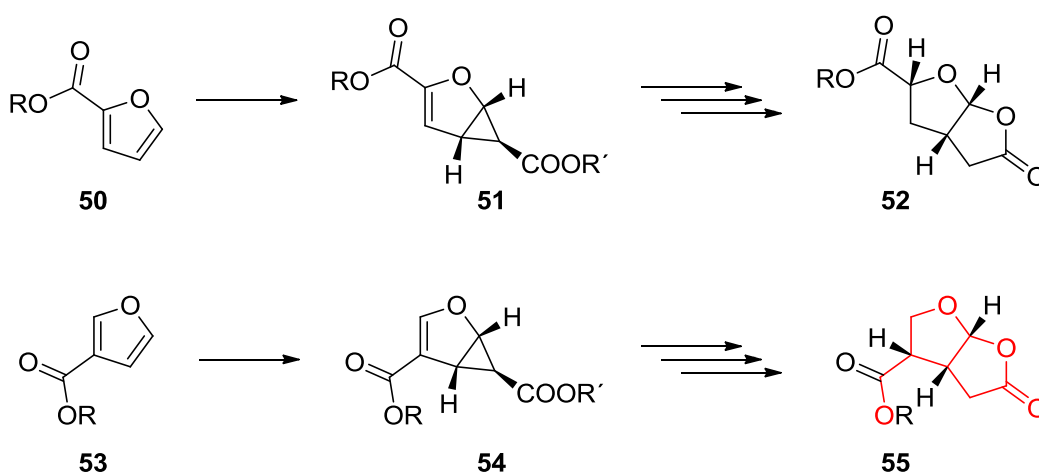


Reagents and conditions: a) DMP, TsOH, THF; b) i. (COCl)₂, DMSO, Et₃N; ii. Ph₃P=CHCO₂Et, DCM, 84% over two steps based on **44**; c) (BzO)₂, benzene, 79%; d) HCl, EA, 91%; e) BzCl, py, 98%.

In conclusion, both syntheses of Zhang *et al.* start from a monoterpene (diastereoselective synthesis) or a comparable carbon skeleton (racemic synthesis). This starting materials, **27** and **13**, are both transferred over several steps virtually to almost the same aliphatic key intermediate (**42** and **25**), which undergo a hemiacetal-formation/lactonization cascade to accomplish the final steps toward Paeonilide in one-pot. The most recently published synthesis by Du *et al.*, employs again the furo-lactone formation via the same aliphatic intermediate, but not starting from an (almost) monoterpene carbon body. In contrast to Zhang *et al.*, the C-10 skeleton is constructed by the combination of a C-6 and a C-4 building block.

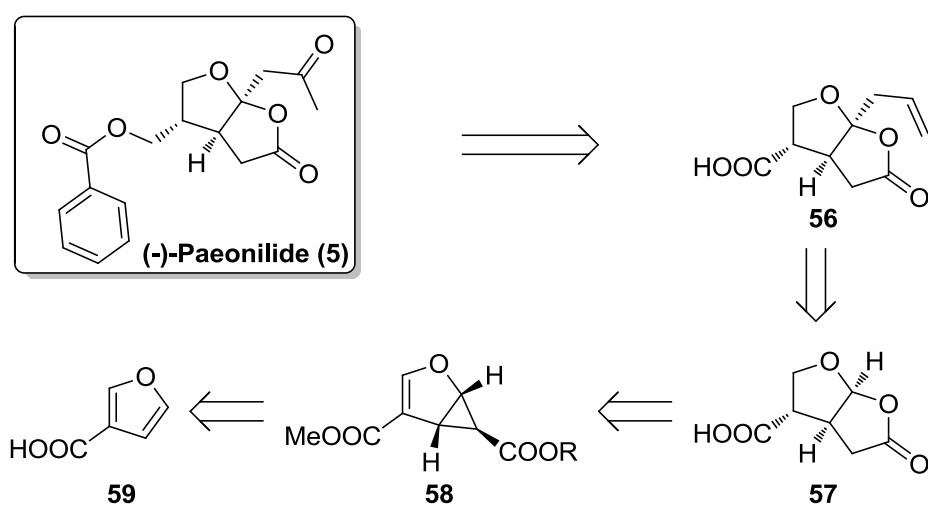
Despite of these results no enantioselective total synthesis is known so far, neither for (+)- nor for (-)-Paeonilide.

Scheme 6: Transfer of an established method to a new substrate scope (similarities to Paeonilide structure are marked in red).



The retro synthetic analysis (Scheme 7) of the target compound **5** does not start from a chiral starting material in contrast to the published diastereoselective synthesis, but employs commercially available 3-furoic acid (**59**). The chiral information is introduced by a copper(I)-catalyzed cyclopropanation reaction using a chiral bis(oxazoline) ligand to yield the bi-cycle **58**. The subsequent lactonization gives rise to the core skeleton **57** of the desired monoterpene. Key step of this synthesis is the so far literature unknown side chain introduction proceeding under substrate control concerning the stereochemistry and providing the functionalized furo-lactone **56**, which is finally transformed to the unnatural enantiomer (-)-Paeonilide (**5**)

Scheme 7: Retrosynthesis of (-)-Paeonilide (**5**).

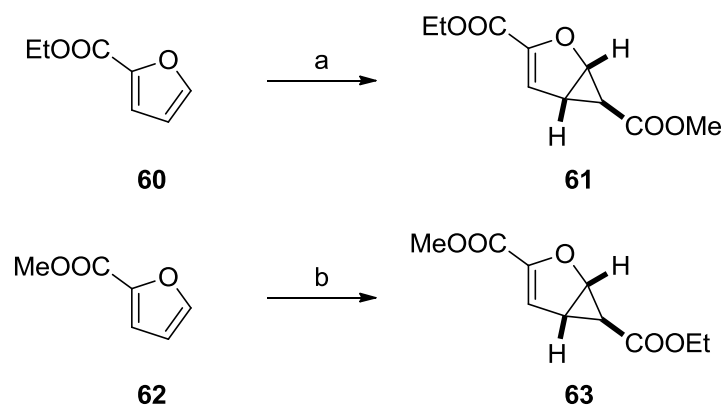


B. Main Part

Although cyclopropanes are a highly strained entity, they are found as a pivotal structural element in a wide range of natural products, including pheromones, unnatural amino acids, fatty acid metabolites and terpenes.²⁹⁻³³ This interesting moiety is also present in biologically active compounds, as natural and synthetic cyclopropanes are endowed with a large range of biological properties, such as enzyme inhibition, insecticidal, antifungal, herbicidal, antimicrobial, antibiotic, antibacterial, antitumor and antiviral activities.³⁴

The history of cyclopropanations of furans started already more than two decades ago. In 1988 Saltykova *et al.* reported the first racemic synthesis of cyclopropanated 2-furoic ethyl ester **60**, catalyzed by rhodium acetate dimer (Scheme 8, top).³⁵

Scheme 8: First reported syntheses of cyclopropanated furan esters.



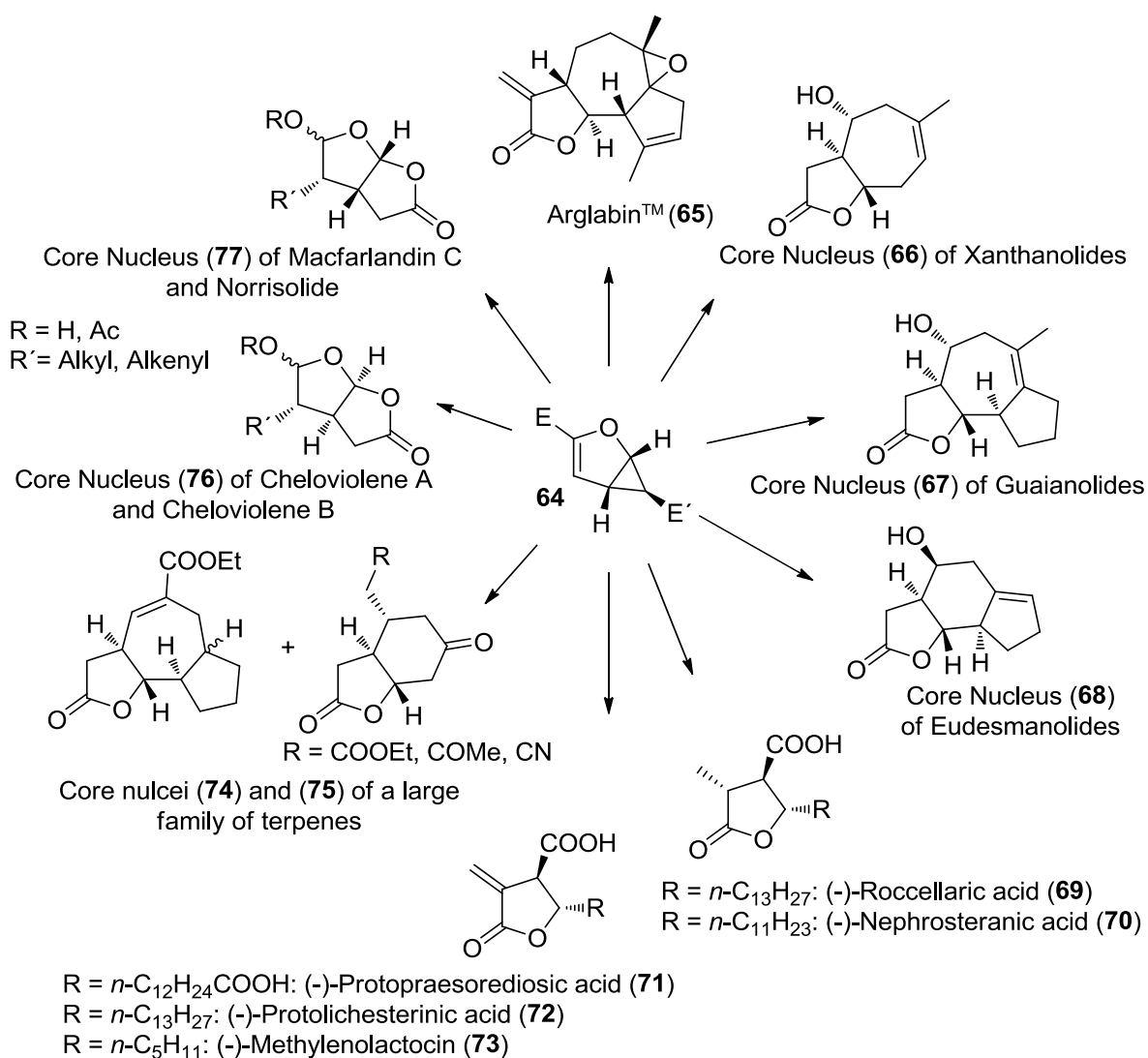
Reagents and conditions: a) $\text{N}_2\text{CHCOOMe}$ (1 eq), **60** (3 - 5 eq), $\text{Rh}_2(\text{OAc})_4$ (0.5 - 10 mol%), r.t., 18 - 22%; b) $\text{N}_2\text{CHCOOEt}$ (1 eq), $\text{Rh}_2(\text{OAc})_4$ (0.3 mol%), r.t., 12 h, 55 %.

Two years later, in 1990, Wenkert *et al.* published the racemic cyclopropanation of 2-furoic methyl ester **62** with diazo glycine ethyl ester (**63**), also catalyzed by dirhodium acetate, but providing higher yields than Saltykova *et al.* (Scheme 8, bottom).³⁶

As this scaffold is an interesting and very convenient gateway for natural product synthesis it was extensively utilized to enter a several natural product families (Scheme 9). **64** provided an access to the core nuclei of *trans* seven-membered sesquiterpenes **66** (Xanthanolides).³⁷⁻³⁸ Furthermore, the core structure of 5,6,5-tricyclic (Eudesmanolides)³⁷⁻³⁸ and 5,7,5-tricyclic (Guaianolides)³⁷ sesquiterpenes **67**

and **68** became available. In 2007 Reiser *et al.* reported the enantioselective synthesis of Arglabin™ (**65**)³⁹, a member of the guaianolide family. **65** is already successfully used for the treatment of breast, colon, ovarian and lung cancer in Kazakhstan. **64** was also used as starting material for the total synthesis of paraconic acids,⁴⁰ i.e. roccellaric acid (**69**),⁴¹ nephrosteranic acid (**70**) and protopraesorediosic acid (**71**). Methylene lactocin (**73**) and protolichesterinic acid (**72**) were accessed in a formal total synthesis.⁴⁰ The γ -lactone moiety in these natural products and natural product skeletons mentioned before, was synthesized via ozonolysis of **64** and subsequent retro-aldol reaction. Contrary to those lactones, the furo-lactones **76** and **77** were built via a lactonization of the cyclopropane ring.²⁸

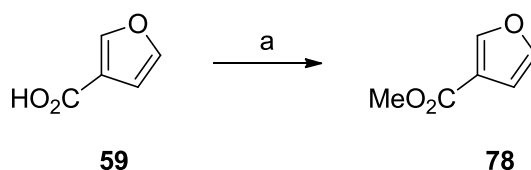
Scheme 9: **64** as versatile building block for natural product synthesis (E = ester).



1. Preparatory work for the asymmetric cyclopropanation

By choosing commercially available 3-furoic acid (**59**) as starting material for the planned synthesis of (-)-Paeonilide (**5**) a protection of the free carboxylic acid by esterification proved to be necessary to avoid unwanted side reactions.⁴² The ester was formed under strongly acidic conditions, *i.e.* in the presence of sulfuric acid (Scheme 10).

Scheme 10: Esterification of 3-furoic acid (**59**).⁴³

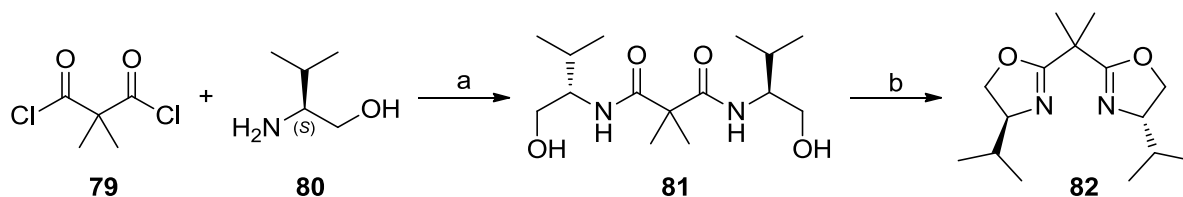


Reagents and conditions: a) MeOH, H₂SO₄, r.t., 24 h, 82 %.

The tool that brings chirality in the copper(I) mediated cyclopropanation is a complex of a chiral ligand and a metal center. A plethora of these catalytic systems has been applied for the cyclopropanation of olefins, *e.g.* bis(oxazoline)-ligands. Alternative ligands and cyclopropanation shall be discussed later in this chapter. The bis(oxazoline)-ligands were already successfully applied in the transformation of 2-furoic esters with diazo esters,⁴⁰ but a few reactions concerning 3-furoic esters were published as well.^{40, 44} Therefore, a bis(oxazoline) system was chosen for the asymmetric reaction between 3-furoic ester **78** and a diazo compound.

(4*S*,4'*S*)-2,2'-(propane-2,2-diyl)bis(4-*isopropyl*-4,5-dihydrooxazole) (**82**) was prepared starting from L-valinol (**80**) and 2,2-dimethylpropanedioyl dichloride (**79**) reacting under amide formation to intermediate **81**, which was cyclized to afford ligand **82** (Scheme 11).⁴⁵

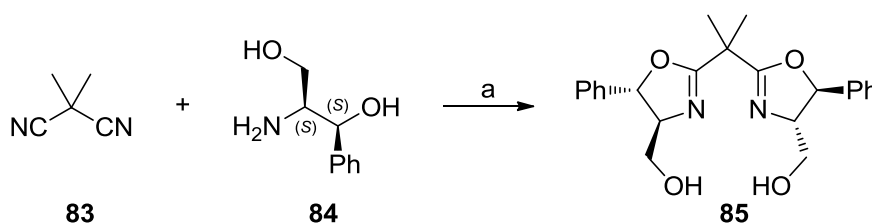
Scheme 11: Synthesis of (4*S*,4'*S*)-2,2'-(propane-2,2-diyl)bis(4-*isopropyl*-4,5-dihydrooxazole) (**82**).



Reagents and conditions: a) L-valinol (2.0 eq), NEt_3 (2.5 eq), DCM 0 °C to r.t., 70 min, 84 %; b) DMAP (10 mol %), NEt_3 (4.0 eq), TsCl (2.0 eq), DCM, r.t., 27 h, 83%.

The second ligand used for cyclopropanation within this thesis was also a bis(oxazoline)-ligand, possessing a secondary binding site. It was synthesized from the amino alcohol (1*S*,2*S*)-2-amino-1-phenyl-1,3-propanediol (**84**), which is not derived from a natural amino acid. This amino alcohol **84** was converted with 2,2-dimethylmalononitrile (**83**)⁴⁶ in an one-pot reaction to ((4*S*,4'*S*,5*S*,5'*S*)-2,2'-(propane-2,2-diyl) bis (5-phenyl-4,5-dihydrooxazole-4,2-diyl)) dimethanol (**85**), catalyzed by cadmium acetate (Scheme 12).^{44, 47}

Scheme 12: Synthesis of ((4*S*,4'*S*,5*S*,5'*S*)-2,2'-(propane-2,2-diyl)bis(5-phenyl-4,5-dihydrooxazole-4,2-diyl))dimethanol (**85**).



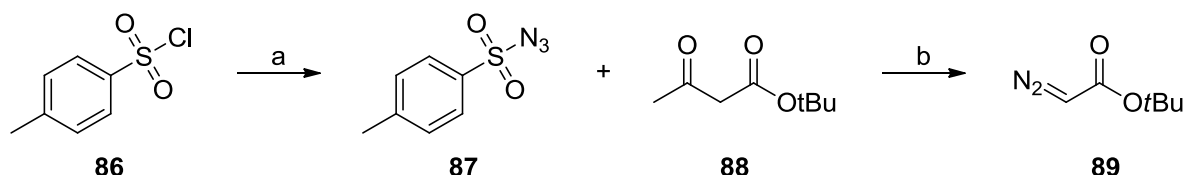
Reagents and conditions: a) amino alcohol **84** (2.5 eq), $\text{Cd}(\text{OAc})_2 \cdot 2\text{H}_2\text{O}$ (5 mol%), chlorobenzene, reflux, 14 h, 39%.

After substrate and ligand, the final compound, which needs to be prepared, is the diazo compound presenting the precursor for the reactive species in the cyclopropanation.

The *tert*-butyl diazo compound **89** was synthesized according to literature precedents following a two-step protocol utilizing the Regitz diazo transfer⁴⁸ from tosyl azide (**87**) to *tert*-butyl acetoacetate (**88**) under phase transfer conditions⁴⁹ yielding *tert*-butyl diazo acetate (**89**) as a solution in *n*-pentane (Scheme 13). Since this solvent is not suitable for the subsequent reaction due to solubility problems of the

copper(I)-complex, it was inevitable to remove the solvent. The remaining yellow diazo ester **89** was then diluted with anhydrous DCM. This procedure exhibits the advantage of preparing a diazo ester-DCM solution which can be adjusted to a certain wt% by calculating the amount of DCM added.

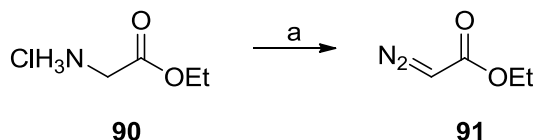
Scheme 13: Synthesis of *tert*-butyl diazo acetate (**89**).



Reagents and conditions: a) NaN₃ (1.1 eq), EtOH, r.t., 3 h, 76%; b) NaOH (2.8 eq), Bu₄NBr (2 mol%), H₂O, *n*-pentane, 0 °C to r.t., 20 h, 88%.

The corresponding ethyl diazo ester **91** was prepared in an one-step procedure starting from glycine ethyl ester hydrochloride (**90**) (Scheme 14).⁵⁰ This method does not provide the advantage of an adjustable wt%. It depends on the amount of DCM used for the reaction and work up. Typically, solutions of 10 - 15 wt% are obtained.

Scheme 14: Synthesis of ethyl diazo acetate (**91**).



Reagents and conditions: a) NaNO₂ (1.3 eq), H₂SO₄ (cat), H₂O/DCM, -20 °C to r.t., 1 h, 96%.

2. Cyclopropanation

2.1 General information

Although the history of transition metal catalyzed cyclopropanations started in 1906,⁵¹ more than a century ago, there were only small developments until the late 1960s when the catalyst development became more interesting, not only for natural product synthesis.

Besides the biological attributes, cyclopropanes are also of synthetic interest, since they can be used for the formation of highly functionalized cycloalkanes⁵²⁻⁵⁸ or acyclic compounds.⁵⁹⁻⁶² The main reason for the broad interest in this special moiety is the reactivity of cyclopropanes, which is usually associated with electron-donating and/or electron-accepting substituents.

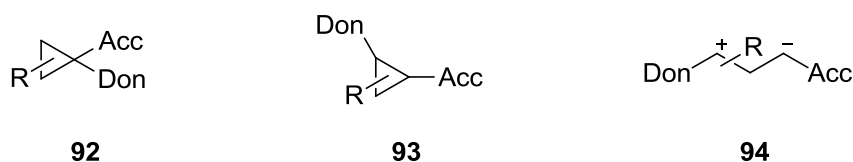
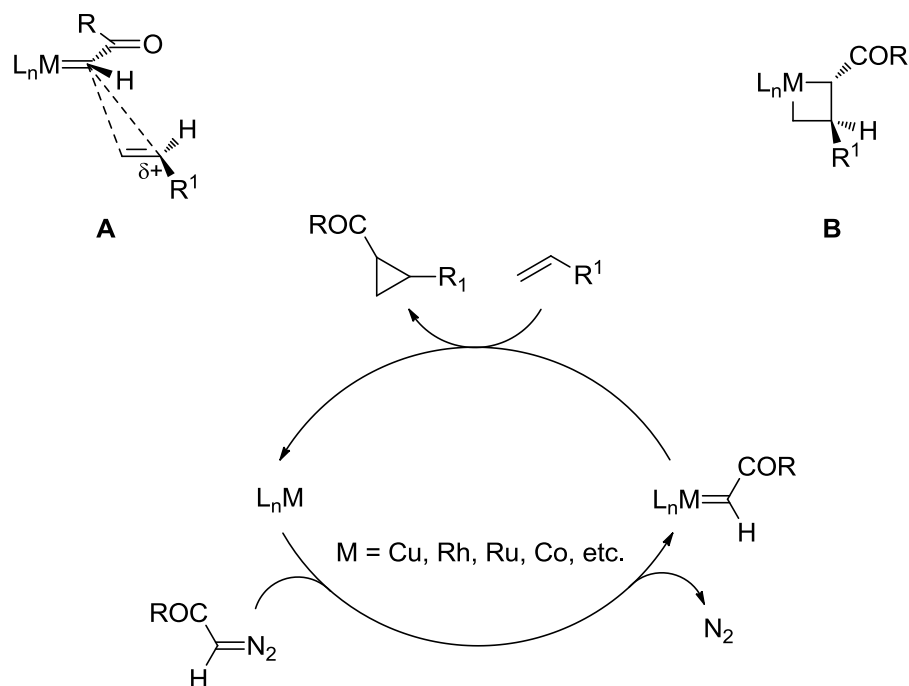


Figure 5: Donor (Don) - Acceptor (Acc) substituted cyclopropanes; geminal (**92**), vicinal (**93**), 1,3-dipolar synthon (**94**).⁶³

The synthetic use of geminal donor-acceptor substituted cyclopropanes, which have no synergistic substituent effect, is only reported in a few publications. Vicinal substituted cyclopropanes are very attractive for organic synthesis, since they are utilized as 1,3-dipolar synthons in a plethora of organic transformation (Figure 5).⁶⁴⁻⁶⁵

Among others, one way *en route* to donor-acceptor substituted cyclopropanes is the transition-metal catalyzed decomposition of a diazo compound, which results in extrusion of nitrogen and the formation of a transition-metal-carbene complex. Calculations⁶⁶ and Hammett studies⁶⁷ support the addition of a very reactive metal-carbene intermediate in the early transition state to the substrate in a concerted, yet strongly asynchronous pathway with a cationic substrate character on one alkene carbon. This is represented by transition state A, rather than in the metallacyclobutane B (Scheme 15).

Scheme 15: Catalytic cycle of metal-catalyzed carbenoid cyclopropanation reaction with diazo compounds.⁶⁸

The use of copper, rhodium and, more recently, also ruthenium catalysts proved to be highly effective. Palladium catalysts have advantages in reactions with electron-deficient alkenes, while other late transition metals like iron or osmium are only reported occasionally.⁶⁸ Regarding copper, Kochi⁶⁹ was the first to show that $Cu(OTf)$ is a highly effective catalyst. $Cu(II)$ -complexes are applicable as well, but need to be reduced *in-situ* since $Cu(I)$ is the active species⁷⁰ in carbene reactions. This can be achieved by treatment with DIBAL-H, substituted hydrazines, or the diazo agent itself. In order to perform the cyclopropanations in an enantioselective manner, a chiral environment is needed to transfer stereochemical information to the olefin substrate. This is achieved by using chiral ligands for complexing the metal ion. A short overview is provided in Figure 6.

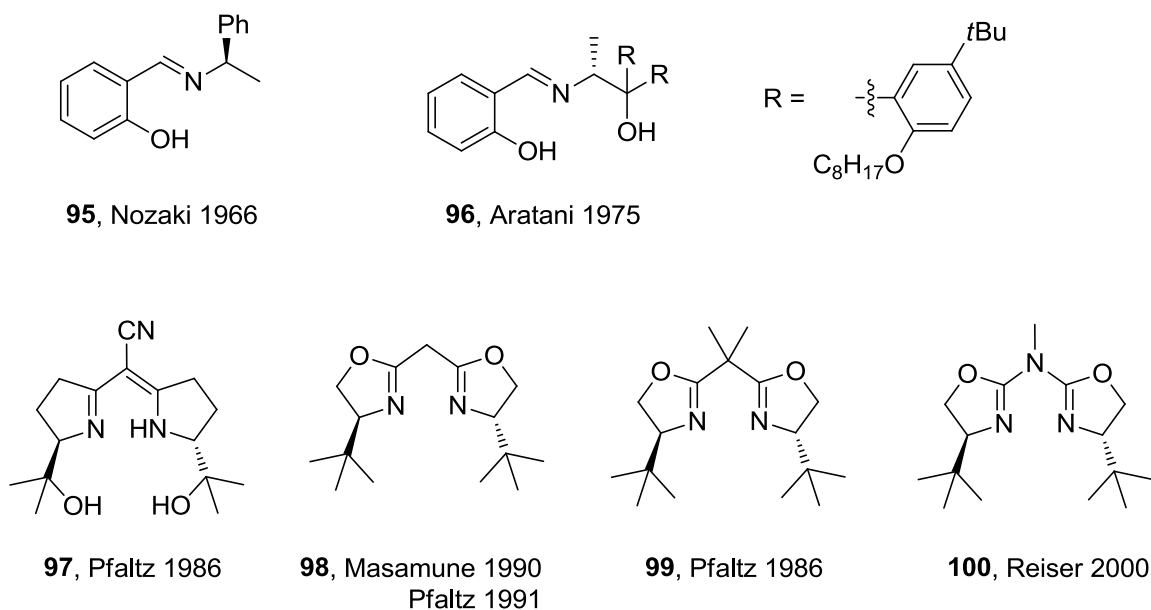


Figure 6: Short overview of chiral ligands for asymmetric cyclopropanations.⁶⁸

The diazo compounds have a rather broad scope regarding tolerated functional groups and substitution patterns, both, mono- and disubstituted ones (Figure 7). The most exhaustively studied diazo reagents are the α -diazo esters (**101**, Y = OR).

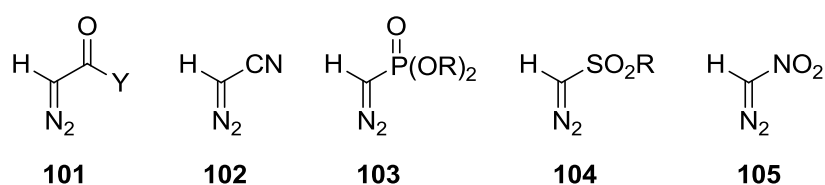


Figure 7: Different α -diazo compounds.⁶⁸

Attempts to use diazo compounds containing chiral auxiliaries for asymmetric cyclopropanation of styrene resulted only in poor diastereoselectivity (Figure 8).⁷¹⁻⁷³

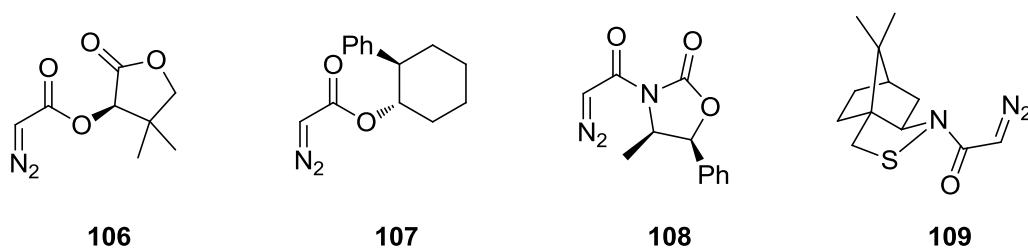
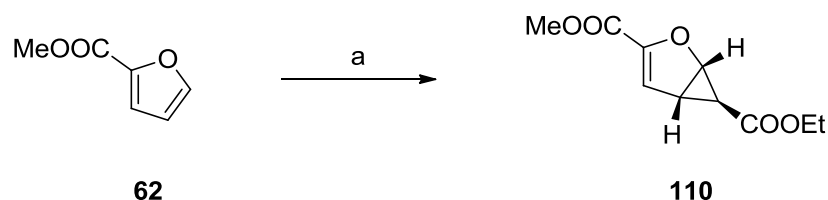


Figure 8: Diazo compounds bearing chiral auxiliaries.

2.2 Furan cyclopropanation

The copper(I) catalyzed cyclopropanation of furan derivatives like **62** comes along with some features. It proceeds regioselectively, since the highly electrophilic copper-carbene complex **111** (Figure 9, left) attacks only the less hindered and presumably more electron rich C-C double bond, as long as the diazo compound is not added in a huge excess. Furthermore, the reaction is diastereoselective, as the ester group at the introduced cyclopropanes is exclusively directed to the convex face of the fused ring system.⁴¹

Scheme 16: Copper(I) catalyzed cyclopropanation of furan ester **62**.



Reagents and conditions: a) i. $\text{N}_2\text{CHCOOEt}$ (2.67 eq.), $\text{Cu}(\text{OTf})_2$ (0.66 mol%), (*S,S*)-*i*Pr-BOX (0.84 mol%), PhNHNH_2 (0.70 mol%), DCM, 0 °C, 54%, 85-90% ee; ii. recrystallization (DCM, *n*-pentane), >99% ee, 37%.

The stereochemical outcome can be explained by a model for the asymmetric cyclopropanation of olefins as suggested by Pfaltz⁷⁴ and Andersson:⁷⁵

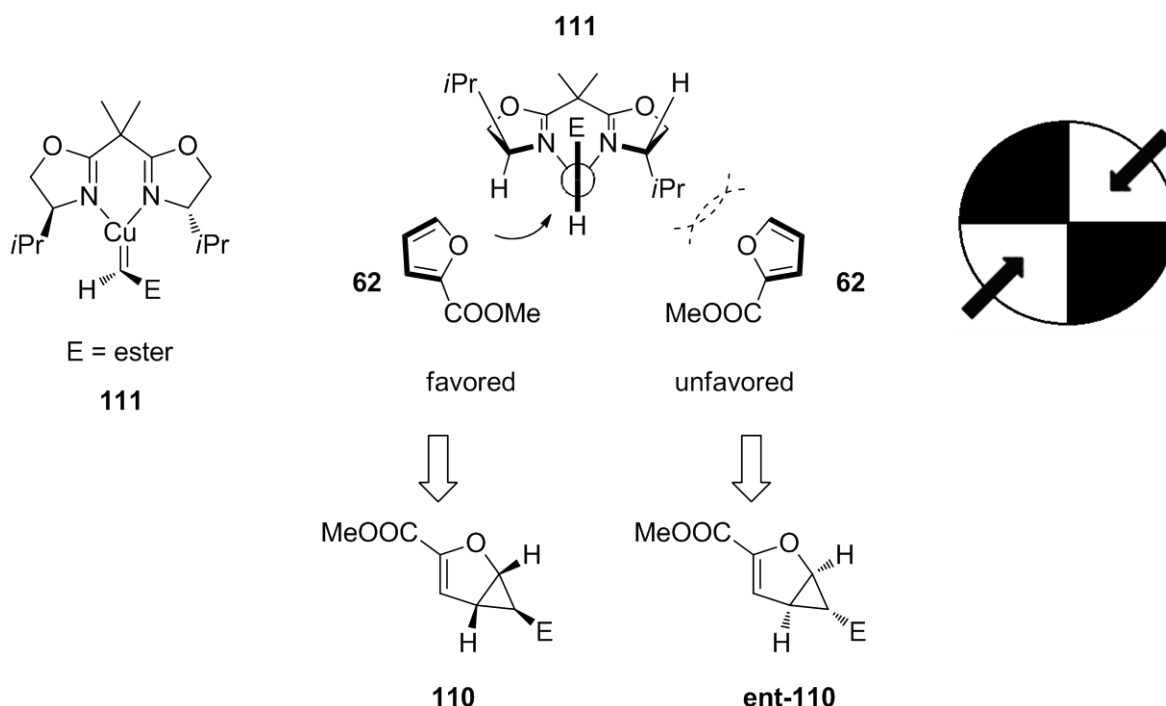


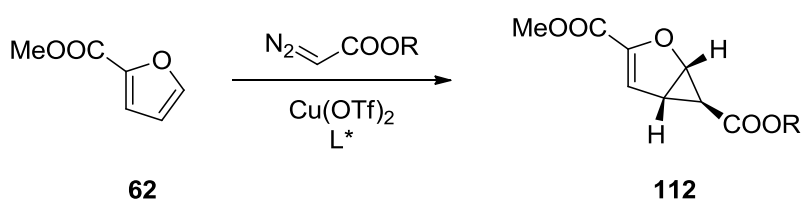
Figure 9: Reactive complex **111** (left) in the asymmetric cyclopropanation with (*S,S*)-*i*Pr-BOX ligand **82**, Cu(I), and ethyl diazo-acetate (**91**, E = COOEt); model for asymmetric cyclopropanation (center and right).

The pathway in which **62** approaches from the left is favored over an approach from the right side of the complex **111** (Figure 9, center), since the latter bears a strong repulsive steric interaction between the approaching olefin and the *i*Pr group of the ligand. This model indicates that the high enantioselectivity depends also on the structure of the olefin, since the COOMe substituent on the furan tends to be pointing away from the ligand framework which results in high enantioselectivity. As the *i*Pr groups of the ligand block the upper left and lower right quadrant of the complex, the substrate attacks from the unhindered quadrants (Figure 9, right). With this complex being C₂-symmetric, the approach via these unblocked quadrants leads to the same enantiomer of **110**.

The ligand and diazo ester screening for the asymmetric cyclopropanation of **62** showed that the bis(oxazoline) ligands (Table 2, entry 1 - 6) are superior to the aza-bis(oxazolines) (Table 2, entry 7 - 10) in terms of isolated yield and slightly superior in

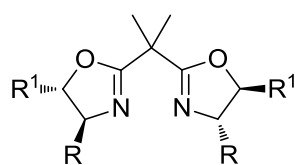
terms of enantiomeric excess obtained.⁴⁰ It turned out that ligand **99** bearing the bulky *t*Bu groups delivered the best results. However, recrystallization of the product furnished the enantiomerically pure cyclopropanation product **112**. Hence, **82** is the ligand of choice for economic reasons (readily available from L-valine in contrast to ligand **99**, which is produced from the expensive unnatural amino acid *tert*-butyl leucine). The steric demand of the diazo ester is another issue. It turned out that exchanging the ethyl group with a *tert*-butyl group has a beneficial effect on the stereochemical outcome of the reaction (Table 2, entry 4 and 6).

Table 2: Ligand and diazo acetate screening for the conversion of 2-furoic ester **62**.⁴⁰



Entry	Diazo acetate R	Ligand L*	Yield [%]	Selectivity [%] ee
1	Me	85	45	69
2	Me	99	55	85
3	Et	99	63	91 ^[a]
4	Et	82	35	81 ^[a]
5	Et	ent-82	33	75 ^[a]
6	<i>t</i> Bu	82	38	95 ^[a]
7	Me	113	23	94
8	Me	100	36	91
9	Me	114	18	91
10	Me	115	31	85

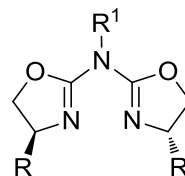
[a]: 99% ee after single recrystallization [isolated yield 53% (entry 3), 32% (entry 4), 29% (entry 5) and 27% (entry 6)].



85: R = CH₂OH, R¹ = Ph

99: R = *t*Bu, R¹ = H

82: R = *i*Pr, R¹ = H



113: R = *t*Bu, R¹ = H

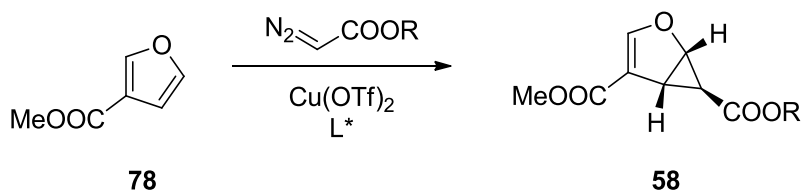
100: R = *t*Bu, R¹ = Me

114: R = *i*Pr, R¹ = H

115: R = *i*Pr, R¹ = Me

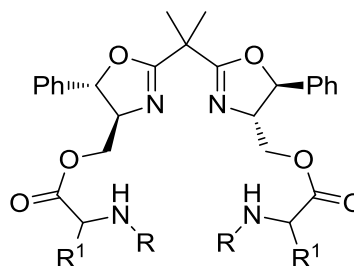
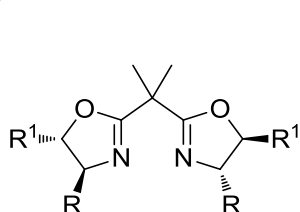
In order to extend the scope of the asymmetric cyclopropanation of furan derivatives, the copper(I)-bis(oxazoline)-diaz-ester system was also examined with 3-furoic methyl ester (**78**) (Table 3). In contrast to the 2-substituted cyclopropanation product **112**, the 3-substituted **58** was formed in slightly lower yields but significantly lower enantiomeric excess.

Table 3: Ligand and diazo acetate screening for the conversion of 3-furoic ester **78**.



Entry	Diazo acetate R	Ligand L*	Yield [%]	Selectivity [%] ee
1 ^[a]	Et	85	27	74
2	<i>t</i> Bu	85	38	65
3 ^[b]	Et	116	31	68
4 ^[b]	Et	117	19	40
5 ^[a]	Et	99	22	74
6	Et	82	31	83
7	<i>t</i> Bu	82	38	83

[a]: Ref. ⁴⁰; [b]: Ref. ⁷⁶.



In the case of ligands **85**, **116** and **117** (Table 3, entry 1 - 4) carrying secondary binding sites, this difference in selectivity can be explained via the substrate-complex coordination. Since the steric demand of the side chains is relatively low compared to an *i*Pr or *t*Bu group, the OH group of **85** (NH for **116** and **117**, respectively) is suggested to act as a hydrogen bond donor (Figure 10, left).⁷⁶ This fact explains the

higher enantiomeric excess of the 2-substituted cyclopropanated furan **112** over the 3-substituted one **58**. The latter is supposed to be unable of forming hydrogen bonds with the ligand-OH/NH group, as the distance between the ester and the OH/NH group is too long (Figure 10, right). Thus, the missing hydrogen bond cannot compensate the relatively low steric demand of the side chains, which results in lower ee values.

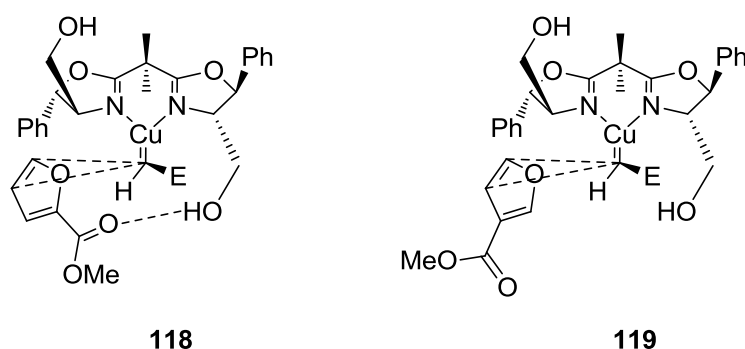


Figure 10: Complex of 2-furoic ester **62** (left)⁷⁶ and 3-furoic ester **78** (right) with ligand **85** bearing a secondary binding site (the same applies to ligand **116** and **117** with the NH groups acting as hydrogen donor); E = ester.

There is a different explanation for the comparable but mostly lower enantiomeric excess using ligands without secondary binding sites **99** and **82** (Table 3, entry 5 - 7). As mentioned above, the substrate approaches to the complex in a way that the furan-COOMe group points away from the bulky moieties (*i*Pr or *t*Bu) of the ligand. This fact, combined with the C₂-symmetry of the complex, is responsible for the stereoselectivity (Figure 11, left column). The exchange of 2-furoic ester with 3-furoic ester should lead to a lower steric repulsion between the furan-COOMe group and the ligand residue, due to the lengthened distance. This steric difference can be responsible for an initially unfavored approach turning into a likely pathway (Figure 11, right column). Although this hypothesis has yet to be proven, it gives an explanation for the lower enantioselectivity of this cyclopropanations and makes the way for further optimization. In order to increase the steric repulsion, more bulky ester groups could be introduced into the 3-furoic acid (**59**) to enable a screening process. If the hypothesis is accurate, the ee values should increase with the bulkiness of the ester (Me < Et < *i*Pr < *t*Bu).

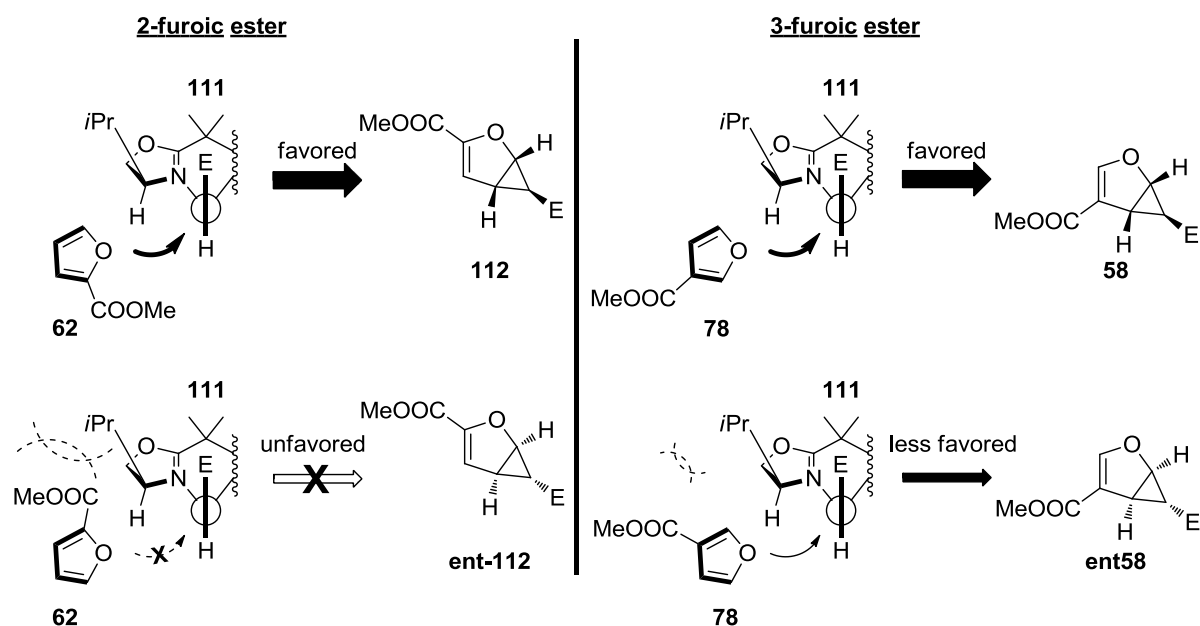


Figure 11: Selectivity comparison of the cyclopropanation of two different substrates (E = ester).

In contrast to the diazo compound screening for the conversion of the 2-furoic ester **62**, the exchange of ethyl diazo glycine (**91**) by *tert*-butyl diazo glycine (**89**) gave no advantage for the stereoselectivity when using 3-furoic ester **78** (Table 3, entry 6 and 7).

Contrary to the 2-furoic-ester-pathway, the 3-furoic-ester pathway does not allow the purification of the desired enantiomer by crystallization. The ethyl ester derivative **119** did not form a solid and stayed a sticky oil even during storage at -18 °C for several weeks. In contrast, the *tert*-butyl derivative **118** crystallizes already as a white solid, while being concentrated under reduced pressure after column chromatography. All attempts to recrystallize it in order to increase the enantiomeric excess, either in the established *n*-pentane/DCM mixture or other solvent mixtures, failed due to the high solubility in almost all common organic solvents (even in neat *n*-pentane at low temperatures).

The stereochemistry of the *tert*-butyl substituted cyclopropanation product **118** was confirmed by X-ray crystallography (Figure 12).

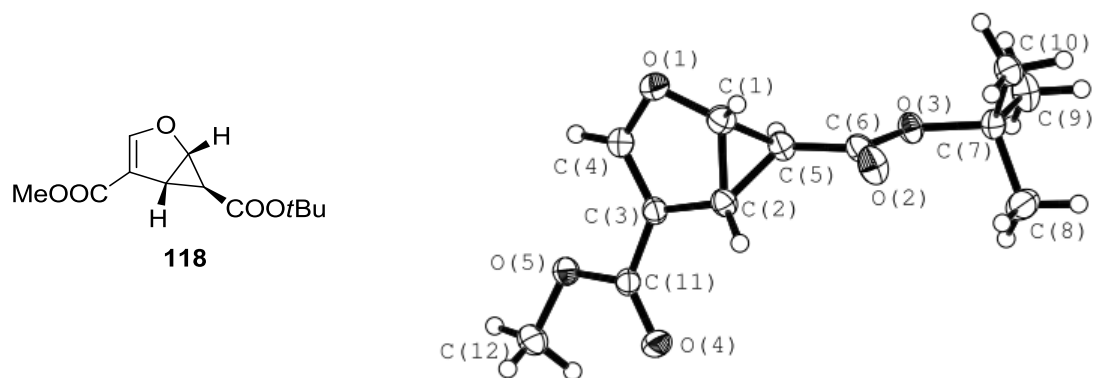
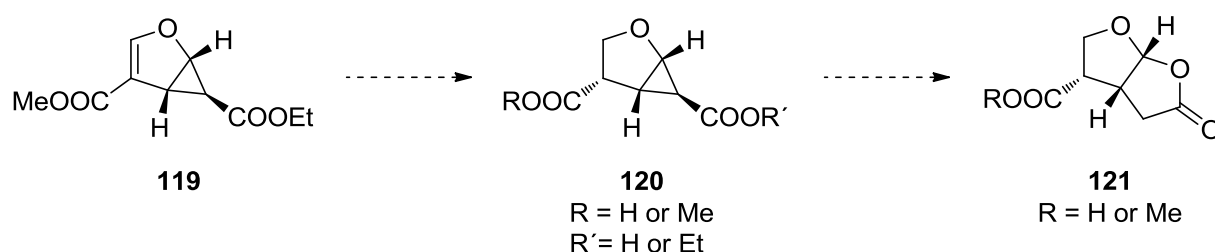


Figure 12: X-ray structure of **118**.

3. Toward the furo-lactone formation

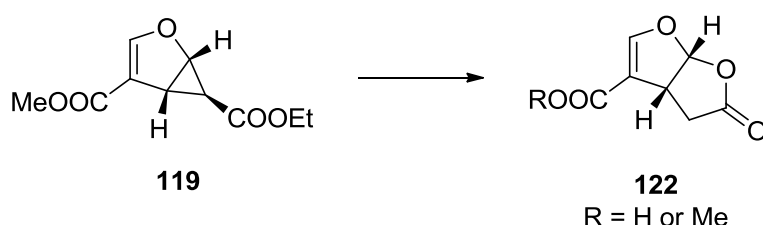
Due to the easier accessibility of the ethyl diazo glycine (**91**), even on multi gram scale, the further experiments toward the furo-lactone **121** were carried out with the ethyl ester derivative **119** of the cyclopropanated furan (Scheme 17).

Scheme 17: From the cyclopropanated furan **119** to the furo-lactone moiety **121**, the core structure of Paeonilide (**5**).



A preliminary account was the straightforward direct lactonization of the cyclopropane **119** to the furo-lactone **121** to yield the core skeleton of the desired target molecule. In order to achieve this reaction several literature known lactonization methods were carried out.

Table 4: Direct lactonization attempts.

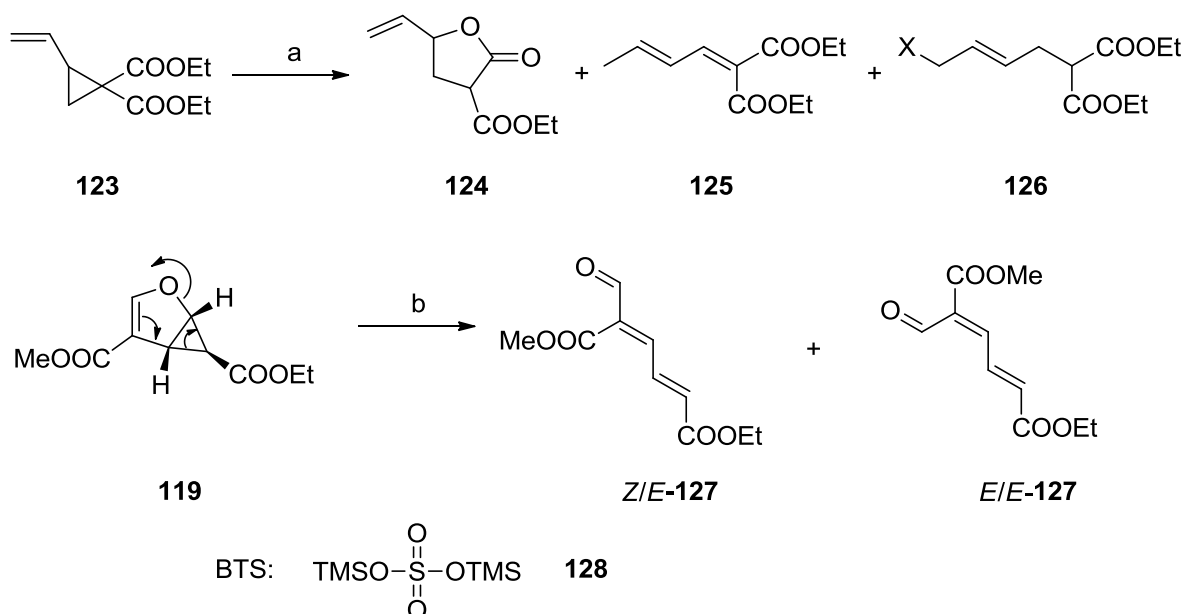


Entry	Reagents	Conditions	Yield [%]	Observations
1 ^[a]	6 M HCl / dioxane	24 h, r.t.	-	saponification
2 ^[b]	MeSO ₃ H (3.3 eq), acetone	24 h, r.t.	-	intractable mixture
3 ^[c]	BTS (2 eq), DCM	14 h, 0 °C to r.t.	87 (127)	formation of acyclic isomers

[a]: Ref ²⁸; [b]: Ref ⁷⁷; [c]: Ref ⁷⁸.

The acid mediated lactonization (Table 4, entry 1), already used in the synthesis of the core nuclei **76** and **77** of Macfarlandin C, Norrisolide and Cheloviolene A/B (Scheme 9), usually applied on saturated systems afforded in present case, e.g. an unsaturated substrate, only a mixture of partially and completely saponified starting material. The use of methane sulfonic acid, successfully employed in the one-pot ring expansion of cyclopropane rings by Theodorakis *et al.*, resulted in the case of **119** in a complex mixture of components. Hiyama *et al.* reported the utilization of bis(trimethylsilyl) sulfate (**128**, BTS, synthesized according to reference ⁷⁹) for the transformation of activated cyclopropane carboxylates into γ -butyrolactones.⁷⁸ So far BTS - highly Lewis acidic and less nucleophilic - was limited to the silylation of active hydrogen compounds.⁸⁰⁻⁸¹ According to Hiyama BTS was superior to other Lewis and Brønsted acids like H₂SO₄, TMS-OTf, TMS-I, BF₃·OEt₂ or TiCl₄, which gave unsaturated aliphatic byproducts in different quantities, depending on the acid used (Scheme 18, top). The treatment of **X** with BTS did not afford desired lactone but exclusively a mixture of unsaturated aliphatic isomers (*Z/E*-**127** and *E/E*-**127** 1.7:1, Scheme 18, bottom). According to Reissig *et al.*, this kind of transformation is one of the most frequently applied reactions in the class of small ring molecules.⁶³ Although these reactions usually provide 1,4-dicarbonyl compounds, **119** delivers 1,6-dicarbonyls due to its fused ring system.

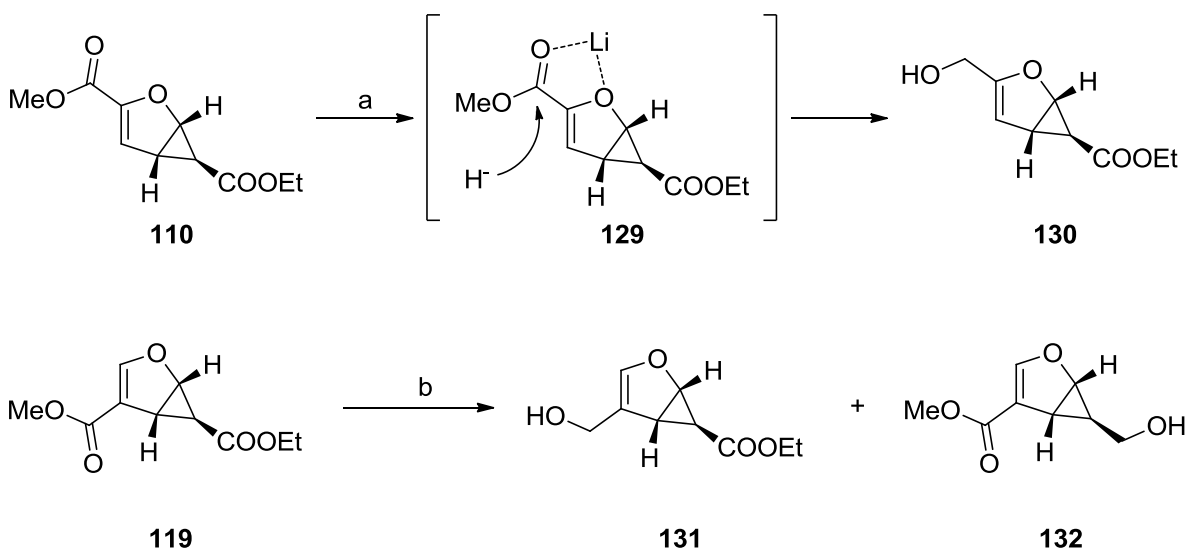
Scheme 18: Lactonization by Hiyama *et al.*, literature example (top) ⁷⁸ and application of **119** (bottom).



Reagents and conditions: a) Lewis or Brønsted acid (2 eq), DCM or DCE, reflux, 98% **124** (for acid = BTS); b) BTS (2 eq), DCM, 0 °C to r.t., 14 h, 87% (**Z/E-127** and **E/E-127** 1.7:1).

Parallel to these efforts on the lactonization, the selective reduction of the furan-COOMe group was attempted, which probably would be advantageous for the later steps, since the COOMe group needs to be transformed into a hydroxyl group anyway.

Scheme 19: Attempted selective methyl ester reduction.

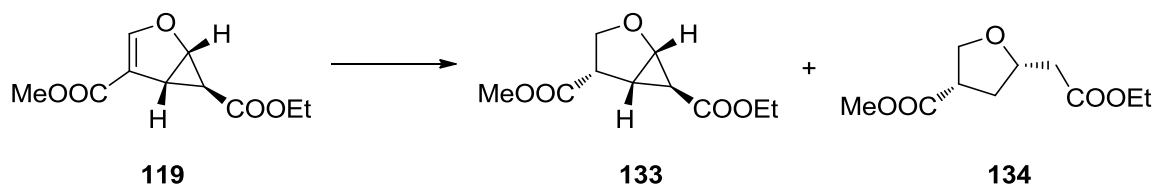


Reagents and conditions: a) LiAlH_4 (0.6 eq), THF, 0 °C, 1 h, 87%; b) LiAlH_4 (0.6 eq), THF, 0 °C, 1 h, 34% **131** and 32% **132**.

The reduction of the 2-substituted derivative **110** with LiAlH_4 proceeded in a selective way, which can be explained via chelating of the oxygen atoms by a lithium ion, probably activating the methyl ester carbonyl (Scheme 19, top).⁸² Due to the 3-position of the methyl ester in **119**, it is not possible to chelate the oxygen atoms, which results in a mixture of both possible alcohols **131** and **132** (Scheme 19, bottom). Because of this selectivity problem, experiments concerning this route were ceased.

To circumvent the problems occurring in the direct lactonization (Table 4) or the selective reduction pathway (Scheme 19), it was envisaged first to reduce the C-C double bond and then implement further modifications toward the furo-lactone core skeleton. In order to achieve this goal, standard methods for C-C double bond hydrogenation were applied (Table 5).

Several attempts in different solvents showed the high dependency of this reactions to the applied solvent, *e.g.* methanol and ethyl acetate proved to be completely ineffective. Moreover, variation of the catalyst (*e.g.* palladium on charcoal, palladium hydroxide on charcoal, ruthenium on aluminum oxide) did not result in consumption of starting material (Table 5, entry 1 - 4).

Table 5: C-C double bond hydrogenation.

Entry	Reagents ^[a]	Conditions	Yield [%]		Observation
			133	134	
1	Pd/C, MeOH, H ₂	24 h, r.t.	-	-	no reaction
2	Pd(OH) ₂ , MeOH, H ₂	24 h, r.t.	-	-	no reaction
3	Pd/C, EA, H ₂	24 h, r.t.	-	-	no reaction
4	Rh/AlOx, EA, H ₂	24 h, r.t.	-	-	no reaction
5	Pd/C, EtOH/H ₂ O (95:5), H ₂	24 h, r.t.	25	8	
6	entry 5 + AcOH (cat)	12 h, r.t.	23	48	
7	Pd/C, EtOH (abs), H ₂	>3 d, r.t.			extremely slow
8	Mg (1 eq), MeOH	0.5 h, 0 °C	-	38	transesterification 2x COOMe (135)
9	RhCl(Ph ₃ P) ₃ , ^[b] EtOH/THF (9:1), H ₂ ^[c]	18 h, r.t.			

[a]: if not stated otherwise H₂ applied via balloon; [b]: Wilkinson's catalyst [c]: balloon 1 h (no reaction), autoclave 20 bar 2 h (no reaction), autoclave 30 bar 15 h (no reaction).

Changing the catalytic system from heterogeneous to homogeneous, *i.e.* by application of Wilkinson's catalyst,⁸³ gave no conversion as well, even when hydrogen pressure was applied up to 30 bar in an autoclave.

The use of aqueous ethanol together with palladium on charcoal finally resulted in conversion of **119**. However, the reaction in EtOH/H₂O with Pd/C provided not only the desired product **133**, but also byproduct **134** from hydrogenation of one cyclopropane bond. The structure of **134** could be confirmed by 2D-NMR analysis. A similar byproduct was also observed when derivatives of the 2-substituted cyclopropanated furan **110** was submitted to hydrogenation conditions, albeit opening of the furan occurred next to addition to the cyclopropane ring.⁸⁴ It could be shown that the presence of water promoted the reaction, since the conversion in anhydrous ethanol was negligible even after 3 days (according to TLC control). The addition of catalytic amounts of acetic acid accelerated the product formation but

gave also an increase in ring opened **134**. The same effect was observed when different acids like *p*-TSA, oxalylic acid or TFA were used. Product **133** was formed as expected, exhibiting the methyl ester group on the concave side of the fused ring system, since the hydrogenation takes place from the less hindered, convex side. The stereochemistry of **133** was confirmed by X-ray crystallography (Figure 13).

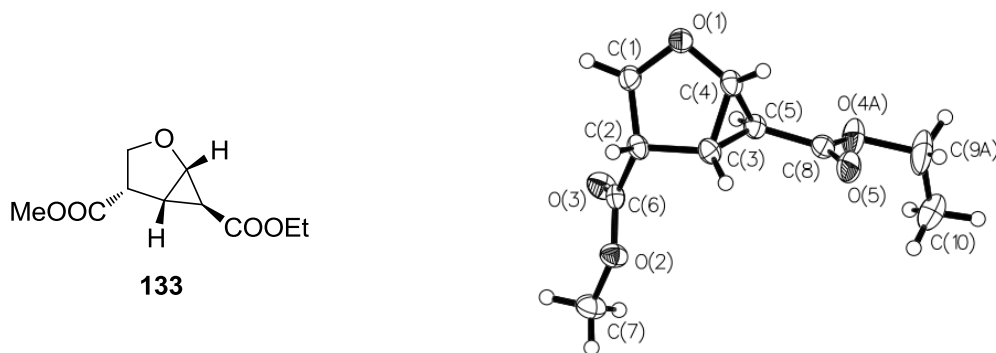
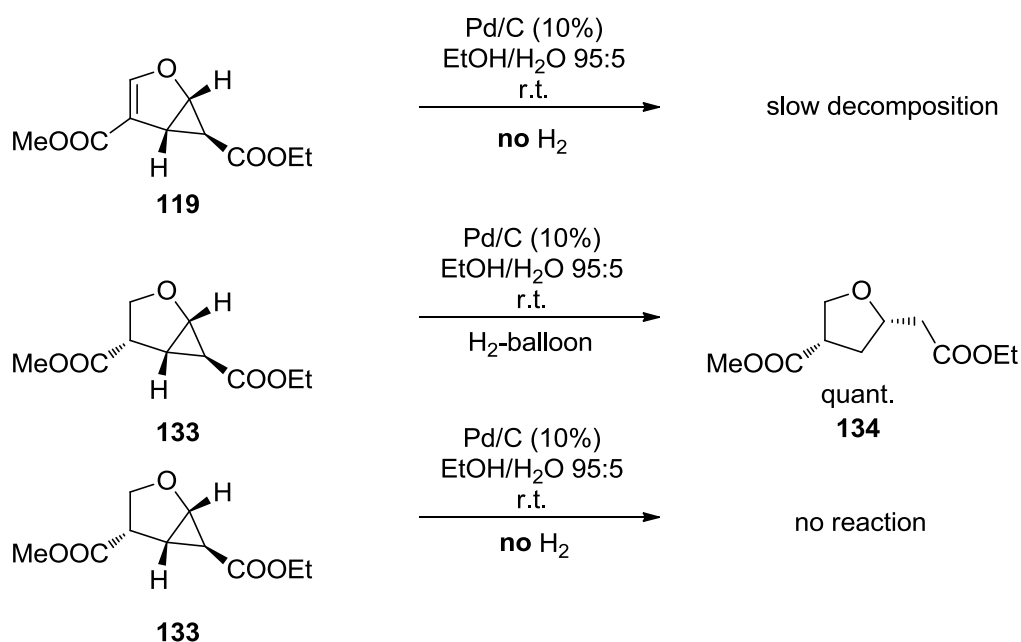


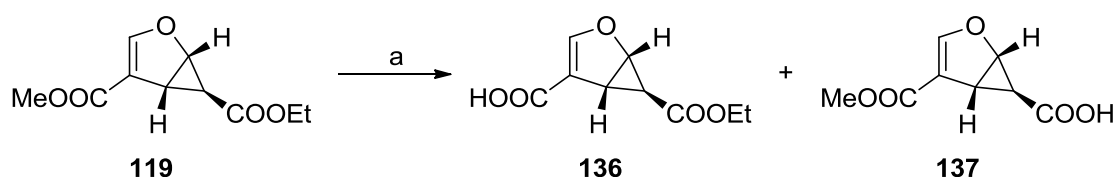
Figure 13: X-ray structure of **133**.

A screening should give rise to the origin of the byproduct **134** (Scheme 20). To this end, olefin **119** was stirred in the presence of palladium on charcoal but without any hydrogen to determine whether the side reaction occurs on the catalyst surface itself, but only very slow decomposition could be observed (Scheme 20, top). The desired hydrogenation product **133** reacted fast under hydrogenation conditions to the opened cyclopropane **134** (Scheme 20, middle). Contrary to these results, treatment of **133** only with solvent and catalyst without hydrogen gave no new compounds on TLC, therefore it seems to be stable under these conditions (Scheme 20, bottom).

Scheme 20: Studies on byproduct formation.

A final hydrogenation was attempted with *in situ* generated hydrogen by treating the starting material **119** with magnesium in methanol.⁸⁵⁻⁸⁶ According to literature precedents, this method was successfully applied on α,β -unsaturated esters and tolerates several functional groups, e.g. esters, epoxides and ethers. The recommended 10 equivalents of magnesium caused a rapid formation of multiple compounds within a few minutes. Changing the conditions to 1 equivalent of magnesium and cooling to 0 °C gave rise to the opened cyclopropane **135**, which is similar to **134**, but transesterificated to a double methyl ester. In contrast to **134**, which was formed as a single diastereomer, **135** was produced as a 1:1 mixture of two diastereomers, which could not be exactly identified yet.

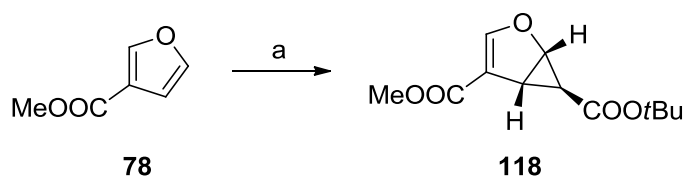
As the aforementioned lactonization directly after cyclopropanation was unsuccessful, the alternative approach of reducing the C-C double bond was further envisaged to be optimized, since a product formation was already observed. To circumvent these problems, saponification of the methyl ester was envisaged. In order to perform this reaction selectively, with respect to the COOMe group, very mild conditions were chosen. A small excess of lithium hydroxide in aqueous THF at 0 °C did not give the desired product but an inseparable 1:1 mixture of both possible mono-saponified products **136** and **137** (Scheme 21).

Scheme 21: Attempt of selective saponification.

Reagents and conditions: a) LiOH (1.1 eq), H₂O/THF 2:1, 0 °C, 6 h, 85% (**136/137** = 1:1).

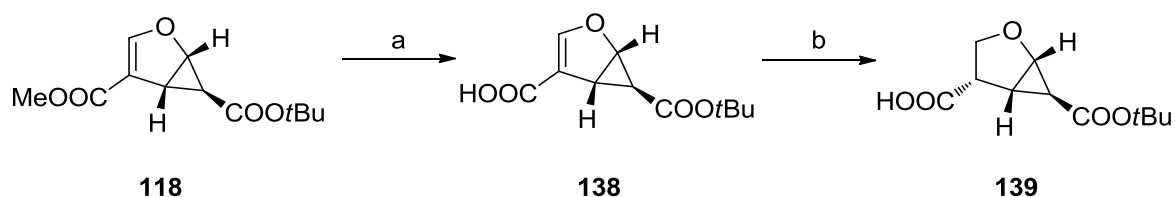
Literature known procedures for a selective conversion of a methyl ester like the reaction of sodium cyanide in DMPU, did not furnish the desired product either, but only a complex mixture which could not be analyzed.⁸⁷⁻⁸⁸

Due to the small difference in reactivity regarding the hydrolysis of the methyl and ethyl ester of **119**, a change of these groups was needed. For this reason the initial cyclopropanation was performed with *tert*-butyl diazo glycine (**89**) to accomplish the cyclopropanated furan **118** (Scheme 22, X-ray structure Figure 12), now bearing a methyl and a *tert*-butyl ester (for a closer discussion of furan-cyclopropanation see chapter 2.2). All further reactions found on this molecule.

Scheme 22: Asymmetric cyclopropanation with *tert*-butyl diazo glycine (**89**).

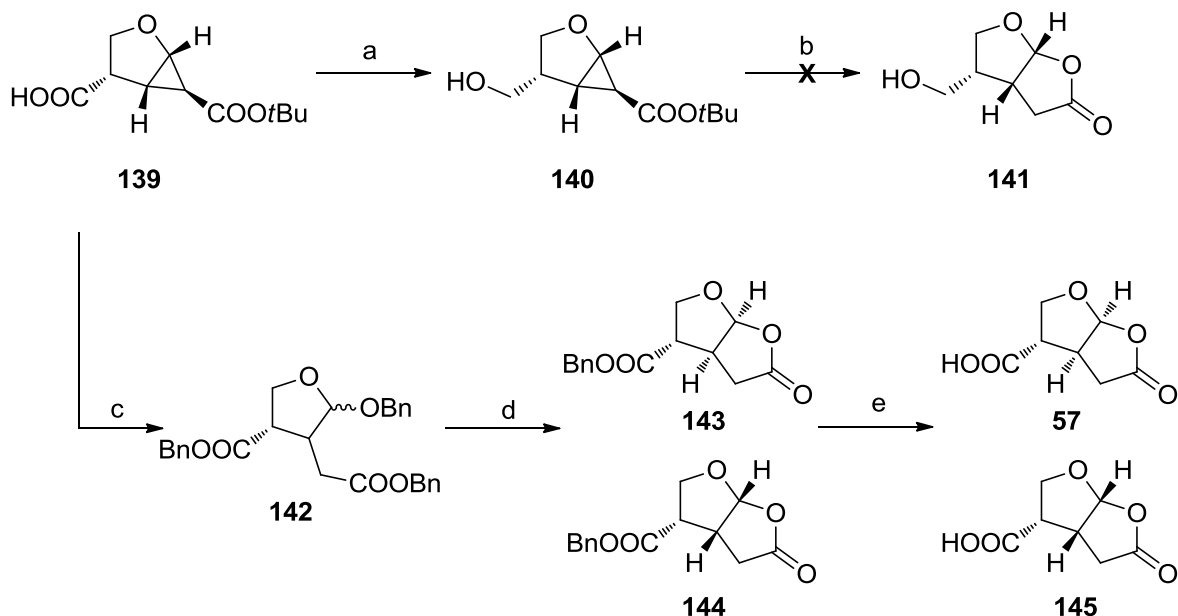
Reagents and conditions: a) Cu(OTf)₂ (1.12 mol%), (*S,S*)-*i*Pr-BOX (**82**) (1.5 mol%), PhNHNH₂ (1.12 mol%), N₂CHCOOtBu (1.3 eq), DCM, 0 °C, 38% (53% brsm), 83% ee.

The subsequent hydrolysis of the methyl ester in the presence of the *tert*-butyl ester performed by the utilization of lithium hydroxide now worked as desired in a chemoselective way, delivering the carboxylic acid **138** in excellent yield (Scheme 23). The synthesis was even applicable on multi gram scale. The following C-C double bond hydrogenation was first tested with the so far best solvent-catalyst system according to the prior hydrogenation screening, palladium on charcoal in ethanol-water 95:5. Already the first reaction proceeded smoothly to the product **139** (Scheme 23). Due to steric reasons the reduction should proceed from the less hindered, convex side of the fused ring system, which was confirmed later.

Scheme 23: Hydrogenation and hydrolysis to **139**.

Reagents and conditions: a) LiOH (1.1 eq), H₂O/THF 3:1, r.t., 6 h, 85% (quant. brsm); b) Pd/C (10%), EtOH/H₂O 95:5, H₂ (balloon), r.t., 6 h, quant.

Having **139** in hands, there were two alternative routes to proceed in the synthesis. Either reduction of the free carboxylic acid group to the corresponding alcohol, followed by the lactonization, or *vice versa*. Both ways were examined. The reduction of the acid group was performed in THF by the use of a borane-THF-complex, which selectively reduces carboxylic acids to the corresponding alcohol in the presence of esters if not added in too large excess.⁸⁹ The reaction itself worked as desired but problems during the work up were encountered, since the product **140** seemed to be unstable under these conditions (Scheme 24).

Scheme 24: Different lactonization pathways.

Reagents and conditions: a) BH₃·THF (1.2 eq), THF, 0 °C to r.t., 13 h, 22%; b) 6 M HCl, THF, r.t., 6 h; c) BnOH, H₂SO₄ (2.8 eq), 0 °C to r.t., 14 h, 30%; d) i: MeSO₃H (6 eq), DCM, -20 °C to r.t., 12 h, (**143/144** = 1.4:1); ii: DBU (1.1 eq), DCM, H₂O (cat), reflux, 2h, 70% (**143/144** = 5:1); e) THF, Pd/C (10%), H₂ (balloon), r.t., 2 h, 85%.

The obtained alcohol **140** was analyzed by X-ray crystallography (Figure 14). This structure proved the assumption that the reduction of the C-C double bond occurred in a way that led to the carboxylic acid **139** (Scheme 23) exhibiting the acid group on the concave side of the fused ring system.

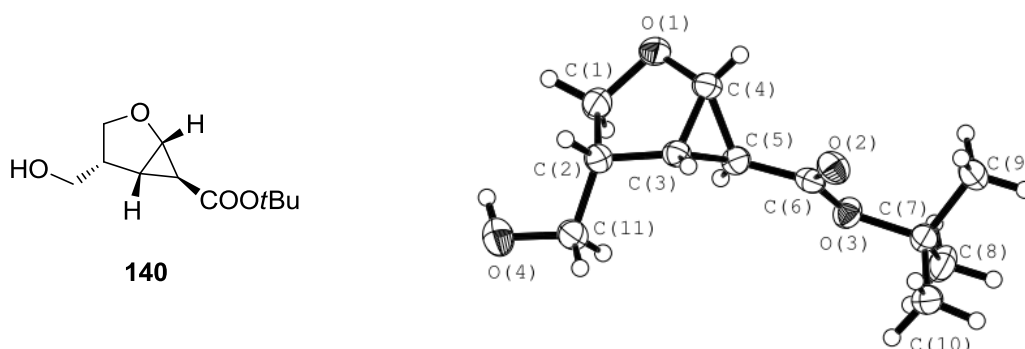


Figure 14: X-ray structure of **140**.

The ensuing lactonization attempt of **140**, following the acid mediated lactonization protocol,²⁸ resulted in a complex mixture of unidentified, highly polar compounds. Since this route seemed incapable of generating the desired fused ring system, the second route was examined.

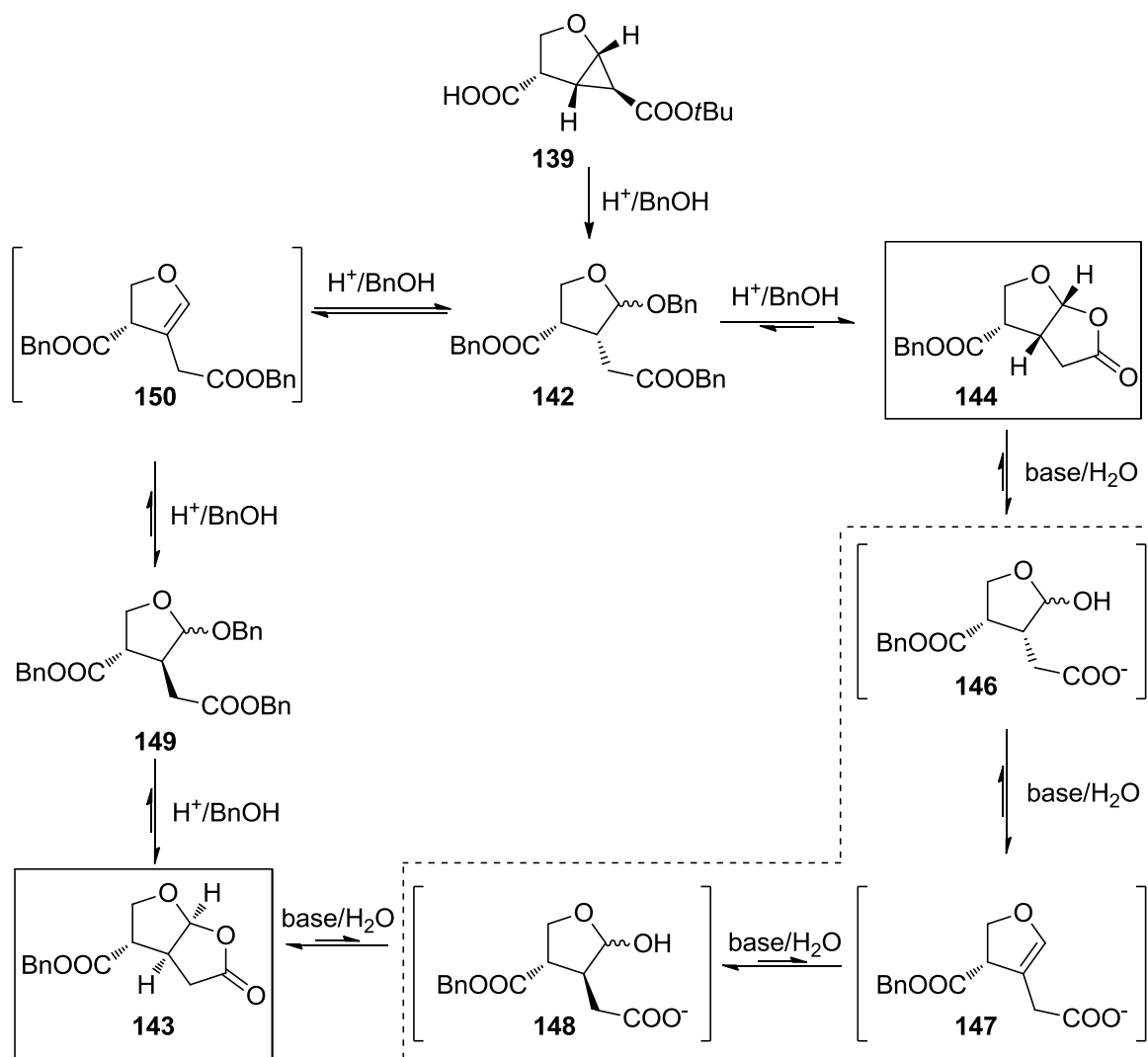
It is possible to form the bi-cyclic system either in an one-pot acid mediated or a two-step reaction. The latter was published by Theodorakis *et al.* for the total synthesis of the spongiane diterpene norrisolide and starts with an acidic opening of the cyclopropane moiety to form the acetal **142**.⁹⁰ Under these conditions all containing ester or carboxylic acid groups are transesterificated or esterificated respectively, depending on the used alcohol (in this case benzyl alcohol). The product was obtained in a diastereomeric mixture and isolated in an impure form by column chromatography. The subsequent lactone closure was accomplished by using methanesulfonic acid furnishing two different diastereomers **143** and **144** in a 1.4:1 ratio.

The formation of the two appearing diastereomers is illustrated in Scheme 25 and can be explained by a mechanism published by Reiser *et al.*²⁸ The expected diastereomer is lactone **144**, which is formed when the backward-directed CH_2COOBn of **142** substitutes the OBn group on the furan. Under acidic conditions, which occur in the cyclopropane ring opening reaction, benzyl alcohol can be reversibly eliminated from compound **142** to yield the enol **150**. This enol can undergo a re-addition of benzyl alcohol to the acetal **149**, now possessing the

CH₂COOBn group on the steric less hindered upper side of the furan ring. This thermodynamically more favored acetal is converted under benzyl alcohol elimination to the lactone **143**, bearing the benzyl ester on the convex side of the bicycles.

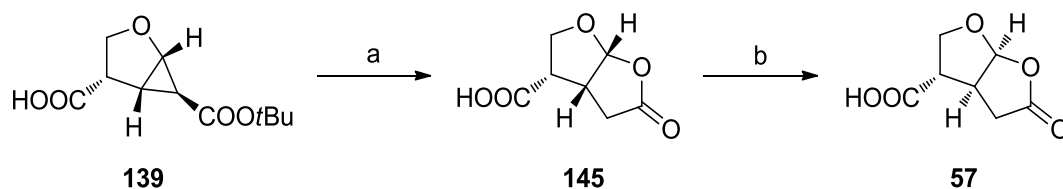
It could also be shown that treatment with DBU shifted the diastereomeric ratio from 1.4:1 to 5:1. This can be explained by the base mediated lactone opening of **144** to the hemiacetal **146** and a subsequent water elimination to enol **147**, followed by re-addition of water to form again a hemiacetal **148** (Scheme 25, dashed box). Possessing the two substituents in anti position **148** is thermodynamically more favored than **146**. The final ring closure gives rise to the furo-lactone **143**.

Scheme 25: Acid mediated formation of lactone diastereomers **143** and **144** (boxes); base mediated lactone isomerization (dashed box).



Although the one-pot acid mediated lactonization was never applied to a cyclopropanated furan having the ester substituent in 3-position, like **139**, it seemed worthwhile to adopt it for that substrate, since the two-step lactonization procedure lacks diastereoselectivity. First attempts with 6 M hydrochloric acid at ambient temperature afforded the lactone **145**, but only as a part of a multi component mixture, which was inseparable due to the high polarity of the compounds.²⁸ A slight modification of the conditions improved the outcome of this reaction (Scheme 26): using 2 M hydrochloric acid and cooling to 0 °C during the acid addition made the starting material **139** react smoothly to the desired product **145**. Since the subsequent base mediated transformation to the other lactone diastereomer was already known from the two-step lactonization discussed before (Scheme 24), this methodology was applied as well. In contrast to the use of DBU, pyridine could be employed without refluxing the reaction mixture, thus avoiding the formation of byproducts to give rise to the core ring system of (-)-Paeonilide (**5**) as the substituent in 3-position was already on the convex side.

Scheme 26: One-pot lactonization and subsequent isomerization.



Reagents and conditions: a) 2 M HCl/THF 3:1, 0 °C to r.t., 12 h, not isolated; b) py, H₂O, r.t., 2 h, 75% over 2 steps.

The absolute stereochemistry of both lactone isomers was confirmed by X-ray crystallography (Figure 15). It should be mentioned that **57** could only be crystallized by the following technique: dissolving **57** in a small amount of acetonitrile on a watch glass, addition of one equivalent of (*R*)-1-(4-chlorophenyl)ethylamine and slow evaporation of the solvent during storage in the refrigerator.

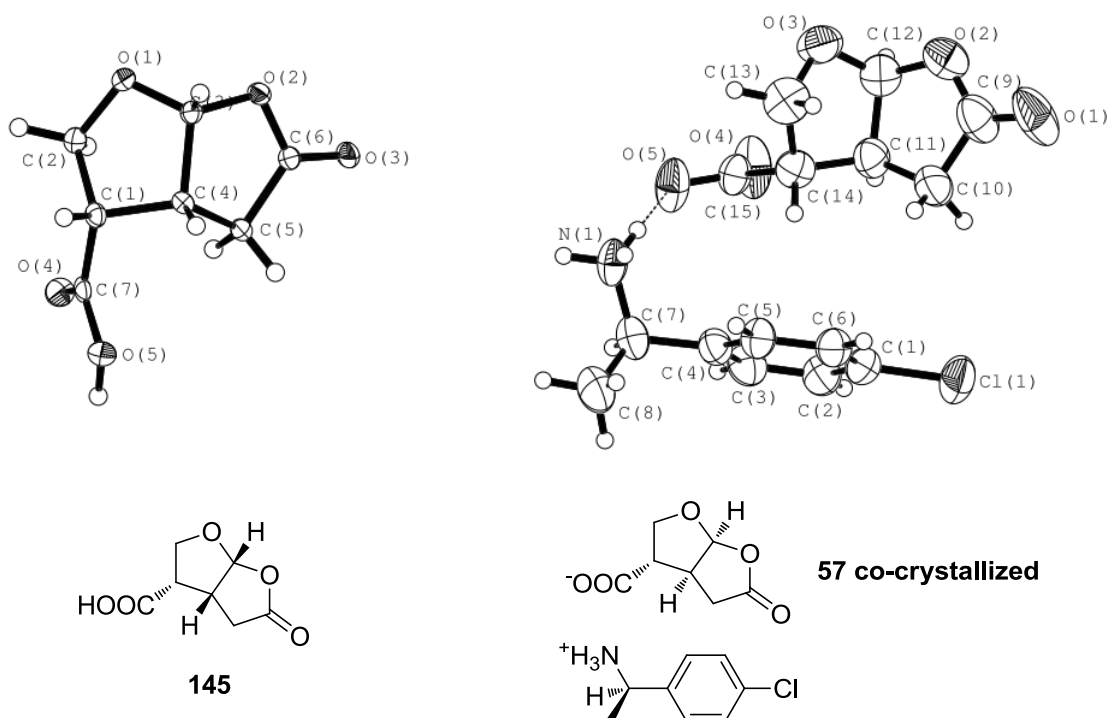
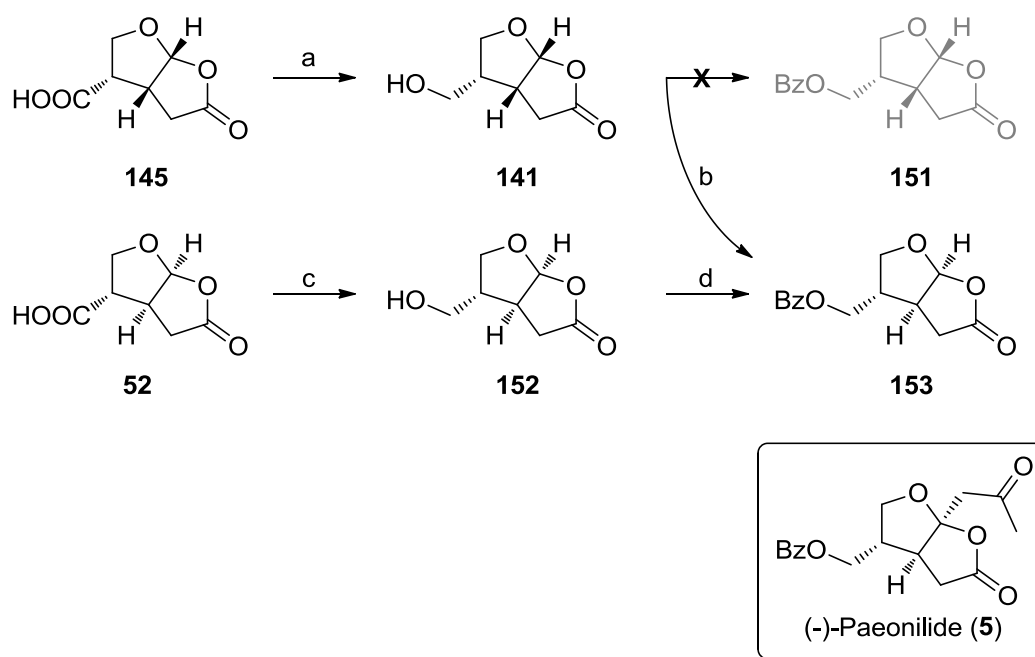
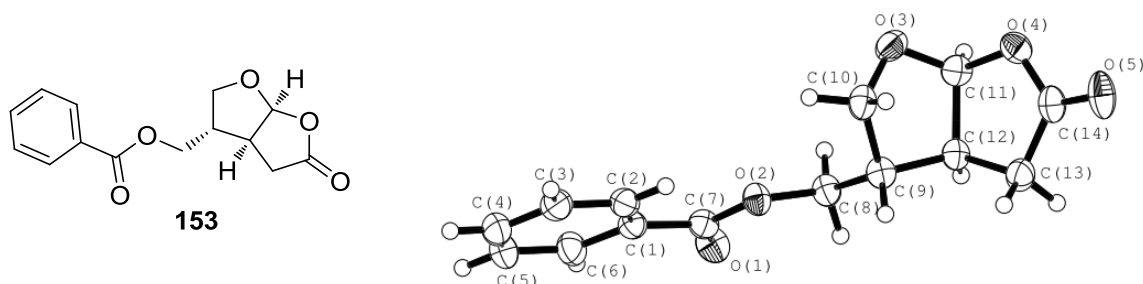


Figure 15: X-ray structures of lactone **145** and **57**, the latter co-crystallized with (*R*)-1-(4-chlorophenyl)ethylamine.

The following experiments were performed in parallel with both lactone diastereomers. In order to complete the final steps toward (-)-Paeonilide (**5**), except for the ketone side chain, the free carboxylic acid was reduced to the corresponding alcohol with the aid of borane.⁸⁹ The best results were obtained when the reaction mixture was heated up to 40 °C once the addition of the reducing agent was finished. Using this procedure, both alcohols **141** and **152** could be obtained in good to excellent yield. The subsequent protection step of the alcohol to the final benzoyl ester was done following the literature reaction of the already published Paeonilide synthesis by Du *et al.*²⁵ The measurement of the optical rotation of both products of the protection reactions gave the same α value, which indicated the isomerization of one of both alcohols, either **141** or **152**. The absolute stereochemistry of the obtained isomer could be confirmed by X-ray crystallography (Scheme 27).

Scheme 27: Reduction and protection reaction; X-ray structure of **153**.

Reagents and conditions: a) $\text{BH}_3\cdot\text{THF}$ (1 eq), THF, 0 °C to 40 °C, 3 h, 68%; b) BzCl (2 eq), py, r.t., 3 h, 36%; c) $\text{BH}_3\cdot\text{THF}$ (1 eq), THF, 0 °C to 40 °C, 3 h, 97%; d) BzCl (2 eq), py, r.t., 3 h, 39%.



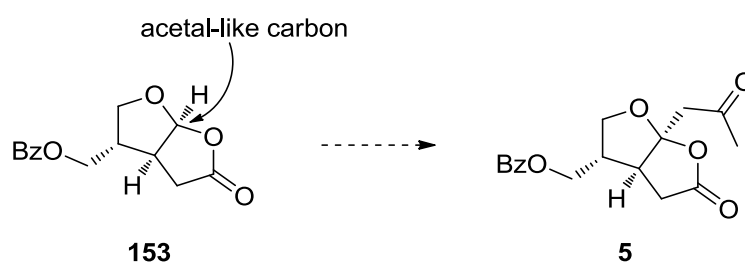
This means both protection reactions provide the same product **153**. The isomerization is supposed to proceed in the same way as previously discussed, especially concerning the base mediated lactone-isomerization (Scheme 25, dashed box). Like in that case, the formation of the steric less hindered and therefore thermodynamically favored lactone **153** is privileged.

4. Side chain introduction by C-H insertion

4.1 General information

The final transformation to the target compound **5** was planned to be accomplished by the utilization of a metal catalyzed carbene C-H insertion in the acetal-like C-H bond (Scheme 28).

Scheme 28: Planned C-H insertion in acetal-like position.



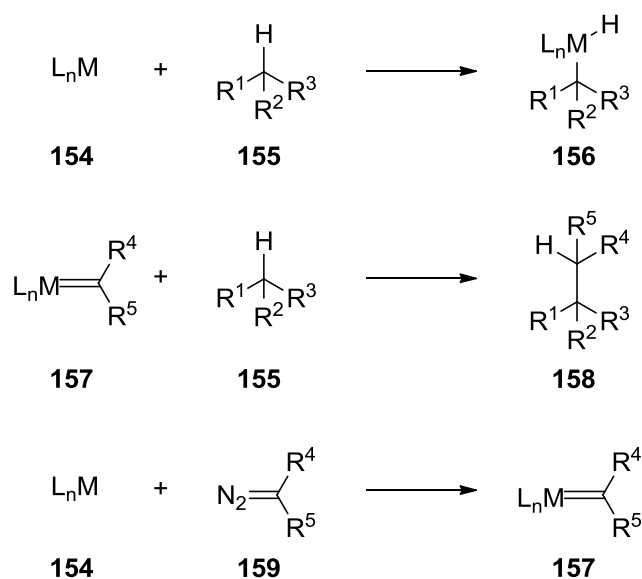
Since its first observation more than 60 years ago⁹¹ and due to its novel chemistry at that time described as unusual reaction, C-H insertions became of great interest not only because of mechanistic implications but also in natural product synthesis. In the latter case, this kind of conversion exhibits huge benefits: Traditional reactions take advantage of functional groups which can hamper the synthesis due to the formation of unwanted byproducts. In contrast to functional group conversions, C-H insertions can be utilized to streamline reaction sequences and to diminish the generation of byproducts. Despite years of investigation in this area, the number of known catalytic processes for these transformations is still limited.⁹²⁻⁹⁴ Several reasons might account for this.⁹⁵

First, predominant investigations on “classic” C-H activations including the formation of an organometallic compound, and second, the big energy requirement for cleaving a C-H bond combined with the arising selectivity problems.

Regarding the first point, most effort in this field was put in studies concerning “classic” C-H activation reaction including the formal insertion of a metal center into the C-H bond to form a σ -organyl derivative (Scheme 29, top). In this case, the relative stability of the newly formed carbon-metal and carbon-hydrogen bonds gave rise to an inert organometallic compound **156**, which paralyzes subsequent

transformations. In contrast to this fact, the transient metallo-carbene **157** with a C-H bond would give rise to the formation of a new carbon-carbon bond **158** by a formal insertion of a carbene into a carbon-hydrogen bond (Scheme 29, middle). Simultaneously, the metal center is released and reused in the catalytic cycle by the *in situ* reaction of the metal complex **154** with an diazo compound **159** (Scheme 29, bottom).⁹⁶⁻⁹⁷

Scheme 29: C-H activation: C-M bond formation (top), carbene insertion (middle), *in situ* formation of metallo-carbene intermediate (bottom).⁹⁵



This alternative route via the transient metal-carbene was first reported by Scott *et al.* using inorganic copper sulfate and chloride as catalyst for the insertion of an ethyl diazo glycine (**91**) derived carbene into a C-H bond of cyclohexane.⁹⁸ The employment of $Cu(acac)_2$, as published by Wulfmann *et al.* in 1976, gave similar results.⁹⁹ Besides copper also rhodium complexes, like $Rh_2(TFA)_4$, were employed. Focusing on Rh containing catalysts, Teyssié, Noels and co-workers reported several articles, which showed superior yields compared to the copper catalyzed reaction mentioned before.¹⁰⁰⁻¹⁰⁴ Therefore, many related rhodium catalysts were applied within the following years, which might be considered as interesting from the mechanistic point of view, but with limited value for synthetic chemistry, at least at that time.¹⁰⁵

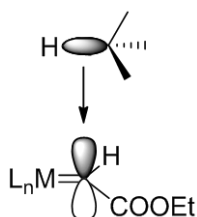
The second reason why C-H insertion chemistry had a rather small impact in recent years is regioselectivity. While established methods rely on selectivity control by

steric and electronic means, the biggest challenge within C-H insertions is to reach comparable level of selectivity as in functional-group based chemistry. This is especially true, because there are typically more than one C-H bond in a common organic substrate molecule. Additionally, the required energy for C-H bond cleavage is quite high. Studies showed that the C-H bond energy values are as follows:¹⁰⁶

carbon center:	CH ₄	primary	secondary	tertiary
C-H bond energy [kcal/mol]:	105	101	99	97

For this reason, reactive reagents like the applied metal carbenes, generated by the decomposition of diazo compounds under nitrogen evolution by transition metals, are required. It is assumed that the newly formed carbon-carbon bond is generated by the interaction of the empty p-orbital of the metal-carbene complex and the filled σ -molecule orbital of the C-H bond (Scheme 30).

Scheme 30: Interaction of metal-carbene complex with a C-H bond.



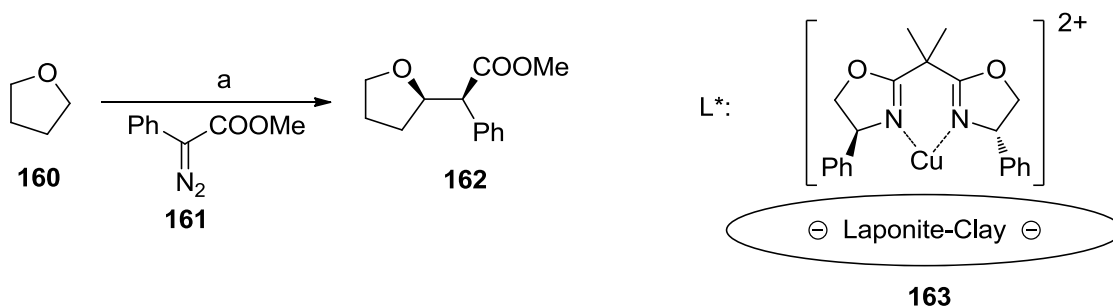
The first transition metal carbene was reported by Greuter *et al.* in 1958 utilizing copper oxide.¹⁰⁷ Although the origins of transition metal catalyzed C-H insertion chemistry started with the employment of copper,¹⁰⁸ nowadays dirhodium complexes are the most utilized catalysts. This originates from the increased conversion attained by dirhodium complexes at mild reaction conditions compared to the copper counterparts.¹⁰⁹

Within the last years, there were a few reports on C-H insertions, dealing with furans or acetals as substrates, which are of great interest for the key step in the synthesis of (-)-Paeonilide (**5**), since it was necessary to find a C-H insertion reaction which can be applied to the acetal-like position in **153** (Scheme 28).

In 2007, Mayoral and Fraile reported an enantioselective C-H insertion of methyl phenyldiazoacetate (**161**) in 2-position of THF (**160**) catalyzed by bis(oxazoline) ligand **163** immobilized on laponite clay (Scheme 31).¹¹⁰ It is worth to mention, that

the immobilized ligand was superior to the homogeneous counterpart, both, in terms of enantiomeric excess and diastereoselectivity. Due to the fact, that THF was used as solvent and as substrate, this methodology is not suitable for natural product synthesis and therefore it needs to be adjusted.

Scheme 31: Copper catalyzed C-H insertion using an immobilized bis(oxazoline) ligand **163** by Fraile and Mayoral.¹¹⁰



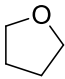
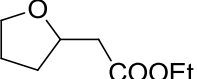
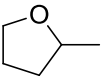
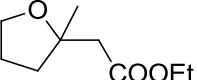
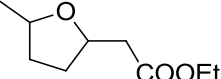
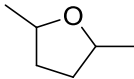
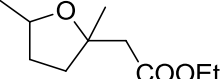
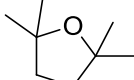
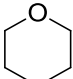
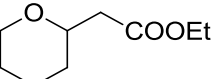
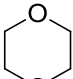
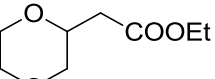
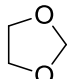
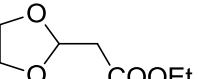
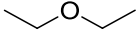
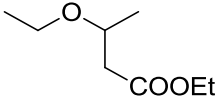
Reagents and conditions: a) THF excess, L* (2 mol%), diazo compound **161** (1 eq), reflux, 2 h, 66 % based on **161**, up to 88% ee (*dr* 75:25).

The same reaction as described in Scheme 31 was also reported by Davies *et al.* using optimized conditions and a Rh₂(S-DOSP)₄ ligand, which provided the product **162** in 67% yield and 97% ee (*dr* 2:1).¹¹¹

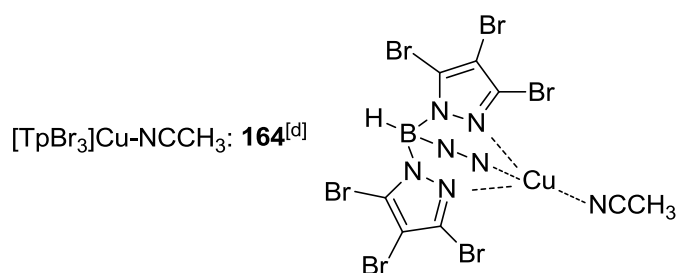
A second study came from Pérez *et al.* in 2002, utilizing a different class of ligand, employed on a broader substrate scope, albeit in racemic reactions.¹¹² The substrate scope could be even extended according to a related publication in 2003.⁹⁵ They applied a homoscorpionate-copper(I) catalyst (**164**) to the successful functionalization of (mostly cyclic) aliphatic ethers and also of acetals by ethyl diazo glycine (**91**) (Table 6). In all cases, only the carbon center adjacent to the oxygen was functionalized, which is in agreement with the results of Adams *et al.*, who reported the same observation using a rhodium catalyst more than ten years ago.¹¹³ The high reactivity of these α-carbons is expounded by its bond energy, since methanol, bearing a comparable electronic environment, exhibits a value of 96 kcal/mol for the H-CH₂OH bond, which is very close to the energy of the reactive tertiary, aliphatic C-H bonds (97 kcal/mol).¹⁰⁶ The inert behavior of the β-carbon center can be explained by the contribution of Nakatani, who showed the deactivation of the C-H bond in β-position to an electron-withdrawing group.¹¹⁴ This fact might give an

explanation for the comparable low yield of the conversion of dioxane (Table 6, entry 6), since in this molecule each carbon center is in the activated α -position as well as the deactivated β -position.

Table 6: Functionalization of ethers and acetals by using a homoscorpionate-copper(I) catalyst **164**.

.Entry	Substrate	Product	Yield [%] ^[a]
1 ^[b]			>99
2 ^[b]			38
			62
3 ^[b]			41
4 ^[b]		---	no reaction
5 ^[c]			84
6 ^[c]			20
7 ^[b]			>99
8 ^[b]			>99

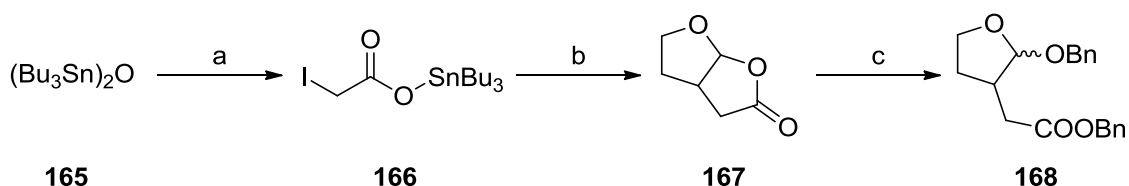
[a]: Determined at the end of the reaction by GC after total consumption of $\text{N}_2\text{CHCOOEt}$. Diethyl fumarate and maleate accounted for 100% of $\text{N}_2\text{CHCOOEt}$ [b]: Ref ⁹⁵; [c]: Ref ¹¹²; [d]: Third pyrazole ring indicated by N-N for better lucidity.



4.2 Preparatory work for the C-H insertion reaction

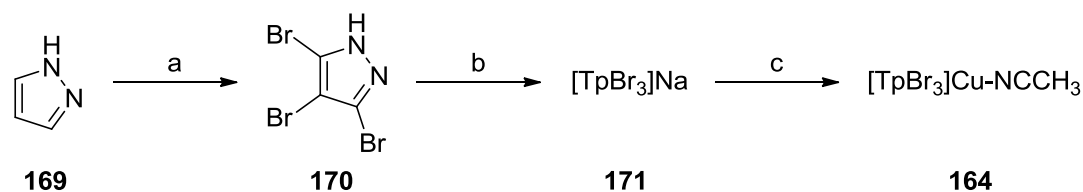
In order to find a model system for the C-H insertion an unsubstituted furo-lactone system was chosen, bearing the same acetal-like position as compound **153**, but being easily producible, even on gram scale.¹¹⁵ The first step involved the formation of tin ester **166** by the neat reaction of hexabutyldistannoxane (**165**) with iodoacetic acid. The subsequent radical reaction with 2,3-dihydrofuran gave the desired, unsubstituted furo-lactone **167**. As C-H insertion reactions in the acetal-like C-H of furo-lactones have not been published so far, a second model compound was prepared, exhibiting a “real” acetal C-H position. This was accomplished by the aforementioned method already employed for the two-step lactonization (Scheme 24) using benzyl alcohol under strongly acidic conditions to furnish **168** as a diastereomeric mixture.

Scheme 32: Synthesis of model substrates.



Reagents and conditions: a) ICH_2COOH (2 eq), 130 °C, 30 min, quant; b) 2,3-dihydrofuran (3 eq), AIBN (5 mol%), benzene, reflux, 8 h, 68%; c) H_2SO_4 (3 eq), BnOH, r.t., 12 h, 86 %.

Besides the model substrates, also the homoscorpionate-copper(I) catalyst **164** was prepared as acetonitrile complex. According to literature procedures,¹¹⁶ commercially available 1H-pyrazole (**169**) was converted to perbromo pyrazole **170**, which was subsequently treated with a shortfall of NaBH_4 at 260 °C by the help of a metal bath (Wood’s metal).¹¹⁷ Remaining **170** was removed by multiple sublimation from the caramel-like sodium boropyrazole (**171**, $[\text{TpBr}_3]\text{Na}$). In order to exchange the sodium cation by Cu(I) yielding the catalytically active catalyst, **171** was stirred with CuI in degassed solvents.¹¹⁸ The final complex $[\text{TpBr}_3]\text{Cu}-\text{NCCH}_3$ (**164**), is very sensitive to moisture and oxygen, but can be stored under inert atmosphere at ambient temperature.

Scheme 33: Synthesis of homoscorpionate [TpBr₃]Cu-NCCH₃ (**164**).

Reagents and conditions: a) NaOH (4 eq), Br₂ (3 eq), H₂O, r.t., 4 h, 76%; b) NaBH₄ (0.25 eq), 260 °C, 82%; c) CuI (1 eq), MeCN (degassed), r.t., 10 h, 75%.

Although the C-H bond of substrate **167**, which is the target of the planned functionalization, is an acetal-like moiety, there might arise several problems. Due to the fact that it is not a “real” acetal, since one of the oxygen atoms belongs to the lactone moiety, the electronic properties of this carbon center are different. There is so far no literature precedence for this kind of conversion, employing such an acetal-like position for C-H insertion chemistry. Therefore, various metal salts were tested in the decomposition of diazo compounds, being the key step in the subsequent reactivity studies (Figure 16 and Table 7). For this reason each salt was treated with ethyl diazo glycine (**91**) and screened for the evolution of nitrogen gas. As a benchmark, established catalysts for this reaction, such as Sc(OTf)₃, Cu(OTf)₂, and Rh₂(OAc)₄ were tested. It is worth mentioning, that FeCl₃ and SbCl₅ showed the most violent nitrogen gas evolution among the tested metal salts.

Besides transition metal salts, a handful of lanthanoide salts were also tested since they might have been interesting, due to their high oxophilic properties and large ionic radii, which would make them suitable for coordinating the oxygen atoms of the constrained substrates **167** (Scheme 28).¹¹⁹ However, from the tested lanthanoide salts, only Gd(OTf)₃ catalyzed the decomposition of the diazo compound.

B. Main Part

H																	He
Li	Be											B	C	N	O	F	Ne
Na	Mg											Al	Si	P	S	Cl	Ar
K	Ca	Sc	Ti	V	Cr	Mn	Fe	Co	Ni	Cu	Zn	Ga	Ge	As	Se	Br	Kr
Rb	Sr	Y	Zr	Nb	Mo	Tc	Ru	Rh	Pd	Ag	Cd	In	Sn	Sb	Te	I	Xe
Cs	Ba	*	Hf	Ta	W	Re	Os	Ir	Pt	Au	Hg	Tl	Pb	Bi	Po	At	Rn
Fr	Ra	**	Rf	Db	Sg	Bh	Hs	Mt	Ds	Rg	Cn						

*	La	Ce	Pr	Nd	Pm	Sm	Eu	Gd	Tb	Dy	Ho	Er	Tm	Yb	Lu
**	Ac	Th	Pa	U	Np	Pu	Am	Cm	Bk	Cf	Es	Fm	Md	No	Lr

Figure 16: Periodic table of elements, salts of marked elements were employed for diazo compound decomposition screening.

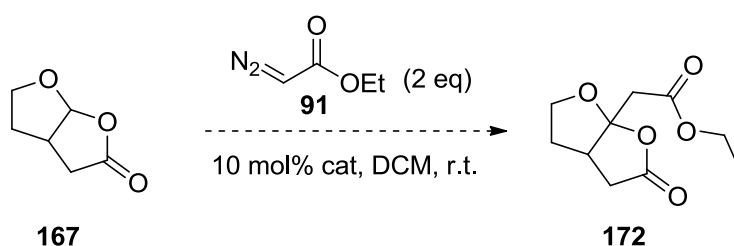
Table 7: Screened metal salts.

no N ₂ gas evolution observed		N ₂ gas evolution observed		
LiBF ₄	NaBF ₄	NaSbF ₆	MgBr ₂ ·OEt ₂	Sc(OTf) ₃
K ₂ PtCl ₄	CaCl ₂	Cp ₂ TiCl ₂	CrCl ₂	MnCl ₂
Ca(OiPr) ₂	CrCl ₃	FeCl ₃	(NH ₄) ₂ Fe(SO ₄) ₂	Fe(BF ₄) ₂
Fe(OAc) ₂	NH ₄ Fe(citrate) ₂	Fe(acac) ₃	Ni(acac) ₂	Cu(OTf) ₂
Co(OAc) ₂	NiCl ₂	CuI	Cu(MeCN) ₄ BF ₄	ZnBr ₂
NbCl ₅	(NH ₄) ₆ (Mo ₇ O ₂₄)	YCl ₃	RuCl ₃	Rh ₂ (OAc) ₄
Sb ₂ S ₃	LaCl ₃	PdBr ₂	AgClO ₄	SbCl ₅
CeCl ₃	Eu(NO ₃) ₃	TaCl ₅	IrCl ₃	Gd(OTf) ₃
EuCl ₃				

4.3 C-H insertion experiments

The first screening with the evaluated metal salts was performed by employing 10 mol% of catalyst and 2 equivalents of ethyl diazo glycine (**91**) in dichloromethane at ambient temperatures as a standard procedure for the furo-lactone substrate (Table 8). According to TLC control, in most cases no conversion of the starting material could be observed, only the dimerization of **91** to diethyl maleate and diethyl fumarate was found. The two very strong Lewis acids FeCl_3 and SbCl_5 showed lactone opening reactions, very rapidly in the latter case. The only catalyst, which was somewhat active, was $\text{Fe}(\text{BF}_4)_2 \cdot 6\text{H}_2\text{O}$. However, this reaction proceeded not in a clean way.

Table 8: First reaction screening.

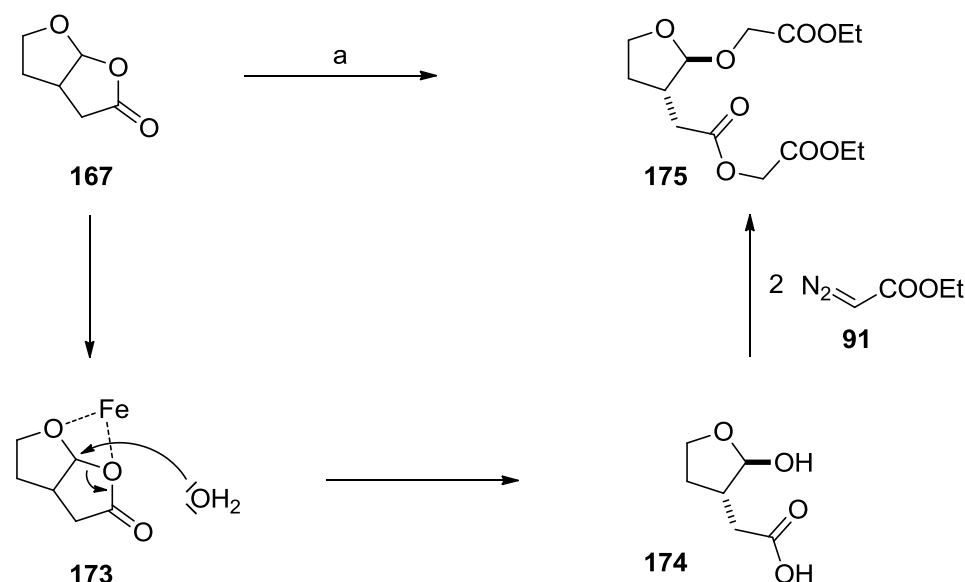


Entry	Catalyst	Observations ^[a]
1	FeCl_3	lactone opening
2	$\text{Fe}(\text{BF}_4)_2 \cdot 6\text{H}_2\text{O}$	slow conversion, complex mixture
3	$\text{Cu}(\text{OTf})_2$	no reaction
4	$\text{MgBr}_2 \cdot \text{OEt}_2$	no reaction
5	$\text{Sc}(\text{OTf})_3$	no reaction
6	ZnBr_2	no reaction
7	Cp_2TiCl_2	no reaction
8	PdBr_2	no reaction
9	TaCl_5	no reaction
10	AgOCl_4	no reaction
11	SbCl_5	rapid lactone opening
12	$\text{Rh}_2(\text{OAc})_4$ ^[b]	no reaction
13	$\text{Gd}(\text{OTf})_3$	no reaction

[a]: Plenty of dimerization products observed in all cases; [b]: 2 mol%.

To optimize this reaction, it was carried out at 0°C, which was envisaged to lead to the formation of less byproducts.

Scheme 34: Lewis acid catalyzed lactone opening of **167** in the presence of ethyl diazo glycine (**91**).

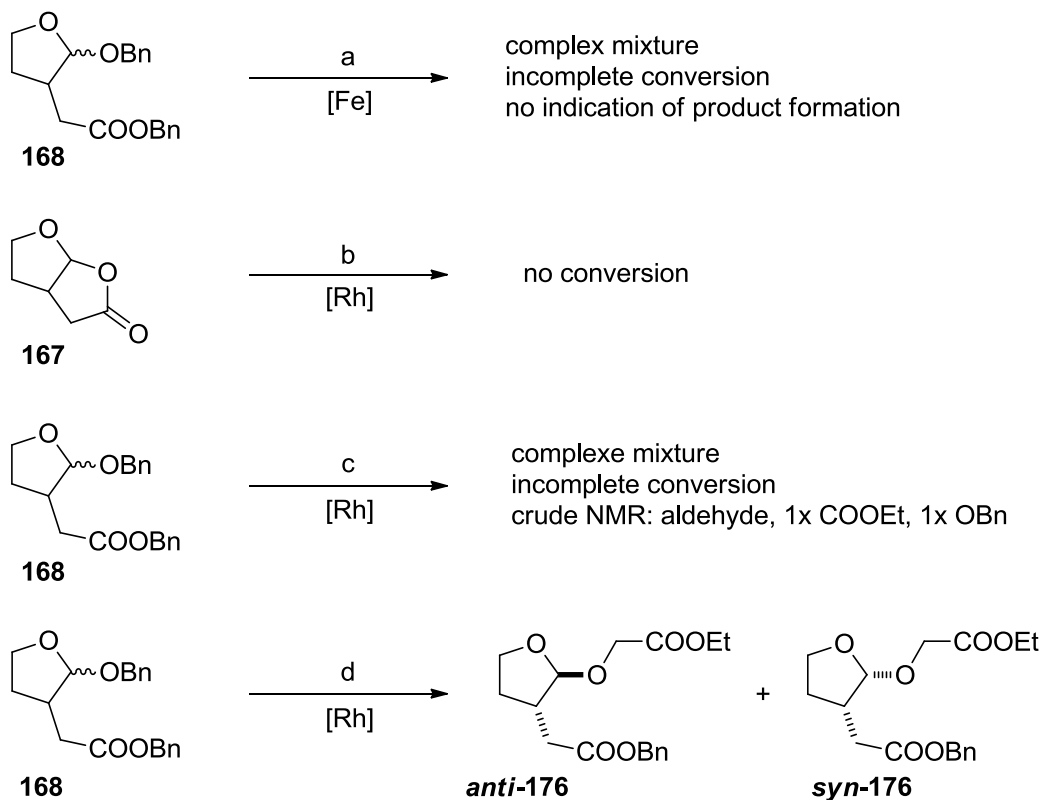


Reagents and Conditions: a) $\text{N}_2\text{CHCOOEt}$ (2 eq), $\text{Fe}(\text{BF}_4)_2 \cdot 6\text{H}_2\text{O}$ (10 mol%), DCM, r.t., 6 h, 32% (combined yield).

Although the reaction provided still many byproducts, two diastereomers of a lactone opening product could be isolated from the mixture (Scheme 34). The Lewis acidic iron(II) salt catalyzes the lactone opening by water, which is originating from the catalyst. The new hydroxyl group and the free carboxylic acid of **174** react with **91** to the corresponding esterified acetal **175**, which was formed as a 1:1 mixture of diastereomers, possessing the two substituents in *anti* conformation to each other. As the iron catalyst showed some activity it was also tested on the second model compound **168** (Scheme 35). This reaction was carried out at ambient temperatures and at 0 °C, but in both cases TLC control showed massive byproduct formation and an incomplete conversion of the starting material **168**. The ^{13}C -NMR of the crude reaction mixture showed no indication for the presence of desired product, which was expected to give a signal at about 110 ppm for the newly formed quaternary acetal carbon center. Besides the iron catalyst, dirhodium was also tested, since rhodium complexes are the most used catalysts for C-H insertion reactions (see chapter 4.1).

Therefore, rhodium(II) acetate dimer was employed in the following reactions (Scheme 35).

Scheme 35: Insertion test reaction.

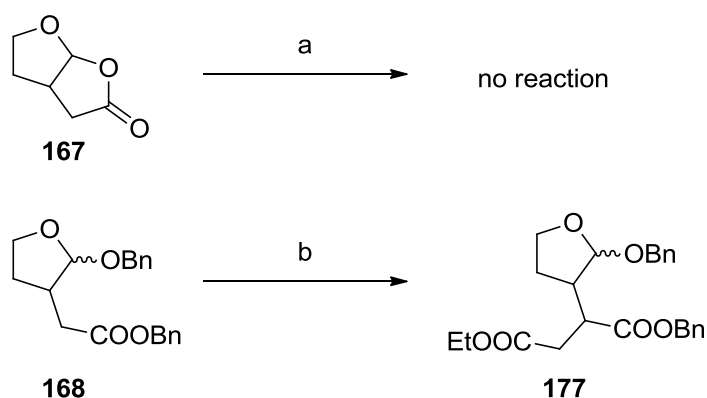


Reagents and conditions: a) $\text{N}_2\text{CHCOOEt}$ (2 eq), $\text{Fe}(\text{BF}_4)_2 \cdot 6\text{H}_2\text{O}$ (10 mol%), DCM, r.t. and 0°C , 6 h; b) $\text{N}_2\text{CHCOOEt}$ (2 eq), $\text{Rh}_2(\text{OAc})_4$ (2 mol%), DCM, r.t. 6 h; c) $\text{N}_2\text{CHCOOEt}$ (2 eq), $\text{Rh}_2(\text{OAc})_4$ (2 mol%), DCM, r.t., $^\circ\text{C}$, 6 h; d) $\text{N}_2\text{CHCOOEt}$ (2 eq), $\text{Rh}_2(\text{OAc})_4$ (2 mol%), DCM, 0°C , 6 h, **anti-176/syn-176** = 1:1, 38% (combined yield).

The expected conversion of furo-lactone **167** did not proceed at all, except for the dimerization of ethyl diazo glycine (**91**). Using acetal-substrate **168** at room temperature, many spots occurred on TLC, although the starting material was not converted completely. The analysis of the crude NMRs showed that the main compound possesses an aldehyde, one ethyl ester and one benzyl group, but it could not be isolated from the other compounds. The same reaction at 0°C gave less spots on TLC and a diastereomeric compound mixture could be isolated by column chromatography. It turned out, that the benzyl ether was cleaved within the reaction, followed by ether formation by the reaction with the diazo ester **91** yielding **176** as a 1:1 mixture of diastereomers.

The literature known reaction conditions were screened as well. The reactions, utilizing the homoscorpionate-copper(I) complex **164** (Table 6), were performed in degassed dichloromethane, due to the instability of **164** against oxygen.⁹⁵ The reaction with furo-lactone **167** afforded only the dimerization products of the diazo ester **91**, as mentioned before in the dirhodium catalyzed reaction. When using the acetal substrate **168** a new compound was furnished and separated from few other byproducts. It turned out, that also in this case no desired acetal-insertion occurred. The insertion took place on the α -position of the benzyl ester, which seems to be the most active site in this molecule. According to literature, the acetal-position of **168** and the acetal-like position of **167** should be privileged for C-H insertion reactions, as they are tertiary centers with comparable low C-H bond energy (97 kcal/mol, see chapter 4.1).¹⁰⁶ Additionally, they are in α -position to the oxygen atoms, electron withdrawing groups, which should activate these C-H bonds even more.¹⁰⁶ Nonetheless, the most active site bears **168** on the α -carbon of the benzyl ester, being the only site where an insertion reaction took place providing **177** as a diastereomeric mixture. In contrast, the α -position of the lactone moiety of **167** was absolutely inactive.

Scheme 36: Insertion attempts by employing homoscorpionate-copper(I) complex **164**.⁹⁵

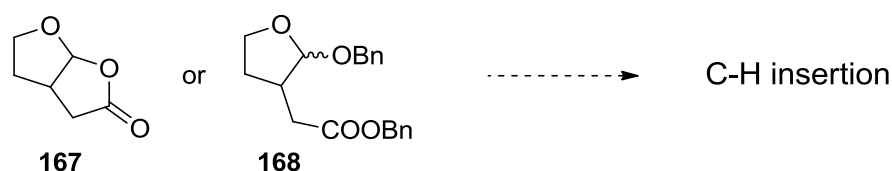


Reagents and conditions: a) $\text{N}_2\text{CHCOOEt}$ (2 eq), $[\text{TpBr}_3]\text{Cu-NCCH}_3$ (**164**) (5 mol%), DCM (degassed), r.t., 6 h; b) $\text{N}_2\text{CHCOOEt}$ (2 eq), $[\text{TpBr}_3]\text{Cu-NCCH}_3$ (**164**) (5 mol%), DCM (degassed) r.t., 6 h, 27%.

Finally, the C-H insertion conditions of Mayoral were applied to both test substrates. As in the original conditions THF was utilized as substrate and as solvent, the conditions needed to be adjusted for natural product synthesis. For this reason the

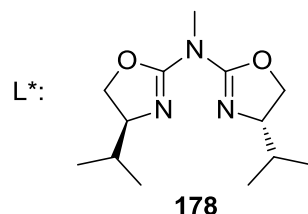
substrate was dissolved together with the catalyst in a small amount of dichloromethane, refluxed and dropwise treated with diazo ester **91**. As Mayoral *et al.* mentioned in their publication, even $\text{Cu}(\text{OTf})_2$ itself was catalytically active in this insertion reaction, therefore both, the $\text{Cu}(\text{OTf})_2$ alone and the corresponding aza-bis(oxazoline)-complex were tested (Table 9). All experiments provided exclusively the dimerization products of the diazo compound **91** but no conversion of the starting material could be observed. As this might have been a result of the maximal applicable reaction temperature, dichloromethane was exchanged by chloroform, exhibiting almost the same boiling point as THF (Table 9, entry 3 and 6). However, the higher temperature provided again no conversion of the starting material.

Table 9: C-H insertion screening applying $\text{Cu}(\text{OTf})_2$.¹¹⁰



Entry	Substrate	Reagents and conditions ^[a]	Observation ^[b]
1	167	$\text{Cu}(\text{OTf})_2$, DCM, reflux	no reaction
2	167	$\text{Cu}(\text{OTf})_2$, L*, DCM, reflux	no reaction
3	167	$\text{Cu}(\text{OTf})_2$, L*, CHCl_3 , reflux	no reaction
4	168	$\text{Cu}(\text{OTf})_2$, DCM, reflux	no reaction
5	168	$\text{Cu}(\text{OTf})_2$, L*, DCM, reflux	no reaction
6	168	$\text{Cu}(\text{OTf})_2$, L*, CHCl_3 , reflux	no reaction

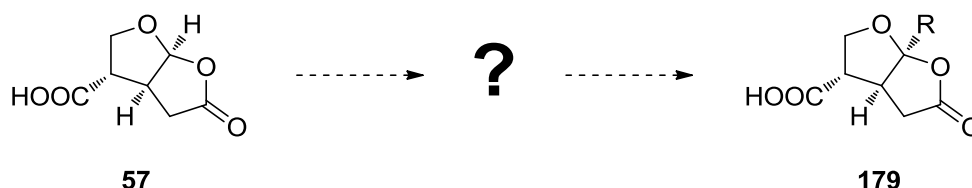
[a]: All reactions carried out with 4 mol% of $\text{Cu}(\text{OTf})_2$, 4.4 mol% of ligand L***178** (if mentioned), and 2 eq of $\text{N}_2\text{CHCOOEt}$; [b]: formation of diazo ester dimerization products in all reactions.



5. Side chain introduction by established chemistry

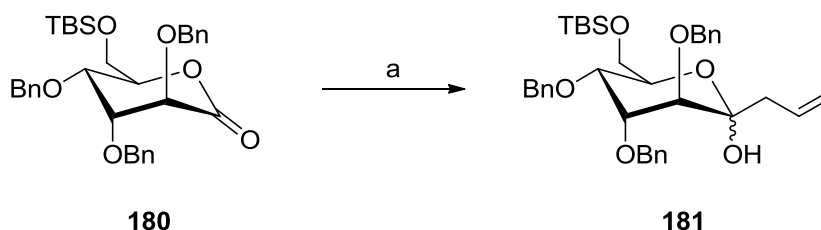
As the C-H activation turned out to give not the desired results for the side chain introduction, the attempts concerning this approach were ceased. The focus was put on the utilization of “traditional” chemistry for the transformation of furo-lactone **57** into an intermediate that gives rise to the acetal-functionalized skeleton **179** (Scheme 37).

Scheme 37: Functionalization via an intermediate.



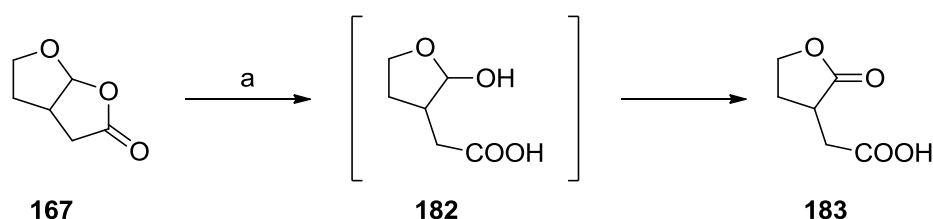
Matsuda *et al.* reported in 2008 within their synthesis of a partially benzylated derivative of the anhydro-D-*altro*-heptulose the functionalization of δ -lactone using Grignard-reagents attacking the lactone carbonyl center (Scheme 38).¹²⁰

Scheme 38: Conversion of a hydrocarbon lactone derivative with allyl-MgBr.



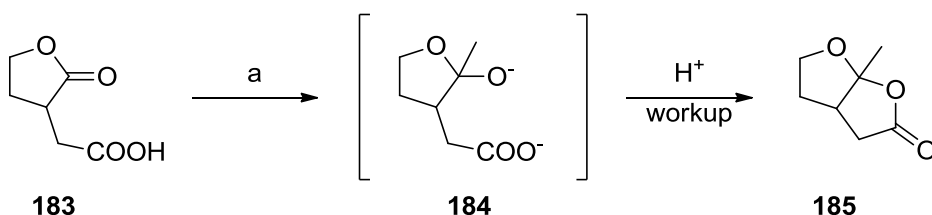
Reagents and conditions: a) allyl-MgBr (1.2 eq), THF, -78 °C, 1.5 h, 92%.

According to this consideration, an acidic lactone opening under oxidative conditions should force the formation of a α,β -substituted γ -lactone as synthon for **179**. To reach this intermediate, the model substrate **167**, already applied for the C-H insertion attempts, was treated with 2.5 M Jones-reagent in acetone (Scheme 39). The applied conditions opened the lactone moiety, setting free a hemiacetal which was further on oxidized to the corresponding lactone **183** by Cr(VI) oxide in excellent yield.

Scheme 39: Conversion of model substrate **167** to lactone **183** by Jones-reagent.

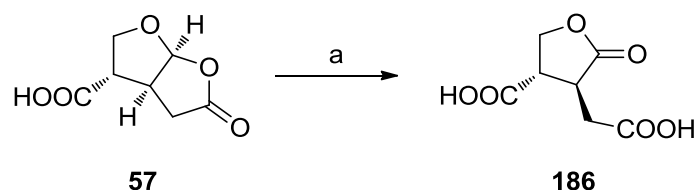
Reagents and conditions: a) Jones-reagent (3.5 eq), acetone, 0 °C to r.t., 3 h, 94%.

This α -substituted lactone **183** was subsequently treated with a Grignard-reagent that was envisaged to preferentially attack the lactone carbonyl in presence of the carboxylate. As the free carboxylic acid consumes one equivalent of the Grignard-reagent, at least two equivalents are needed to be employed for the planned conversion. Already the first test reactions provided the desired, functionalized furo-lactone **185**, using 2.5 equivalents of Me-MgBr at -78 °C (Scheme 40). It should be noted that the final product **185** was formed during the acidic quenching of the residual Grignard-reagent, by the addition of 2 M hydrochloric acid. Since the nucleophilic attack of Me-MgBr at the lactone carbonyl center delivers a hemiacetal as intermediate, the proton source is needed to enable the lactone closure.

Scheme 40: Side chain introduction by utilizing the methyl Grignard-reagent.

Reagents and conditions: a) Me-MgBr (2.5 eq), THF, -78 °C to 0 °C, 2 h, 19%.

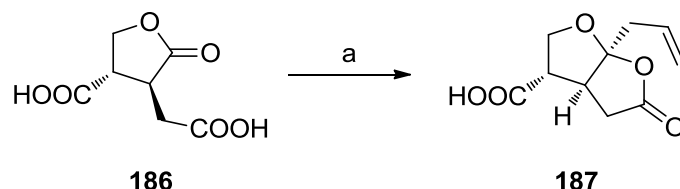
The isolated product showed the characteristic quaternary carbon peak at 117 ppm in the ¹³C-NMR. Although the yield was relatively low, this sequence was tested on the actual furo-lactone **57**. As described before, it was necessary to open the lactone moiety first under oxidative conditions, which was again accomplished by employing Jones-reagent to lactone **57**, deriving the desired α,β -substituted γ -lactone **186** in excellent yield.

Scheme 41: Oxidative lactone opening.

Reagents and conditions: a) Jones-reagent (2.5 eq), acetone, 0 °C to r.t., 6h, 88%.

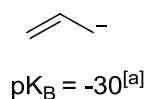
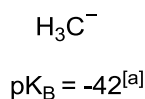
Having this precursor in hands, it was essential to find an appropriate Grignard-reagent that introduces a side chain being convertible to the final keto-group. For that reason allyl-MgBr was chosen to introduce the allyl side chain which should be oxidizable to the necessary methyl ketone moiety. First attempts were carried out by employing 3.2 equivalents of the reagent, since theoretically 2 equivalents are decomposed by the two free carboxylic acid functions, affording the allylated product **187** in 68% yield (Table 10). Further tests proved, that 2.5 equivalents are the optimal amount for this conversion giving an enhanced yield of 73% for **187**.

Table 10: Allyl side chain introduction and reaction optimization.



Reagents and conditions: a) allyl-MgBr, THF, -78 °C to 0 °C, 2 h.

Entry	Allyl-MgBr (eq)	Yield [%]
1	2	53
2	2.5	73
3	3.2	68

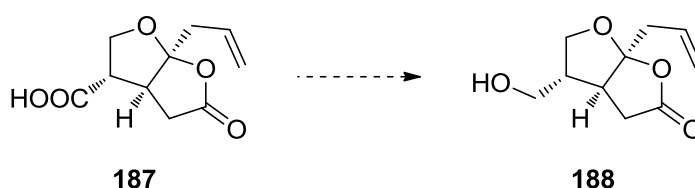


[a]: pK_B values calculated from corresponding pK_A values of methane and propene in DMSO; Ref ¹²¹

The increased yield of the allyl-Grignard reaction (Table 10) compared to the Me-MgBr one (Scheme 40) might be ascribed to the stronger basicity of the methyl-anion and therefore the resulting higher reactivity (Table 10, bottom). This fact is in compliance with the TLC monitoring of the reactions: the Me-MgBr reaction showed much more byproduct formation than the reaction using allyl-MgBr.

According to literature, there is no precedence of a furo-lactone functionalized on the acetal-like center. To the best of knowledge, this is a new methodology, using well-established chemistry for this kind of side chain introduction.

Table 11: Envisaged reduction by $\text{BH}_3 \cdot \text{THF}$.



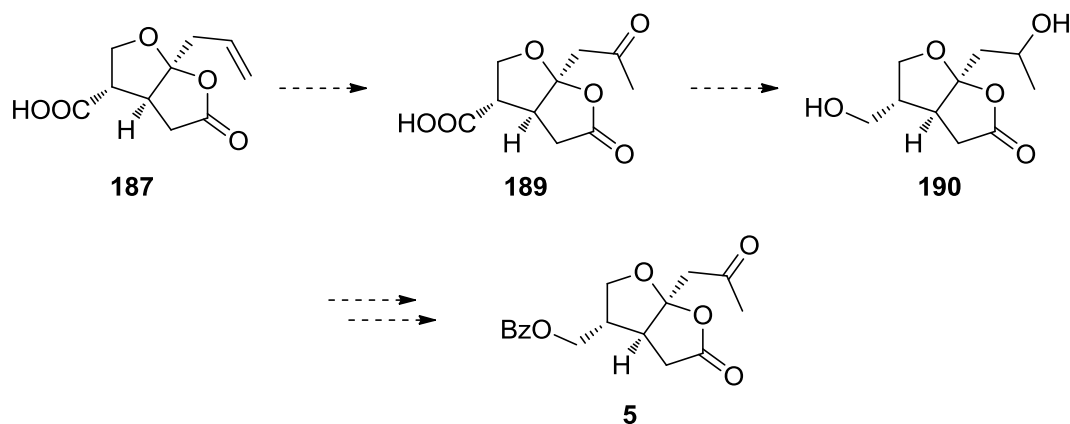
Entry	Reagents and conditions	Yield [%]
1 ^[a]	BH ₃ ·THF (1 eq), THF, -10°C to r.t., 6 h	traces
2	BH ₃ ·THF (1 eq), THF, -30°C to r.t., 8 h	traces
3 ^[b]	Zn(BH ₄) ₂ (1 eq), ClCOOEt (1 eq), NEt ₃ (1 eq) THF, 0 °C to r.t., 1 h	traces

57

A third method was the application of zinc borohydride to accomplish the reaction, which was prepared following a literature protocol.¹²⁴ This reagent was already successfully used for the reduction of a carboxylic acid in the presence of a lactone by Helmchen *et al.*, although the acid group was *in situ* converted to a mixed anhydride before $\text{Zn}(\text{BH}_4)_2$ was added.¹²³ Additionally, this borohydride reagent was used by Crimmins *et al.* for ketone reduction on a molecule bearing a terminal olefin, without harming the latter.¹²⁵ Although the reaction looked promising according to TLC monitoring, **188** proved to be unstable during workup.

Therefore, one additional reaction step was crucial in the sequence toward (-)-Paeonilide (**5**) (Scheme 42). The allyl chain was planned to be oxidized using Wacker-chemistry, followed by a reduction to the corresponding diol **190**. This compound allows two ways to the target molecule **5**: either selective oxidation of a secondary alcohol, followed by a benzyl protection, or selective protection of the primary alcohol followed by oxidation of the secondary alcohol.

Scheme 42: Final reaction sequence incorporating diol **190**.

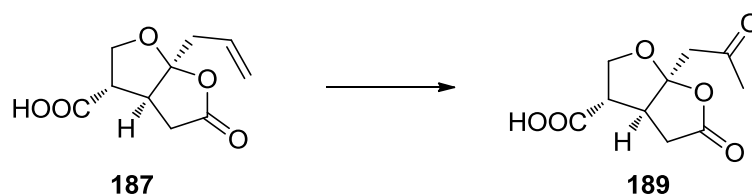


The conversion of the olefin was envisaged to be accomplished by the Wacker-oxidation to give rise to the keto-moiety (Table 12). This reaction is one of the best studied palladium promoted reactions and has important applications in industry¹²⁶⁻¹²⁸ as well as in academia.¹²⁹⁻¹³⁰

Common Wacker-oxidation protocols apply PdCl_2 or $\text{Pd}(\text{OAc})_2$ as catalyst together with a stoichiometric co-catalyst (e.g. CuCl), under one atmosphere of oxygen gas in a DMF/water- or DMA/water-mixture.

The first tests were carried out according to these conditions, following a procedure by Lowary *et al.*, who employed the Wacker-oxidation for the total synthesis of Buergerinin F and G (Table 12, entry 1).¹³¹ It turned out, that his protocol afforded only low conversion of the starting material **187**, although additional catalyst and co-catalyst were added after five hours. Raising the temperature did not give any advantage either. The isolated product showed impurities of the corresponding aldehyde, which was inseparable from the desired product by column chromatography. This lack of product selectivity was also described by Lowary *et al.* Additionally, the product mixture contained small amounts of DMA, exhibiting almost the same R_f value like **189**.

Table 12: Olefin oxidation.



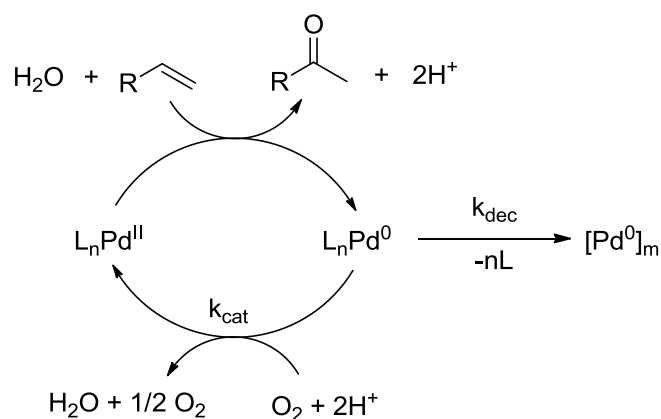
Entry	Reagents and conditions ^[a]	Yield [%]
1 ^[b]	PdCl ₂ (10 mol%), CuCl (1 eq) O ₂ , DMF/H ₂ O 3:1, r.t. to 70 °C, 10 h	19% ^{[c][d]}
2 ^[e]	PdCl ₂ (10 mol%), O ₂ , DMA/H ₂ O 15:1, 70 °C, 6 h	62% ^[d]
3 ^[f]	Jones-reagent (2.5 eq), Hg(OAc) ₂ (0.25 eq), acetone/H ₂ O 4:1, 0 °C to r.t., 15 h	79%

[a]: O₂ applied via balloon; [b]: Ref ¹³¹ [c]: mixture of ketone and aldehyde; [d]: containing inseparable solvent residues; [e]: Ref ¹³²; [f]: Ref ¹³³.

A second approach, following the procedure of Kaneda *et al.*, where the copper co-catalyst was abandoned, which is usually used to facilitate the re-oxidation of the Pd(0) by oxygen and to prevent the formation of palladium black.¹³² Kaneda *et al.* showed the beneficial effect of using DMA instead of DMF for this reaction, which provides the advantage of faster catalyst regeneration. Their proposed catalytic cycle (Scheme 43) illustrates the competition between the rate determining step of catalyst recycling (k_{cat}) and catalyst decomposition, which forms inactive Pd(0) metal (k_{dec}). It was demonstrated that k_{cat}/k_{dec} in DMA was almost 2.3 times higher than observed in DMF.

These data showed the ability of DMA to promote the re-oxidation of Pd(0) to the active catalyst and to suppress the competing Pd(0) aggregation.

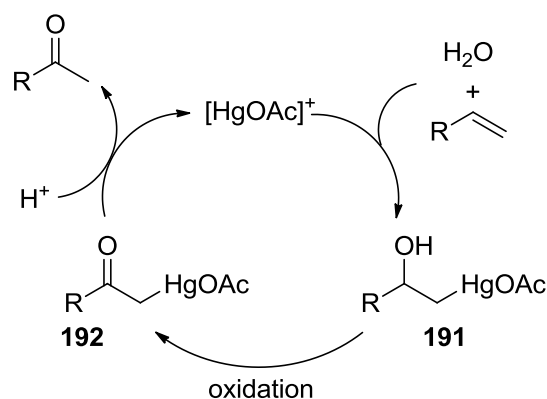
Scheme 43: Proposed catalytic cycle by Kaneda *et al.* (k_{cat} = rate of the re-oxidation, k_{dec} = rate of the decomposition).¹³²



The application of this protocol to substrate **189** afforded the desired product in significantly higher yield compared to the procedure before, delivering only the desired ketone **189** without formation of the corresponding aldehyde (Table 12, entry 2). However, the problem of inseparable DMA contamination in the isolated product after column chromatography arose once more.

Another method, also delivering the desired Wacker-product, utilizes a $\text{Hg}(\text{OAc})_2$ mediated oxymercuration combined with subsequent oxidation by Jones-reagent.¹³⁴ As Hg(II) resembles Pd(II) in its ability to activate a C-C double bond for nucleophilic attack, it is an interesting candidate for catalytic oxidation.¹³⁵

Scheme 44: Catalytic cycle of Hg(II).¹³⁴

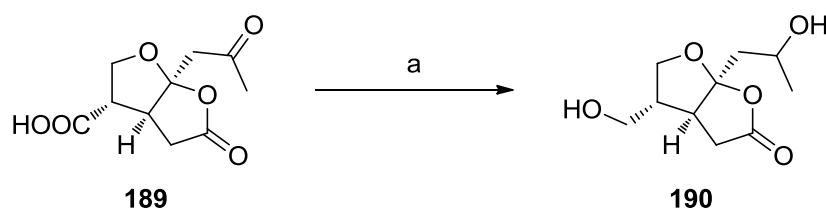


The reaction is driven in the direction of the thermodynamically less stable hydrated form **191**, by trapping this intermediate with the help of the oxidation to the corresponding ketone **192**.

The actual experiment, using **187** as starting material, was carried out following the procedure of Zou *et al.*, who used this methodology for the oxidation of an allyl group connected to carbohydrate derivatives.^{133, 136} Already the first tests showed a cleaner reaction compared to the Wacker-oxidations applied before (Table 12, entry 3). There was also no problem during the isolation of the product concerning solvent residues after column chromatography, as occurred when using DMF or DMA, respectively. In this way the desired ketone **189** was obtained in good yields.

Having ketone **189** in hands, both, the free carboxylic acid and the ketone needed to be reduced to the diol **190**, as a selective reduction of the COOH group in presence of the ketone moiety was not possible, due to the higher reactivity of the latter. The reduction was again achieved by using the $\text{BH}_3\cdot\text{THF}$ -complex at lower temperatures (Scheme 45).

Scheme 45: Reduction of ketone **189** to diol **190**.

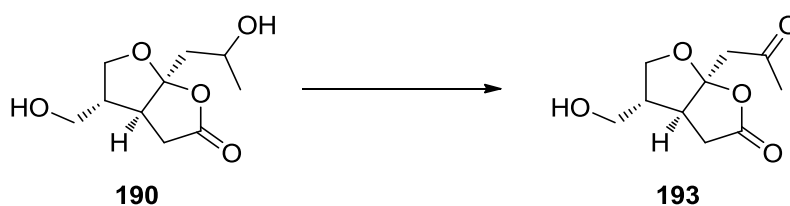


Reagents and conditions: a) $\text{BH}_3\cdot\text{THF}$ (2.1 eq), THF, $-15\text{ }^\circ\text{C}$ to r.t., 4 h, 16%.

Unfortunately, this diol **190** proved to be unstable against the purification procedures like the alcohol **188** mentioned before (Table 11), although the reaction itself proceeded smoothly to the desired product (according to TLC monitoring). Nevertheless, a small amount of **190** could be isolated in an impure manner, but was tried to be converted in a selective oxidation of the secondary OH group in presence of the primary OH. For this reason, several oxidation procedures were implemented (Table 13). First attempts employed cerium(IV) catalysis, applicable for selective oxidation of secondary alcohols in the presence of primary ones.¹³⁷ Either cerium(IV) sulfate (Table 13, entry 1) or cerium(IV) ammonium nitrate (CAN) (Table 13, entry 2) was used as catalyst and sodium bromate as co-catalyst.

This method was also applied by Meinwald *et al.*, who used cerium sulfate for the synthesis of (±)-Palasonin.¹³⁸ However, in the case of the diol **190** both reagents did not give success. While cerium sulfate showed only traces in the NMR of the crude mixture, CAN gave no conversion at all. Applying more equivalents of oxidation reagent and longer reaction times, afforded a mixture of highly polar components in both cases.

Table 13: Attempts for the selective oxidation of the secondary alcohol group.



Entry	Reagents and conditions	Yield [%]
1 ^{[a][b]}	Ce(SO ₄) ₂ ·H ₂ SO ₄ (10 mo%), NaBrO ₃ (1 eq), MeCN/H ₂ O 7:3, 80 °C, 3 h	traces
2 ^[a]	CAN (10 mol%), NaBrO ₃ (1 eq), MeCN/H ₂ O 7:3, 80 °C, 6 h	no reaction
3 ^[c]	NaOCl (1 eq), HOAc, 0 °C to r.t., 1.5 h	slow decomposition
4 ^[d]	NBS (1.5 eq), DME/H ₂ O 9:1, 0 °C to r.t., 1 h	complex mixture

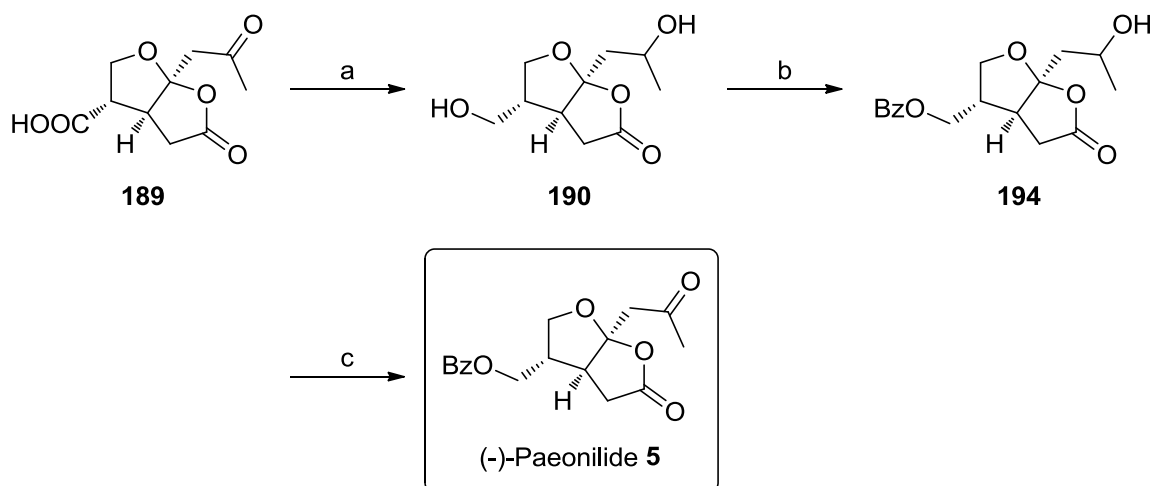
[a]: Ref ¹³⁷; [b]: Ref ¹³⁸; [c]: Ref ¹³⁹; [d]: Ref ¹⁴⁰.

The utilization of a sodium hypochlorite solution in acetic acid, a common mixture for selective oxidation of secondary alcohols, resulted in slow decomposition of the starting material **190** (Table 13, entry 3).^{139, 141} The last applied protocol was the use of *N*-bromosuccinimide in aqueous DME generating a complex mixture of compounds in short time (Table 13, entry 4).¹⁴⁰

As the approach of a selective oxidation of the secondary OH group of diol **190** did not deliver the desired results, a selective protection of the primary alcohol moiety of **190** as a benzoyl ester was planned, as this group is finally required in (-)-Paeonilide **5**. A subsequent oxidation of the remaining OH group would then give rise to the target monoterpenoid **5**. An advantage of this procedure is the possibility to use a bigger variety of oxidative agents, since the primary OH would already be converted to the final OBz group. To reach this goal, the following steps were carried

out in an one-pot manner, without purification of the intermediates by column chromatography, as the alcohol **188** and the diol **190** proved to give problems during their purification.

Scheme 46: The endgame.



Reagents and conditions: a) BH₃·THF (2.1 eq), THF, -15 °C to r.t., 4 h; b) BzCl (1.05 eq), NEt₃ (6 eq), DMAP (0.1 eq), DCM, -40 °C to -10 °C, 1.5 d; c) DMP (1 eq), DCM, 0 °C, 3 h, 44% over 3 steps, based on **189**.

The final steps started again with a simultaneous reduction of the ketone and the carboxylic acid of **189** by BH₃·THF-complex, which smoothly provided diol **190** (Scheme 46). After removing the solvent under reduced pressure, the crude mixture was dissolved in DCM and treated with a small excess of benzoyl chloride in the presence of an excess of triethylamine and catalytic amounts of DMAP. This procedure of selectively protecting a primary OH followed the protocol of Schlessinger *et al.*, who applied this methodology to the racemic synthesis of Senepoxide.¹⁴² These conditions afforded one new compound with negligible byproduct formation, according to TLC monitoring. In order to remove the amines, the crude mixture was washed with an ammonium chloride solution, to give rise to crude **194**, which was again dissolved in dichloromethane and finally treated with Dess-Martin periodinane for the oxidation of the secondary alcohol.¹⁴³ The oxidation reaction was purified by column chromatography and subsequent crystallization from methanol.¹¹ This reaction sequence gave rise to the target monoterpenoid (-)-Paeonilide **5** in an overall yield of 44% over the last 3 steps, based in **189** correlating with an average yield of 76% for each of the last 3 reactions.

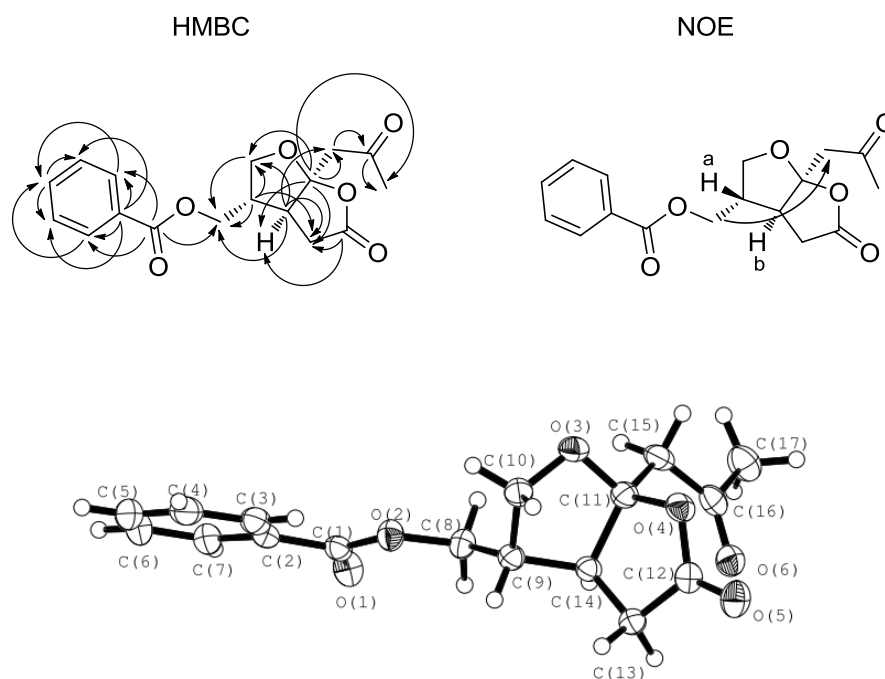
The complete synthesis, starting from commercially available 3-furoic acid (**59**) afforded (-)-Paeonilide (**5**) in a 12 step, straightforward synthesis with an overall yield of 4.4% (7.7% brsm).

In comparison to the so far published syntheses (see chapter A. Introduction), the most significant difference of this work is the way of introducing enantioselectivity. Starting from an achiral substrate and implementing the chiral information in a later step, instead of applying an already chiral starting material and maintaining its stereoinformation throughout the complete synthetic route. Another important distinction is the introduction of a new way for the construction of the bi-cyclic system to the Paeonilide-chemistry. This new strategy ceases ring formation, which applies a reaction sequence used in all of the so far published Paeonilide-syntheses. Last but not least, the installation of the keto-side chain is performed in a novel way, instead of using a starting material, which already contains the required functional groups.

7. Characterization and biological evaluation of (-)-Paeonilide

(-)-Paeonilide (**5**) was obtained as thin, colorless needles. The ^1H - and ^{13}C -NMR spectroscopic data are in accordance with the published data as well as the HMBC-correlations (Scheme 47, left). The assignment of the NOE signals were complicated by the overlap of the signals of the protons H^{a} and H^{b} by other proton signals. But there is an unambiguous NOE signal between the two side chains of the furo-lactone core skeleton (Scheme 47, right), which indicates the position of those two arms on the same side of the bi-cycle. Nevertheless, the absolute stereochemistry was confirmed by X-ray crystallography.

Scheme 47: Significant C-H correlations by HMBC (indicated by arrows, left); NOE signal (indicated by arrow, right); X-ray structure of (-)-Paeonilide (**5**).



The measured optical rotation of the obtained sample of (-)-Paeonilide (**5**) showed a $[\alpha]_{\text{D}}^{20}$ value of -42.0° (CHCl_3 , $c = 0.14$) which differs from the measured value of the originally isolated (+)-Paeonilide ($[\alpha]_{\text{D}}^{20} = +54.3^\circ$; CHCl_3 , $c = 0.44$), published by Liu *et al.*, concerning the absolute value.¹¹ This observation is in accordance with the fact, that the copper(I)-catalyzed asymmetric cyclopropanation delivered the cyclopropane **118** with an ee value of 83%. Furthermore, the enantiomeric excess could not be enriched during the synthesis, as (re)crystallization of the respective

compounds was either not possible or resulted in the same optical rotation values as before.

Attempts to measure the enantiomeric excess of one of the final compounds via chiral HPLC were not successful, since all applied columns and conditions did not provide a separation of the two enantiomers.

Anyway, if the *ee* value of the obtained (-)-Paeonilide (**5**) is calculated from the measured optical rotation, which is of course only a rule of thumb and not accurate for all chiral compounds,¹⁴⁴ one expects an *ee* of approximately 85%, which would be in accordance with the enantiomeric excess, achieved from the cyclopropanation.

So far, only the natural enantiomer (+)-Paeonilide (+)-(**5**) was applied for investigating the biological activities (see chapter A. Introduction). As (+)-**5** shows structural similarities to the ginkgolide family, it was tested against the PAF induced thrombocyte-aggregation and provided an IC_{50} value of 8 $\mu\text{g/mL}$ (25 μM). Having the enantiomerically enriched (-)-Paeonilide (**5**) in hands, it was submitted for biological assays in order to compare the behavior of both Paeonilide enantiomers (Table 14).

Table 14: Obtained data from rabbit-thrombocyte-aggregation assay (kindly measured by Schwabe GmbH & Co. KG, Karlsruhe, Germany).

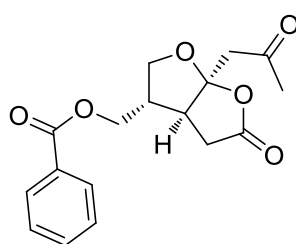
Entry	Concentration of 5 [$\mu\text{g/mL}$]	Inhibited aggregation [%]		Average value of inhibition [%]
		experiment 1	experiment 2	
1	1	5.9	8.6	7.3
2	3	-12.5	24.9	6.2
3	10	-10.4	20.2	4.9
4	30	26.8	13.2	20

The thrombocyte aggregation was inhibited by 20% at a concentration of 30 $\mu\text{g/mL}$ (94 μM) of **5**, hence (-)-Paeonilide (**5**) seems to be much less active than the eutomer (+)-**5** (IC_{50} = 8 $\mu\text{g/mL}$, 25 μM respectively). Presumably, the antagonism is caused by the impurity of the eutomer (+)-**5** in the investigated sample. These results imply that the unnatural distomer of Paeonilide is not active against the PAF receptor, at least not up to concentrations of 30 $\mu\text{g/mL}$.

C. Summary & Schematic Overview

1. Summary

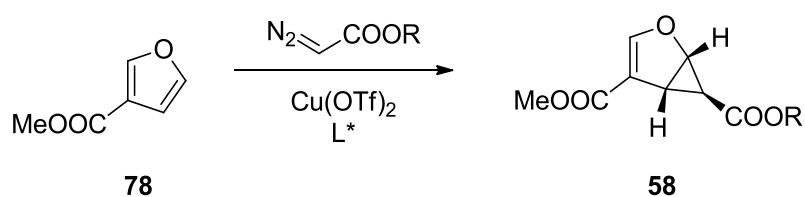
A plethora of new interesting compounds was discovered in the realm of plants. One of them was the monoterpene (+)-Paeonilide (+)-**(5)**, which was isolated, characterized and submitted to biological assays. The target of this thesis was the development of an enantioselective synthesis of the monoterpene (-)-Paeonilide **(5)** (Figure 17) based on commercially available 3-furoic acid (**59**). This goal was envisaged to be achieved by the application of an asymmetric copper(I)-catalyzed cyclopropanation introducing the stereochemical information into the achiral precursor.



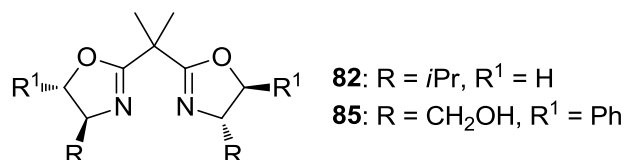
(-)-Paeonilide (**5**)

Figure 17: Structure of (-)-Paeonilide (**5**).

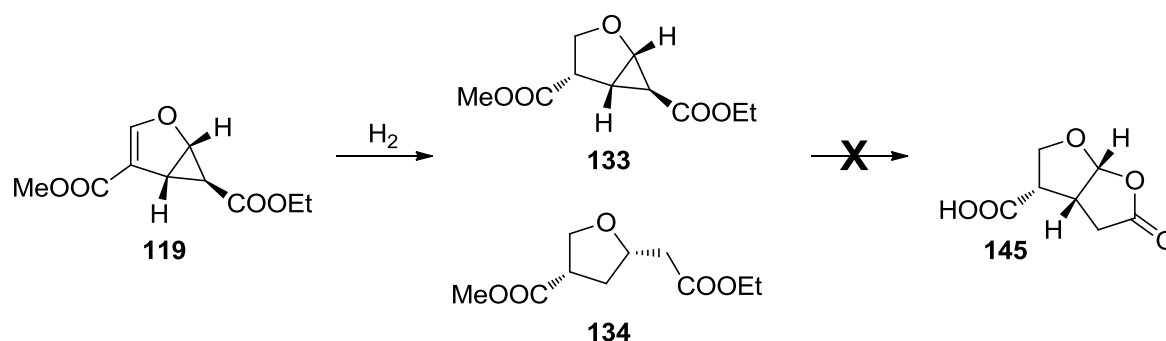
The cyclopropanation utilizing diazo glycine ethyl ester (**91**) and the corresponding *tert*-butyl ester **89** in the presence of different bis(oxazoline)-ligands **82** or **85** provided the cyclopropanated product **58**. It was possible to improve the achieved yields and *ee*-values within this screening, compared to literature precedents (Table 15).

Table 15: Ligand and diazo ester screening.

Entry	Diazo acetate R	Ligand L*	Yield [%]	Selectivity [%] ee
1 ^[a]	Et	85	27	74
2	<i>t</i> Bu	85	38	65
3	Et	82	31	83
4	<i>t</i> Bu	82	38	83

[a]: Ref. ⁴⁰.

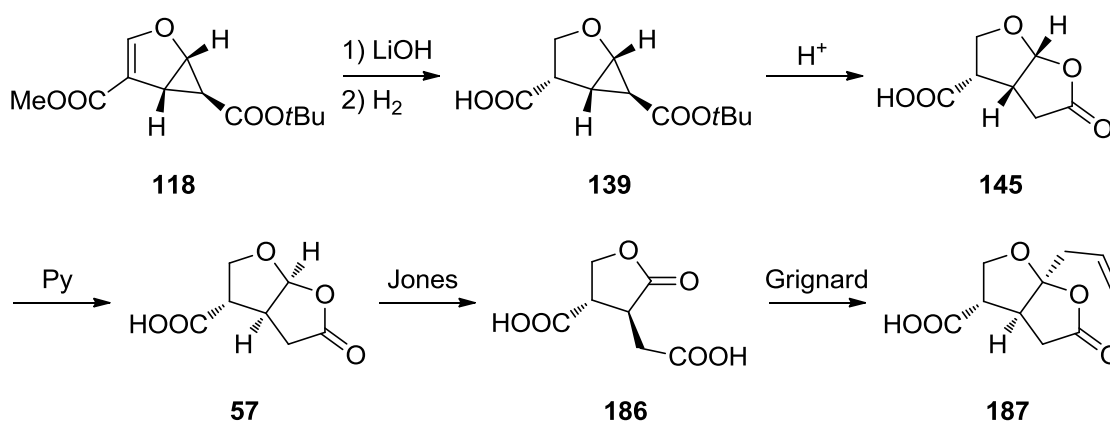
Using the ethyl substituted cyclopropane derivative **119**, the straightforward synthesis via C-C double bond hydrogenation and subsequent lactonization failed due to byproduct formation during the hydrogenation and inappropriate lactonization conditions (Scheme 48).

Scheme 48: Employment of the ethyl substituted cyclopropane **119**.

Changing the used diazo ester to the *t*Bu-substituted **89** provided a straightforward synthesis toward the lactone **145**, which could be converted into lactone **57**, applying a base (Scheme 49).

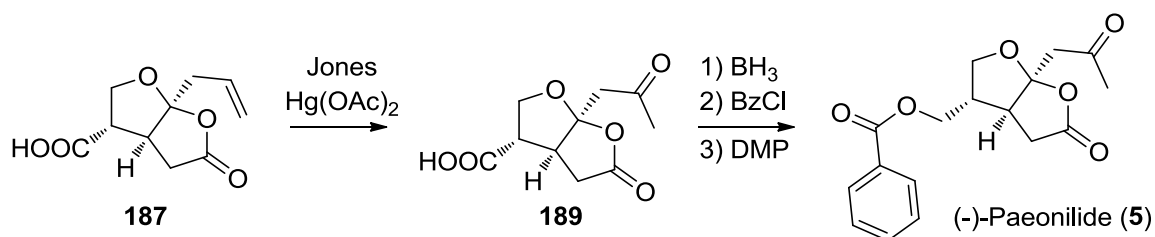
The further steps included an oxidative lactone opening giving rise to the disubstituted lactone **186**. A subsequent treatment with a Grignard-reagent afforded the allyl-substituted furo-lactone **187**. Having the substituted lactone **187** in hands, oxymercuration-oxidation chemistry provided the ketone **189**, which was converted in a three-step-one-pot manner to the final compound, since the intermediates proved to be unstable when purified (Scheme 50).

Scheme 49: Synthetic route employing *t*Bu-substituted cyclopropane **118**.



Ketone **189** was reduced to the corresponding diol, which was selectively protected on the primary hydroxyl group and finally the secondary alcohol was re-oxidized to the ketone, to yield the target monoterpenoid (-)-Paeonilide (**5**).

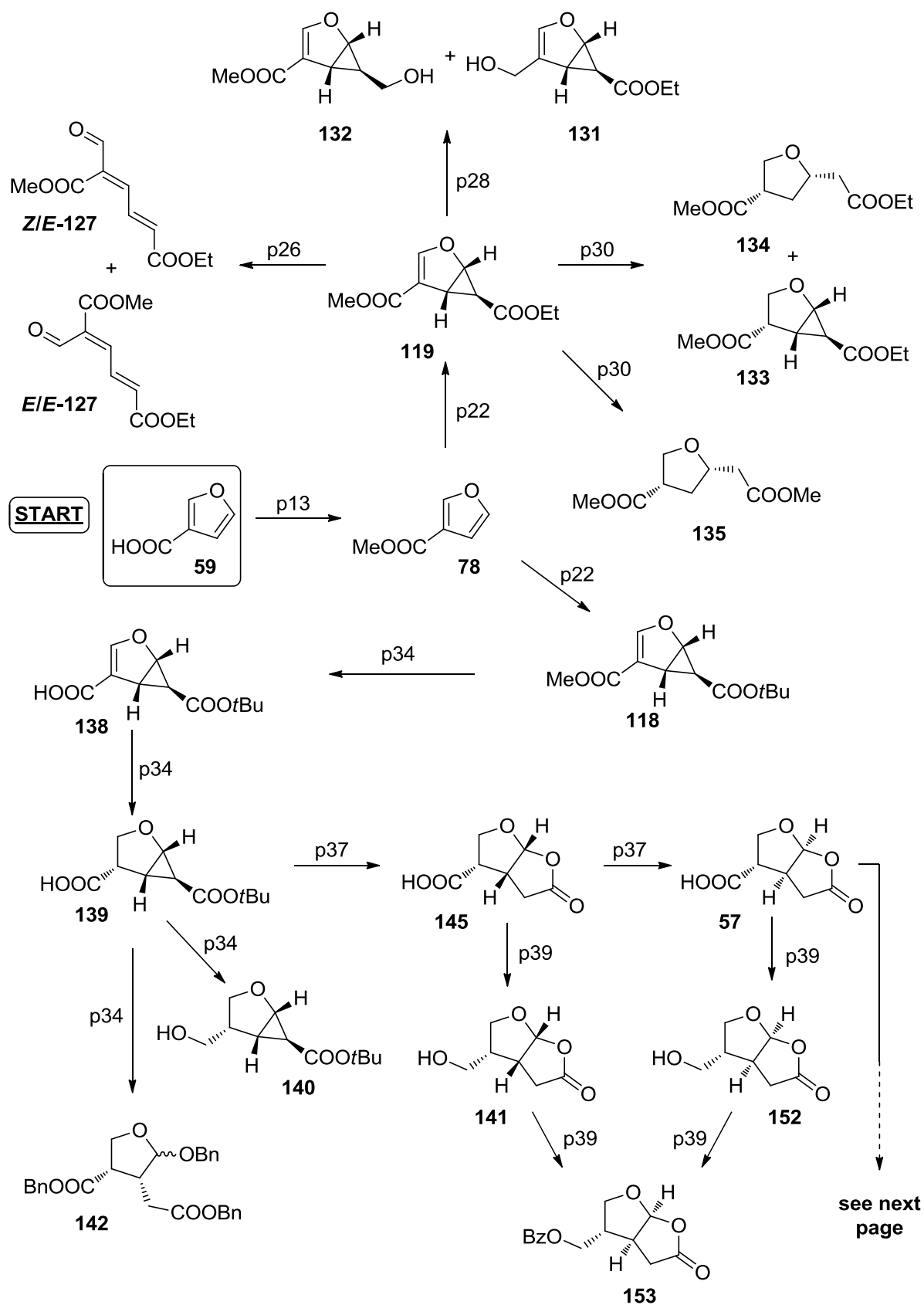
Scheme 50: Completion of the synthesis of (-)-Paeonilide (**5**).

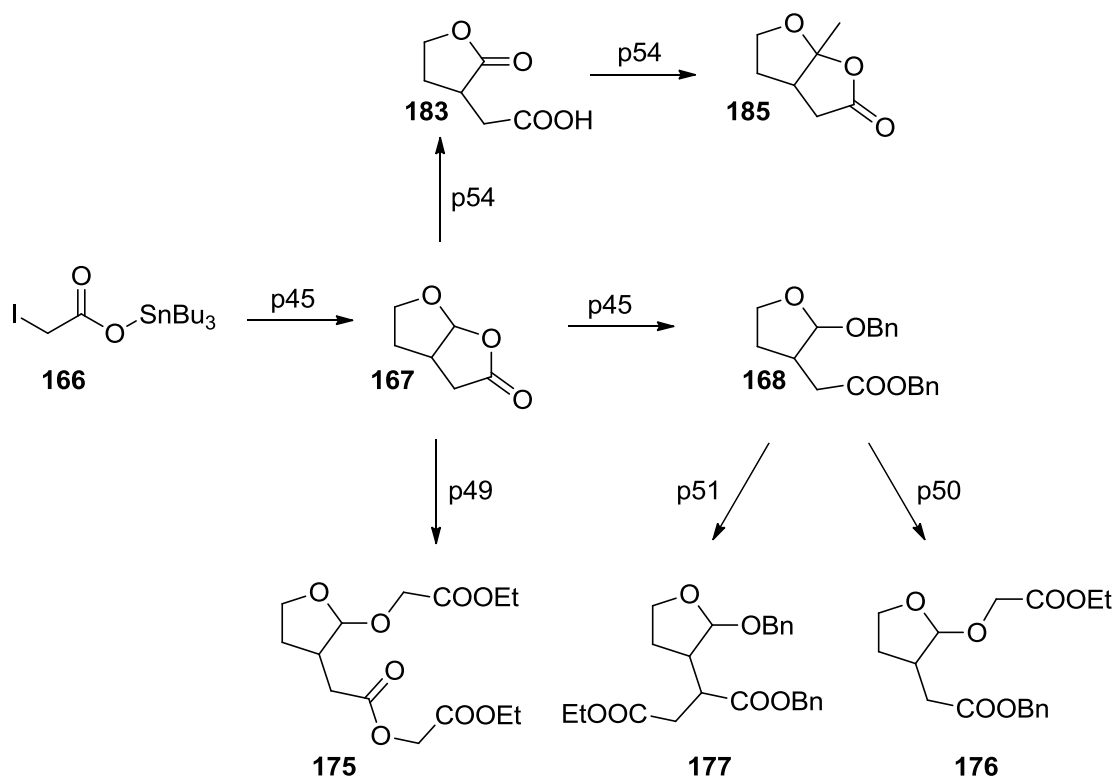
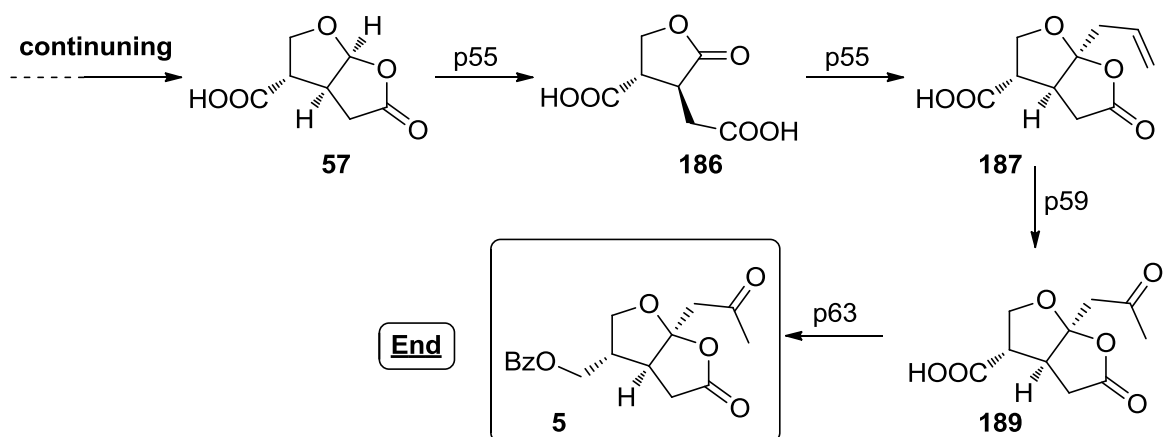


This synthetic route presents a straightforward access to the synthesis of the unnatural (-)-Paeonilide (**5**) within 12 steps and an overall yield of 4.4% (7.7% brsm). Although this synthesis did not provided absolutely enantiomerically pure (-)-Paeonilide (obtained $[\alpha]_{\text{D}}^{20}$ = of -42.0° (CHCl_3 , $c = 0.14$); literature value $[\alpha]_{\text{D}}^{20} = +54.3^\circ$ (CHCl_3 , $c = 0.44$)), it was submitted for biological assays in order to get an inkling of the activity of the unnatural enantiomer. The target compound **5**

showed activity against the thrombocyte aggregation although the inhibition was much less than found for the natural enantiomer (+)-**5**. Presumably, this small measured effect is caused by the impurity of the eutomeric (+)-**5** in the measured sample. These results imply that the unnatural distomer of Paeonilide is not active against the PAF receptor, at least not in the tested range of concentrations.

2. Schematic overview of synthesized compounds





D. Experimental

1. General comments

All reactions were carried out in oven dried glassware under atmospheric conditions unless otherwise stated. Commercially available chemicals were used as received, without any further purification.

The following solvents and reagents were purified prior to use:

Dichloromethane (CH_2Cl_2) was distilled from SICAPENT[®]. Ethanol (EtOH) and methanol (MeOH) were distilled from magnesium and stored over molecular sieves (3 Å). Tetrahydrofuran (THF) was distilled from sodium wire. Toluene was dried with CaH_2 , distilled and stored over sodium wire. Ethyl acetate (EA) and hexanes (PE) for chromatographic separations were distilled prior to use. Benzoyl chloride was distilled prior to use. Triethylamine and pyridine were distilled from KOH.

Analytical thin layer chromatography was performed on Merck TLC aluminium sheets silica gel 60 F 254. Visualization was accomplished with UV light (254 nm). For staining vaniline or permanganate solutions followed by heating were used. Liquid chromatography was performed using Merck flash silica gel 60 (0.040-0.063 mm).

¹H- and ¹³C-NMR:

NMR-spectra were recorded on FT-NMR-spectrometers of the type Bruker Avance 300 (300 MHz for ¹H, 75 MHz for ¹³C), Avance 400 (400 MHz for ¹H, 101 MHz for ¹³C) or Avance III 600 (600 MHz for ¹H, 151 MHz for ¹³C) at ambient temperature. Data are as follows: Chemical shift in ppm from internal CHCl_3 (7.26 ppm) as standard on the δ scale, multiplicity (s = singlet, bs = broad singlet, d = doublet, t = triplet, q = quartet, dd = doublet of doublet, ddd = doublet of doublet of doublet, dddd = doublet of doublet of doublet of doublet, dt = doublet of triplet, td = triplet of doublet, tt = triplet of triplet, tdd = triplet of doublet of doublet, tdt = triplet of doublet of triplet, ddt = doublet of doublet of triplet, dtd = doublet of triplet of doublet, dq = doublet of quartet, qd = quartet of doublet and m = multiplet), integration and coupling constant (Hz). ¹³C chemical shifts are reported in ppm from internal CHCl_3 (77 ppm) as standard on the δ scale. The ¹³C signals were assigned with the help of DEPT 90, DEPT 135 or HSQC techniques ((+) = CH or CH_3 , (-) = CH_2 , (C_q) = quaternary carbon).

X-ray analysis:

All X-ray measurements were performed by the crystallographic department of the University of Regensburg.

Melting points:

The melting points were measured on a Büchi SMP-20 apparatus in a silicon oil bath or on a SRS MPA 100 OptiMelt. Values thus obtained were not corrected.

Mass spectrometry:

Mass spectrometry was performed using Varian MAT 311A, Finnigan MAT 95, Thermoquest Finnigan TSQ 7000 or Agilent Technologies 6540 UHD Accurate-Mass Q-TOF LC/MS at the Central Analytical Laboratory (University of Regensburg). The percentage set in brackets gives the peak intensity related to the basic peak ($I = 100\%$). High resolution mass spectrometry (HRMS): The molecular formula was proven by the calculated precise mass.

Elemental analysis:

Elemental analysis was measured on a Vario EL III or Mikro-Rapid CHN (Heraeus) (micro analytic section of the University of Regensburg).

IR spectroscopy:

ATR-IR spectroscopy was carried out on a Biorad Excalibur FTS 3000 spectrometer, equipped with a Specac Golden Gate Diamond Single Reflection ATR-System.

Optical rotation:

The optical rotation was determined in a Perkin Elmer 241 polarimeter at 589 nm wavelength (sodium-d-line) in a 1.0 dm measuring cell of ca. 2 mL volume.

HPLC:

High performance liquid chromatography was carried out using Varian 920-LC with DAD.

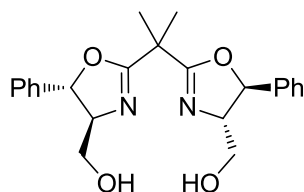
Phenomenex Lux Cellulose-2 or Chiralcel OD-H served as chiral stationary phase.

2. Synthesis of literature-known compounds and reagents

2,2-dimethylmalonyl dichloride (**79**),¹⁴⁵ (S)-2-amino-3-methylbutan-1-ol (**80**),¹⁴⁵
N1,N3-bis((S)-1-hydroxy-3-methylbutan-2-yl)-2,2-dimethylmalonamide (**81**),⁴⁵
(4S, 4'S)-2,2'-(propane-2,2-diyl)bis(4-isopropyl-4,5-dihydrooxazole) (**82**),⁴⁵ 2,2-
dimethyl-malononitrile (**83**),⁴⁶ ethyl 2-diazoacetate (**91**),⁵⁰ bis(trimethylsilyl) sulfate
(BTS, **128**),⁷⁹ 3,4,5-tribromo-1H-pyrazole (**170**),¹¹⁷ (S)-4-isopropyl-N-((S)-4-isopropyl-
4,5-dihydrooxazol-2-yl)-N-methyl-4,5-dihydrooxazol-2-amine (**178**),¹⁴⁶ Jones-
reagent,¹⁴⁷ $\text{Zn}(\text{BH}_4)_2$.¹²⁴

3. Syntheses

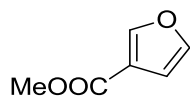
((4*S*,4'*S*,5*S*,5'*S*)-2,2'-(propane-2,2-diyl)bis(5-phenyl-4,5-dihydrooxazole-4,2-diyl))dimethanol (**85**)



Dinitrile **83** (791 mg, 8.41 mmol, 1 eq), (1*S*,2*S*)-2-amino-1-phenyl-1,3-propanediol (**84**) (3.52 g, 21.03 mmol, 2.5 eq) and Cd(OAc)₂·2H₂O (112 mg, 0.42 mmol, 5 mol%) were put together with 40 mL chlorobenzene. While refluxing it for 14 h it became a clear solution. The solvent was removed under reduced pressure and the remaining residue was dissolved in 20 mL DCM and washed with water (3 x 15 mL). The combined aqueous layers were washed with 20 mL DCM. The combined organic layers were dried over Na₂SO₄, filtered and concentrated under reduced pressure. The crude product was purified by silica column chromatography (DCM/MeOH = 95:5) to afford the product as yellow solid which was re-crystallized from EA to obtain the clean **85** as white crystals (1.29 g, 3.28 mmol, 39%).

R_f (EA/MeOH = 10:1) = 0.23. - $[\alpha]_D^{20} = -84.5$ (DCM, $c = 1$).

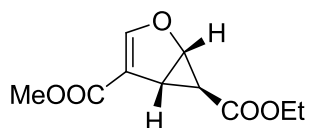
¹H NMR (300 MHz, CDCl₃): δ = 7.42 - 7.22 (m, 10H), 5.52 (d, $J = 6.3$ Hz, 2H), 4.32 (d, $J = 5.8$ Hz, 2H), 4.11 (dt, $J = 6.3, 3.1$ Hz, 2H), 3.93 (d, $J = 11.8$ Hz, 2H), 3.74 - 3.61 (m, 2H), 1.68 (s, 6H). - **¹³C NMR** (75 MHz, CDCl₃): δ = 171.1(C_q), 140.4(C_q), 128.8(+), 128.4(+), 125.6(+), 83.3(+), 75.7(+), 63.7(-), 39.7(C_q), 23.8(+). - **IR** (neat): $\tilde{\nu}$ = 3335, 3288, 2923, 2821, 1650, 1459, 1333, 1270, 1150, 1117, 1088, 972, 935, 762, 695, 635 cm⁻¹. - **mp**: 153 °C.

methyl furan-3-carboxylate (78)

Furan-3-carboxylic acid (25 g, 223.3 mmol) was dissolved in 120 mL MeOH. After cooling to 0 °C, 25 mL conc. H₂SO₄ were added dropwise. The reaction was stirred for 1 d at room temperature, 50 mL distilled water were added and transferred in a separation funnel. The mixture was extracted with 3 portions of 100 mL Et₂O. The combined organic layers were washed with a saturated NaHCO₃ solution, dried over Na₂SO₄ and concentrated under reduced pressure. The crude product was distilled at 15 mbar, 85 °C oil bath and 55 - 60 °C boiling point to yield the ester in 82% as colorless oil, which crystallized while storing at -18 °C.

R_f (PE/EA = 3:1): 0.69.

¹H NMR (300 MHz, CDCl₃): δ = 8.05 - 7.97 (m, 1H), 7.42 (t, *J* = 1.7 Hz, 1H), 6.78 - 6.70 (m, 1H), 3.84 (s, 3H). - **¹³C NMR** (75 MHz, CDCl₃): δ = 163.4 (C_q), 147.6(+), 143.7(+), 119.2(C_q), 109.7(+), 51.4(+). - **IR** (neat): $\tilde{\nu}$ = 3153, 3000, 2954, 1725, 1579, 1508, 1440, 1310, 1194, 1156, 1075, 984, 874, 793, 760, 601 cm⁻¹.

(1*S*,5*R*,6*S*)-6-ethyl 4-methyl 2-oxabicyclo[3.1.0]hex-3-ene-4,6-dicarboxylate (119)

A flame dried flask under nitrogen atmosphere was charged with 1 mL of dry DCM and $\text{Cu}(\text{OTf})_2$ (32 mg, 0.089 mmol, 0.56 mol%). To this suspension (*S,S*)-*i*Pr-bis(oxazoline)-ligand (**82**) (31.7 mg, 0.12 mmol, 0.75 mol%) was added, which caused the suspension to turn into a blue solution, which was stirred for 1 h. This solution was transferred using a syringe filter to another flame dried flask under nitrogen atmosphere, equipped with a mineral oil bubbler and containing **78** (2 g, 15.07 mmol) dissolved in 1 mL dry DCM at 0 °C. Phenylhydrazine (8.5 μL , 0.089 mmol, 0.56 mol%) was added dropwise turning the solution to a dark red-brown color. After 15 min the dropwise addition of ethyl diazo glycine (20.2 g solution of 11.6 wt%, 20.6 mmol, 1.3 eq) in DCM was started (one drop every 10 sec). During the addition of diazo-compound at 0 °C nitrogen was evolved. After completion of the reaction, the mixture was allowed to warm to room temperature and was filtered through a plug of basic alumina followed by 50 mL of DCM. The organic layers were concentrated under reduced pressure to afford a yellow-brown oil. The residue was purified by fractioned distillation under reduced pressure ($p = 15$ mbar, $\text{bp} = 55 - 66$ °C) in order to recover the starting material (607 mg, 4.8 mmol, 32%). The brown residue was purified by column chromatography (PE/EA = 10:1) to yield the desired product as a slightly yellow solid (990 mg, 4.67 mmol, 31%, brsm: 45%, 83% ee).

R_f (PE/EA = 3:1) = 0.47. - $[\alpha]_D^{20} = -21.8$ (DCM, $c = 1$).

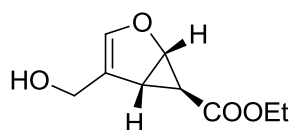
^1H NMR (300 MHz, CDCl_3): $\delta = 7.18$ (s, 1H), 4.99 (d, $J = 5.7$ Hz, 1H), 4.12 (q, $J = 7.1$ Hz, 2H), 3.73 (s, 3H), 3.06 (dd, $J = 5.6, 2.9$ Hz, 1H), 1.24 (t, $J = 7.1$ Hz, 3H), 1.11 (d, $J = 2.7$ Hz, 1H). - **^{13}C NMR** (75 MHz, CDCl_3): $\delta = 171.5(\text{C}_q)$, 164.0(C_q), 156.4(+), 115.7(C_q), 68.9(+), 61.0(-), 51.5(+), 29.5(+), 21.5(+), 14.1(+). - **IR** (neat): $\tilde{\nu} = 3104, 2984, 2956, 2912, 1708, 1602, 1440, 1375, 1320, 1263, 1171, 1096, 1030, 1008, 961, 933, 896, 834, 791, 764, 729$ cm^{-1} . - **MS** (EI-MS, 70 eV): m/z (%) = 212 (M^+ , 10), 139 (100), 108 (15), 107 (24), 95 (12), 79 (13), 52 (10), 51 (17). - **HRMS** (EI-MS, m/z): 212.0684 ($\text{C}_{10}\text{H}_{19}\text{O}_5$, calc. 212.0685 [M^+]). - **HPLC analysis** (Chiralcel OD-H, *n*-heptane/*i*PrOH 95:5, 1.0 mL/min, 254 nm): $t_r = 6.07$, $t_r = 7.26$; 83% ee.

(2Z,4E)-6-ethyl 1-methyl 2-formylhexa-2,4-dienedioate (Z/E-127) and (2E,4E)-6-ethyl 1-methyl 2-formylhexa-2,4-dienedioate (E/E-127)

In a flame dried flask under nitrogen atmosphere **119** (300 mg, 1.41 mmol) was dissolved in 5 mL of dry DCM and 10 pieces of 3 Å molecular sieves were added. The solution was cooled to 0 °C and BTS (**128**) (686 mg, 2.82 mmol, 2 eq) dissolved in 2 mL of dry DCM was added dropwise. The reaction was allowed to warm to room temperature and stirred for 14 h. The mixture was transferred to a separation funnel and diluted with 20 mL of DCM and washed with a saturated NaHCO₃ solution (2 x 5 mL). The organic layer was dried over Na₂SO₄, filtered and concentrated under reduced pressure. The crude product was purified by silica column chromatograph (PE/EA = 10:1) to afford a 1.7:1 (**Z/E-127** / **E/E-127**) mixture of isomers (260 mg, 1.22 mmol, 87%).

R_f (PE/EA = 3:1) = 0.43.

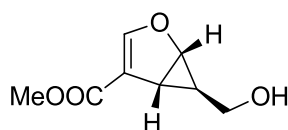
¹H NMR (600 MHz, CDCl₃): δ = 10.12 (d, *J* = 2.7 Hz, 1H, minor), 9.84 (s, 1.7H, major), 8.25 (dd, *J* = 15.5, 12.0 Hz, 1H, minor), 8.00 (dd, *J* = 15.4, 12.0 Hz, 1.7H, major), 7.51 (ddd, *J* = 12.0, 2.7, 0.8 Hz, 1H, minor), 7.37 (dd, *J* = 12.0, 0.7 Hz, 1.7H, major), 6.42 (dd, *J* = 15.4, 0.8 Hz, 1.7H, major), 6.38 (dd, *J* = 15.5, 0.8 Hz, 1H, minor), 4.21 (dq, *J* = 2.8, 7.1 Hz, 5.4H, major+minor), 3.89 (s, 5.1H, major), 3.85 (s, 3H, minor), 1.27 (dt, *J* = 1.1, 7.1 Hz, 8.1H, major+minor). - **¹³C NMR** (151 MHz, CDCl₃): δ = 190.1(C_q, minor), 188.9(C_q, major), 165.3(C_q, minor), 165.0(C_q, minor), 165.0(C_q, major), 164.2(C_q, major), 145.9(+, minor), 145.4(+, major), 137.0(+, major), 136.8(+, minor), 136.0(+, minor), 135.2(+, major), 132.7(C_q, major), 129.7(C_q, minor), 61.1(-, major), 61.1(-, minor), 52.4(+, minor), 52.3(+, major), 14.0(+). - **IR** (neat): $\tilde{\nu}$ = 3411, 2982, 1711, 1583, 1438, 1369, 1303, 1267, 1235, 1196, 1148, 1103, 1029, 984, 858, 734 cm⁻¹. - **MS** (CI-MS, NH₃): *m/z* (%) = 230 (MNH⁴⁺, 100), 213 (MH⁺, 10). - **HRMS** (EI-MS, *m/z*): 212.0684 (C₁₀H₁₂O₅, calc. 212.0685 [M⁺]).

(1*S*,5*R*,6*S*)-ethyl 4-(hydroxymethyl)-2-oxabicyclo[3.1.0]hex-3-ene-6-carboxylate (131)

In a flame dried flask under an atmosphere of nitrogen **119** (300 mg, 1.45 mmol, 1 eq) was dissolved in dry THF (5.7 mL) and cooled to 0 °C. LiAlH₄ (32 mg, 0.85 mmol, 0.6 eq) was added carefully, which caused hydrogen evolution. After 1 h the reaction was quenched by the addition on 1 mL water, transferred to a separation funnel and 5 mL Et₂O were added. It was washed with a saturated Rochelle salt solution (3 x 2 mL). The organic layer was dried over Na₂SO₄, filtered and concentrated under reduced pressure. The purification by silica column chromatography (PE/EA = 1:1) afforded alcohol **131** as colorless solid (90 mg, 0.49 mmol 34%)

R_f (PE/EA = 1:1) = 0.39. - $[\alpha]_D^{20} = -59.1$ (DCM, c = 1).

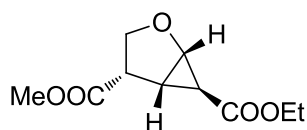
¹H NMR (300 MHz, CDCl₃): δ = 6.37 (s, 3H), 4.87 (dt, *J* = 5.5, 0.8 Hz, 3H), 4.30 (s, 6H), 4.13 (q, *J* = 7.1 Hz, 7H), 2.84 (dd, *J* = 5.6, 2.7 Hz, 3H), 1.63 (s, 2H), 1.26 (t, *J* = 7.1 Hz, 11H), 1.08 (d, *J* = 2.6 Hz, 3H). - **¹³C NMR** (75 MHz, CDCl₃): δ = 172.6(C_q), 143.8(+), 121.2(C_q), 67.6(+), 60.8(-), 57.3(-), 32.0(+), 22.0(+), 14.2(+). - **IR** (neat): $\tilde{\nu}$ = 3412, 2952, 2879, 1703, 1600, 1442, 1378, 1312, 1173, 1105, 1034, 976, 784, 760, 722 cm⁻¹. - **MS** (EI-MS, 70 eV): *m/z* (%) = 184 (M⁺, 17), 166 (15), 127 (11), 111 (100), 81 (14), 55 (12), 53 (13), 39 (12). - **HRMS** (PI-EIMS, *m/z*): 184.0738 (C₉H₁₂O₄, calc. 184.0736 [M⁺]). - **mp**: 66 °C.

(1*S*,5*R*,6*R*)-methyl 6-(hydroxymethyl)-2-oxabicyclo[3.1.0]hex-3-ene-4-carboxylate (132)

In a flame dried flask under nitrogen atmosphere, **119** (300 mg, 1.45 mmol, 1 eq) was dissolved in dry THF (5.7 mL) and cooled to 0 °C. LiAlH₄ (32 mg, 0.85 mmol, 0.6 eq) was added carefully, which caused hydrogen evolution. After 1 h the reaction was quenched by the addition on 1 mL water, transferred to a separation funnel and 5 mL Et₂O were added. It was washed with a saturated Rochelle salt solution (3 x 2 mL). The organic layer was dried over Na₂SO₄, filtered and concentrated under reduced pressure. The purification by silica column chromatography (PE/EA = 1:1) afforded alcohol **132** as colorless oil (79 mg, 0.46 mmol, 32%)

R_f (PE/EA = 1:1) = 0.27. - $[\alpha]_D^{20} = +15.2$ (DCM, c = 1).

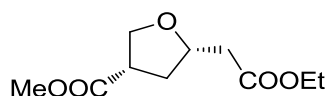
¹H NMR (300 MHz, CDCl₃): δ = 7.11 (s, 1H), 4.62 (d, *J* = 6.8 Hz, 1H), 3.73 (s, 3H), 3.53 (dd, *J* = 7.1, 1.6 Hz, 2H), 2.56 (s, 1H), 2.44 (dd, *J* = 5.9, 3.1 Hz, 1H), 0.75 (tdd, *J* = 7.1, 3.1, 1.0 Hz, 1H). - **¹³C NMR** (75 MHz, CDCl₃): δ = 165.2(C_q), 155.9(+), 115.6(C_q), 66.7(+), 61.6(-), 51.4(+), 23.7(+), 22.0(+). - **IR** (neat): $\tilde{\nu}$ = 3401, 3106, 3003, 2952, 2883, 1688, 1599, 1441, 1377, 1313, 1172, 1100, 1031, 974, 783, 760, 724 cm⁻¹. - **MS** (EI-MS, 70 eV): *m/z* (%) = 169 (M⁺-H, 1), 152 ((M-H₂O)⁺, 2), 139 ((M⁺-CH₂OH)⁺, 100), 53 (12). - **HRMS** (PI-EIMS, *m/z*): 170.0577 (C₈H₁₀O₄, calc. 170.0579 [M⁺]).

(1S,4S,5S,6S)-6-ethyl 4-methyl 2-oxabicyclo[3.1.0]hexane-4,6-dicarboxylate (133)

119 (200 mg, 0.94 mmol, 1 eq) was dissolved in 4 mL of a EtOH/water mixture (95:5) and 20 g Pd/C (10%) were added. The reaction mixture was stirred at room temperature for 24 h under an atmosphere of hydrogen applied via a balloon. After filtration the solution was concentrated under reduced pressure. The purification by silica column chromatography (PE/EA = 5:1) afforded the product as colorless crystals (50 mg, 0.24 mmol, 25%).

R_f (PE/EA = 3:1) = 0.52. - $[\alpha]_D^{20} = +58.3$ (DCM, $c = 0.6$).

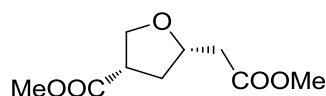
^1H NMR (300 MHz, CDCl_3): $\delta = 4.24$ (dd, $J = 5.4, 1.2$ Hz, 1H), 4.20 - 4.05 (m, 3H), 3.75 (s, 3H), 3.73 (dd, $J = 21.3, 11.4$ Hz, 1H), 3.40 (td, $J = 9.5, 5.3$ Hz, 1H), 2.42 (td, $J = 5.3, 3.8$ Hz, 1H), 2.27 (dd, $J = 3.8, 0.9$ Hz, 1H), 1.24 (t, $J = 7.1$ Hz, 3H). - **^{13}C NMR** (75 MHz, CDCl_3): $\delta = 171.8(\text{C}_q)$, 170.6(C_q), 67.9(-), 65.8(+), 60.7(-), 52.3(+), 44.2(+), 27.9(+), 21.7(+), 14.1(+). - **IR** (neat): $\tilde{\nu} = 3063, 3002, 2170, 1732, 1707, 1440, 1407, 1381, 1312, 1261, 1207, 1180, 1119, 1078, 1029, 988, 922, 865, 780, 694\text{ cm}^{-1}$. - **MS** (EI-MS, 70 eV): m/z (%) = 214 (M^+ , 1), 182 (23), 169 (18), 168 (70), 155 (11), 154 (32), 141 (67), 140 (34), 126 (16), 125 (15), 111 (24), 109 (37), 10 (32), 100 (21), 99 (43), 97 (17), 82 (29), 81 (100), 69 (28), 59 (37), 55 (75), 53 (58), 45 (68). - **HRMS** (PI-EIMS, m/z): 214.0835 ($\text{C}_{10}\text{H}_{14}\text{O}_5$, calc. 214.0841 [M^+]); - **mp**: 68 °C.

(3S,5S)-methyl 5-(2-ethoxy-2-oxoethyl)tetrahydrofuran-3-carboxylate (134)

119 (250 mg, 1.18 mmol, 1 eq) was dissolved in 5 mL of a EtOH/water mixture (95:5) and 25 mg Pd/C (10%) were added. The mixture was stirred for 72 h at room temperature under an atmosphere of hydrogen applied via a balloon. After filtration and the solution was concentrated under reduced pressure and purified by silica column chromatography (PE/EA = 5:1) to afford the product as colorless oil (255 mg, 1.18 mmol, quant.).

R_f (PE/EA = 3:1) = 0.31. - $[\alpha]_D^{20}$ = -10.4 (CHCl₃, c = 1).

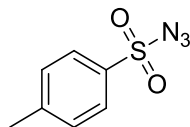
¹H NMR (600 MHz, CDCl₃): δ = 4.26 (dq, J = 8.4, 6.3 Hz, 3H), 4.13 (q, J = 7.1 Hz, 7H), 4.04 (dd, J = 8.9, 6.0 Hz, 3H), 3.92 (t, J = 8.5 Hz, 3H), 3.68 (s, 10H), 3.13 (qd, J = 8.2, 6.0 Hz, 3H), 2.67 (dd, J = 15.7, 7.2 Hz, 3H), 2.53 (dd, J = 15.7, 6.0 Hz, 3H), 2.36 (ddd, J = 12.7, 8.8, 6.3 Hz, 3H), 1.89 (dt, J = 12.7, 8.2 Hz, 3H), 1.24 (t, J = 7.2 Hz, 11H). - **¹³C NMR** (151 MHz, CDCl₃): δ = 173.8(C_q), 170.9(C_q), 75.9(+), 69.8(-), 60.5(-), 52.0(+), 44.0(+), 40.0(-), 34.8(-), 14.1(+). - **IR** (neat): $\tilde{\nu}$ = 2983, 1729, 1438, 1370, 1155, 1064, 1201, 936, 850, 673 cm⁻¹. - **MS** (CI-MS, NH₃): m/z (%) = 235 (21), 234 (MNH₄⁺, 100), 217 (MH⁺, 35). - **HRMS** (ESI, m/z): 217.1069 (C₁₀H₁₇O₅, calc. 217.1071 [MH⁺]).

(3S,5S)-methyl 5-(2-methoxy-2-oxoethyl)tetrahydrofuran-3-carboxylate (135)

In a flame dried flask under nitrogen atmosphere **119** (50 mg, 0.236 mmol) was dissolved in 2.5 mL MeOH. The flask was cooled to 0 °C and Mg turnings (5.7 mg, 0.236 mmol, 1 eq) were added. When the reaction started hydrogen was evolved (mineral oil bubbler) and white precipitate occurred. After 30 min the precipitate and the remaining Mg were filtered off. The solution was concentrated under reduced pressure. The crude mixture was purified by silica column chromatography (PE/EA = 3:1) to afford the product as 1:1 mixture of diastereomers (18 mg, 0.089 mmol, 38%).

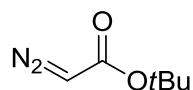
R_f (PE/EA = 3:1) = 0.39. - $[\alpha]_D^{20} = +17.6$ (DCM, $c = 1$).

^1H NMR (600 MHz, CDCl_3): $\delta = 4.40 - 4.34$ (m, 1H, diast. 1), 4.29 (tt, $J = 7.2, 6.2$ Hz, 1H, diast. 2), 4.16 - 4.11 (m, 1H, diast. 1), 4.07 (dd, $J = 8.9, 6.0$ Hz, 1H, diast. 2), 3.94 (t, $J = 8.5$ Hz, 1H, diast. 2), 3.87 (dd, $J = 8.9, 6.7$ Hz, 1H, diast. 1), 3.70 (s, 6H), 3.69 (s, 6H), 3.19 - 3.11 (m, 2H), 2.70 (dd, $J = 15.7, 7.4$ Hz, 1H, diast. 2), 2.61 (dd, $J = 15.3, 7.3$ Hz, 1H, diast. 1), 2.57 (dd, $J = 15.7, 5.8$ Hz, 1H, diast. 2), 2.52 (dd, $J = 15.3, 5.8$ Hz, 1H, diast. 1), 2.46 - 2.40 (m, 1H, diast. 1), 2.38 (ddd, $J = 12.7, 8.8, 6.4$ Hz, 1H, diast. 2), 1.91 (dt, $J = 12.7, 8.2$ Hz, 1H, diast. 2), 1.83 (ddd, $J = 12.8, 9.5, 7.7$ Hz, 1H, diast. 1). - **^{13}C NMR** (151 MHz, CDCl_3): $\delta = 173.8(\text{C}_q)$, 171.4(C_q , diast. 2), 171.2(C_q , diast. 1), 75.9(+, diast. 2), 75.4(+, diast. 1), 70.1(-, diast. 1), 69.9(-, diast. 2), 52.1(+), 52.1(+), 51.8(+), 51.7(+), 44.1(-, diast. 2), 43.6(-, diast. 1), 39.9(-, diast. 1), 39.9(-, diast. 2), 34.9(-, diast. 2), 34.7(-, diast. 1). **IR** (neat): $\tilde{\nu} = 2989, 2955, 1731, 1437, 1371, 1263, 1197, 1171, 1062, 1016, 936, 847 \text{ cm}^{-1}$. - **MS** (EI-MS, 70 eV): m/z (%) = 203 (MH^+ , 1), 171 (41), 170 (16), 142 (62), 129 (92), 116 (54), 102 (12), 101 (61), 97 (13), 87 (18), 83 (11), 82 (14), 81 (14), 74 (18), 69 (100), 59 (53), 55 (23), 45 (13), 43 (22).

4-methylbenzenesulfonyl azide (87)

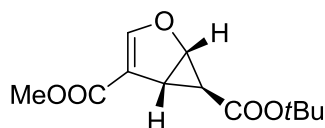
A 2 L flask was charged with sodium azide (71.5 g, 1.1 mol, 1.1 eq) and 400 mL of 90% aqueous EtOH. In an additional 2 L flask tosyl chloride (190.5 g, 1 mol, 1 eq) was dissolved in 1 L of EtOH (it was warmed up to 50 °C for complete dissolving if necessary) and was added to the azide solution. After 3 h the formed NaCl was filtered off. The solvent was removed under reduced pressure (bath temperature 35 °C, minimum applied pressure 110 mbar). The crude product was transferred to a separation funnel, 1 L water was added (without shaking) to induce phase separation. The product phase (lower one) was separated and washed with water (2 x 100 mL), dried over Na₂SO₄ and filtered to afford the desired product as an oil, which crystallized while storing at -18 °C (150 g, 0.76 mol, 76%).

¹H NMR (300 MHz, CDCl₃): δ = 7.83 (d, *J* = 8.3 Hz, 2H), 7.40 (d, *J* = 8.3 Hz, 2H), 2.47 (s, 3H). - **¹³C NMR** (75 MHz, CDCl₃): δ = 146.3(C_q), 135.4(C_q), 130.0(+), 127.5(+), 21.7(+). - **IR** (neat): $\tilde{\nu}$ = 2121, 1595, 1366, 1161, 1084, 813, 743, 655 cm⁻¹.

***tert*-butyl 2-diazoacetate (**89**)**

A three-necked 2 L flask, equipped with an internal thermometer, a mineral oil bubbler and a stopper was charged with 900 mL *n*-pentane and cooled to 0 °C. At that temperature tosyl azide (**87**) (62.6 g, 318 mmol, 1 eq), *tert*-butyl acetoacetate (**88**) (52.8 mL, 318 mmol, 1 eq) and Bu₄NBr (2.05 g, 6.36 mmol, 2 mol%) were added. The resulting mixture was treated with a cold sodium hydroxide solution (36 g, 0.9 mol, 2.8 eq, dissolved in 300 mL water), which was added in portions over a period of 15 min. When the addition was finished, the ice bath was removed, the flask was equipped with a mineral oil bubbler and stirring was continued for 20 h. The resulting white solid was removed via suction by the help of Celite, and the pad was washed with 100 mL *n*-pentane. The filtrate was transferred to a separation funnel, the phases were separated and the aqueous phase was washed with *n*-pentane (3 x 100 mL). The combined organic layers were washed with water (2 x 200 mL) and brine (1 x 200 mL) and dried over MgSO₄. After filtration the solvent was removed under reduced pressure (water bath 15 °C, minimum pressure 110 mbar) to afford pure product **89** as yellow liquid (39.6 g, 279 mmol, 88%). This liquid was diluted in the necessary amount of DCM to adjust the required wt% in DCM for the further reaction.

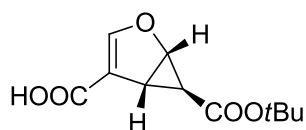
¹H NMR (300 MHz, CDCl₃): δ = 4.55 (s, 1H), 1.40 (s, 9H).

(1*S*,5*R*,6*S*)-6-*tert*-butyl 4-methyl 2-oxabicyclo[3.1.0]hex-3-ene-4,6-dicarboxylate (118)

A flame dried flask under nitrogen atmosphere was charged with 3 mL of dry DCM and $\text{Cu}(\text{OTf})_2$ (884 mg, 2.28 mmol, 1.12 mol%). To this suspension (*S,S*)-*i*Pr-bis(oxazoline)-ligand (813 mg, 3.05 mmol, 1.5 mol%) was added, which caused the suspension to turn into a blue solution, which was stirred for 1 h. This solution was transferred using a syringe filter to another flame dried flask under nitrogen atmosphere, equipped with a mineral oil bubbler and containing **78** (25.64 g, 203.5 mmol) dissolved in 10 mL DCM at 0 °C. Phenylhydrazine (225 mL, 2.28 mmol, 1.12 mol%) was added dropwise turning the solution to a dark red-brown color. After 15 min the dropwise addition of *tert*-butyl diazo glycine (561.5 g solution of 6.7 wt%, 264.6 mmol, 1.3 eq) in DCM was started (one drop every 10 sec). During the addition of diazo-compound at 0 °C nitrogen is evolved. After completion, the mixture was allowed to warm to room temperature and was filtered through a plug of basic alumina followed by 500 mL of DCM. The organic layers were concentrated under reduced pressure to afford a yellow-brown oil. The residue was purified by fractioned distillation under reduced pressure ($p = 15$ mbar, $bp = 55 - 66$ °C) to recover starting material (7.26 g, 77.3 mmol, 38%). The brown residue was purified by column chromatography (PE/EA = 15:1) to yield the desired product as a slightly yellow solid (18.56 g, 77.3 mmol, 38%, brsm: 53%, 83% ee).

R_f (PE/EA = 5:1) = 0.61. - $[\alpha]_D^{20} = -20.5$ (DCM, $c = 1$).

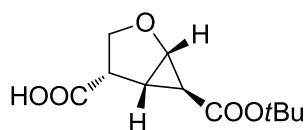
^1H NMR (300 MHz, CDCl_3): $\delta = 7.15$ (s, 1H), 4.91 (dt, $J = 5.6, 0.8$ Hz, 1H), 3.72 (s, 3H), 2.99 (dd, $J = 5.6, 2.9$ Hz, 1H), 1.42 (d, $J = 9.0$ Hz, 9H), 1.05 - 0.97 (m, 1H). - **^{13}C NMR** (75 MHz, CDCl_3): $\delta = 170.7(\text{C}_q)$, 164.1(C_q), 156.3(+), 115.7(C_q), 81.3(C_q), 68.8(+), 51.4(+), 29.0(+), 28.0(+), 22.4(+). - **IR** (neat): $\tilde{\nu} = 3109, 3071, 2977, 1699, 1599, 1444, 1367, 1271, 1157, 1097, 1045, 975, 830, 792, 760, 720$ cm^{-1} . - **MS** (EI-MS, 70 eV): m/z (%) = 240 (M^+ , 1), 184 (78), 176 (30), 166 (14), 155 (12), 152 (17), 139 (100), 108 (19), 107 (19), 57 (91). - **HRMS** (PI-EIMS, m/z): 240.0999 ($\text{C}_{12}\text{H}_{16}\text{O}_5$, calc. 240.0998 [M^+]). - **mp**: 72 °C. - **HPLC analysis** (Phenomenex Lux Cellulose-2, *n*heptane/*i*PrOH 99:1, 1.0 mL/min, 254 nm): $t_r = 13.17$, $t_r = 17.81$; 83% ee.

(1*S*,5*R*,6*S*)-6-(*tert*-butoxycarbonyl)-2-oxabicyclo[3.1.0]hex-3-ene-4-carboxylic acid (138)

118 (12.31 g, 51.3 mmol) was dissolved in 400 mL of a 3:1 water-THF mixture. To the resulting turbid solution LiOH (1.35 g, 56.4 mmol, 1.1 eq) was slowly added, which turns the color to yellow. After 6 h of stirring, the reaction mixture was transferred to a separation funnel and washed with Et₂O (2 x 150 mL) to recover remaining starting material (15%). The aqueous layer was acidified with HCl (2M) to a pH of about 2 and extracted with Et₂O (3 x 150 mL). The combined organic layers were dried over Na₂SO₄, filtered and concentrated under reduced pressure to afford the desired product as a colorless solid (9.85 g, 43.6 mmol, 85%, brsm: 100%).

R_f (PE/EA = 1:1) = 0.26. - $[\alpha]_D^{20} = -23.8$ (MeOH, c = 1).

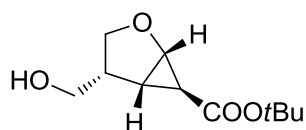
¹H NMR (300 MHz, Acetone): δ = 10.23 (s, 1H), 7.36 (s, 1H), 5.03 (d, *J* = 5.6 Hz, 1H), 2.92 (dd, *J* = 5.6, 2.8 Hz, 1H), 1.44 (s, 10H), 1.05 (d, *J* = 2.6 Hz, 1H). - **¹³C NMR** (75 MHz, Acetone): δ = 171.2(C_q), 164.8(C_q), 157.5(+), 116.6(C_q), 81.5(C_q), 69.2(+), 29.7(+), 28.2(+), 22.9(+). - **IR** (neat): $\tilde{\nu}$ = 3038, 2976, 1711, 1655, 1602, 1447, 1385, 1365, 1275, 1159, 1107, 975, 897, 836, 760, 717 cm⁻¹. - **MS** (EI-MS, 70 eV): *m/z* (%) = 226 (M⁺, 1), 170 (45), 153 (24), 152 (15), 125 (58), 107 (10), 57 (100), 51 (11), 41 (32), 39 (10). - **HRMS** (EI-MS, *m/z*): 226.0841 (C₁₁H₁₄O₅, calc. 226.0841 [M⁺]). - **mp**: 142 °C.

(1S,4S,5S,6S)-6-(tert-butoxycarbonyl)-2-oxabicyclo[3.1.0]hexane-4-carboxylic acid (139)

138 (9.3 g, 41.2 mmol) was dissolved in 200 mL of an EtOH/water mixture (95:5) and 900 mg Pd/C (10%) were added. After two times vacuum-hydrogen-spilling hydrogen was applied via a balloon. When the starting material was consumed (about 4 h), the mixture was filtered through celite and washed with 100 mL EtOH, twice. The organic layer was concentrated under reduced pressure to afford the desired product as colorless oil (9.4 g, 41.2 mmol, 100%) which crystallizes at ambient temperature after some days.

R_f (PE/EA = 1:1) = 0.2. - $[\alpha]_D^{20} = +62.4$ (MeOH, $c = 1$).

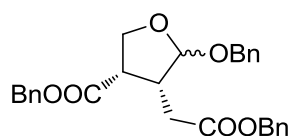
^1H NMR (300 MHz, CDCl_3): $\delta = 8.77$ (s, 1H), 4.23 - 4.11 (m, 2H), 3.69 (t, $J = 9.8$ Hz, 1H), 3.42 (td, $J = 9.5, 5.4$ Hz, 1H), 2.41 (td, $J = 5.4, 3.8$ Hz, 1H), 2.21 (dd, $J = 3.7, 0.8$ Hz, 1H), 1.42 (s, 9H). - **^{13}C NMR** (75 MHz, CDCl_3): $\delta = 176.9(\text{C}_q)$, 169.8(C_q), 81.2(C_q), 67.7(-), 65.7(+), 44.2(+), 28.0(+), 27.4(+), 22.7(+). - **IR** (neat): $\tilde{\nu} = 3192, 2984, 1703, 1401, 1366, 1320, 1197, 1152, 1116, 1073, 981, 952, 870, 841, 779, 725, 674\text{ cm}^{-1}$. - **MS** (ESI-MS): m/z (%) = 456 (19), 455 ($(2\text{M-H})^-$, 82), 274 (14), 273 ($(\text{M}+\text{HCOO}^-)$, 100), 227 ($(\text{M-H})^-$, 3). - **HRMS** (ESI-MS, m/z): 227.0927 ($\text{C}_{11}\text{H}_{15}\text{O}_5$, calc. 227.0925 [$(\text{M-H})^-$]). - **mp**: 92 °C.

(1*S*,4*R*,5*S*,6*S*)-tert-butyl-4-(hydroxymethyl)-2-oxabicyclo[3.1.0]hexane-6-carboxylate (140)

In a flame dried flask under nitrogen atmosphere **139** (377 mg, 1.65 mmol) was dissolved in 30 mL of dry THF and cooled to 0°C. $\text{BH}_3\cdot\text{THF}$ (2 mL of 1 M solution in THF, 1.2 eq) was added dropwise, which caused hydrogen evolution. The reaction was stirred for 1 h at 0 °C, warmed to room temperature and stirred for additional 12 h. The reaction was quenched by the addition of 1 mL of water. It was transferred to a separation funnel, mixed with 2 mL of a saturated NH_4Cl solution and extracted with EA (3 x 40 mL). The combined organic layers were dried over Na_2SO_4 , filtered and concentrated under reduced pressure. The crude product was purified by silica column chromatography (PE/EA = 3:1) to afford the product as colorless crystals (78 mg, 0.363 mmol, 22%).

R_f (PE/EA = 1:1) = 0.40. - $[\alpha]_D^{20} = +54.8$ (MeOH, $c = 1$).

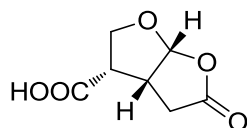
^1H NMR (300 MHz, CDCl_3): δ = 4.16 (d, $J = 5.5$ Hz, 1H), 4.07 (t, $J = 9.1$ Hz, 1H), 3.77 (dd, $J = 10.6, 6.9$ Hz, 1H), 3.64 (dd, $J = 10.6, 6.9$ Hz, 1H), 3.14 (t, $J = 9.8$ Hz, 1H), 2.88 - 2.73 (m, 1H), 2.13 (dd, $J = 9.3, 5.2$ Hz, 1H), 1.97 (s, 1H), 1.93 (d, $J = 3.9$ Hz, 1H), 1.41 (s, 9H). - **^{13}C NMR** (75 MHz, CDCl_3): δ = 170.3(C_q), 80.7(C_q), 69.1(-), 65.6(+), 62.9(-), 42.3(+), 28.1(+), 26.8(+), 21.8(+). - **IR** (neat): $\tilde{\nu}$ = 3503, 3389, 3314, 2977, 2823, 1705, 1691, 1398, 1368, 1314, 1261, 1153, 1106, 1064, 1038, 981, 947, 924, 883, 837, 719, 694, 658 cm^{-1} . - **MS** (CI-MS, NH_3): m/z (%) = 232 (MNH_4^+ , 100), 215 (MH^+ , 14), 176 (45). - **HRMS** (LSI-MS, m/z): 215.1278 ($\text{C}_{11}\text{H}_{19}\text{O}_4$, calc. 215.1283 [MH^+]). - **mp**: 55-70 °C.

(3*S*,4*R*)-benzyl-5-(benzyloxy)-4-(2-(benzyloxy)-2-oxoethyl)tetrahydrofuran-3-carboxylate (142)

139 (500 mg, 2.19 mmol) was dissolved in 25 mL BnOH cooled to 0 °C and conc. H₂SO₄ (0.33 mL, 6.19 mmol, 2.8 eq) was added by an addition funnel over 15 min. The mixture was allowed to warm to room temperature and stirred over night. NEt₃ (1.72 mL, 12.4 mmol, 2 eq based on H₂SO₄) was added dropwise and the solvent was removed by distillation under reduced pressure. The set of diastereomers was separated from by-products by silica column chromatography (PE/EA = 15:1) to afford **142** (303 mg, 0.66 mmol, 30%) as yellow oil, which was used in the next reaction without further separation.

R_f (PE/EA = 10:1) = 0.25 - 0.14.

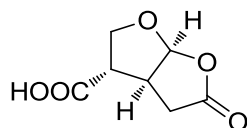
¹H NMR (300 MHz, CDCl₃): δ = 7.40 - 7.21 (m, 15H), 5.30 - 4.95 (m, 5H), 4.68 (dd, *J* = 11.9, 5.4 Hz, 1H), 4.42 (dd, *J* = 20.8, 11.9 Hz, 1H), 4.25 - 4.09 (m, 2H), 3.70 - 3.51 (m, 1H), 3.13 - 2.92 (m, 1H), 2.77 - 2.31 (m, 2H). - **¹³C NMR** (75 MHz, CDCl₃): δ = 172.9(C_q), 171.8(C_q), 171.5(C_q), 171.5(C_q), 137.9(C_q), 137.8(C_q), 135.7(C_q), 135.5(C_q), 128.6(+), 128.6(+), 128.6(+), 128.4(+), 128.4(+), 128.4, 128.3(+), 128.3(+), 128.2(+), 127.7(+), 127.7(+), 127.6(+), 106.8(+), 103.3(+), 69.2(-), 68.9(-), 68.5(-), 67.8(-), 66.9(-), 66.7(-), 66.5(-), 66.4(-), 46.9(+), 45.2(+), 44.0(+), 43.9(+), 33.2(-), 32.2(-). - **IR** (neat): $\tilde{\nu}$ = 3033, 2944, 2898, 1731, 1497, 1455, 1388, 1347, 1245, 1166, 1098, 1055, 1006, 948, 913, 734, 695 cm⁻¹. - **MS** (ESI-MS, *m/z*): 943 (18), 939 (37), 938 (2MNH₄⁺, 45), 479 (11), 478 (MNH₄⁺, 58), 354 (27), 353 (MNH₄⁺-BnOH, 100).

(3*S*,3*aR*,6*aR*)-5-oxohexahydrofuro[2,3-*b*]furan-3-carboxylic acid (145)

139 (2.64 g, 11.6 mmol) was dissolved in 30 mL THF and cooled to 0 °C. To the cooled solution 90 mL HCl (2 M) were added dropwise within 1 h. The resulting mixture was allowed to warm to room temperature and stirred for 12 h. The solvent was evaporated under reduced pressure to afford the crude product as brownish solid which was used without further purification. For analytic reasons the crude product can be purified by silica column chromatography (toluene/ethyl formate/formic acid = 5:4:1).

R_f (PE/EA = 1:1) = 0.09. - $[\alpha]_D^{20} = -52.2$ (MeOH, $c = 1$).

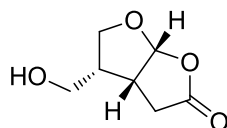
^1H NMR (600 MHz, DMSO): $\delta = 12.85$ (s, 2H), 6.07 (d, $J = 5.4$ Hz, 2H), 4.11 (dd, $J = 9.0, 7.6$ Hz, 2H), 3.86 (dd, $J = 10.9, 9.1$ Hz, 2H), 3.40 (ddd, $J = 15.4, 10.3, 5.0$ Hz, 2H), 3.29 (ddd, $J = 10.9, 9.0, 7.6$ Hz, 3H), 2.80 (dd, $J = 18.8, 10.6$ Hz, 2H), 2.36 (dd, $J = 18.8, 4.7$ Hz, 2H). - **^{13}C NMR** (151 MHz, DMSO): $\delta = 175.1(\text{C}_q)$, 171.4(C_q), 107.7(+), 67.3(-), 46.2(+), 39.8(+), 29.9(-). - **IR** (neat) $\tilde{\nu} = 3086, 3008, 2904, 1773, 1711, 1416, 1367, 1295, 1244, 1182, 1132, 1103, 966, 843, 802, 735, 664\text{ cm}^{-1}$. - **MS** (EI-MS, 70 eV): m/z (%) = 173 (MH^+ , 1), 98 (15), 86 (16), 85 (27), 83 (76), 82 (100), 81 (12), 73 (10), 69 (10), 68 (16), 55 (50), 54 (10). - **HRMS** (EI-MS, m/z): 173.0454 ($\text{C}_7\text{H}_9\text{O}_5$, calc. 173.0450 [MH^+]). - **mp** = 170 °C.

(3S,3aS,6aS)-5-oxohexahydrofuro[2,3-*b*]furan-3-carboxylic acid (57)

Crude **145** (2 g, 11.6 mmol) was dissolved in 10 mL pyridine together with 10 drops of water and was stirred for 2 h at room temperature. Pyridine was removed by co-distillation with toluene (3 x 5 mL) under reduced pressure. The crude mixture was purified by silica column chromatography (toluene/ethylformate/formic acid = 5:4:1) to afford the desired product as slightly yellow solid (1.49 g, 8.66 mmol, 75% based on **139**).

R_f (PE/EA = 1:1) = 0.09. - $[\alpha]_D^{20} = -19.2$ (MeOH, $c = 1$).

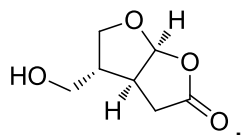
^1H NMR (400 MHz, MeOD): $\delta = 6.09$ (d, $J = 5.5$ Hz, 1H), 4.30 (dd, $J = 9.5, 2.5$ Hz, 1H), 4.11 (dd, $J = 9.5, 6.5$ Hz, 1H), 3.60 - 3.49 (m, 1H), 3.02 (dt, $J = 6.4, 2.5$ Hz, 1H), 2.97 (dd, $J = 18.8, 10.6$ Hz, 1H), 2.60 (dd, $J = 18.8, 3.7$ Hz, 1H). - **^{13}C NMR** (101 MHz, MeOD): $\delta = 177.5(\text{C}_q)$, 175.3(C_q), 110.1(+), 70.6(-), 51.2(+), 43.1(+), 34.7(-). - **IR** (neat): $\tilde{\nu} = 2994, 1771, 1695, 1416, 1358, 1295, 1178, 1103, 966, 929, 885, 855, 803, 670, 614 \text{ cm}^{-1}$. - **MS** (ESI-MS): m/z (%) = 515 ($(3\text{M-H}^+)^-$, 10), 344 (17), 343 ($(2\text{M-H}^+)^-$, 100), 217 (M-HCOO^- , 17), 137 (12). - **HRMS** (ESI-MS, m/z): 171.0298 ($\text{C}_7\text{H}_7\text{O}_5$, calc. 171.0299 [$(\text{M-H})^-$]). - **mp**: 143 °C.

(3a*R*,4*R*,6a*R*)-4-(hydroxymethyl)tetrahydrofuro[2,3-*b*]furan-2(6a*H*)-one (141)

In a flame dried flask under nitrogen atmosphere **145** (1 g, 5.81 mmol) was dissolved in 20 mL of dry THF and cooled to 0 °C. $\text{BH}_3 \cdot \text{THF}$ (5.81 mL of a 1 M solution in THF, 5.81 mmol, 1 eq) was added dropwise. After the addition was finished, the reaction was allowed to warm to room temperature and was then slowly heated up to 40 °C. After 3 h at that temperature, it was cooled to room temperature and 5 g of a slightly wet silica slurry were added to quench the reaction. The solvent was removed under reduced pressure in order to produce the dry-load for silica column chromatography (EA), which afforded the desired product as colorless oil (617 mg, 3.91 mmol, 68%).

R_f (EA) = 0.26. - $[\alpha]_D^{20} = -2.2$ (MeOH, $c = 1$).

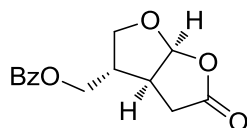
^1H NMR (300 MHz, MeOD): $\delta = 6.08$ (d, $J = 4.7$ Hz, 1H), 3.96 (ddd, $J = 12.0, 9.5, 4.2$ Hz, 2H), 3.47 (dd, $J = 7.4, 1.1$ Hz, 2H), 3.06 - 2.88 (m, 2H), 2.65 - 2.49 (m, 1H), 2.31 - 2.17 (m, 1H). - **^{13}C NMR** (75 MHz, MeOD): $\delta = 178.3(\text{C}_q)$, 110.5(+), 70.2(-), 63.5(-), 49.2(+), 49.0(+), 42.5(+), 35.3(-). - **IR** (neat) $\tilde{\nu} = 3335, 2910, 1744, 1641, 1410, 1316, 1199, 1107, 1035, 968, 928, 819, 744 \text{ cm}^{-1}$. - **HRMS** (ESI-MS, m/z): 159.0653 ($\text{C}_7\text{H}_{11}\text{O}_4$, calc. 159.0652 [MH^+]).

(3aS,4R,6aS)-4-(hydroxymethyl)tetrahydrofuro[2,3-b]furan-2(6aH)-one (152)

In a flame dried flask under nitrogen atmosphere **57** (250 mg, 1.45 mmol) was dissolved in 5 mL of dry THF and cooled to 0 °C. $\text{BH}_3 \cdot \text{THF}$ (1.45 mL of a 1 M solution in THF, 1.45 mmol, 1 eq) was added dropwise. After the addition was finished, the reaction was allowed to warm to room temperature and was then slowly heated up to 40 °C. After 3 h at that temperature, it was cooled to room temperature and 1.3 g of a slightly wet silica slurry were added to quench the reaction. The solvent was removed under reduced pressure to produce the dry-load for silica column chromatography (EA), which afforded the desired product **152** as colorless oil (222 mg, 1.41 mmol, 97%).

R_f (EA) = 0.26. - $[\alpha]_D^{20} = -9.0$ (MeOH, $c = 1$).

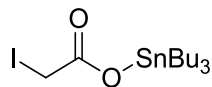
^1H NMR (300 MHz, MeOD): δ = 6.06 (d, $J = 4.6$ Hz, 1H), 3.97 (ddd, $J = 11.9, 9.4, 4.2$ Hz, 2H), 3.46 (d, $J = 7.4$ Hz, 2H), 3.02 - 2.87 (m, 2H), 2.55 (ddd, $J = 15.8, 11.6, 7.7$ Hz, 1H), 2.28 - 2.16 (m, 1H). - **^{13}C NMR** (75 MHz, MeOD): δ = 178.0(C_q), 110.5(+), 70.3(-), 63.7(-), 49.5(+), 42.7(+), 35.4(-). - **IR** (neat) $\tilde{\nu}$ = 3331, 2960, 2884, 1772, 1392, 1353, 1191, 1132, 1101, 1046, 1025, 977, 930, 896 cm^{-1} . - **HRMS** (ESI-MS, m/z): 159.0651 ($\text{C}_7\text{H}_{11}\text{O}_4$, calc. 159.0652 [MH^+]).

((3S,3aS,6aS)-5-oxohexahydrofuro[2,3-*b*]furan-3-yl)methyl benzoate (153)

In a flame dried flask under nitrogen atmosphere **152** (158 mg, 0.69 mmol) was dissolved in 10 mL of dry pyridine and benzoyl chloride (160 μ L, 1.38 mmol, 2 eq) was added dropwise. After 3 h the solvent was removed under reduced pressure by co-distillation with toluene (3 x 10 mL). The residue was purified by silica column chromatography (PE/EA = 1:1) to afford **153** as yellow oil (72 mg, 0.27 mmol, 39%).

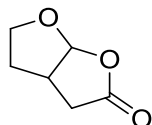
R_f (PE/EA = 1:1) = 0.57. - $[\alpha]_D^{20} = -15$ (DCM, $c = 1$).

^1H NMR (300 MHz, CDCl_3): $\delta = 8.06 - 7.97$ (m, 2H), 7.65 - 7.54 (m, 1H), 7.52 - 7.41 (m, 2H), 6.15 (d, $J = 5.1$ Hz, 1H), 4.29 (qd, $J = 11.1, 7.3$ Hz, 2H), 4.10 (ddd, $J = 12.2, 9.8, 4.1$ Hz, 2H), 3.08 - 2.90 (m, 2H), 2.62 - 2.52 (m, 2H). - **^{13}C NMR** (75 MHz, CDCl_3): $\delta = 174.4(\text{C}_q)$, 166.3(C_q), 133.4(+), 129.6(+), 129.4(C_q), 128.5(+), 108.0(+), 69.2(-), 64.8(-), 45.3(+), 41.8(+), 34.5(-). - **IR** (neat) $\tilde{\nu} = 2970, 2898, 1780, 1717, 1451, 1355, 1315, 1274, 1176, 1112, 1071, 981, 937, 897, 712$ cm^{-1} . - **HRMS** (ESI-MS, m/z): 285.0734 ($\text{C}_{14}\text{H}_{14}\text{NaO}_5$, calc. 285.0733 $[(\text{M}+\text{Na})^+]$).

tributylstannyl 2-iodoacetate (166)

Iodoacetic acid (11.15 g, 60 mmol, 2 eq) was heated together with bis(tributyltin) oxide (**165**) (17.88 g, 30 mmol, 1 eq) at 130 °C for 30 min. During that time a clear solution was formed, containing some drops of water. After cooling to room temperature the mixture was transferred with hot PE to a separation funnel where the water was separated. The solvent was removed under reduced pressure to afford the clean product as a white solid (26.25 g, 55.14 mmol, 92% based on iodoacetic acid).

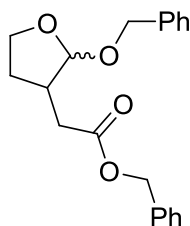
¹H NMR (300 MHz, CDCl₃): δ = 3.70 (s, 2H), 1.78 - 1.45 (m, 7H), 1.42 - 1.16 (m, 13H), 0.91 (t, *J* = 7.3 Hz, 10H). - **¹³C NMR** (75 MHz, CDCl₃): δ = 175.7(C_q), 30.0(-), 29.3(-), 18.9(+), 15.9(-). - **IR** (neat): $\tilde{\nu}$ = 2954, 2922, 2855, 1571, 1428, 1380, 1290, 1159, 1078, 869, 769, 670, 603 cm⁻¹.

tetrahydrofuro[2,3-*b*]furan-2(6*a*H)-one (167)

Tin ester **166** (51.18 g, 107.5 mmol, 1 eq), 2,3-dihydrofuran (24.4 mL, 322.5 mmol, 3 eq) and AIBN (984 mg, 6 mmol, 5 mol%) were refluxed in 120 mL benzene for 8 h. The reaction mixture was transferred to a separation funnel and partitioned between acetonitrile (100 mL) and PE (100 mL). The acetonitrile phase was washed with PE (3 x 100 mL) and concentrated under reduced pressure. The crude product was purified by silica column chromatography (PE:EA = 2:1) to afford the desired product **X** as yellowish oil (9.35 g, 73.1 mmol, 68%).

R_f (PE/EA = 1:1) = 0.31.

^1H NMR (300 MHz, CDCl_3): δ = 6.04 (d, J = 5.4 Hz, 1H), 4.10 - 4.00 (m, 1H), 3.96 - 3.84 (m, 1H), 3.11 (dddd, J = 12.1, 9.0, 5.9, 3.2 Hz, 1H), 2.83 (dd, J = 18.6, 10.2 Hz, 1H), 2.39 (dd, J = 18.6, 3.6 Hz, 1H), 2.16 (dddd, J = 12.8, 10.3, 9.2, 8.2 Hz, 1H), 1.73 (ddt, J = 12.8, 5.7, 2.7 Hz, 1H). - **^{13}C NMR** (75 MHz, CDCl_3): δ = 175.3(C_q), 108.2(+), 67.3(-), 38.3(+), 34.7(-), 32.2(-). - **IR** (neat): $\tilde{\nu}$ = 2982, 2882, 1770, 1356, 1298, 1250, 1170, 1106, 1003, 963, 935, 869, 832, 648 cm^{-1} .

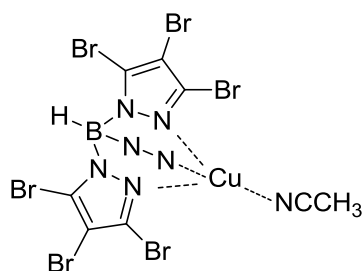
benzyl 2-(2-(benzyloxy)tetrahydrofuran-3-yl)acetate (168)

167 (1.5 g, 11.7 mmol) was dissolved in 50 mL BnOH at 0 °C and conc. H₂SO₄ (2 mL, 37.5 mmol, 3.2 eq) were added by an addition funnel over 15 min. The mixture was allowed to warm to room temperature and was stirred over night. NEt₃ (15.5 mL, 112 mmol, 3 eq based on H₂SO₄) was added dropwise and the solvent was removed by distillation under reduced pressure. The sticky residue was purified by silica column chromatography (PE/EA = 8:1) to afford the product as 1:1.3 mixture of diastereomers (3.1 g, 9.51 mmol, 82%).

R_f (PE/EA = 5:1) = 0.36.

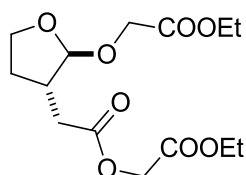
¹H NMR (600 MHz, CDCl₃): δ = 7.39 - 7.26 (m, 23H), 5.14 (d, *J* = 4.4 Hz, 1.3H, major), 5.13 - 5.09 (m, 4H), 4.95 (d, *J* = 1.2 Hz, 1H, minor), 4.73 - 4.69 (m, 2.3H), 4.44 (dd, *J* = 28.1, 12.0 Hz, 2H), 4.02 (td, *J* = 8.8, 3.6 Hz, 1.3H, major), 3.99 - 3.95 (m, 2H, minor), 3.90 (dd, *J* = 16.2, 8.2 Hz, 1.4H, major), 2.77 - 2.68 (m, 2.3H), 2.61 - 2.53 (m, 2.3H), 2.51 (dd, *J* = 15.7, 7.3 Hz, 1H, minor), 2.34 (dd, *J* = 15.7, 8.2 Hz, 1H, minor), 2.29 (dtd, *J* = 13.6, 7.8, 6.0 Hz, 1H, minor), 2.13 - 2.06 (m, 1.3H, major), 1.78 (ddd, *J* = 22.4, 11.2, 9.1 Hz, 1.3H, major), 1.63 - 1.57 (m, 1H, minor). - **¹³C NMR** (151 MHz, CDCl₃): δ = 172.6(C_q,major), 171.8(C_q, minor), 138.4(C_q), 138.1(C_q), 135.9(C_q), 135.8(C_q), 128.5(+), 128.5(+), 128.3(+), 128.3(+), 128.2(+), 128.2(+), 128.2(+), 127.8(+), 127.5(+), 127.5(+), 127.4(+), 106.8(+, minor), 102.6(+, major), 68.9(-, minor), 68.6(-, major), 66.6(-, major), 66.5(-, minor), 66.4(-, minor), 66.2(-, major), 41.8(+, minor), 39.9(+, major), 37.1(-, minor), 33.7(-, major), 29.8(-, minor), 29.0(-, major). - **IR** (neat): $\tilde{\nu}$ = 2942, 2892, 1732, 1497, 1454, 1347, 1263, 1212, 1162, 1022, 916, 734, 695, 613 cm⁻¹. - **MS** (EI-MS, 70 eV): *m/z* (%) = 235 ((M-C₇H₇)⁺, 1), 219 ((M-OC₇H₇)⁺, 24), 129 (18), 91 (C₇H₇⁺, 100). - **Elemental analysis** calcd. (%) for C₂₀H₂₂O₄ (326.15): C 73.60, H 6.79, found C 73.55, H 6.69.

copper(I) tris(3,4,5-tribromo-1H-pyrazole-1-yl)hydroborate acetonitrile complex (164) (third pyrazole ring indicated by N-N for better lucidity)



Perbromo pyrazole **170** (4.41 g, 14.6 mmol, 4 eq) and NaBH₄ (138 mg, 3.65 mmol, 1 eq) are molten in a sublimation apparatus under nitrogen atmosphere at 265 °C (metal bath) until cessation of hydrogen evolution. After cooling to room temperature the resulting solid was crushed. The remaining perbromo pyrazole (**170**) was removed by sublimation under reduced pressure (100 °C, 15 mbar). The crushing-sublimation procedure was done thrice. This provided the crude [TpBr₃]Na (**171**) (3.31 g, 3.50 mmol, 96%), which was used without further purification. For the following procedure all solvents were degassed thrice via pump-freeze-method and all steps were one under nitrogen atmosphere. In a flame dried flask under nitrogen atmosphere [TpBr₃]Na (**171**) (946 mg, 1 mmol) and CuI (190 mg, 1 mmol, 1 eq) were dissolved in 60 mL dry MeCN and stirred over night at room temperature. After removing the solvent under reduced pressure the remaining solid was dissolved in 40 mL dry DCM and filtered to remove NaI. The solvent was removed under reduced pressure until a thick oil was remaining. To this residue 5 mL of PE were added and white crystals (750 mg, 0.73 mmol, 73%) were formed while storing at -18 °C. The complex was stable at room temperature when stored under exclusion of moisture and oxygen.

¹H NMR (300 MHz, CD₂Cl₂): δ = 10.87 (s, 1H), 2.18 (s, 2H). - **¹³C NMR** (75 MHz, CD₂Cl₂): δ = 129.7(C_q), 122.8(C_q), 116.1(C_q), 100.1(C_q), 3.0(+). - **IR** (neat): $\tilde{\nu}$ = 3094, 3011, 2855, 2771, 1527, 1479, 1389, 1349, 1323, 1178, 1123, 1003, 969, 730 cm⁻¹.

ethyl 2-(2-(2-(2-ethoxy-2-oxoethoxy)-5-oxotetrahydrofuran-3-yl)ethoxy)acetate (175)

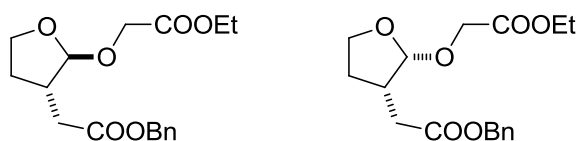
In a flame dried flask under nitrogen atmosphere **167** (250 mg, 1.95 mmol) was dissolved in 2 mL of dry DCM and $\text{Fe}(\text{BF}_4)_2 \cdot 6\text{H}_2\text{O}$ (66 mg, 0.195 mmol, 0.1 eq) was added at 0 °C. The mixture was treated with ethyl diazo glycine (1.96 g of a solution in DCM with 12.7 wt%, 2 eq) by the help of a syringe pump (0.25 mL/h). During the reaction nitrogen was evolved (mineral oil bubbler). After about 6 h, at the end of the addition, the solvent was removed under reduced pressure and the crude mixture was purified by silica column chromatography (PE/EA = 5:1) to afford **175** (two diastereomers) as yellow oil (197 mg, 0.62 mmol, 32% combined yield).

Isomer 1 (92 mg, 0.29 mmol, 15%): R_f (PE/EA = 3:1) = 0.16.

^1H NMR (600 MHz, CDCl_3): δ = 4.97 (d, J = 1.1 Hz, 1H), 4.61 (s, 2H), 4.21 (q, J = 7.1 Hz, 4H), 4.13 (d, J = 2.3 Hz, 2H), 3.95 (t, J = 7.1 Hz, 2H), 2.86 – 2.71 (m, 1H), 2.61 (dd, J = 15.8, 6.8 Hz, 1H), 2.39 (dd, J = 15.8, 8.6 Hz, 1H), 2.33 (ddd, J = 14.6, 12.6, 7.1 Hz, 1H), 1.65 (dtd, J = 12.5, 7.3, 4.2 Hz, 1H), 1.27 (t, J = 7.1 Hz, 3H), 1.27 (t, J = 7.1 Hz, 3H). - **^{13}C NMR** (151 MHz, CDCl_3): δ = 171.2(C_q), 170.4(C_q), 167.6(C_q), 107.3(+), 66.9(-), 64.0(-), 61.4(-), 60.7(-), 41.6(+), 36.3(-), 29.4(-), 14.1(+), 14.0(+). - **IR** (neat): $\tilde{\nu}$ = 2980, 2939, 2909, 1741, 1424, 1382, 1277, 1198, 1155, 1119, 1054, 1028, 957, 924 cm^{-1} . - **MS** (ESI-MS): m/z (%) = 654 (2MNH_4^+ , 28), 336 (MNH_4^+ , 100). - **HRMS** (ESI-MS, m/z): 341.1205 ($\text{C}_{14}\text{H}_{22}\text{NaO}_8$, calc. 341.1207 [($\text{M}+\text{Na}$) $^+$]).

Isomer 2 (105 mg, 0.33 mmol, 17%): R_f (PE/EA = 3:1) = 0.27.

^1H NMR (600 MHz, CDCl_3): δ = 5.09 (d, J = 4.4 Hz, 1H), 4.61 (dd, J = 50.2, 15.9 Hz, 2H), 4.20 (q, J = 7.2 Hz, 2H), 4.16 (dd, J = 7.2, 1.5 Hz, 2H), 4.10 (dd, J = 38.4, 16.5 Hz, 2H), 4.00 (ddd, J = 9.3, 8.5, 3.2 Hz, 1H), 3.86 (dd, J = 16.4, 8.2 Hz, 1H), 2.83 (dd, J = 16.6, 7.1 Hz, 1H), 2.62 (dd, J = 16.6, 7.7 Hz, 1H), 2.59 - 2.50 (m, 1H), 2.16 - 2.09 (m, 1H), 1.81 (tt, J = 11.4, 9.1 Hz, 1H), 1.27 (t, 7.3 Hz, 3H), 1.25 (t, 7.6 Hz, 3H). - **^{13}C NMR** (151 MHz, CDCl_3): δ = 172.1(C_q), 170.4(C_q), 167.7(C_q), 103.3(+), 67.1(-), 63.9(-), 61.3(-), 60.6(-), 60.6(-), 40.0(+), 32.9(-), 28.6(-), 14.1(+), 14.0(+). - **IR** (neat): $\tilde{\nu}$ = 2983, 2949, 2902, 1742, 1423, 1381, 1279, 1198, 1158, 1125, 1092, 1027, 984, 900 cm^{-1} . - **MS** (ESI-MS): m/z (%) = 341 (MNa^+ , 26), 336 (MNH_4^+ , 100). - **HRMS** (ESI-MS, m/z): 341.1205 ($\text{C}_{14}\text{H}_{22}\text{NaO}_8$, calc. 341.1207 [$(\text{M}+\text{Na})^+$]).

benzyl 2-(2-(2-ethoxy-2-oxoethoxy)tetrahydrofuran-3-yl)acetate (176)

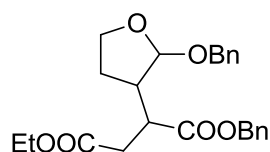
In a flame dried flask under nitrogen **168** (200 mg, 0.613 mmol) was mixed with 1 mL of dry DCM and $\text{Rh}_2(\text{OAc})_4$ (5.4 mg, 0.012 mmol, 2 mol%). The mixture was cooled to 0 °C and treated with ethyl diazo glycine (1.2 g of a solution in DCM with 12 wt%, 2 eq) by the help of a syringe pump (0.25 mL/h). During the reaction nitrogen was evolved (mineral oil bubbler). At the end of the addition the solvent was removed under reduced pressure and the crude mixture was purified by silica column chromatography (1:1) to afford two diastereomers as yellow oil (75 mg, 0.23 mmol, 38% combined yield).

anti-isomer (176) (39 mg, 0.12 mmol, 20%): R_f (PE/EA = 1:1) = 0.60.

^1H NMR (300 MHz, CDCl_3): δ = 7.43 - 7.27 (m, 4H), 5.37 (d, J = 2.5 Hz, 1H), 4.73 (dd, J = 75.9, 11.6 Hz, 2H), 4.20 (q, J = 7.1 Hz, 2H), 4.00 (s, 2H), 3.64 - 3.48 (m, 2H), 2.89 (dd, J = 17.7, 8.7 Hz, 1H), 2.69 - 2.54 (m, 1H), 2.29 (dd, J = 17.8, 4.6 Hz, 1H), 1.87 (dtd, J = 12.3, 6.8, 5.6 Hz, 1H), 1.73 - 1.57 (m, 1H), 1.28 (t, J = 7.2 Hz, 3H). -
 ^{13}C NMR (75 MHz, CDCl_3): δ = 175.8(C_q), 170.1(C_q), 136.4(C_q), 128.9(+), 128.5(+), 128.1(+), 107.2(+), 71.2(-), 69.0(-), 68.2(-), 60.9(-), 39.1(+), 33.7(-), 31.7(-), 14.2(+). -
IR (neat): $\tilde{\nu}$ = 2982, 2935, 1784, 1746, 1451, 1276, 1205, 1131, 1025, 938 cm^{-1} . -
MS (ESI-MS): m/z (%) = 345 (MNa^+ , 26), 340 (MNH_4^+ , 100), 323 (MH^+ , 73). -
HRMS (ESI-MS, m/z): 345.1306 ($\text{C}_{17}\text{H}_{22}\text{NaO}_6$, calc. 345.1309 [($\text{M}+\text{Na}$) $^+$].

syn-isomer (176) (36 mg, 0.11 mmol, 18%): R_f (PE/EA = 1:1) = 0.70.

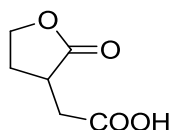
^1H NMR (300 MHz, CDCl_3): δ = 7.44 - 7.27 (m, 5H), 5.55 (d, J = 5.2 Hz, 1H), 4.71 (dd, J = 78.2, 11.8 Hz, 2H), 4.19 (q, J = 7.1 Hz, 2H), 4.01 (s, 2H), 3.61 - 3.46 (m, 2H), 2.84 - 2.70 (m, 1H), 2.60 (dd, J = 17.1, 8.2 Hz, 1H), 2.41 (dd, J = 17.1, 12.0 Hz, 1H), 1.97 (dtd, J = 12.0, 6.9, 5.1 Hz, 1H), 1.90 - 1.76 (m, 1H), 1.27 (t, J = 7.1 Hz, 3H). - **^{13}C NMR** (75 MHz, CDCl_3): δ = 176.5(C_q), 170.3(C_q), 136.6(C_q), 128.9(+), 128.5(+), 128.0(+), 103.3(+), 70.5(-), 69.4(-), 68.1(-), 60.8(-), 37.7(+), 32.6(-), 28.4(-), 14.2(+). - **IR** (neat): $\tilde{\nu}$ = 2925, 1786, 1748, 1455, 1358, 1205, 1175, 1139, 1024, 961, 926 cm^{-1} . - **MS** (ESI-MS): m/z (%) = 345 (MNa^+ , 28), 340 (MNH_4^+ , 100), 323 (MH^+ , 58). - **HRMS** (ESI-MS, m/z): 345.1305 ($\text{C}_{17}\text{H}_{22}\text{NaO}_6$, calc. 345.1309 $[(\text{M}+\text{Na})^+]$).

1-benzyl 4-ethyl 2-(2-(benzyloxy)tetrahydrofuran-3-yl)succinate (177)

A flame dried flask under nitrogen atmosphere, was filled with 8 mL of dry DCM and **168** (326 mg, 1 mmol). The resulting solution was degassed thrice by pump-freeze method and treated with [TpBr₃]Cu-MeCN (**164**) (51 mg, 0.05 mmol, 5 mol%). Ethyl diazo glycine (770 mg of 14.8 wt% DCM solution, 1 mmol, 1 eq) was added by a syringe pump, 0.25 mL/h. During the reaction nitrogen gas was evolved (mineral oil bubbler). When the addition was finished the reaction was stirred for further 30 min, concentrated under reduced pressure. The residue was purified by silica column chromatography (PE/EA = 5:1) to afford a mixture of diastereomers (1:1) as colorless oil (111 mg, 0.27 mmol, 27%).

R_f (PE/EA = 5:1) = 0.25.

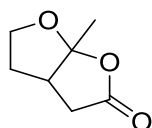
¹H NMR (600 MHz, CDCl₃): δ = 7.39 - 7.25 (m, 20H), 5.17 - 5.03 (m, 5H), 4.92 (s, 1H, isomer 2), 4.74 (d, *J* = 4.0 Hz, 1H), 4.72 (d, *J* = 4.3 Hz, 1H), 4.67 - 4.61 (m, 1H, isomer 1), 4.55 (ddd, *J* = 14.6, 8.1, 6.6 Hz, 1H, isomer 2), 4.42 (d, *J* = 11.6 Hz, 1H), 4.37 (d, *J* = 11.9 Hz, 1H), 4.23 - 4.09 (m, 4H), 2.81 - 2.75 (m, 1H, isomer 2), 2.72 (dd, *J* = 7.8, 3.9 Hz, 1H), 2.71 - 2.68 (m, 2H), 2.67 (d, *J* = 7.8 Hz, 1H), 2.63 (ddd, *J* = 8.7, 7.5, 4.7 Hz, 1H, isomer 1), 2.58 - 2.46 (m, 3H), 2.38 - 2.29 (m, 2H), 2.05 (dt, *J* = 12.9, 7.6 Hz, 1H, isomer 1), 1.93 (ddd, *J* = 12.9, 7.1, 2.1 Hz, 1H, isomer 1), 1.55 (td, *J* = 12.0, 9.0 Hz, 1H, isomer 2), 1.27 (dt, *J* = 1.6, 7.1 Hz, 8H). - **¹³C NMR** (151 MHz, CDCl₃): δ = 172.3(C_q), 171.6(C_q), 171.2(C_q), 171.1(C_q), 138.2(C_q), 137.8(C_q), 135.8(C_q), 135.7(C_q), 128.5(+), 128.5(+), 128.3(+), 128.3(+), 128.2(+), 128.2(+), 128.2(+), 128.2(+), 127.9(+), 127.6(+), 106.9(+, isomer 2), 102.8(+, isomer 1), 75.8(+, isomer 2), 75.6(+, isomer 1), 68.8(-), 68.6(-), 66.4(-), 66.2(-), 60.5(-), 60.4(-), 43.1(-), 42.9(-), 42.2(+, isomer 2), 40.7(+, isomer 1), 36.4(-), 35.2(-, isomer 2), 34.8(-, isomer 1), 33.5(-), 14.2(+). - **IR** (neat): $\tilde{\nu}$ = 2963, 2360, 2340, 1733, 1454, 1261, 1160, 1094, 1024, 799, 736, 697 cm⁻¹. - **MS** (ESI-MS): *m/z* (%) = 431 (27), 430 (MNH₄⁺, 100), 306 (10), 305 (52). - **HRMS** (ESI-EIC-MS, *m/z*): 430.2223 (C₂₄H₃₂NO₆, calc. 430.2224 [(M+NH₄)⁺]).

2-(2-oxotetrahydrofuran-3-yl)acetic acid (183)

167 (1 g, 7.8 mmol) was dissolved in 15 mL acetone and cooled in an ice bath. 2.5 M Jones reagent (11 mL, 27.5 mmol, 3.5 eq) was added by an addition funnel over a period of 1 h. When the addition was finished the reaction was stirred for further 2 h at room temperature. The green mixture was transferred to a separation funnel. After addition of 10 mL of water, the crude product was extracted with EA (4 x 10 mL). The combined organic layers were dried with Na₂SO₄, filtered and concentrated under reduced pressure. The product (1.06 g, 7.35 mmol, 94%) was used without further purification.

R_f (PE/EA = 1:1) = 0.23.

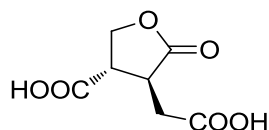
¹H NMR (300 MHz, MeOD): δ = 4.39 (td, J = 8.9, 2.1 Hz, 1H), 4.25 (ddd, J = 10.2, 8.9, 6.7 Hz, 1H), 3.04 - 2.90 (m, 1H), 2.77 (dd, J = 17.3, 4.3 Hz, 1H), 2.59 (dd, J = 17.3, 7.7 Hz, 1H), 2.48 (dddd, J = 12.2, 8.9, 6.8, 2.1 Hz, 1H), 2.10 (dtd, J = 12.4, 10.6, 9.0 Hz, 1H). - **¹³C NMR** (75 MHz, MeOD): δ = 181.3(C_q), 174.7(C_q), 68.3(-), 37.2(+), 34.9(-), 29.2(-). - **IR** (neat) $\tilde{\nu}$ = 3460, 3984, 2924, 1701, 1404, 1381, 1266, 1158, 1020, 960, 897, 830, 782, 713, 668, 616 cm⁻¹. - **MS** (EI-MS, 70 eV): m/z (%) = 144 (M⁺, 1), 100 (12), 82 (13), 58 (29), 57 (10), 56 (22), 55 (100), 54 (31), 45 (19), 43 (24), 42 (19), 41 (46), 39 (26). - **HRMS** (ESI-MS, m/z): 145.0492 (C₆H₉O₄, calc. 145.0495 [MH⁺]).

6a-methyltetrahydrofuro[2,3-b]furan-2(6aH)-one (185)

In a flame dried flask under nitrogen atmosphere **183** (100 mg, 0.69 mmol) was dissolved in 2 mL of dry THF and cooled to -78 °C. Me-MgBr (913 μ L of a 22 wt% solution in THF, 1.725 mmol, 2.5 eq) was added dropwise. After the turbid solution was kept at that temperature for 2 h, it was allowed to warm to 0 °C. Then it was transferred to a separation funnel and 1 mL of water was added. The mixture was acidified to a pH of 2 by HCl (2 M) and extracted with Et₂O (4 x 5 mL). The combined organic layers were dried over Na₂SO₄, filtered and concentrated under reduced pressure. The crude product was purified by silica column chromatography (PE/EA = 1:1) to afford the desired product as colorless oil (18 mg, 0.13 mmol, 19%).

R_f (PE/EA = 1:1) = 0.47.

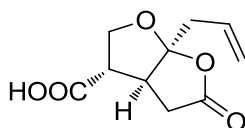
¹H NMR (300 MHz, CDCl₃): δ = 4.07 (td, J = 8.7, 2.5 Hz, 1H), 3.93 (td, J = 9.7, 6.2 Hz, 1H), 2.94 (dd, J = 18.2, 9.8 Hz, 1H), 2.80 (tt, J = 9.6, 2.7 Hz, 1H), 2.50 (dd, J = 18.1, 2.6 Hz, 1H), 2.28 (ddd, J = 18.1, 12.9, 9.3 Hz, 1H), 1.83 - 1.70 (m, 1H), 1.65 (s, 3H). - **¹³C NMR** (75 MHz, CDCl₃): δ = 174.6(C_q), 117.4(C_q), 67.4(-), 42.7(+), 36.5(-), 33.1(-), 23.8(+). - **IR** (neat) $\tilde{\nu}$ = 2987, 2939, 2888, 1761, 1387, 1323, 1259, 1219, 1129, 1084, 1014, 899, 832, 682, 606 cm⁻¹. - **MS** (EI-MS, 70 eV): m/z (%) = 141 (M-H⁺, 1), 127 (M-Me⁺, 5), 98 (38), 97 (16), 83 (12), 55 (31), 54 (14), 43 (100). - **HRMS** (ESI-MS, m/z): 143.0702 (C₇H₁₁O₃, calc. 143.0703 [(M+H)⁺]).

(3S,4S)-4-(carboxymethyl)-5-oxotetrahydrofuran-3-carboxylic acid (186)

57 (1.41 g, 8.2 mmol) was dissolved in 25 mL of acetone and cooled to 0 °C. Within 30 min, 8.2 mL of Jones-reagent (2.5 M) were added. The mixture turned slowly from orange to green. After 6 h it was transferred to a separation funnel, 10 mL of water were added and it was washed with EA (4 x 25 mL). The combined organic layers were dried over Na₂SO₄, filtered and concentrated under reduced pressure. The crude mixture was purified by silica column chromatography (PE/EA = 1:2 + 1 vol% HOAc) to afford the desired product (1.36 g, 7.23 mmol, 88%).

R_f (EA) = 0.27. - $[\alpha]_D^{20} = -29.5$ (MeOH, c = 1).

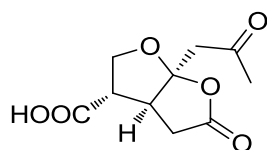
¹H NMR (600 MHz, Acetone): δ = 4.57 (t, *J* = 9.0 Hz, 1H), 4.33 (t, *J* = 9.0 Hz, 1H), 3.64 - 3.53 (m, 1H), 3.19 (dt, *J* = 10.3, 5.1 Hz, 1H), 2.86 (d, *J* = 5.2 Hz, 2H). - **¹³C NMR** (151 MHz, MeOD): δ = 179.2(C_q), 174.2(C_q), 174.0(C_q), 68.6(-), 45.5(+), 40.3(+), 33.4(-). - **IR** (neat) $\tilde{\nu}$ = 3506, 3321, 2977, 1721, 1699, 1408, 1380, 1259, 1188, 1158, 1085, 1029, 861, 714, 692, 648 cm⁻¹. - **MS** (ESI-MS): *m/z* (%) = 563 ((3M-H)⁻, 5), 375 ((2M-H)⁻, 100), 233 (M+HCOO⁻, 18), 187 ((M-H)⁻, 14). - **HRMS** (ESI-MS, *m/z*): 187.0247 (C₇H₇O₆, calc. 187.0248 [(M-H)⁻]).

(3S,3aS,6aS)-6a-allyl-5-oxohexahydrofuro[2,3-b]furan-3-carboxylic acid (187)

In a flame dried flask under nitrogen atmosphere **186** (603 mg, 3.32 mmol) was dissolved in 50 mL of dry THF and cooled to -78 °C. Allyl-MgBr (8.02 mL of a 1 M solution in Et₂O, 8.02 mmol, 2.5 eq) was added dropwise. After the turbid solution was kept at that temperature for 2 h, it was allowed to warm to 0 °C. Then it was transferred to a separation funnel, 20 mL of water were added. The mixture was acidified to a pH of 2 by HCl (2 M). It was extracted with Et₂O (4 x 50 mL). The combined organic layers were dried over Na₂SO₄, filtered and concentrated under reduced pressure. The crude product was purified by silica column chromatography (toluene/ethyl formate/formic acid = 5:4:1) to afford the desired product as colorless oil (514 mg, 2.42 mmol, 73%).

R_f (toluene/ethyl formate/formic acid = 5:4:1) = 0.35. - $[\alpha]_D^{20}$ = -16.2 (MeOH, c = 1).

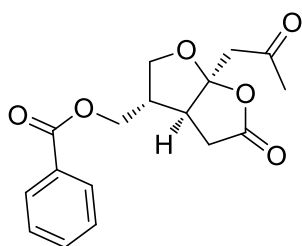
¹H NMR (300 MHz, Acetone): δ = 5.81 (ddt, J = 17.3, 10.2, 7.1 Hz, 1H), 5.29 - 5.08 (m, 2H), 4.32 (dd, J = 9.5, 2.2 Hz, 1H), 4.15 (dd, J = 9.5, 6.6 Hz, 1H), 3.38 (dt, J = 10.4, 2.7 Hz, 1H), 3.21 - 3.09 (m, 1H), 3.02 (dd, J = 18.7, 10.4 Hz, 1H), 2.73 - 2.60 (m, 3H). - **¹³C NMR** (75 MHz, Acetone): δ = 174.6(C_q), 173.6(C_q), 132.3(+), 120.1(-), 118.6(C_q), 70.1(-), 51.6(+), 44.6(+), 41.9(-), 35.9(-). - **IR** (neat) $\tilde{\nu}$ = 3402, 2930, 2848, 1716, 1648, 1414, 1263, 1208, 1089, 1017, 972, 924, 866 cm⁻¹. - **MS** (ESI-MS): m/z (%) = 635 ((3M-H)⁻, 45), 423 ((2M-H)⁻, 100), 325 (M+F₃CCOO⁻, 24), 257 (M+HCOO⁻, 52). - **HRMS** (ESI-MS, m/z): 211.0612 (C₁₀H₁₁O₅, calc. 211.0612 [(M-H)⁻]).

(3*S*,3*aS*,6*aS*)-5-oxo-6*a*-(2-oxopropyl)hexahydrofuro[2,3-*b*]furan-3-carboxylic acid (189)

187 (100 mg, 0.47 mmol) was dissolved in 2 mL of acetone/water (4:1) and cooled to 0°C. At that temperature Hg(OAc)₂ (37.4 mg, 0.118 mmol, 0.25 eq) was added, which turned the solution yellow. After 15 min 470 µL of Jones-reagent (2.5 M) were added dropwise. The mixture was allowed to warm to room temperature and was stirred for additional 15 h. After that time it was transferred to a separation funnel, mixed with 1 mL of water and extracted with Et₂O (4 x 3 ml). The crude product was purified by silica column chromatography (toluene/ethyl formate/formic acid = 5:4:1) to afford the desired product as yellow oil (85 mg, 0.37 mmol, 79%).

R_f (toluene/ethyl formate/formic acid = 5:4:1) = 0.22. - $[\alpha]_D^{20} = -30.7$ (MeCN, c = 1).

¹H NMR (600 MHz, CD₃CN): δ = 4.22 (d, *J* = 9.7 Hz, 1H), 4.02 (dd, *J* = 9.8, 6.0 Hz, 1H), 3.35 (dd, *J* = 21.5, 10.6 Hz, 2H), 3.15 (dd, *J* = 18.7, 10.9 Hz, 1H), 3.00 (dd, *J* = 27.8, 12.1 Hz, 2H), 2.54 (dd, *J* = 18.7, 3.6 Hz, 1H), 2.12 (s, 3H). - **¹³C NMR** (151 MHz, CD₃CN): δ = 206.2(C_q), 175.8(C_q), 174.0(C_q), 116.1(C_q), 69.3(-), 51.8(+), 49.9(-), 45.2(+), 36.3(-), 30.8(+). - **IR** (neat) $\tilde{\nu}$ = 3503, 2998, 2919, 1766, 1712, 1404, 1373, 1275, 1205, 1173, 1112, 1036, 999, 949, 926, 862, 653, 609 cm⁻¹. **HRMS** (ESI-MS, *m/z*): 227.0563 (C₁₀H₁₁O₆, calc. 227.0561 [(M-H)⁻]).

((3*S*,3*aS*,6*aS*)-5-oxo-6*a*-(2-oxopropyl)hexahydrofuro[2,3-*b*]furan-3-yl)methyl benzoate (5**)**

In a flamed dried flask under nitrogen atmosphere **189** (18 mg, 0.079 mmol) was dissolved in 1 mL of dry THF and cooled to -15 °C. To this solution BH₃·THF (solution 1 M in THF, 166 µL, 0.166 mmol, 2.1 eq) was added dropwise. After 4 h at -15 °C it was allowed to warm to room temperature. The solvent was evaporated under reduced pressure. The obtained crude product was dissolved in 1.5 mL of dry DCM, cooled to -40 °C and treated with DMAP (1 mg, 0.008 mmol, 0.1 eq), triethylamine (66 µL, 0.474 mmol, 6 eq) and benzoyl chloride (10 µL, 0.083 mmol, 1.05 eq). The reaction was allowed to warm to -10 °C. After 1.5 d it was transferred to a separation funnel, treated with 1 mL of a half saturated NH₄Cl solution and extracted with Et₂O (3 x 2 mL). The combined organic layers were dried over Na₂SO₄, filtered and concentrated under reduced pressure. The crude product was again dissolved in 2 mL of dry DCM, cooled to 0 °C and treated with solid DMP (33.5 mg, 0.079 mmol, 1 eq). After 3 h at that temperature it was warmed to room temperature and transferred to a separation funnel. The mixture was washed with saturated NaHCO₃ solution (2 x 1 mL). The combined aqueous layers were extracted with DCM (2 x 1 mL). The combined organic layers were dried over Na₂SO₄, filtered and concentrated under reduced pressure. The crude product was purified by silica column chromatography (PE/EA = 2:1) to afford the clean **5** as white needles (11 mg, 0.035 mmol, 44% based on **189**).

R_f (PE/EA = 1:1) = 0.50. -[α]_D²⁰ = -42.0 (CHCl₃, c = 0.17).

¹H NMR (600 MHz, CDCl₃): δ = 8.02 (dd, *J* = 8.1, 1.0 Hz, 2H), 7.60 (tt, *J* = 7.2, 1.2 Hz, 1H), 7.47 (t, *J* = 7.8 Hz, 2H), 4.29 (dd, *J* = 11.0, 7.3 Hz, 1H), 4.19 (dd, *J* = 11.0, 8.0 Hz, 1H), 4.03 (qd, *J* = 9.9, 3.4 Hz, 2H), 3.40 (d, *J* = 17.7 Hz, 1H), 3.34 (dd, *J* = 18.6, 10.5 Hz, 1H), 2.99 - 2.93 (m, 2H), 2.58 - 2.51 (m, 2H), 2.20 (s, 3H).

¹³C NMR (75 MHz, CDCl₃): δ = 204.5(C_q), 174.6(C_q), 166.5(C_q), 133.5(+), 129.7(+), 129.6(C_q), 128.7(+), 115.1(C_q), 68.0(-), 65.0(-), 49.6(-), 46.8(+), 44.5(+), 36.7(-), 31.0(+). - **IR** (neat): $\tilde{\nu}$ = 2984, 1703, 1401, 1366, 1320, 1197, 1152, 1116, 1074, 981, 952, 927, 870, 841, 779, 725, 674 cm⁻¹. - **MS** (ESI-MS, m/z): 456 (19), 455 ((2M-H)⁻, 82), 274 (13), 273 (M+HCOO⁻, 100), 277 ((M-H)⁻, 3). - **HRMS** (ESI-MS, m/z): 227.0927 (C₁₁H₁₅O₅, calc. 227.0925 [(M-H)⁻]). - **mp**: 152 °C.

E. Appendix

1. NMR spectra

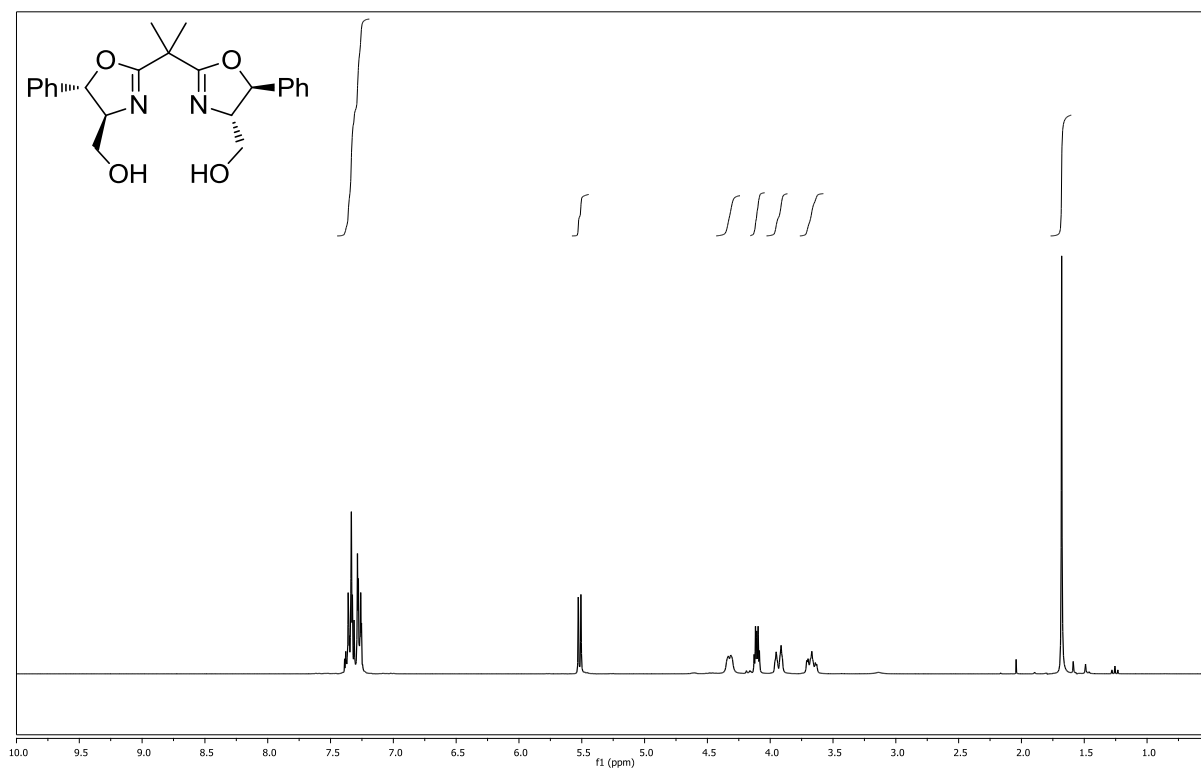
^1H -NMR spectra: upper image

^{13}C -NMR spectra (DEPT 135 integrated): lower image

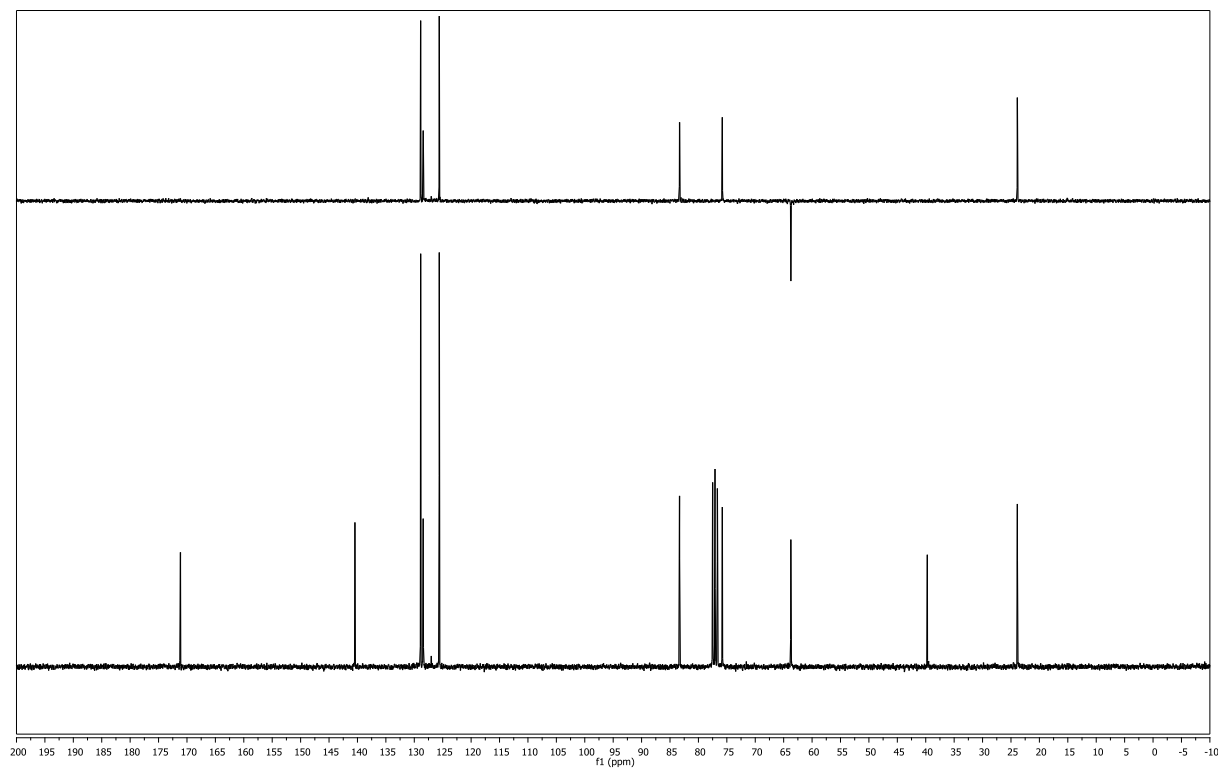
Used solvent and MHz are stated at the actual spectra.

((4*S*,4'*S*,5*S*,5'*S*)-2,2'-(propane-2,2-diyl)bis(5-phenyl-4,5-dihydrooxazole-4,2-diyl))dimethanol (85)

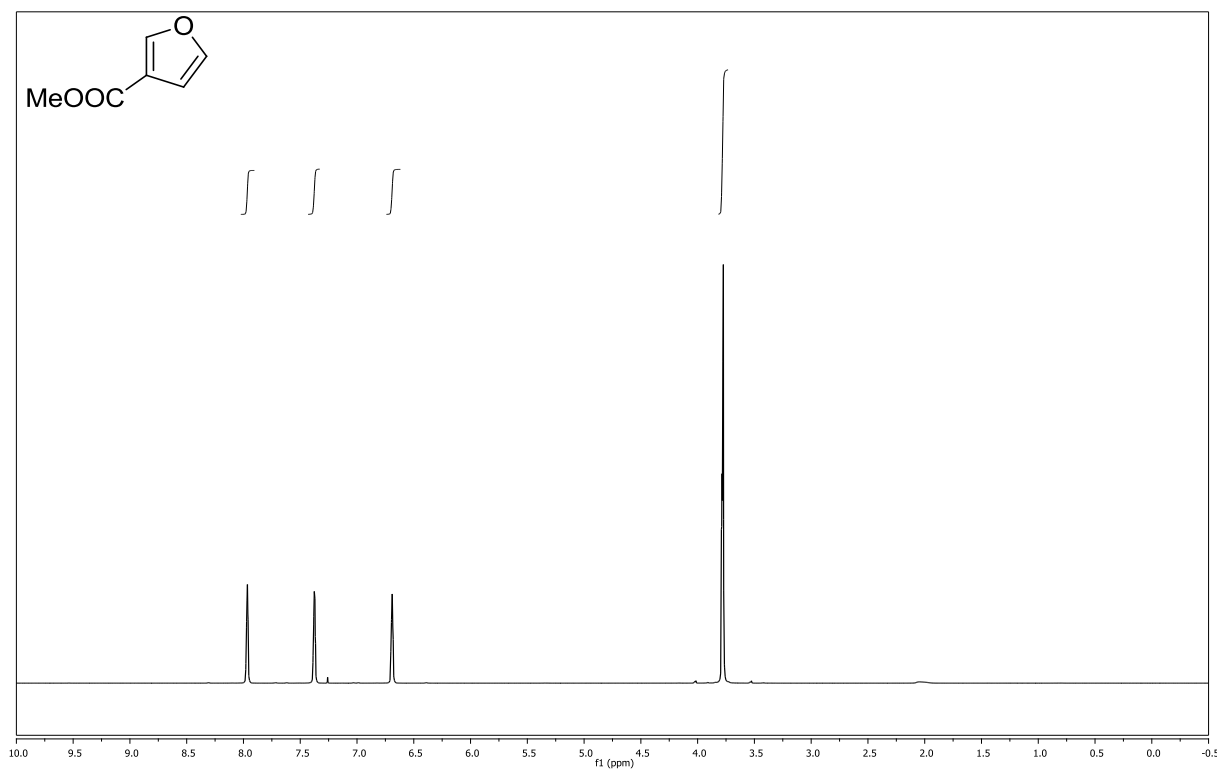
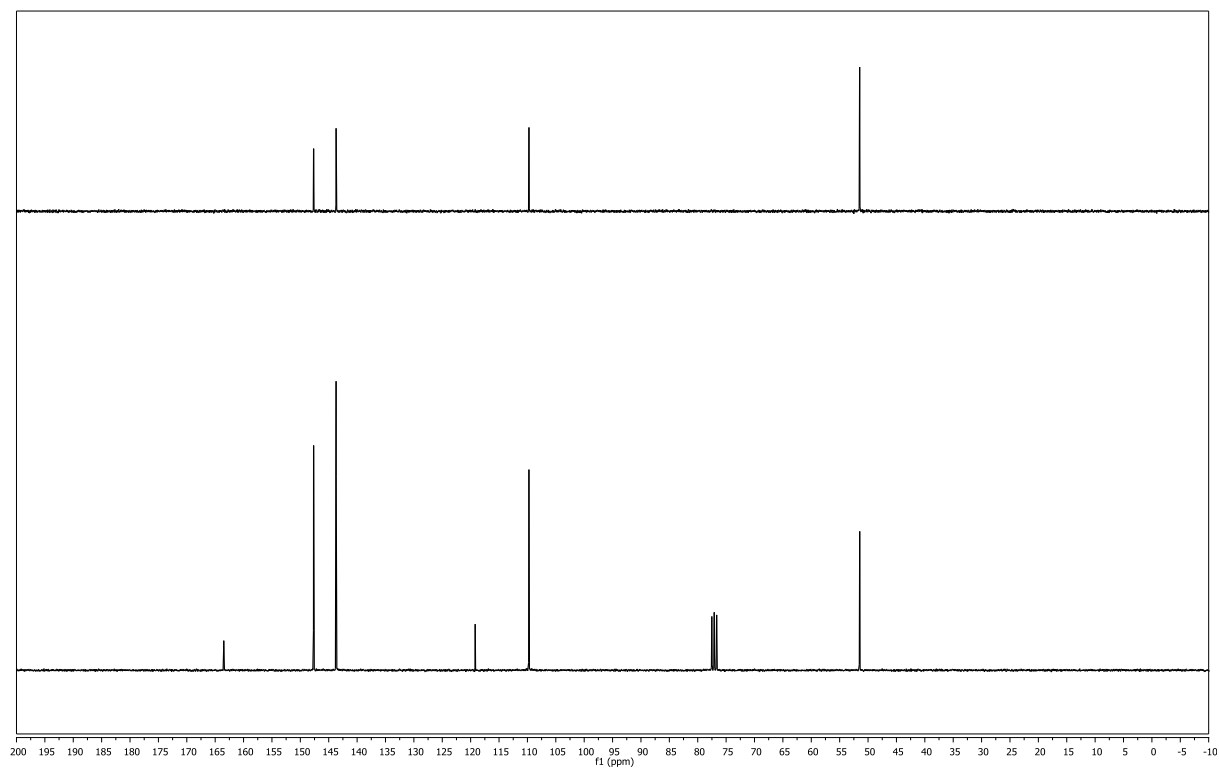
(CDCl₃, 300 MHz)



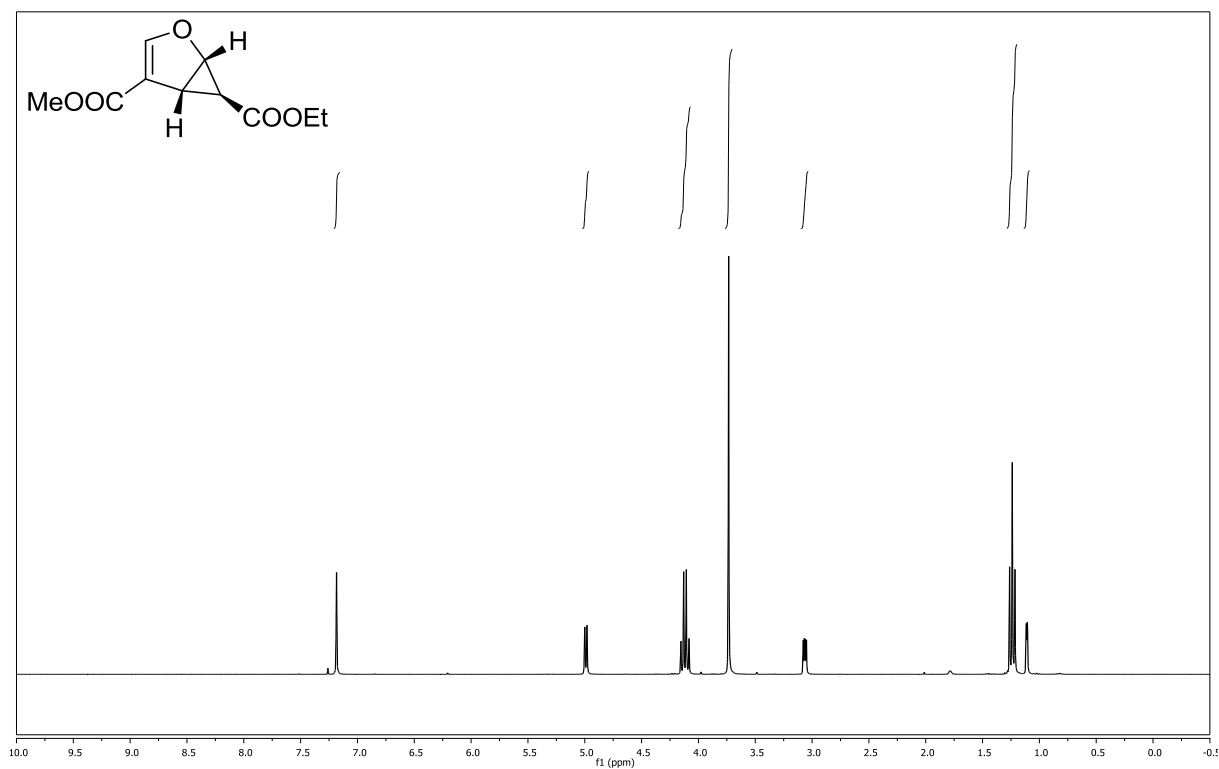
(CDCl₃, 75 MHz)



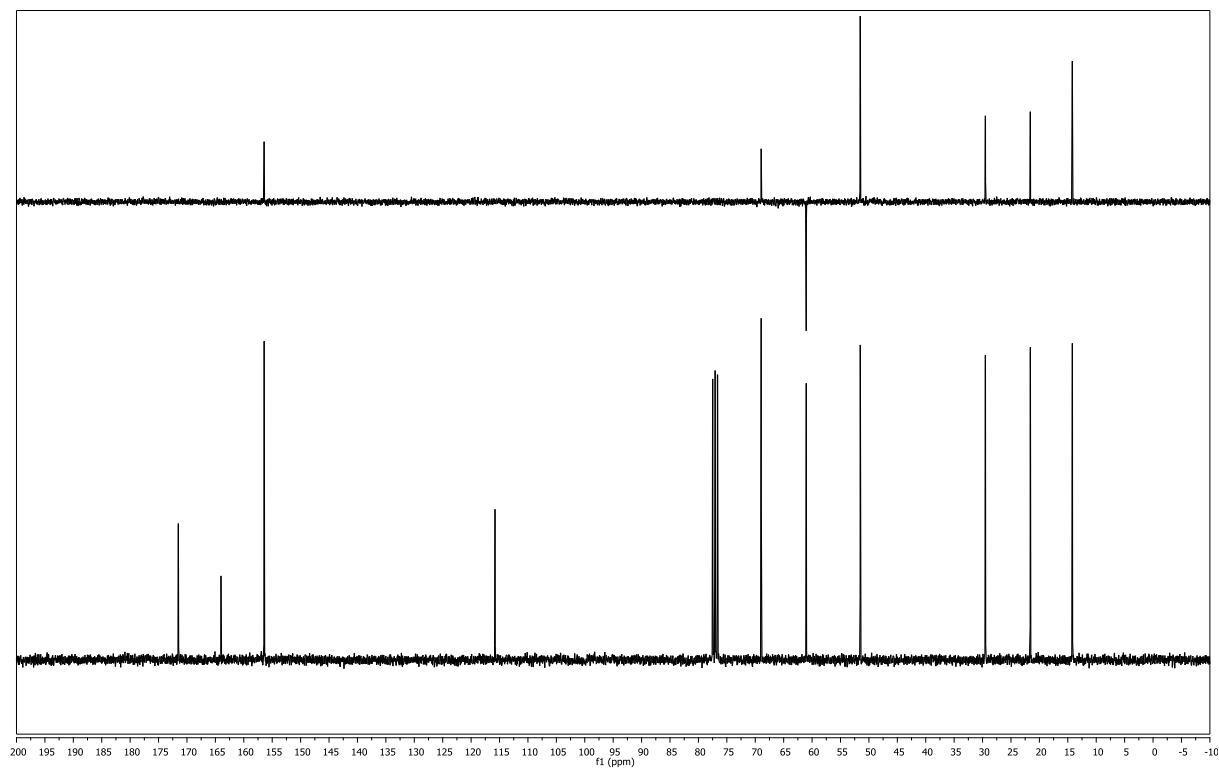
methyl furan-3-carboxylate (78)

(CDCl₃, 300 MHz)(CDCl₃, 75 MHz)

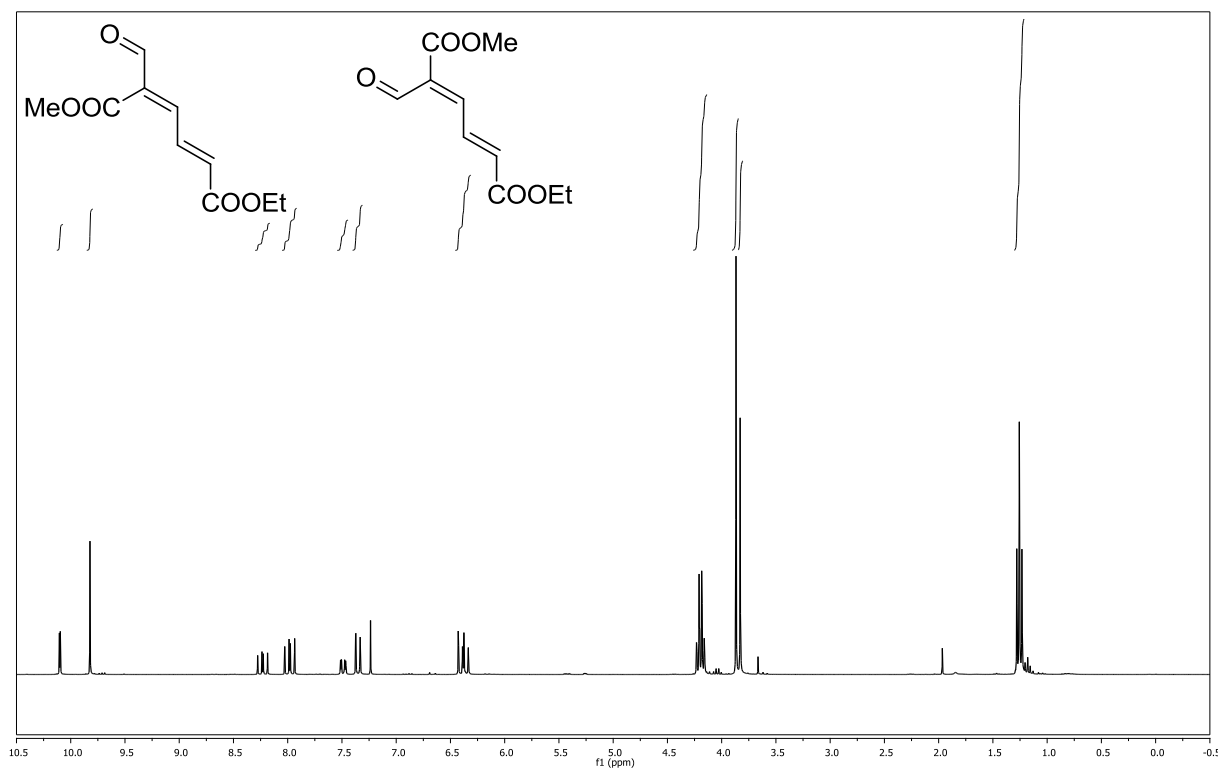
(1*S*,5*R*,6*S*)-6-ethyl 4-methyl 2-oxabicyclo[3.1.0]hex-3-ene-4,6-dicarboxylate
(119) **(CDCl₃, 300 MHz)**



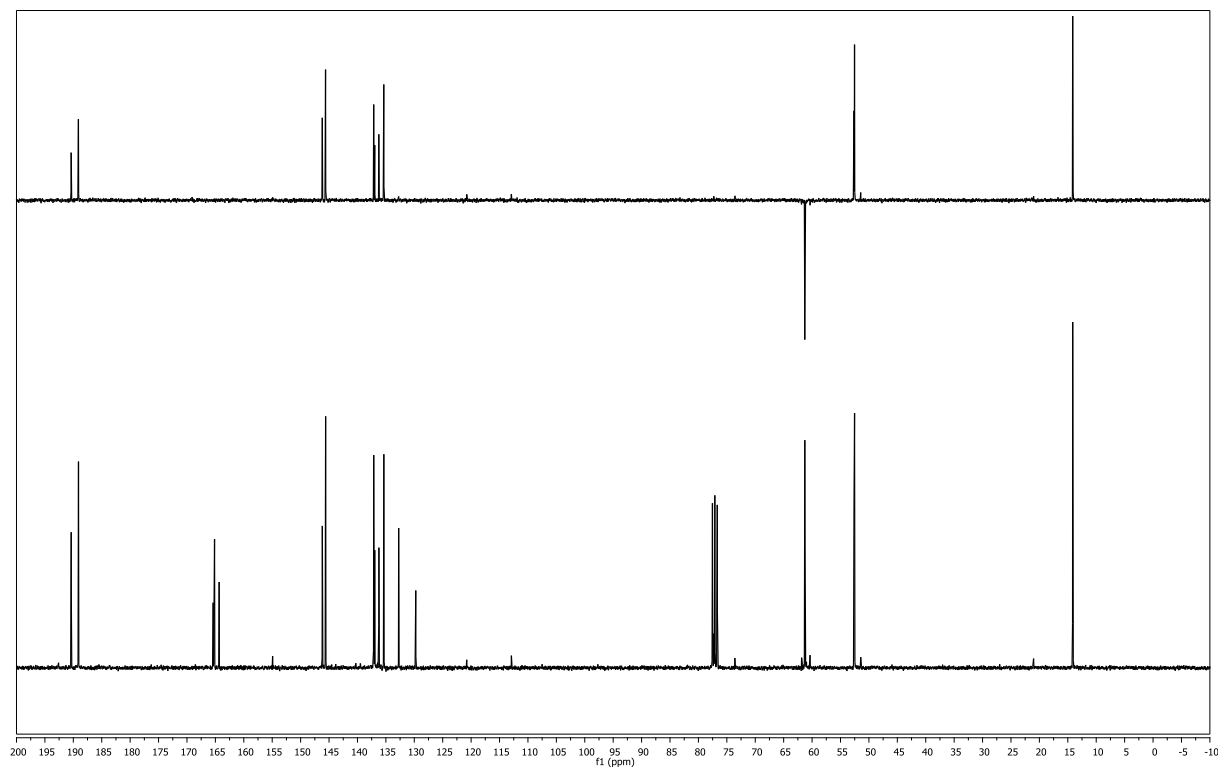
(CDCl₃, 75 MHz)



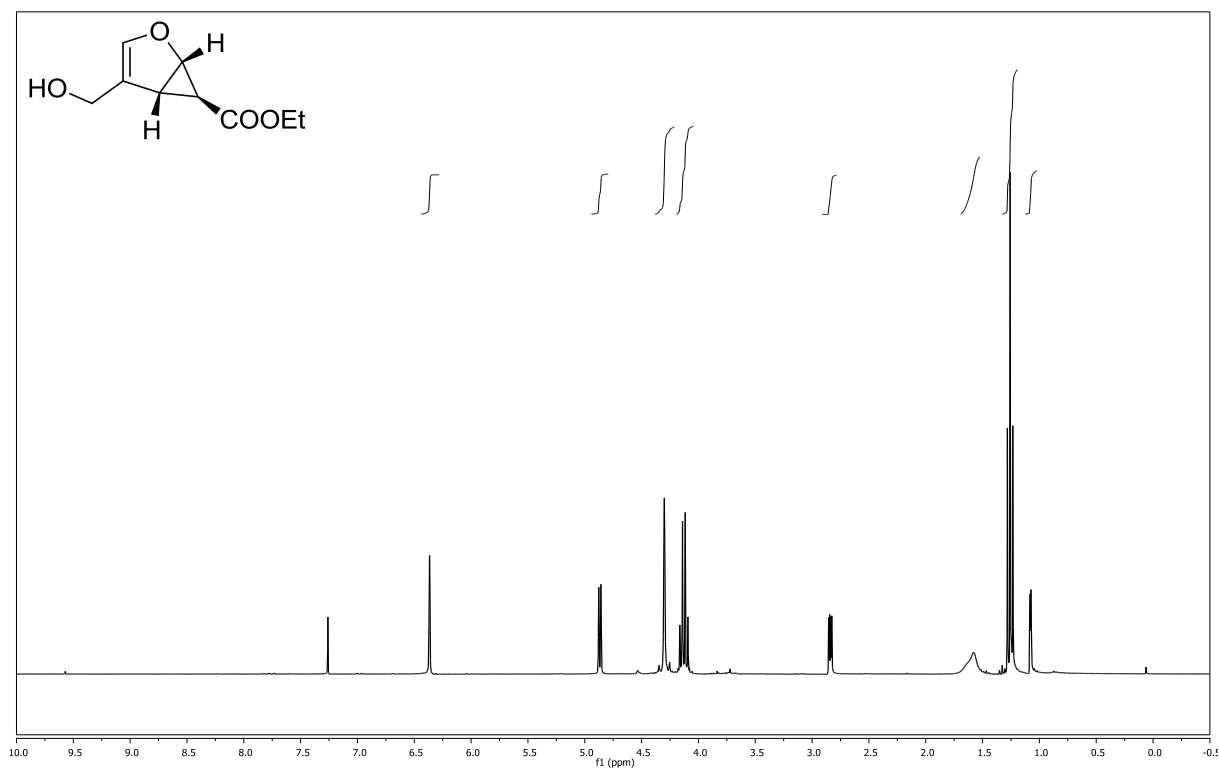
(2Z,4E)-6-ethyl 1-methyl 2-formylhexa-2,4-dienedioate (Z/E-127) and (2E,4E)-6-ethyl 1-methyl 2-formylhexa-2,4-dienedioate (E/E-127) (CDCl₃, 600 MHz)



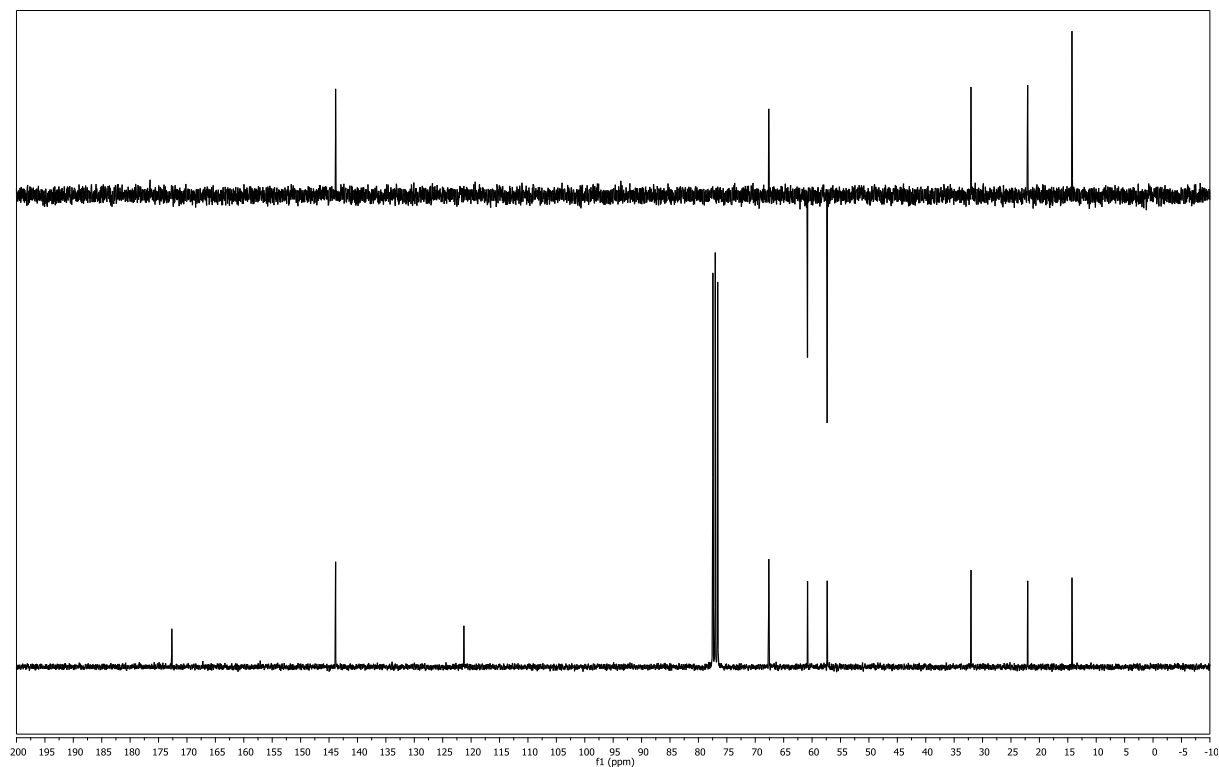
(CDCl₃, 151 MHz)



(1*S*,5*R*,6*S*)-ethyl-4-(hydroxymethyl)-2-oxabicyclo[3.1.0]hex-3-ene-6-carboxylate
(131) **(CDCl₃, 300 MHz)**

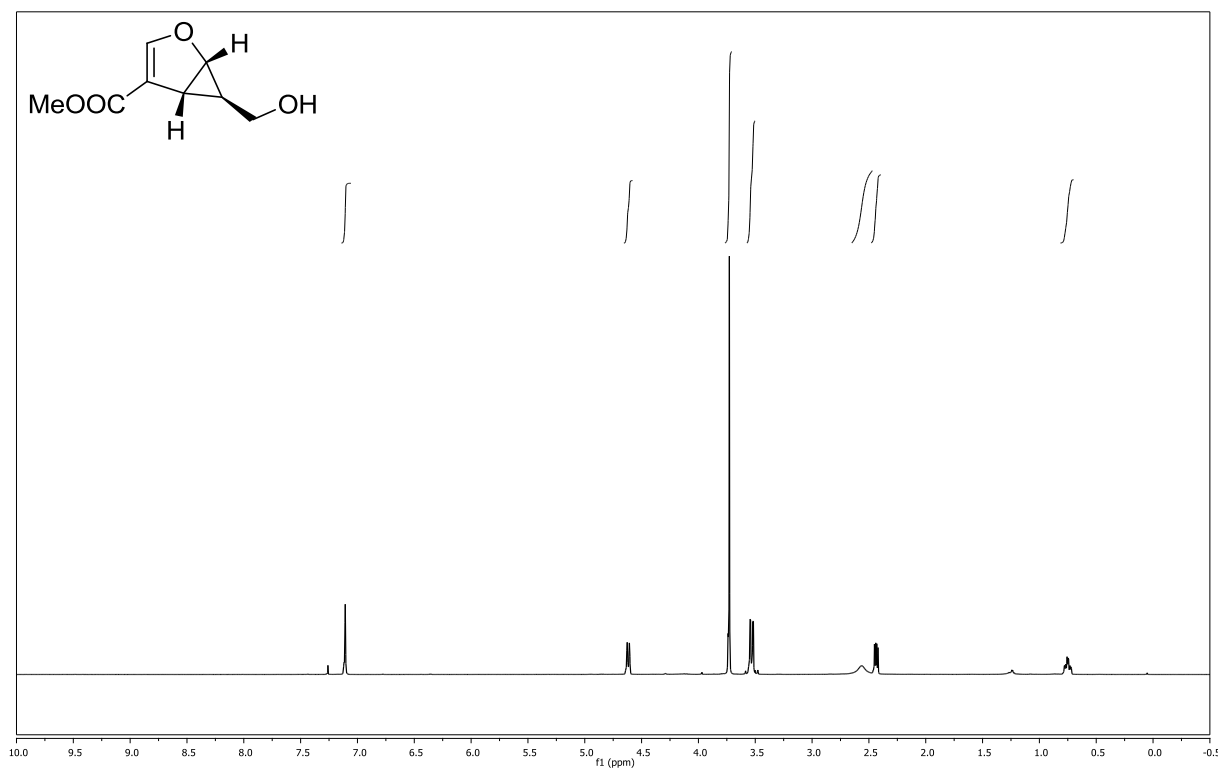


(CDCl₃, 75 MHz)

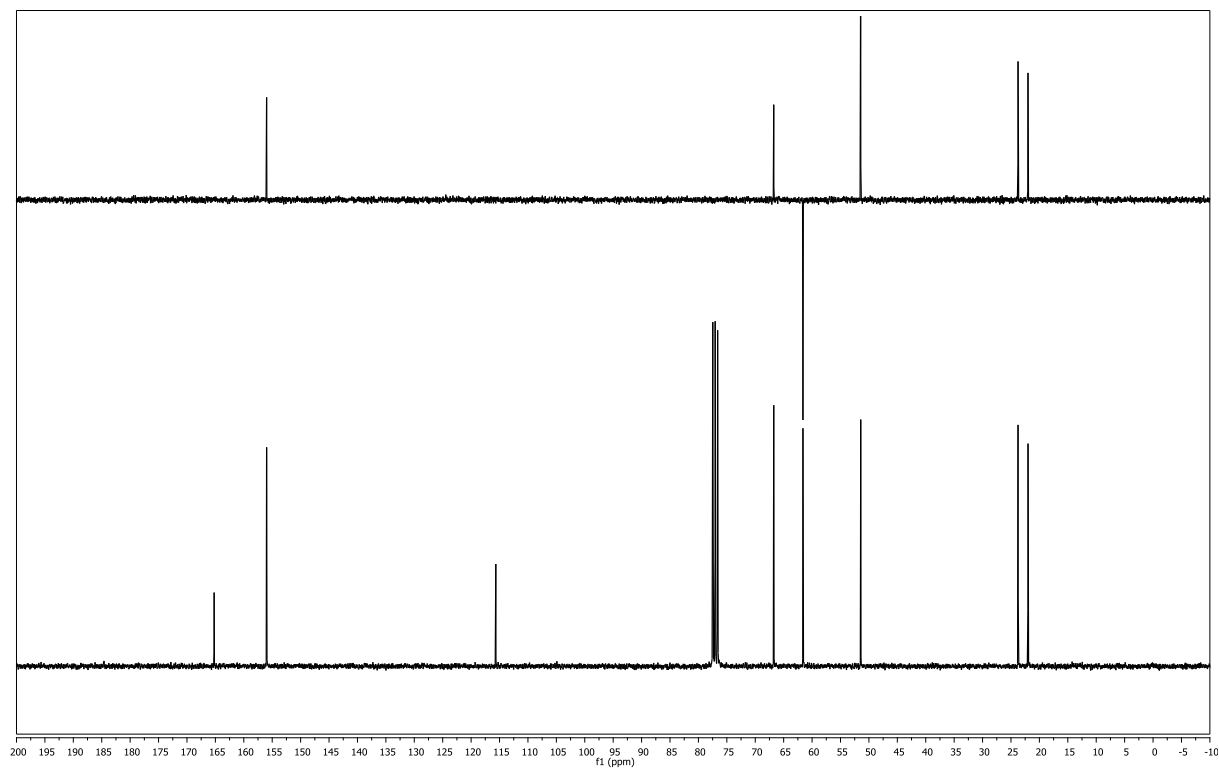


(1*S*,5*R*,6*R*)-methyl-6-(hydroxymethyl)-2-oxabicyclo[3.1.0]hex-3-ene-4-carboxylate (132)

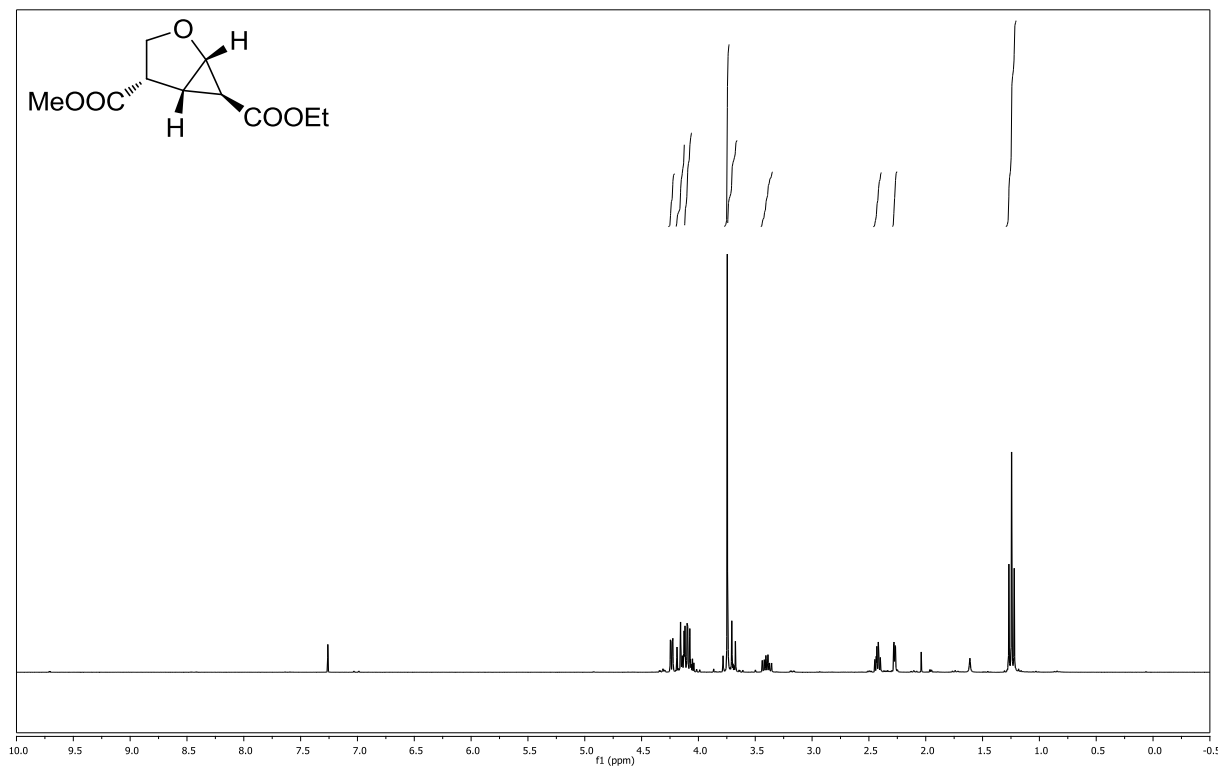
(CDCl₃, 300 MHz)



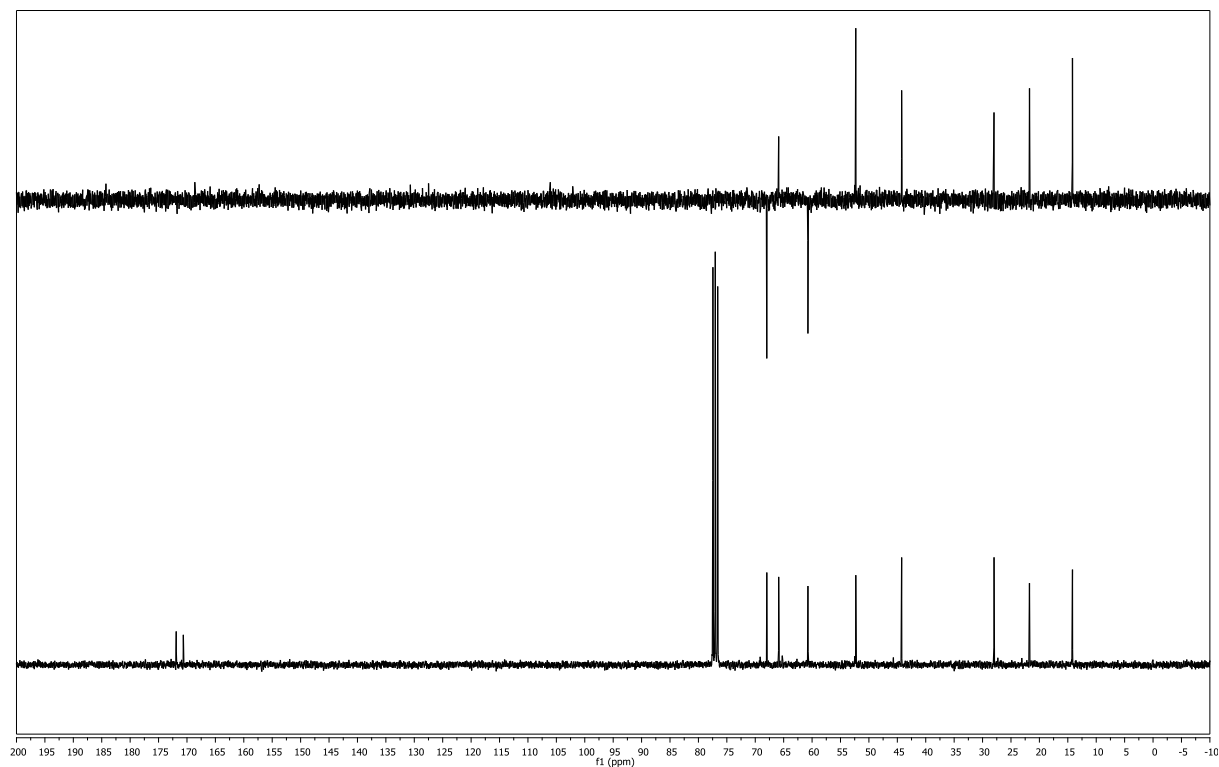
(CDCl₃, 75 MHz)



(1*S*,4*S*,5*S*,6*S*)-6-ethyl 4-methyl 2-oxabicyclo[3.1.0]hexane-4,6-dicarboxylate
(133) **(CDCl₃, 300 MHz)**

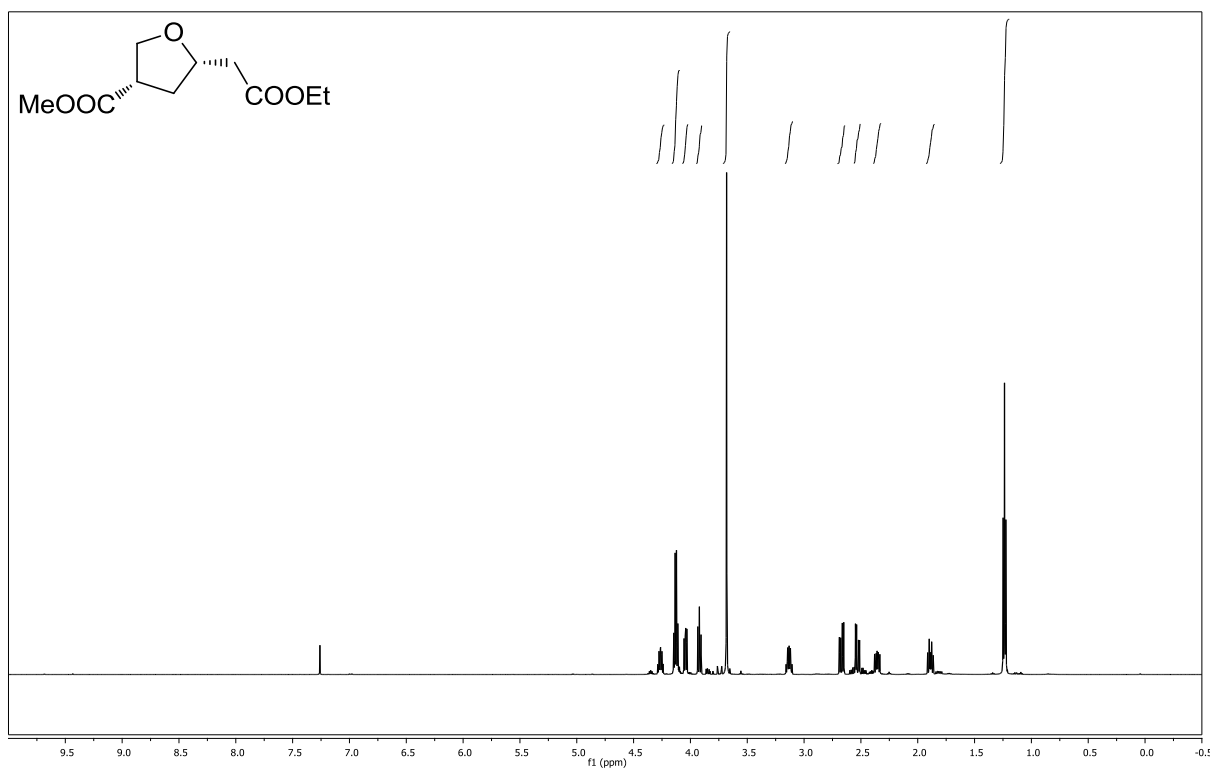


(CDCl₃, 75 MHz)

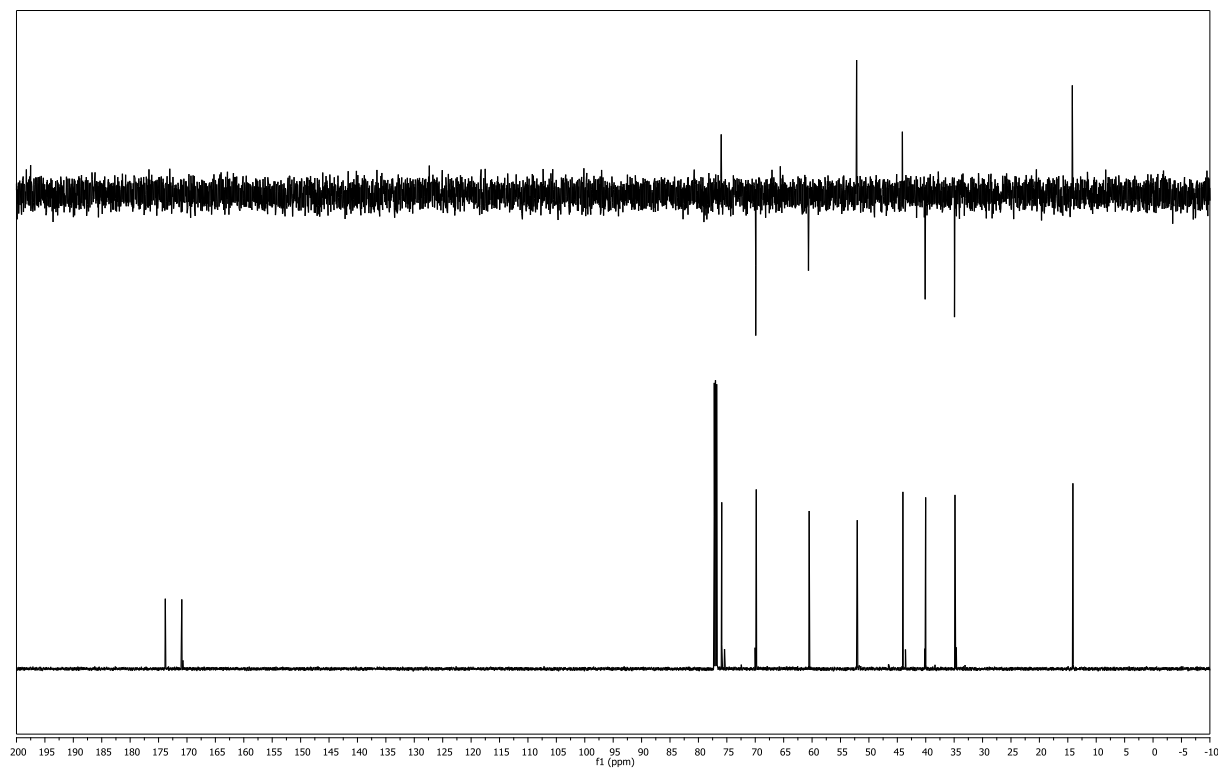


(3*S*,5*S*)-methyl 5-(2-ethoxy-2-oxoethyl)tetrahydrofuran-3-carboxylate (134)

(CDCl₃, 600 MHz)

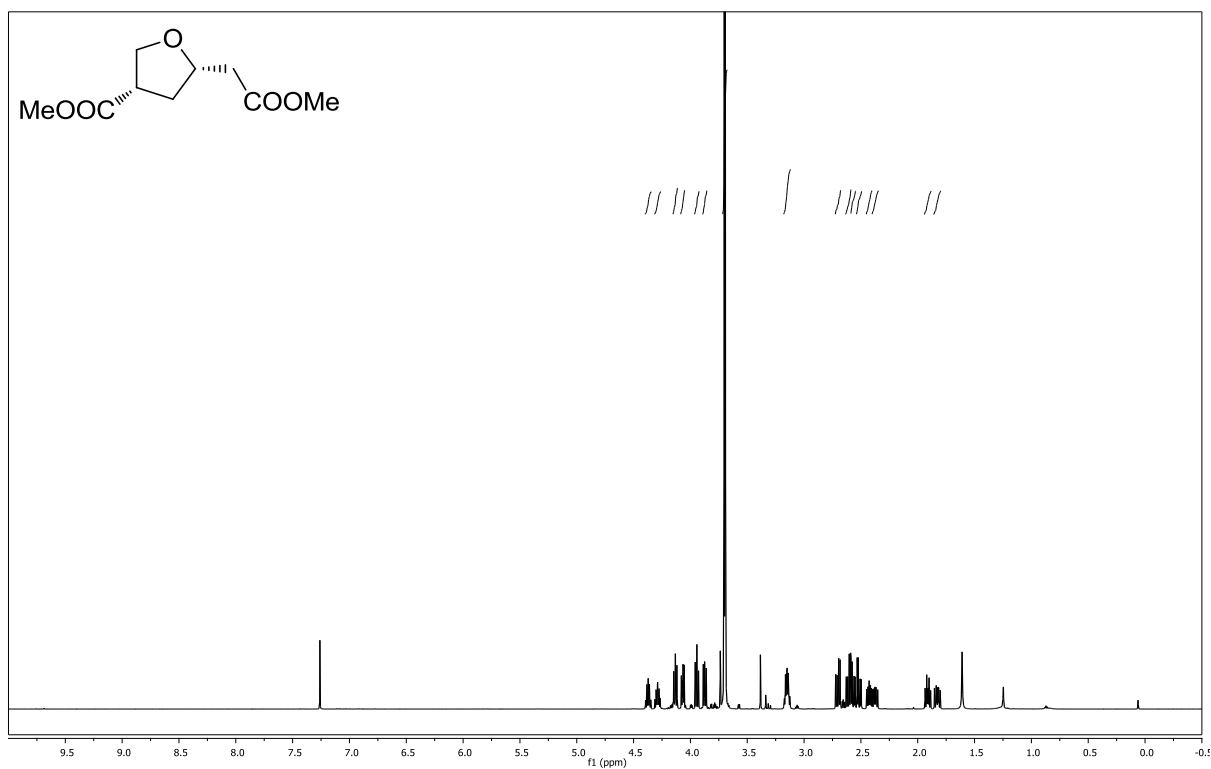


(CDCl₃, 151 MHz)

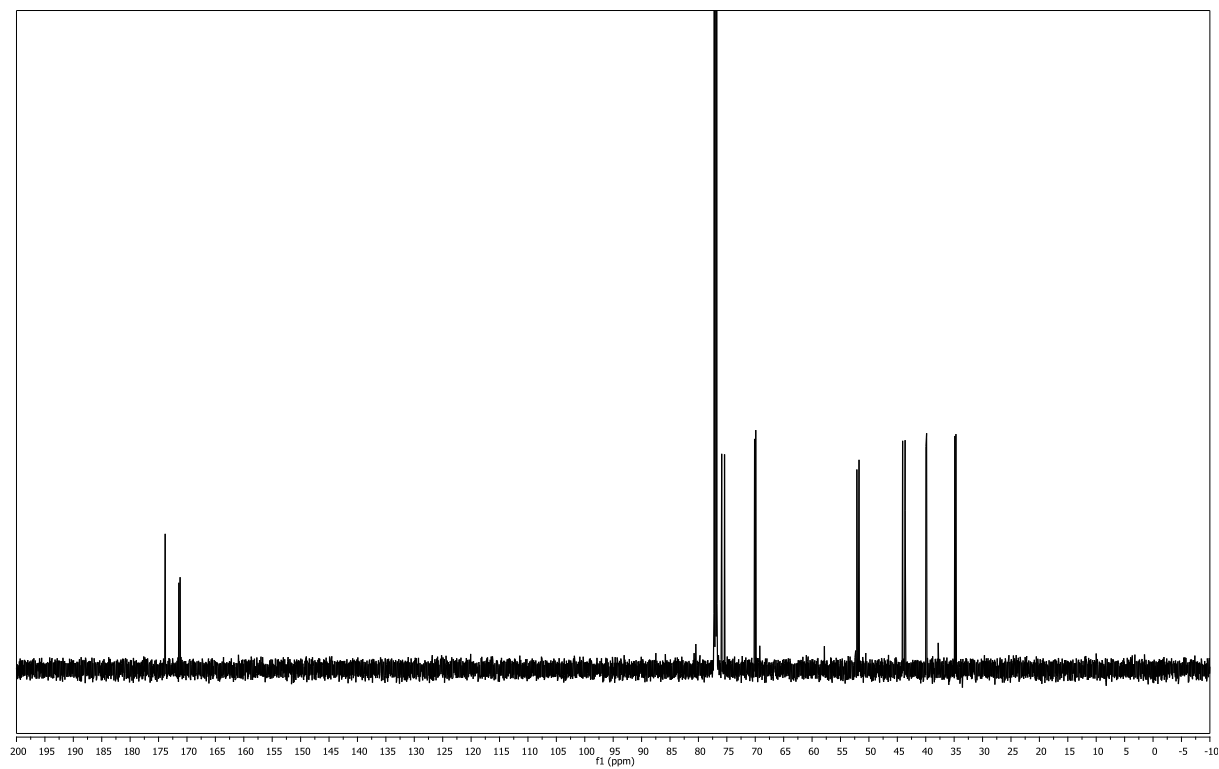


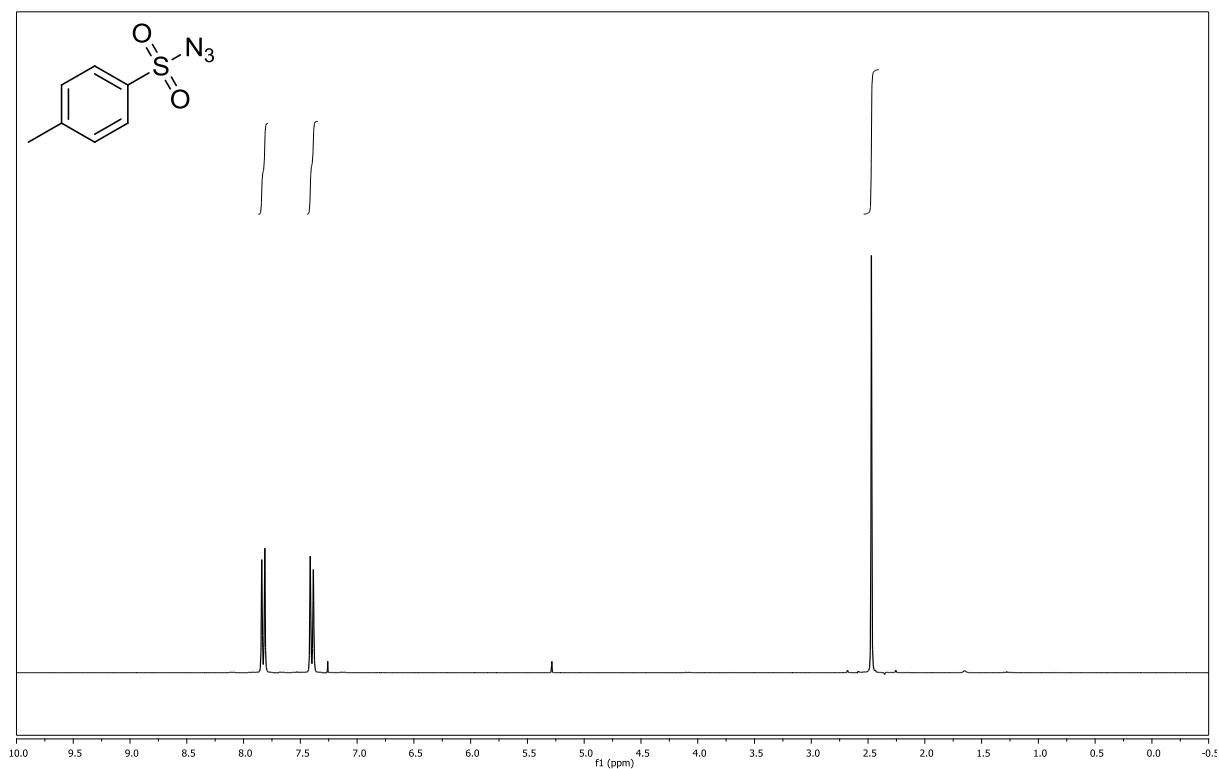
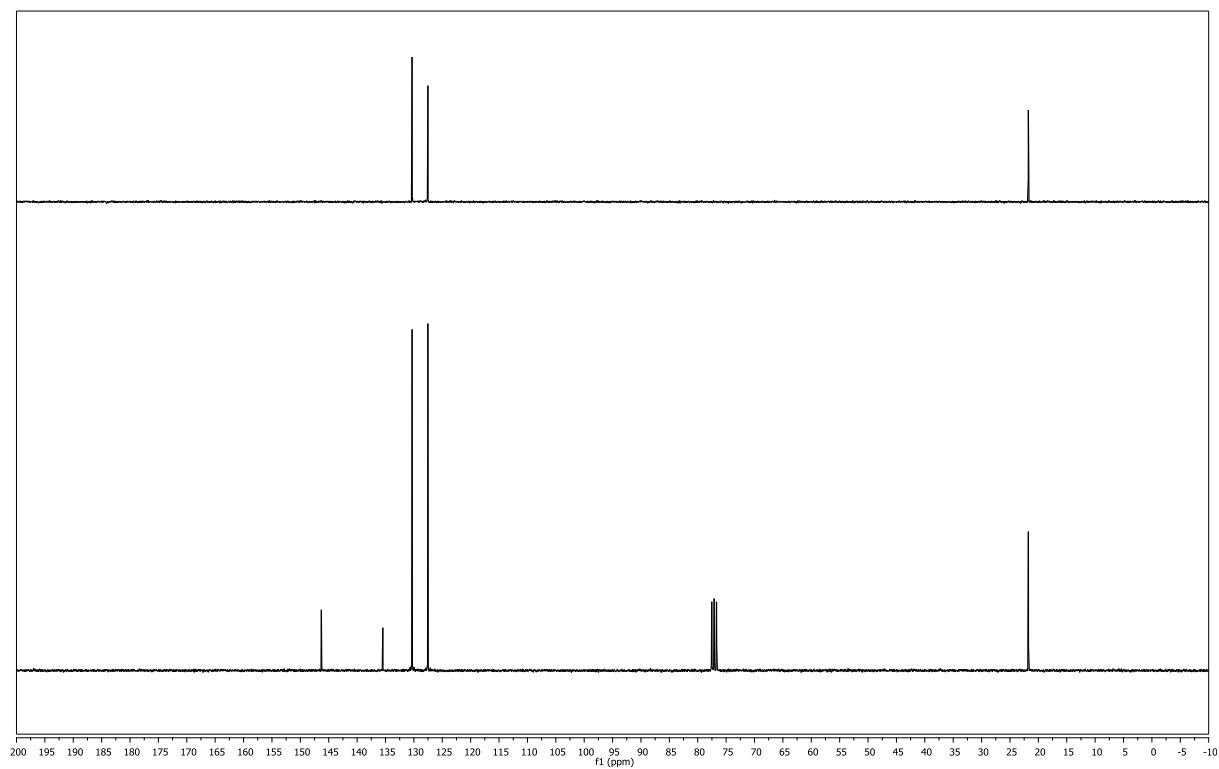
(5*S*)-methyl 5-(2-methoxy-2-oxoethyl)tetrahydrofuran-3-carboxylate (135)

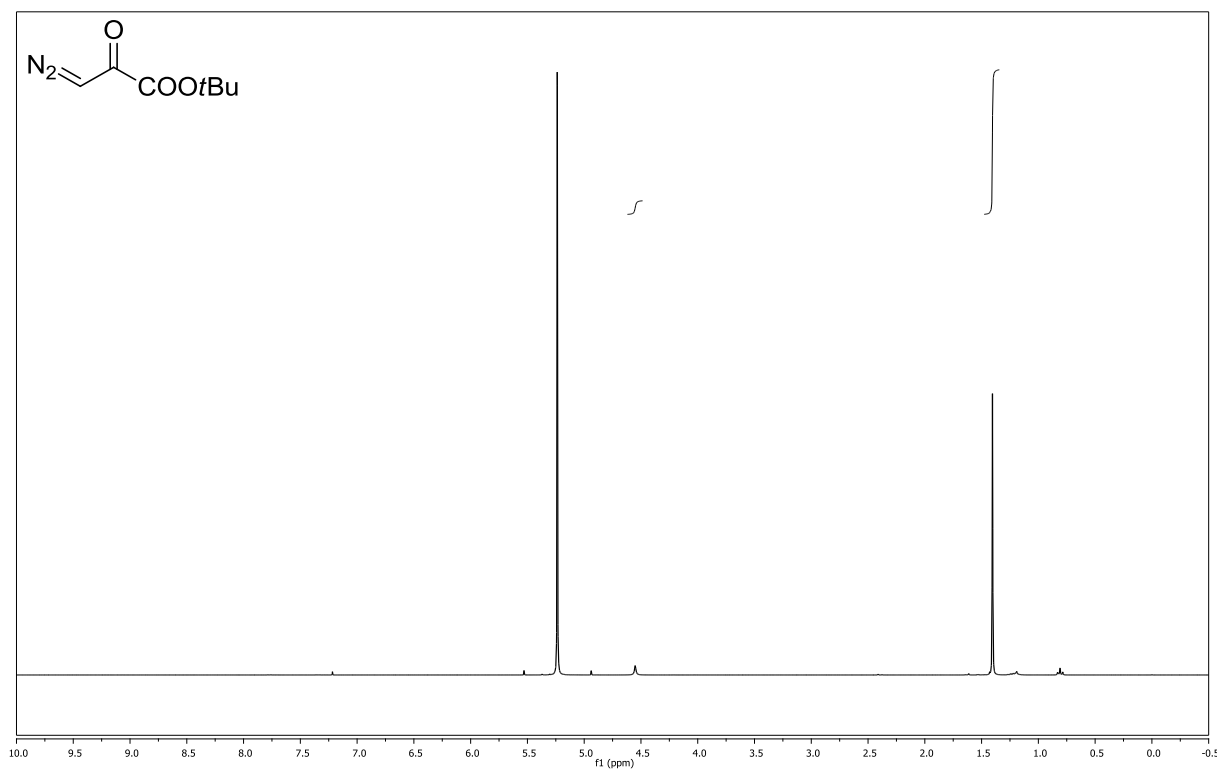
(CDCl₃, 600 MHz)



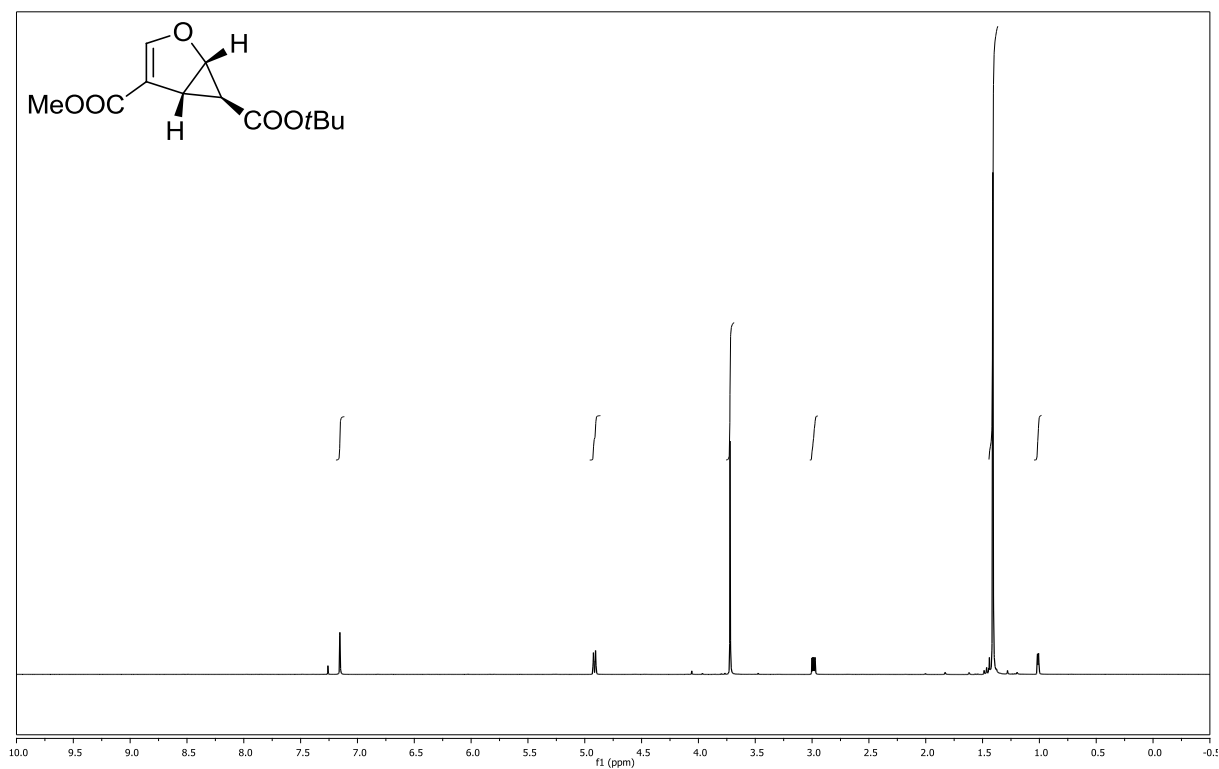
(CDCl₃, 151 MHz)



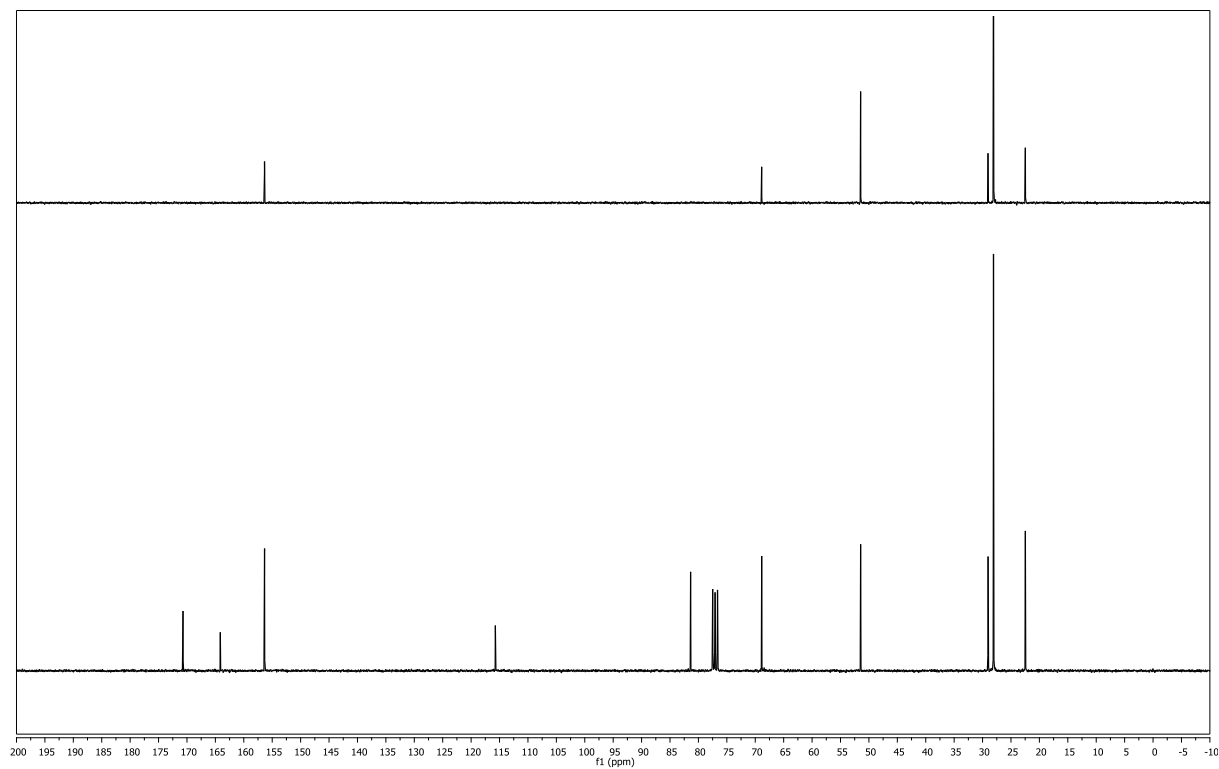
4-methylbenzenesulfonyl azide (87)**(CDCl₃, 300 MHz)****(CDCl₃, 75 MHz)**

tert*-butyl 3-diazo-2-oxopropanoate (89)*(CDCl₃, 300 MHz)**

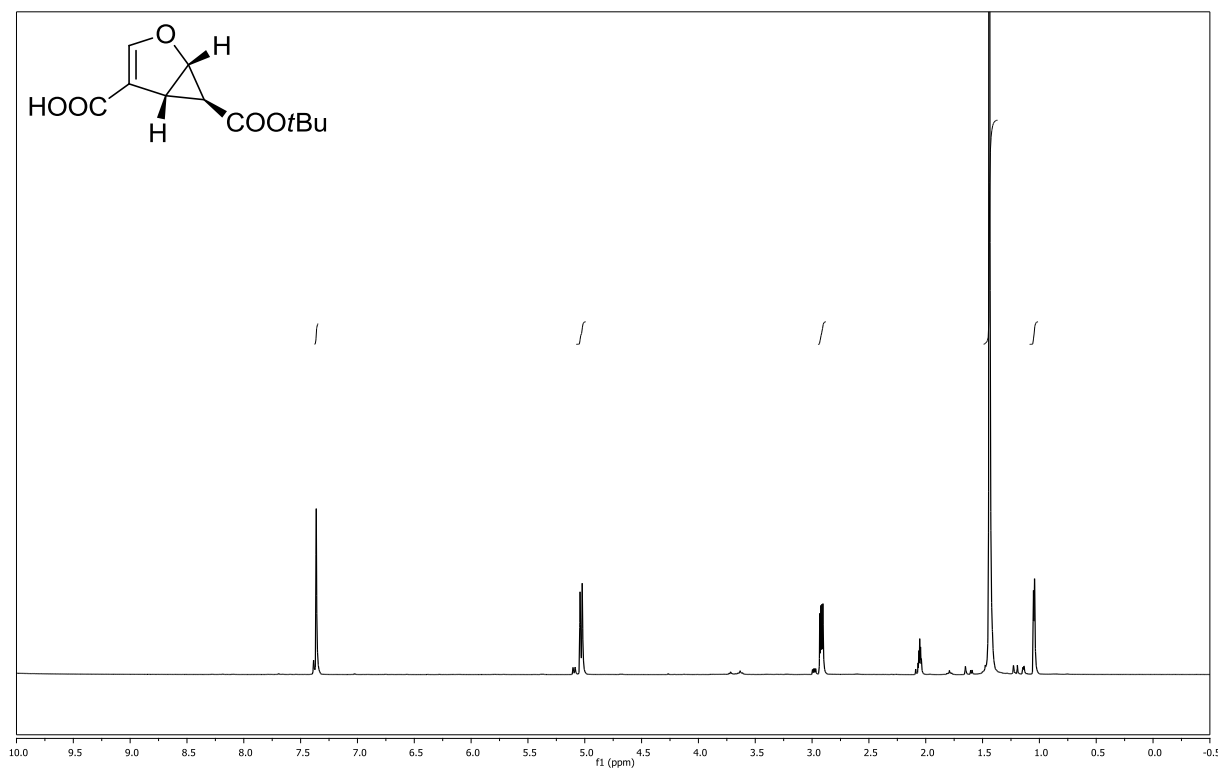
(1*S*,5*R*,6*S*)-6-*tert*-butyl 4-methyl 2-oxabicyclo[3.1.0]hex-3-ene-4,6-dicarboxylate
(118) **(CDCl₃, 300 MHz)**



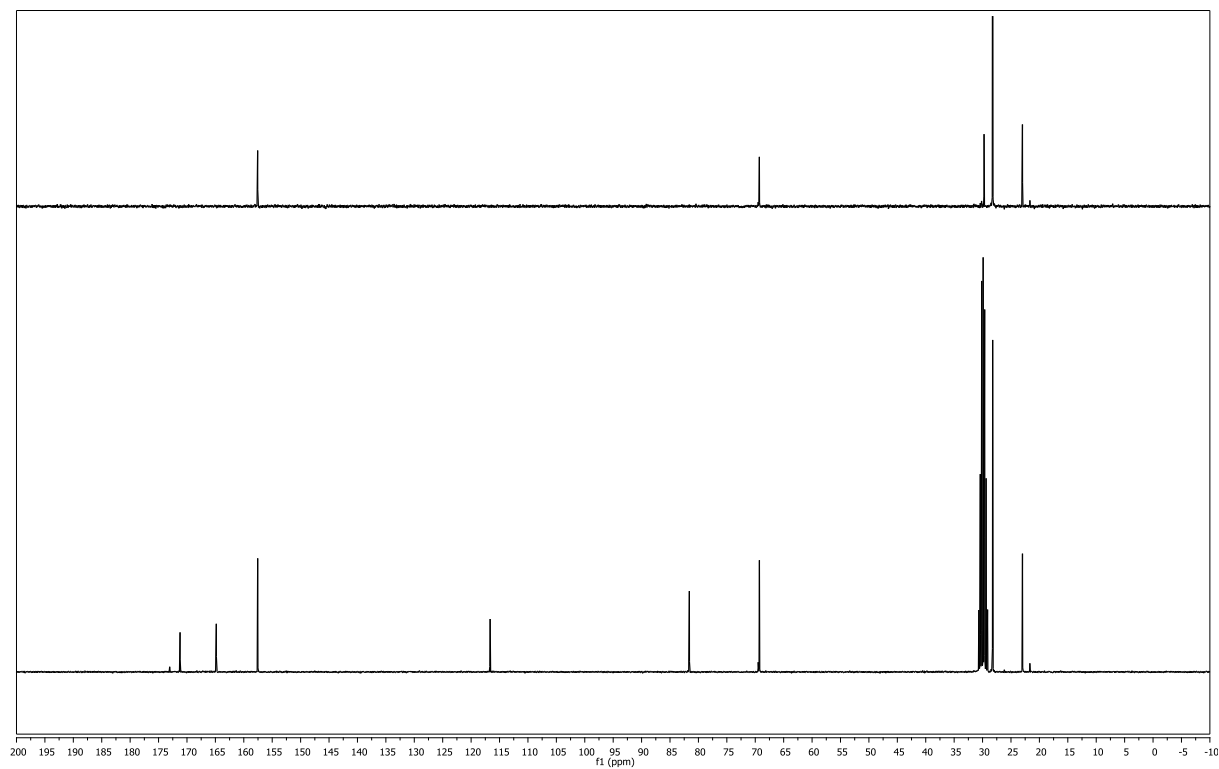
(CDCl₃, 75 MHz)



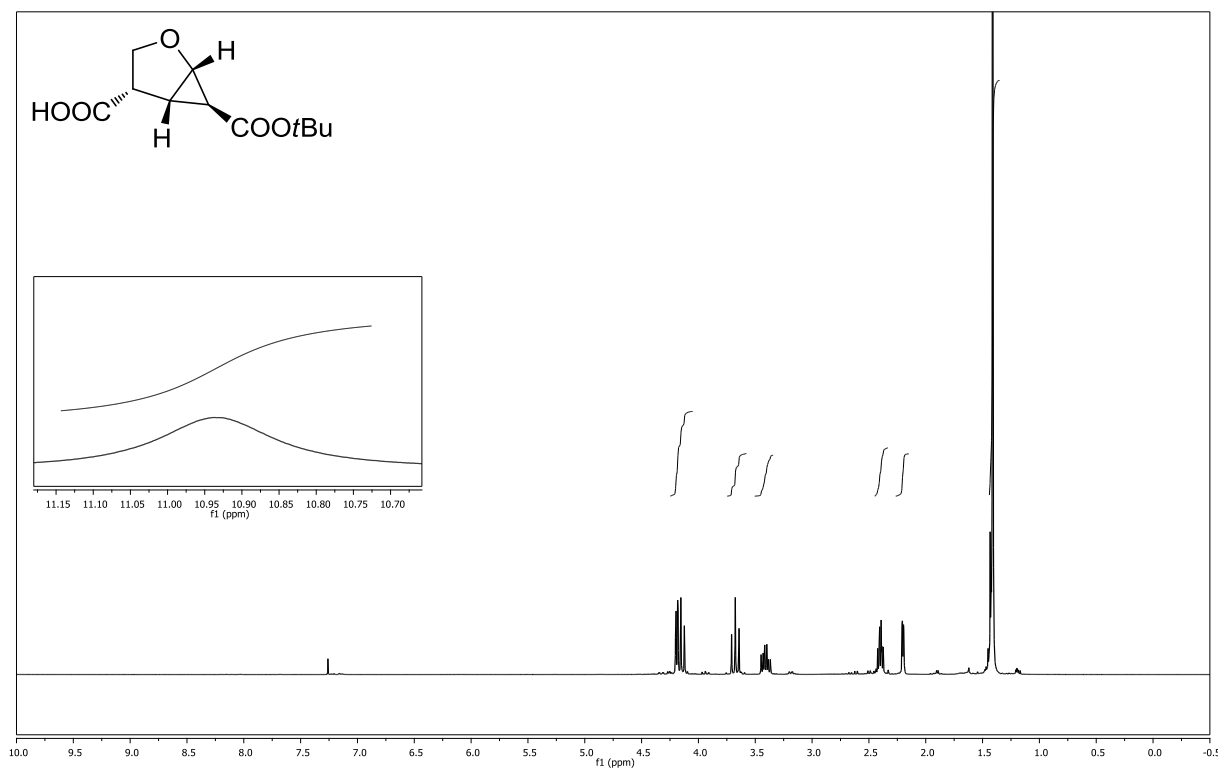
(1*S*,5*R*,6*S*)-6-(*tert*-butoxycarbonyl)-2-oxabicyclo[3.1.0]hex-3-ene-4-carboxylic acid (138)
(acetone-*d*₆, 300 MHz)



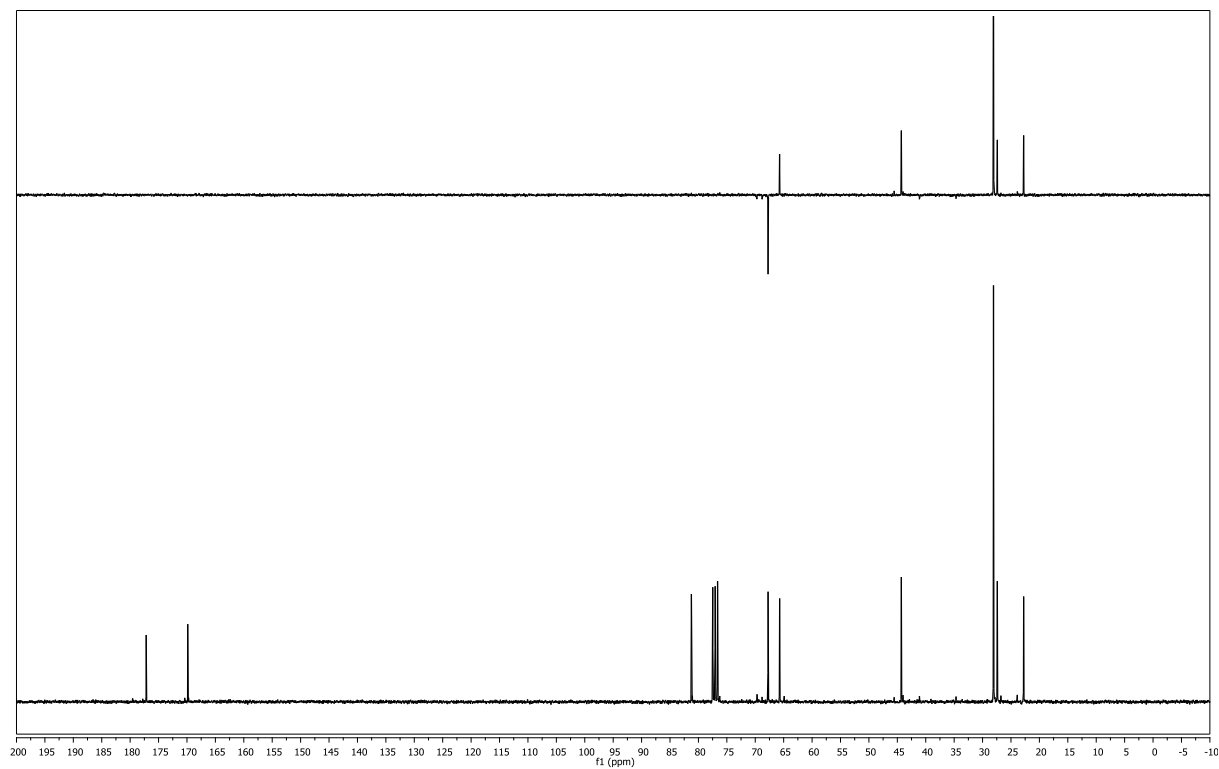
(acetone-*d*₆, 75 MHz)



(1*S*,4*S*,5*S*,6*S*)-6-(*tert*-butoxycarbonyl)-2-oxabicyclo[3.1.0]hexane-4-carboxylic acid (139)
(CDCl₃, 300 MHz)

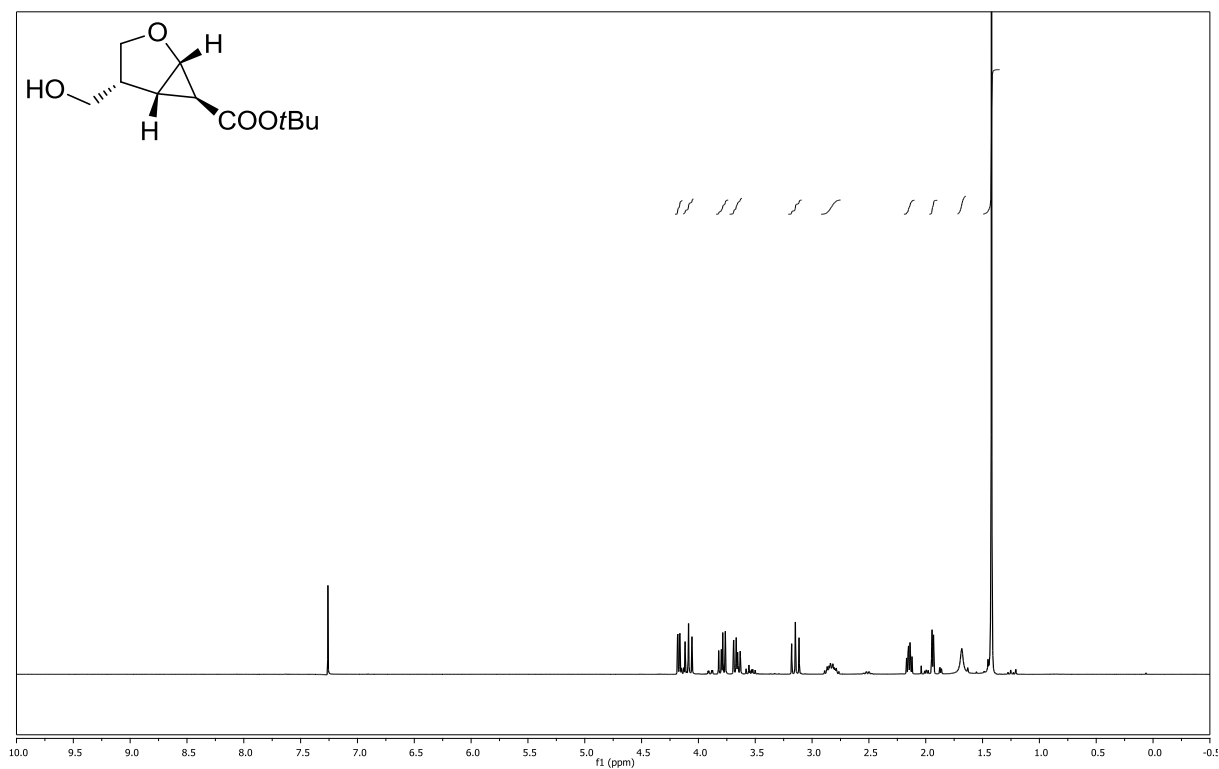


(CDCl₃, 75 MHz)

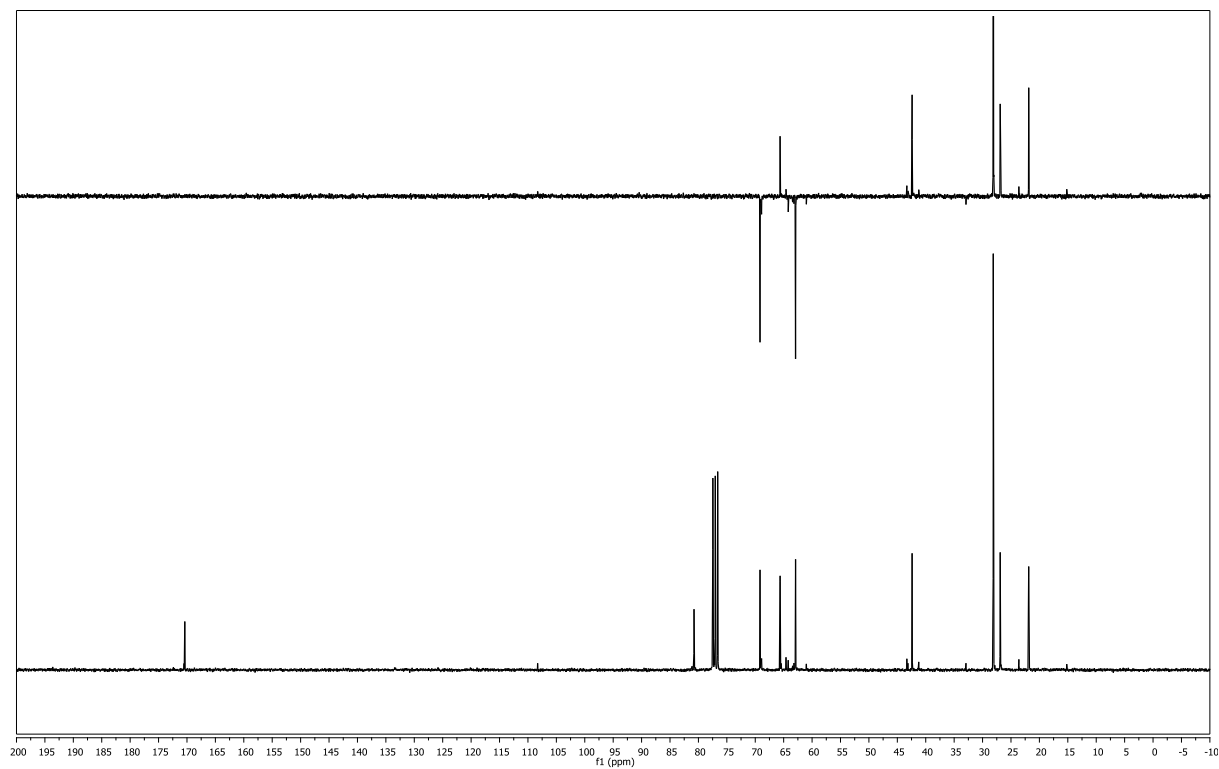


(1*S*,4*R*,5*S*,6*S*)-*tert*-butyl-4-(hydroxymethyl)-2-oxabicyclo[3.1.0]hexane-6-carboxylate (140)

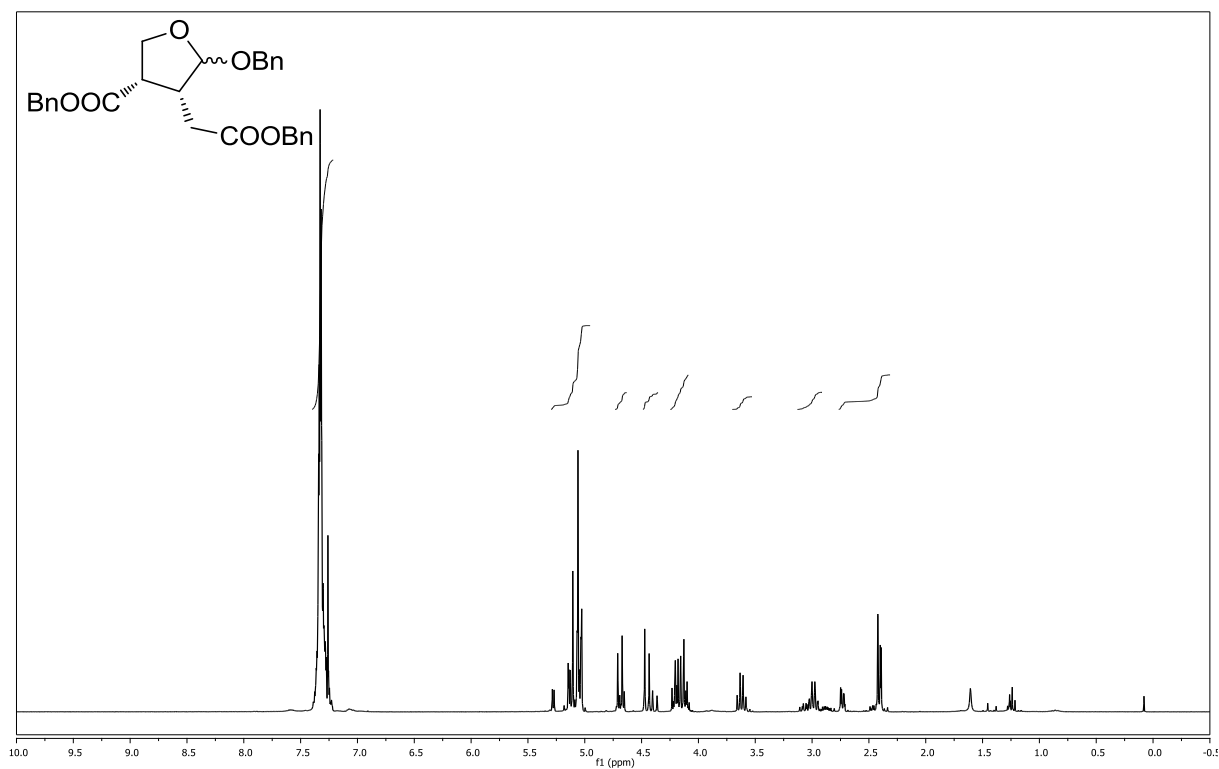
(CDCl₃, 300 MHz)



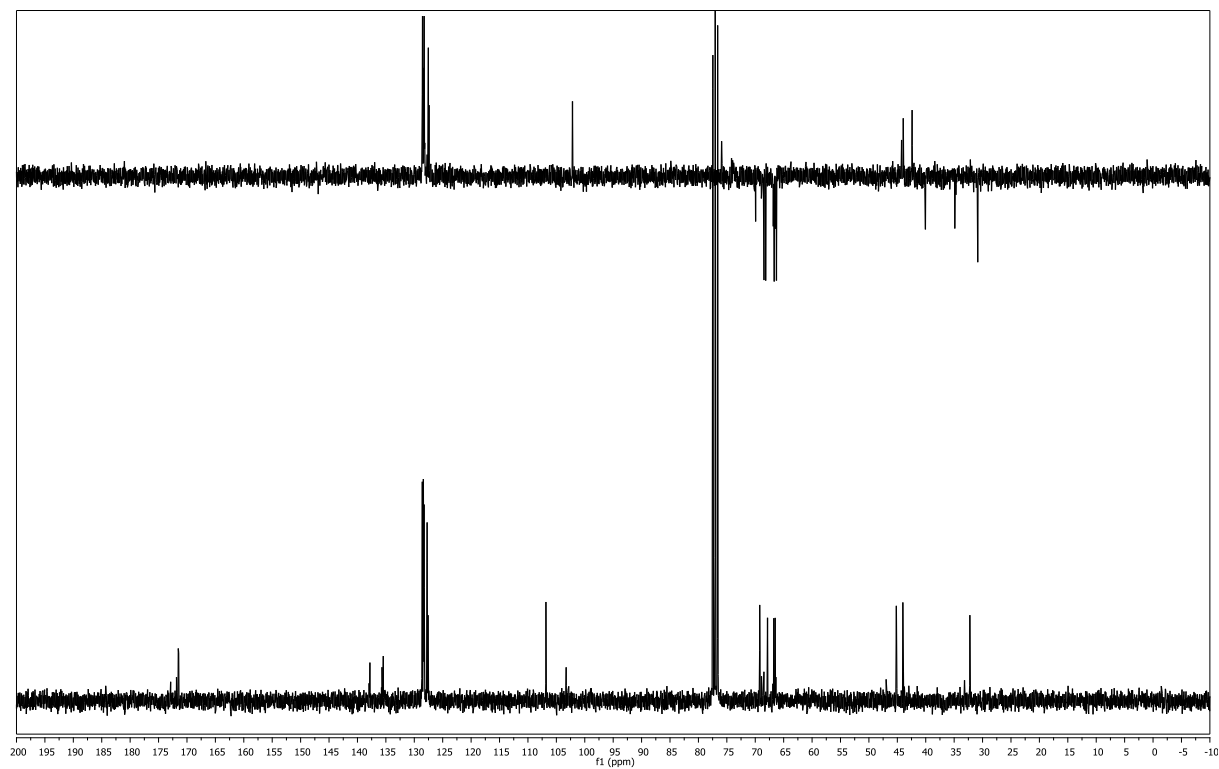
(CDCl₃, 75 MHz)

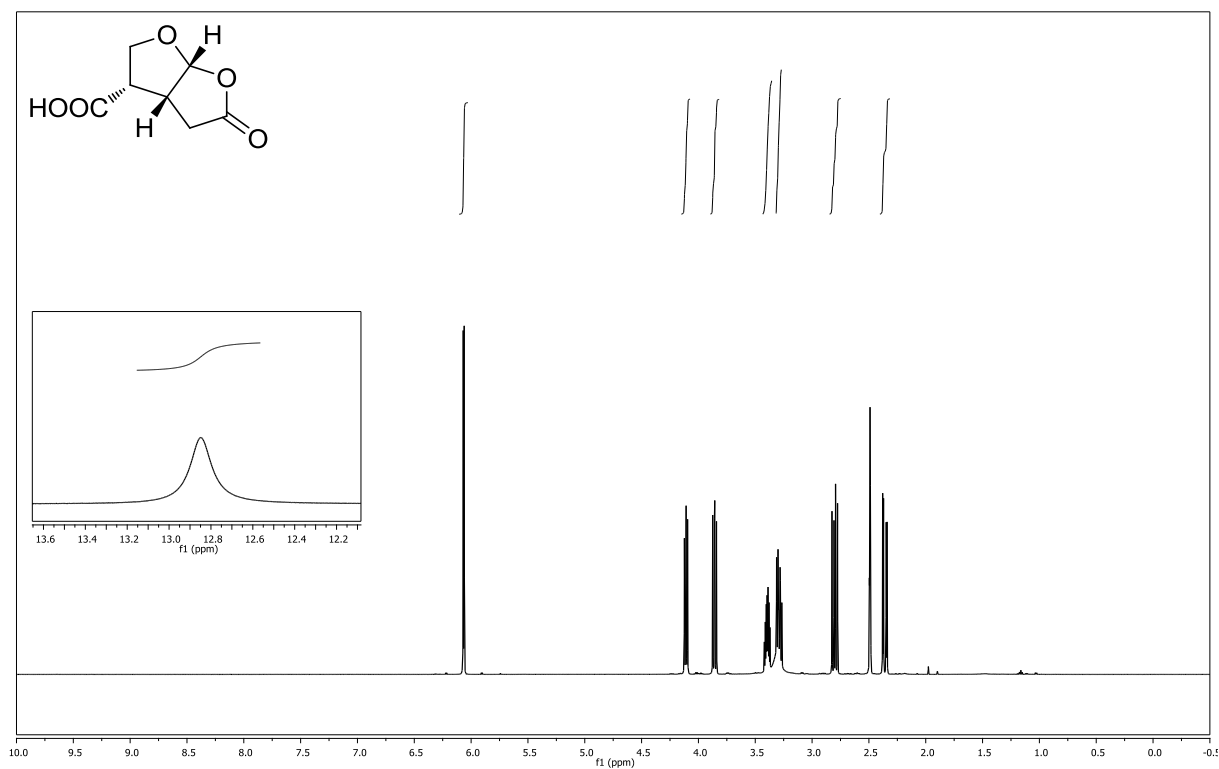
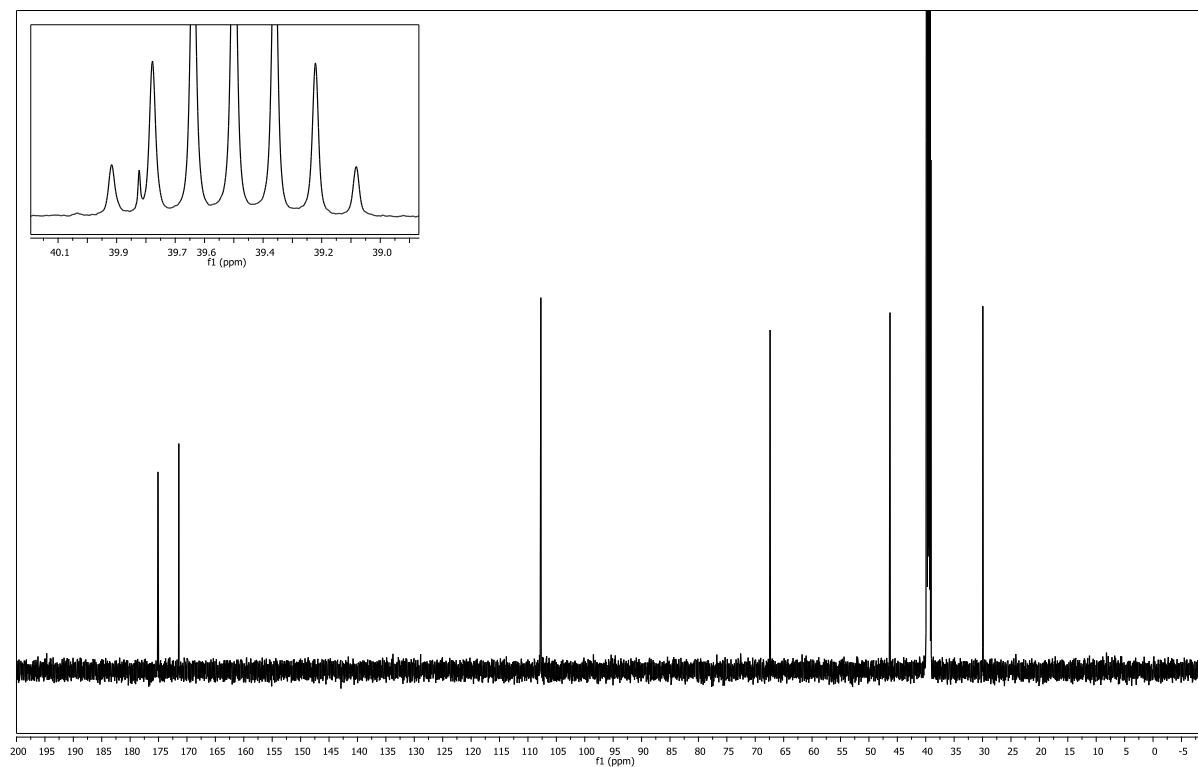


(3*S*,4*R*)-benzyl 5-(benzyloxy)-4-(2-(benzyloxy)-2-oxoethyl)tetrahydrofuran-3-carboxylate (142) **(CDCl₃, 300 MHz)**



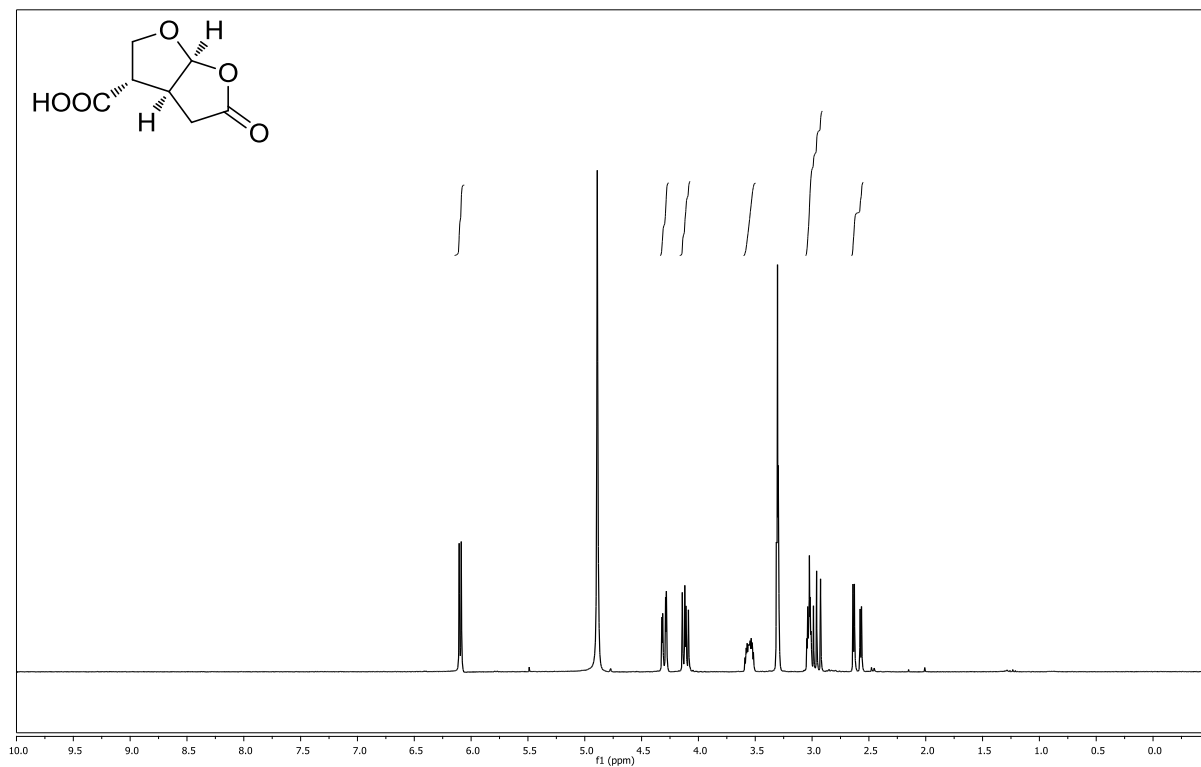
(CDCl₃, 75 MHz)



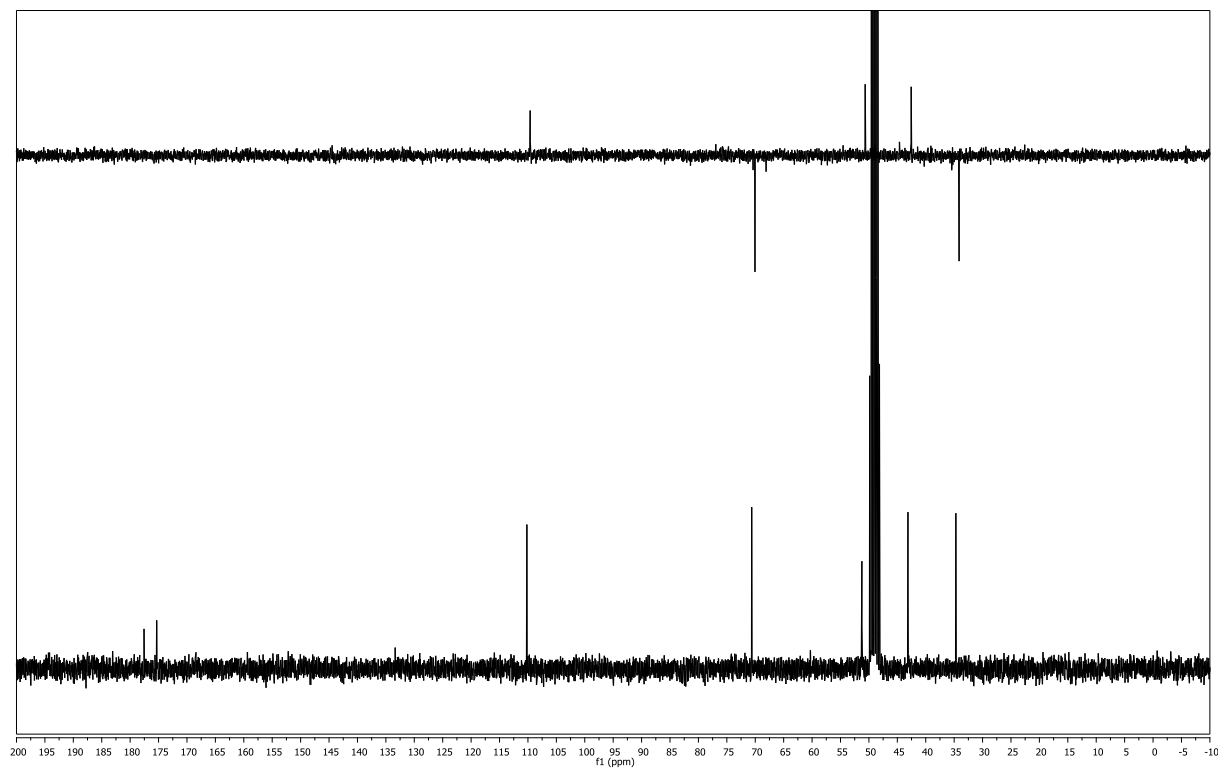
(3*S*,3*aR*,6*aR*)-5-oxohexahydrofuro[2,3-*b*]furan-3-carboxylic acid (145)**(DMSO-*d*₆, 600 MHz)****(DMSO-*d*₆, 151 MHz)**

(3*S*,3*aS*,6*aS*)-5-oxohexahydrofuro[2,3-*b*]furan-3-carboxylic acid (57)

(methanol-*d*₄, 400 MHz)

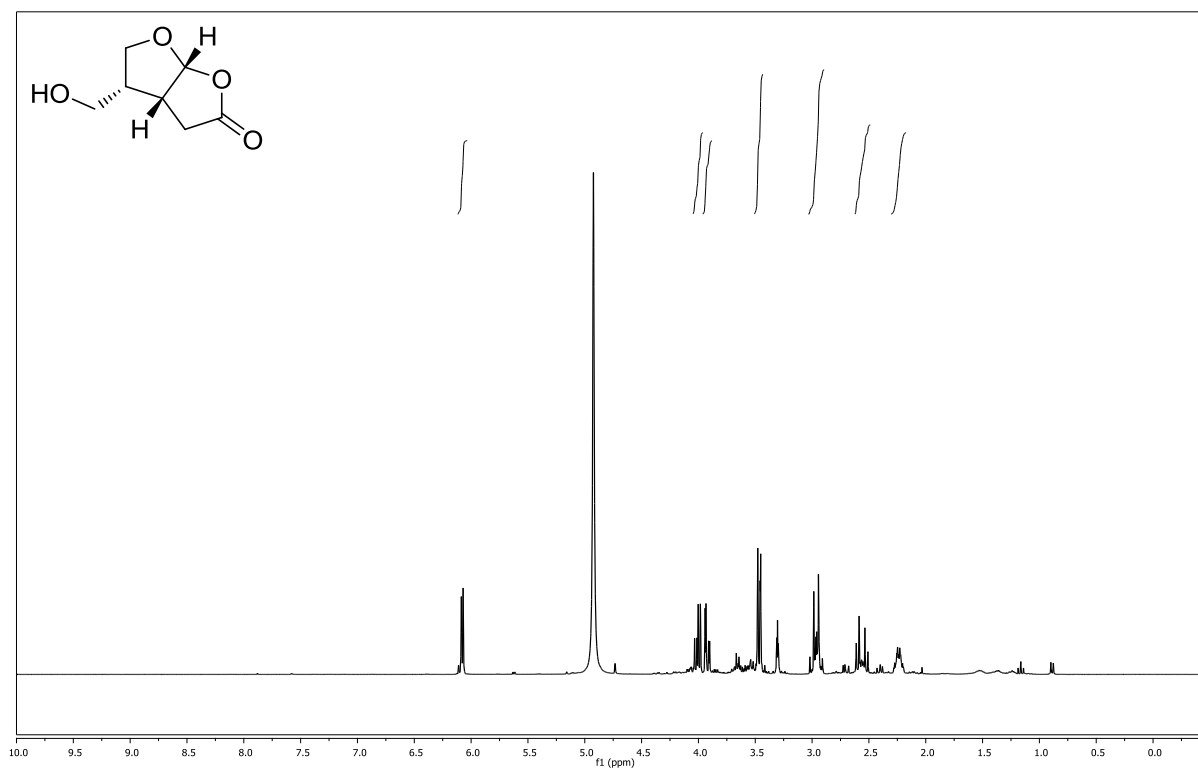


(methanol-*d*₄, 101 MHz)

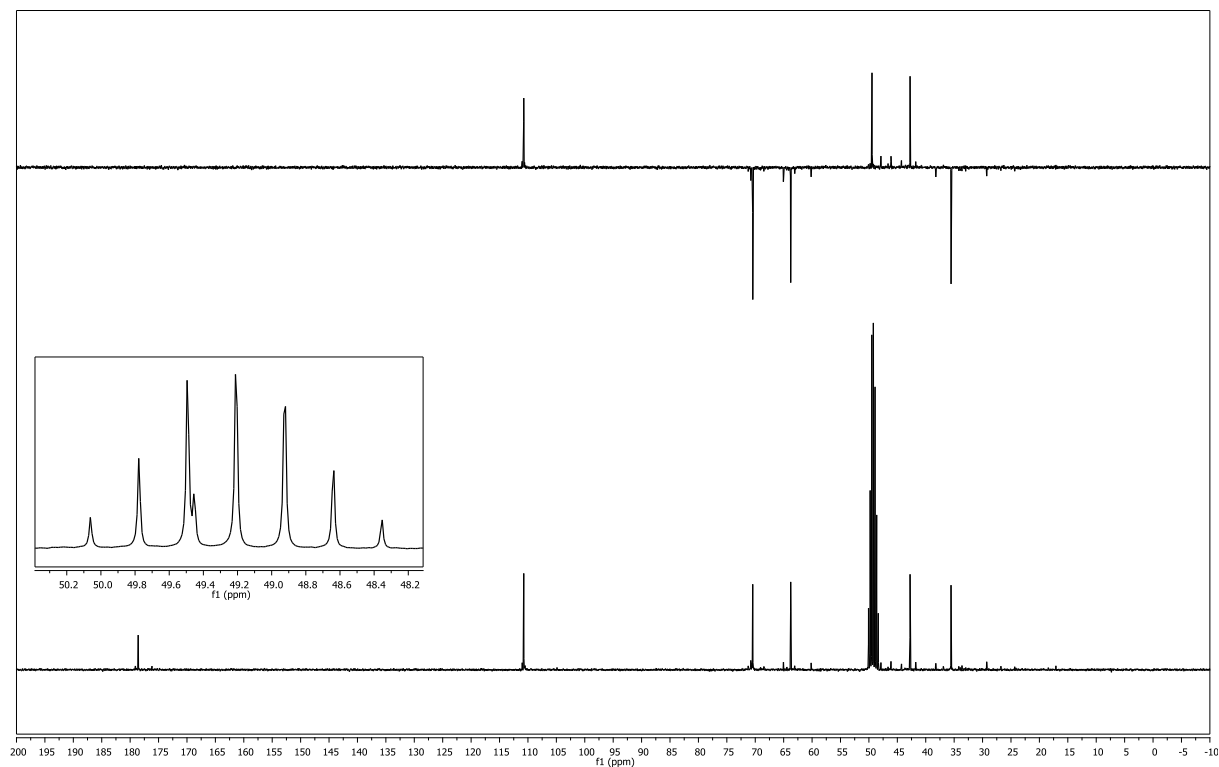


(3*aR*,4*R*,6*aR*)-4-(hydroxymethyl)tetrahydrofuro[2,3-*b*]furan-2(6*aH*)-one (141)

(methanol-*d*₄, 300 MHz)

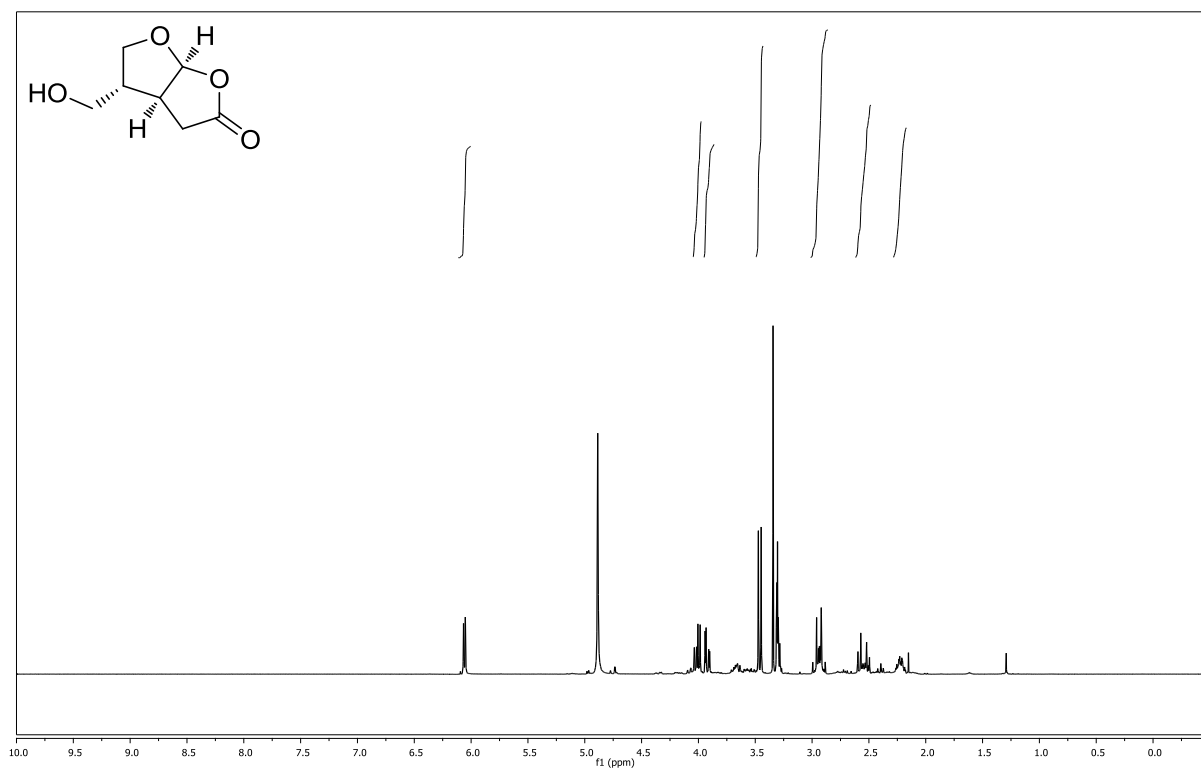


(methanol-*d*₄, 75 MHz)

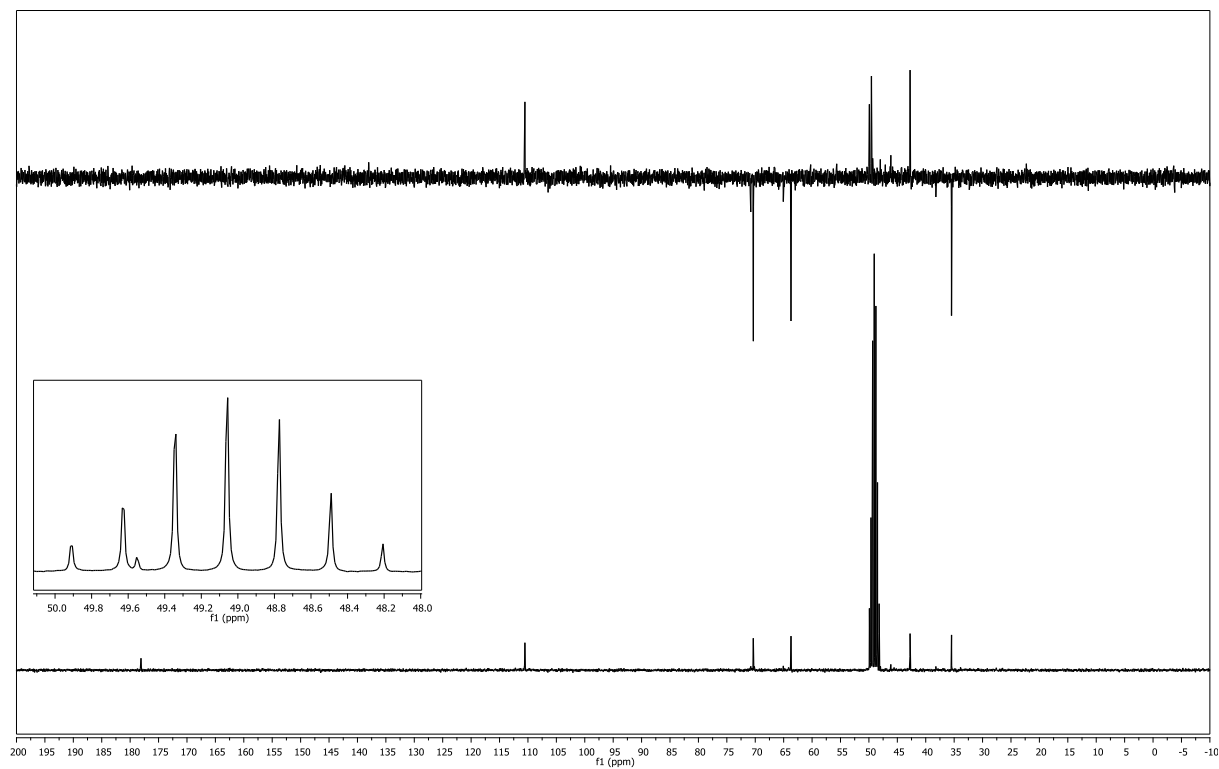


(3a*S*,4*R*,6a*S*)-4-(hydroxymethyl)tetrahydrofuro[2,3-*b*]furan-2(6a*H*)-one (152)

(methanol-*d*₄, 300 MHz)

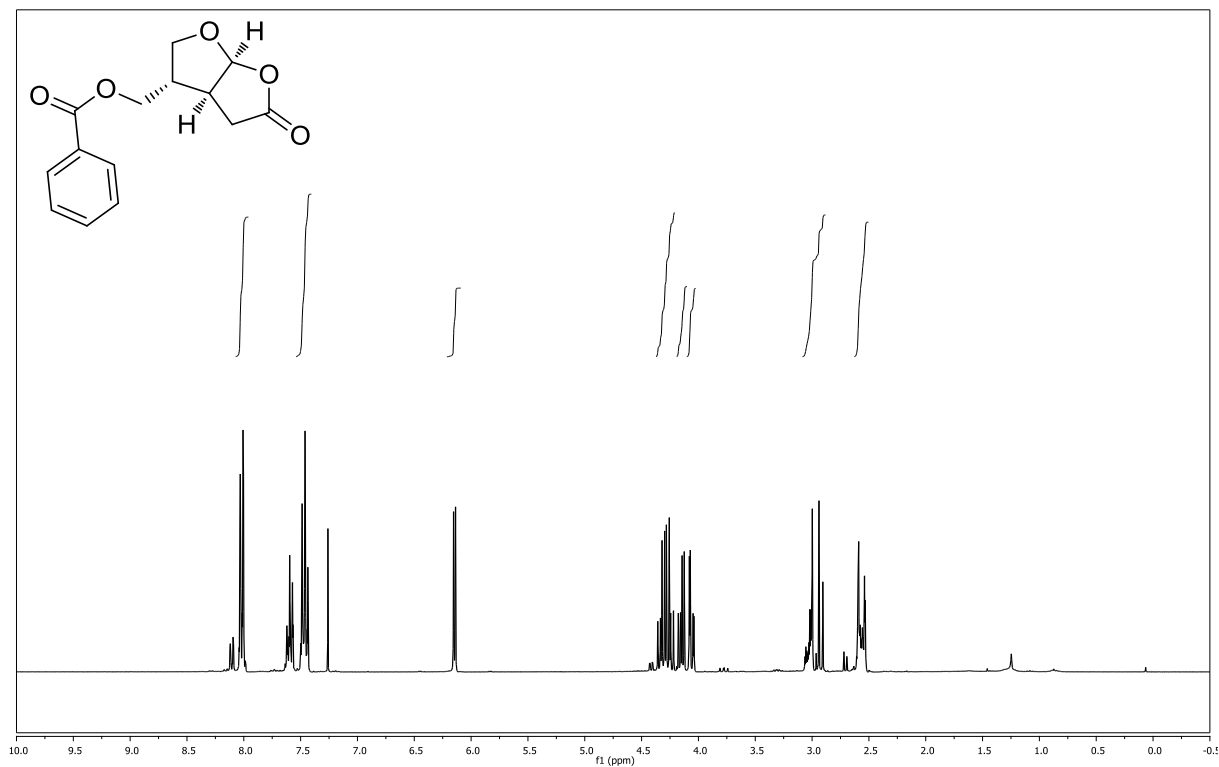


(methanol-*d*₄, 75 MHz)

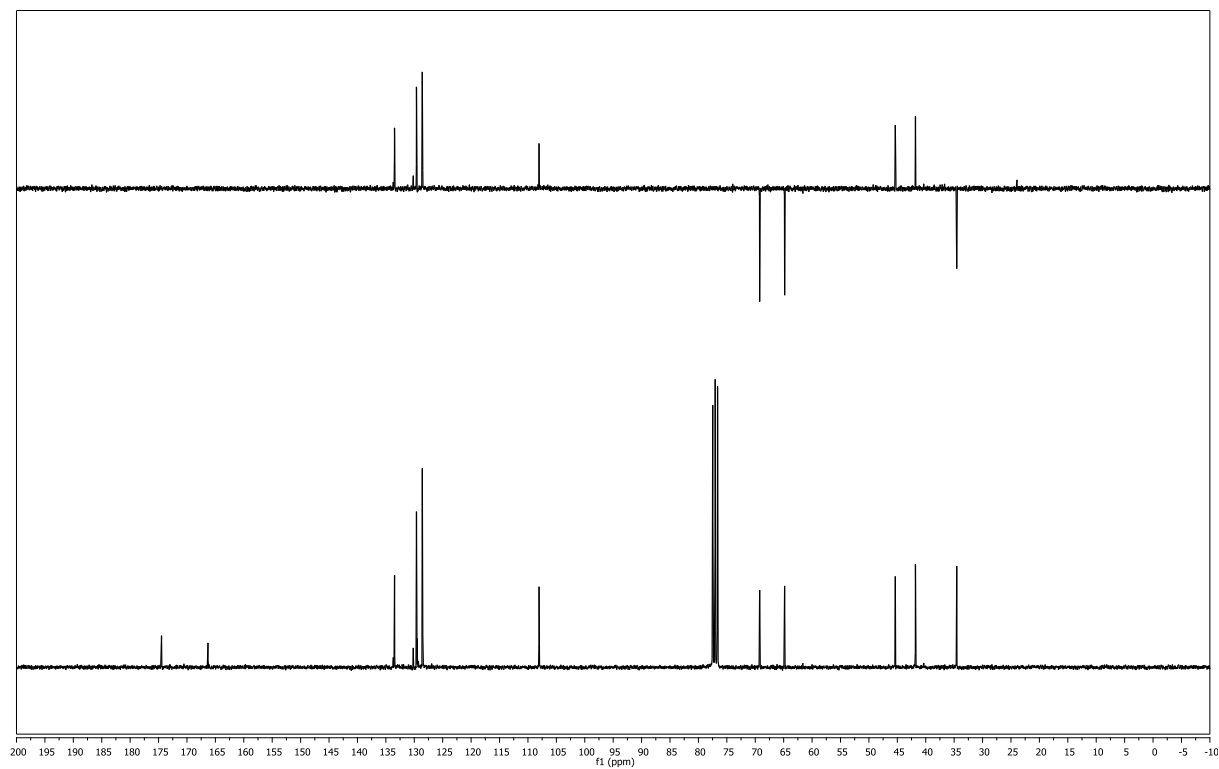


((3*S*,3*aS*,6*aS*)-5-oxohexahydrofuro[2,3-*b*]furan-3-yl)methyl benzoate (153)

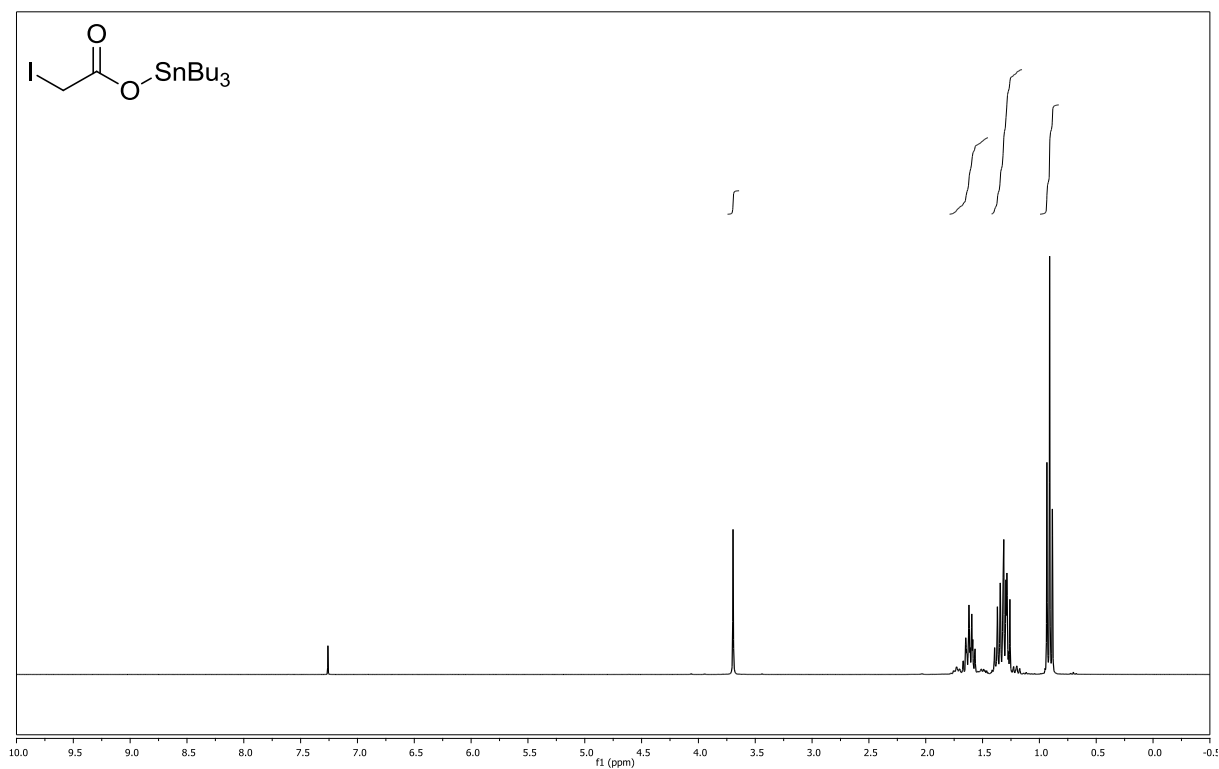
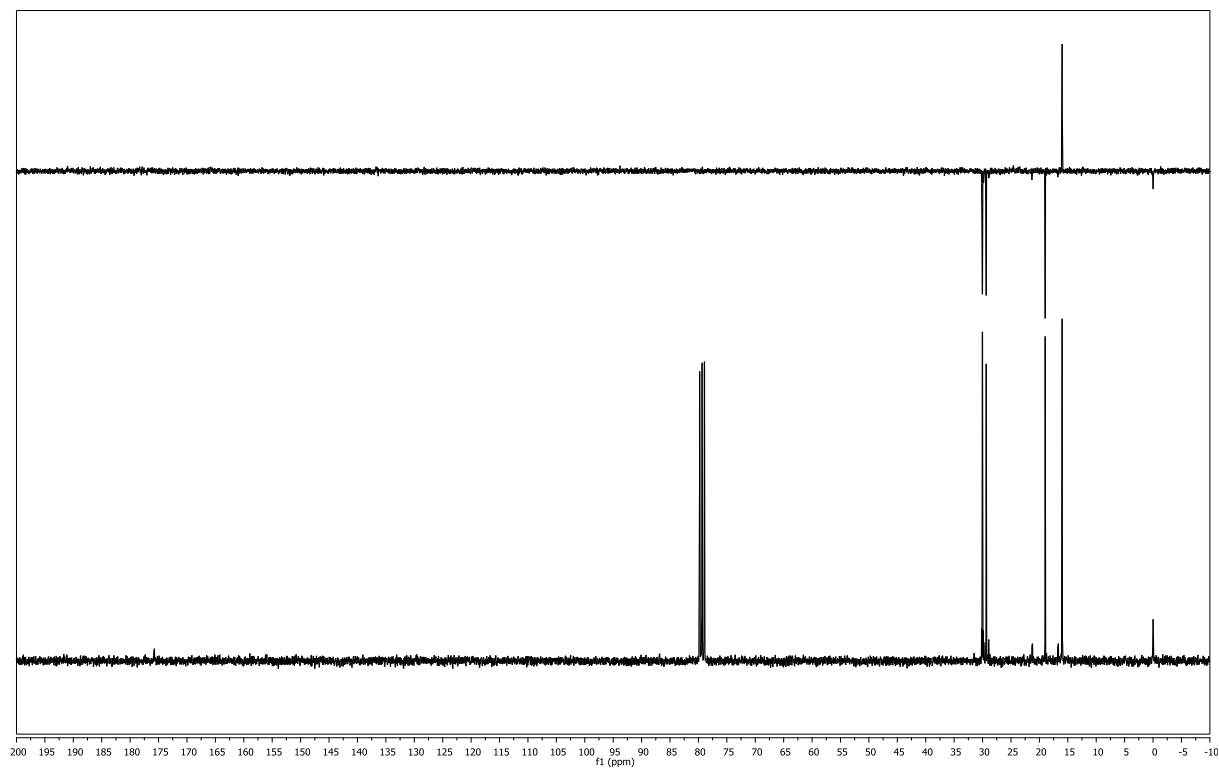
(CDCl₃, 300 MHz)

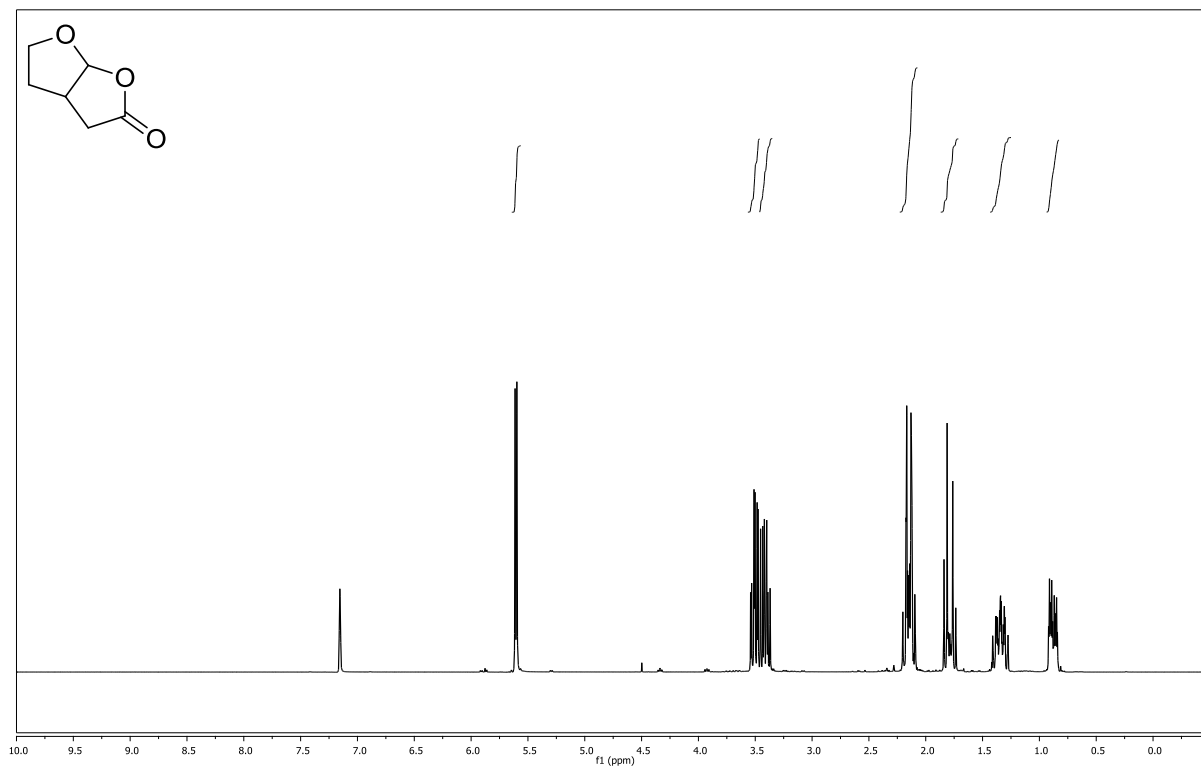
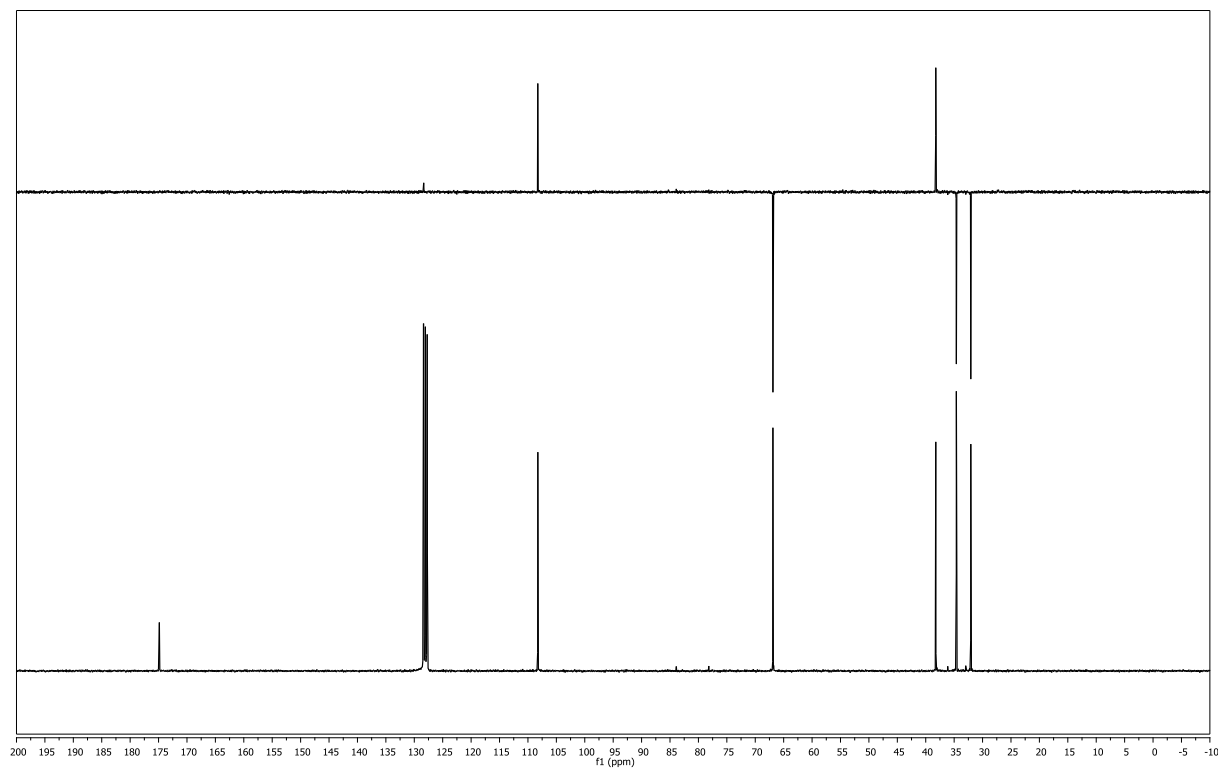


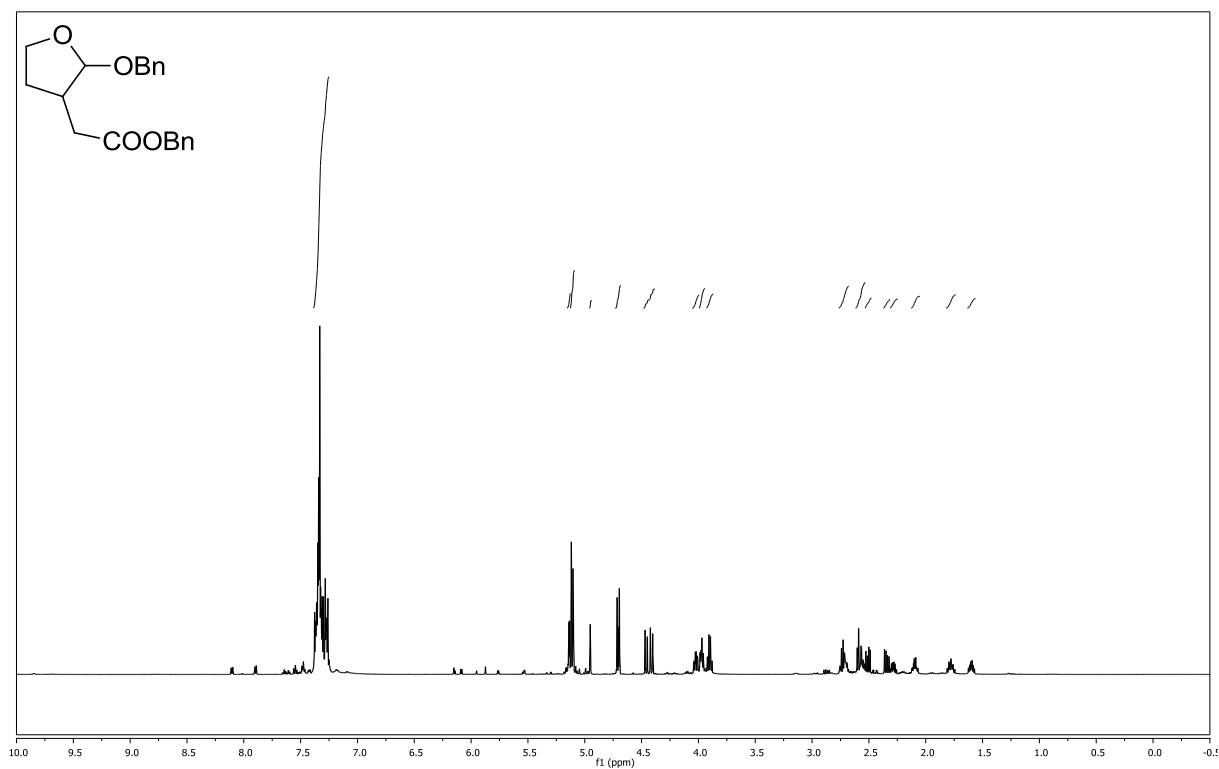
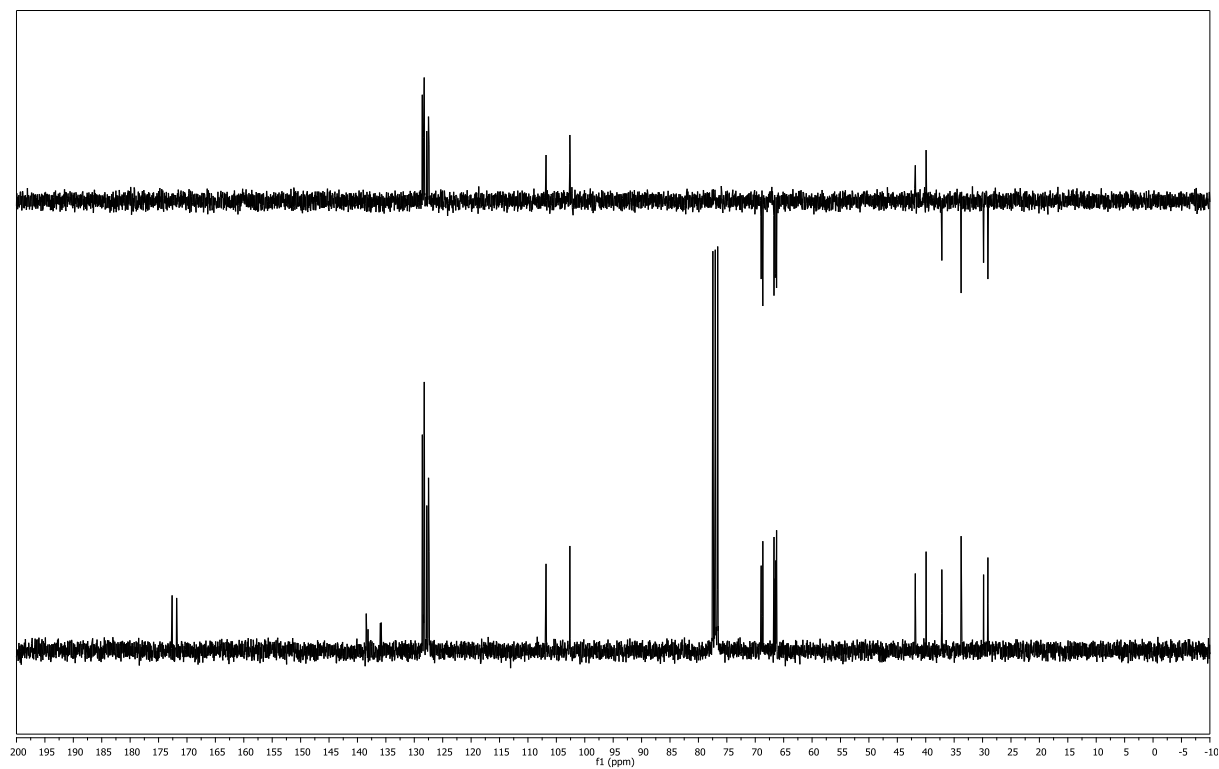
(CDCl₃, 75 MHz)



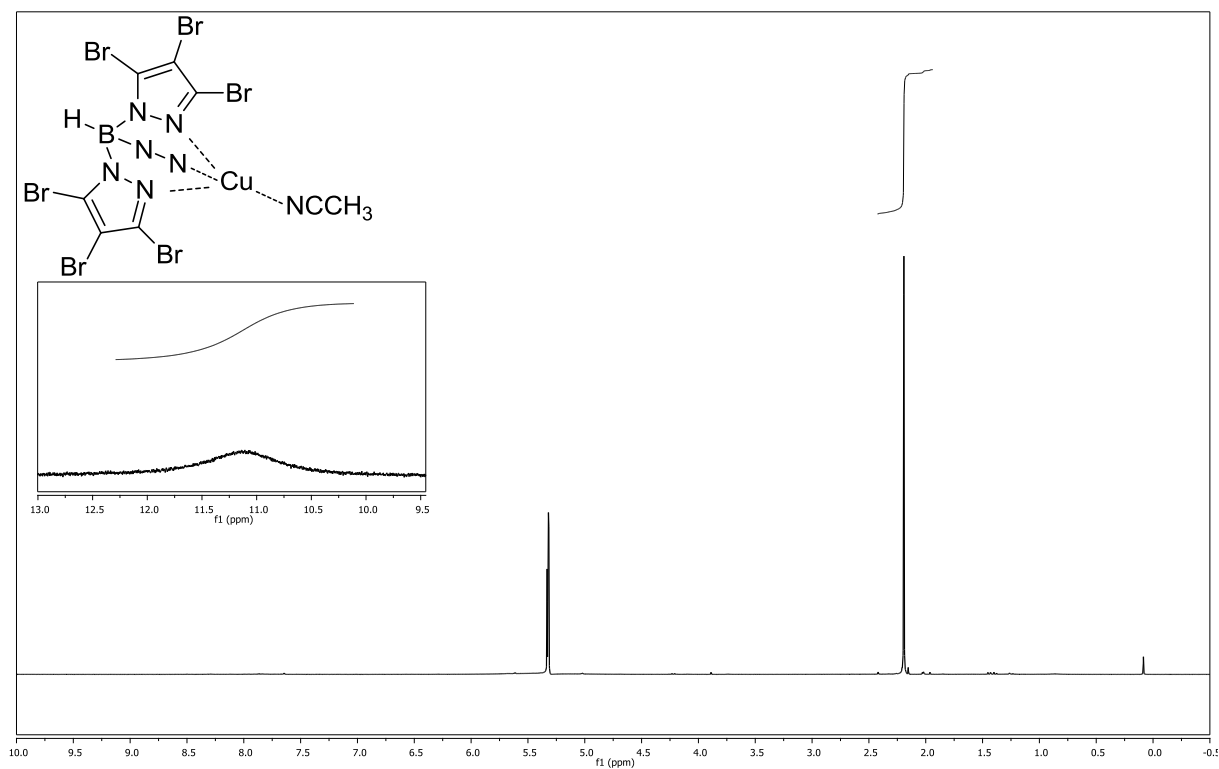
tributylstannyl 2-iodoacetate (166)

(CDCl₃, 300 MHz)(CDCl₃, 75 MHz)

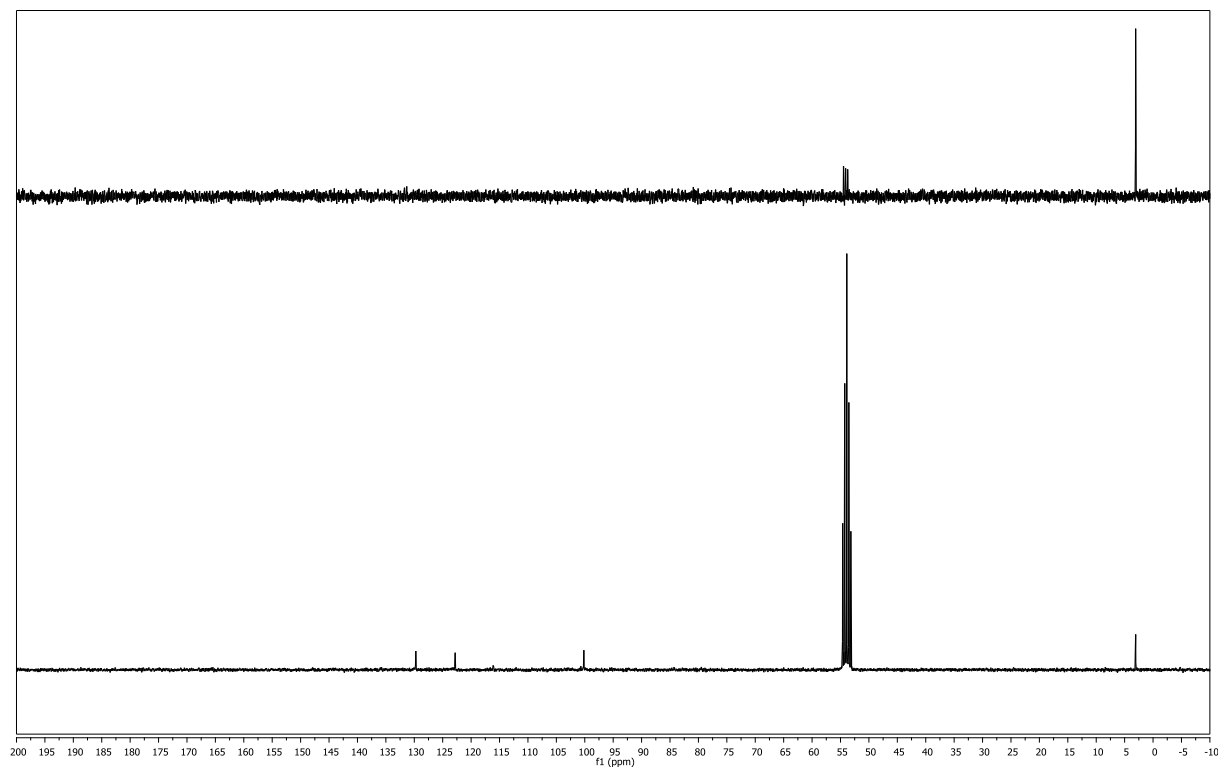
tetrahydrofuro[2,3-*b*]furan-2(6*a*H)-one (167)**(CDCl₃, 300 MHz)****(CDCl₃, 75 MHz)**

benzyl 2-(2-(benzyloxy)tetrahydrofuran-3-yl)acetate (168)**(CDCl₃, 600 MHz)****(CDCl₃, 151 MHz)**

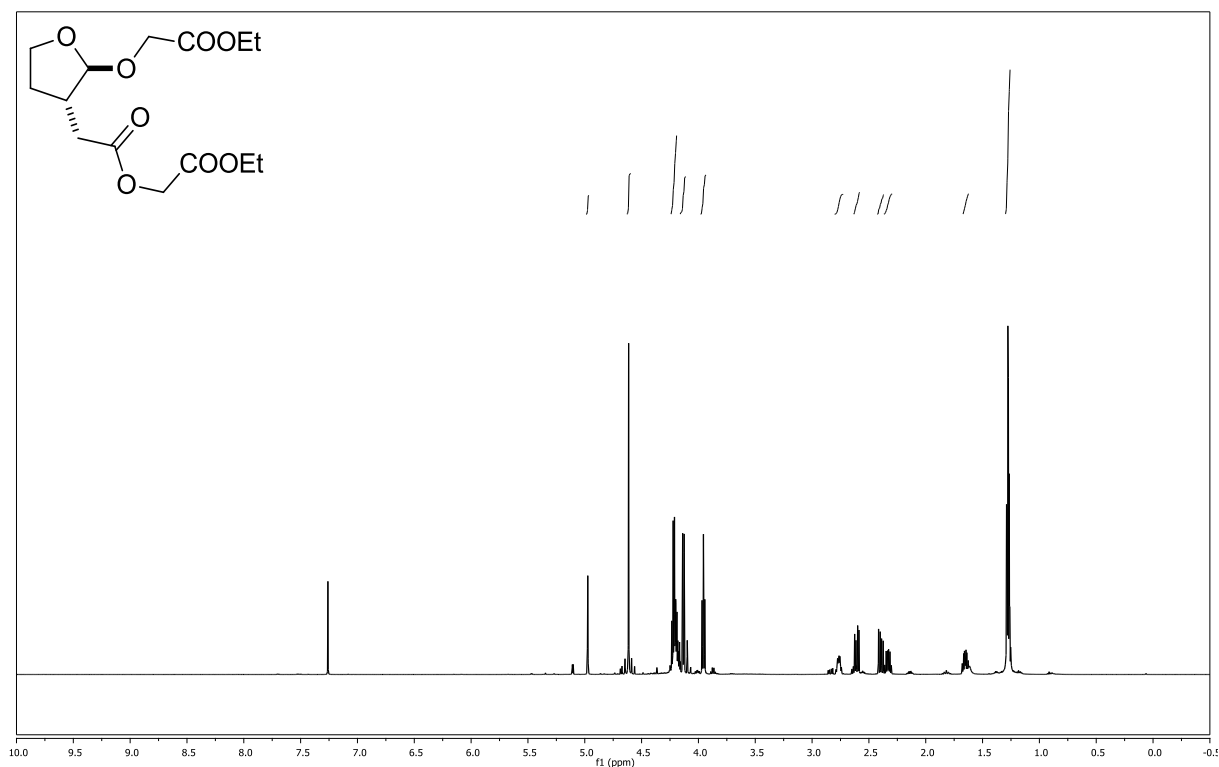
copper(I) tris(3,4,5-tribromo-1H-pyrazole-1-yl)hydroborate acetonitrile complex (164) (third pyrazole ring indicated by N-N for better lucidity) (CD₂Cl₂, 300 MHz)



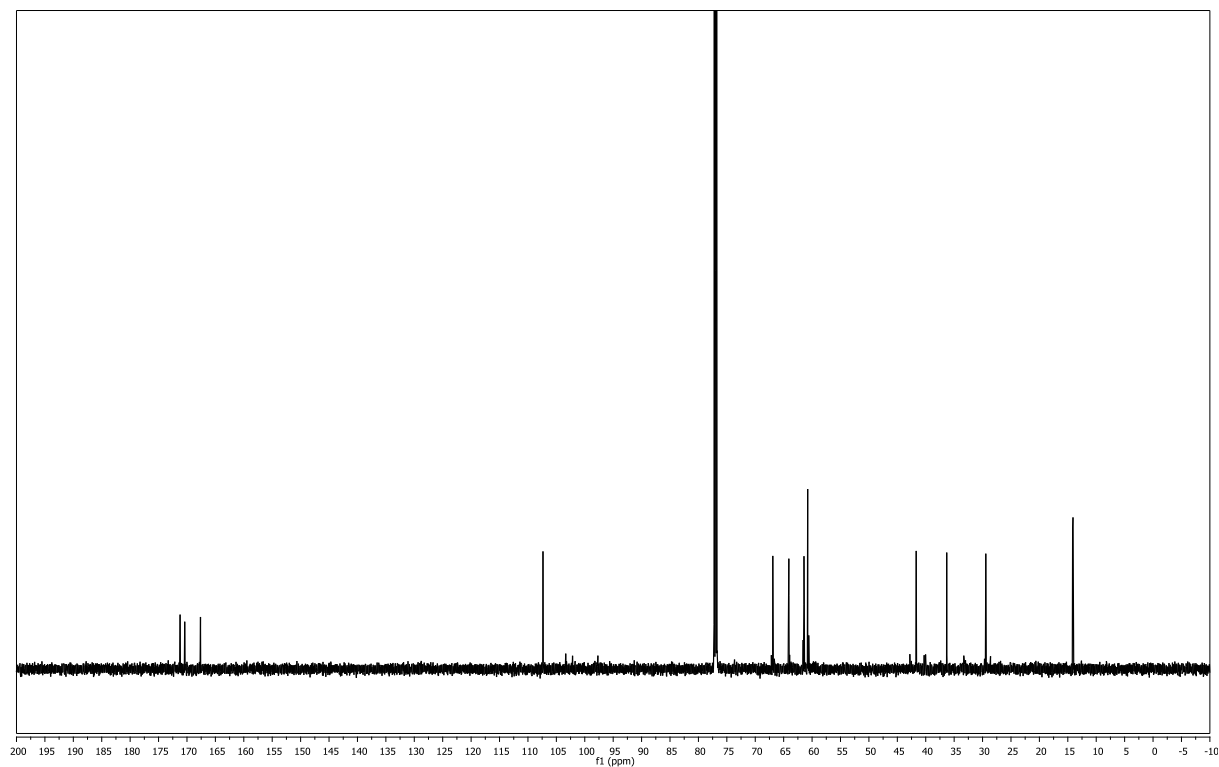
(CD₂Cl₂, 75 MHz)



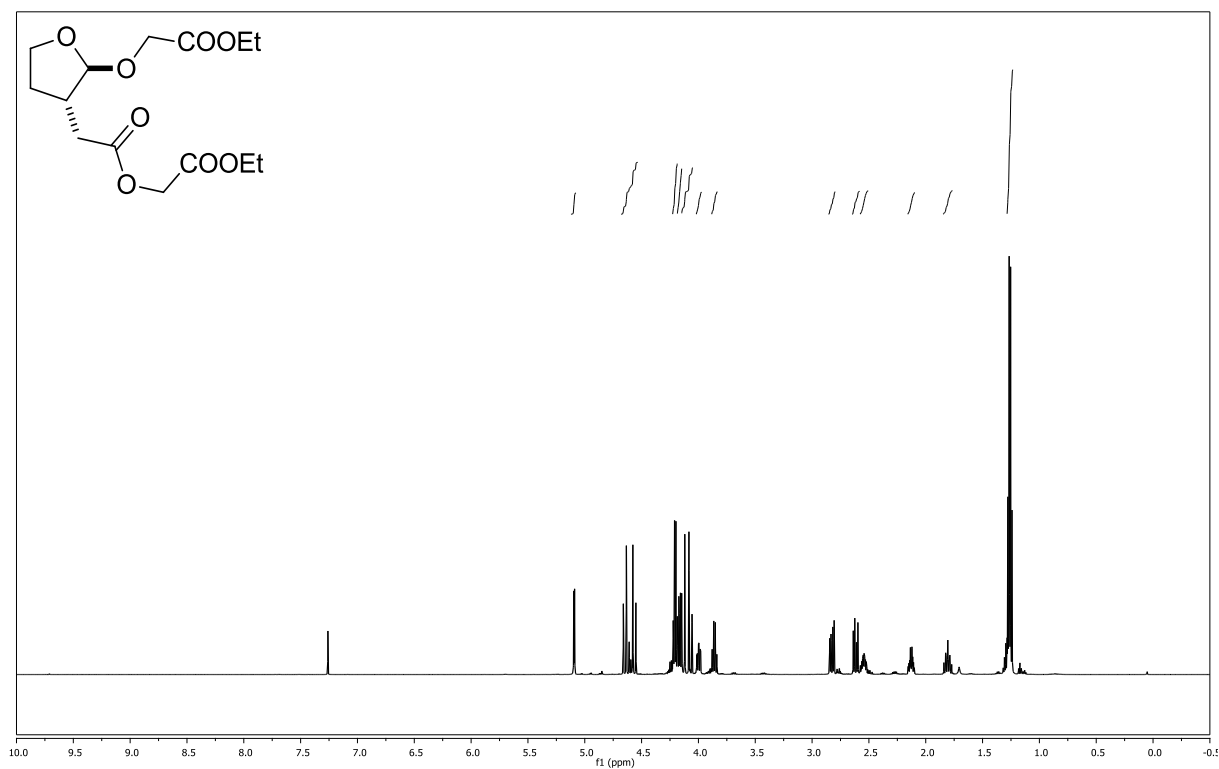
ethyl-2-(2-(2-(2-ethoxy-2-oxoethoxy)-5-oxotetrahydrofuran-3-yl)ethoxy)acetate
(175) Isomer 1 **(CDCl₃, 600 MHz)**



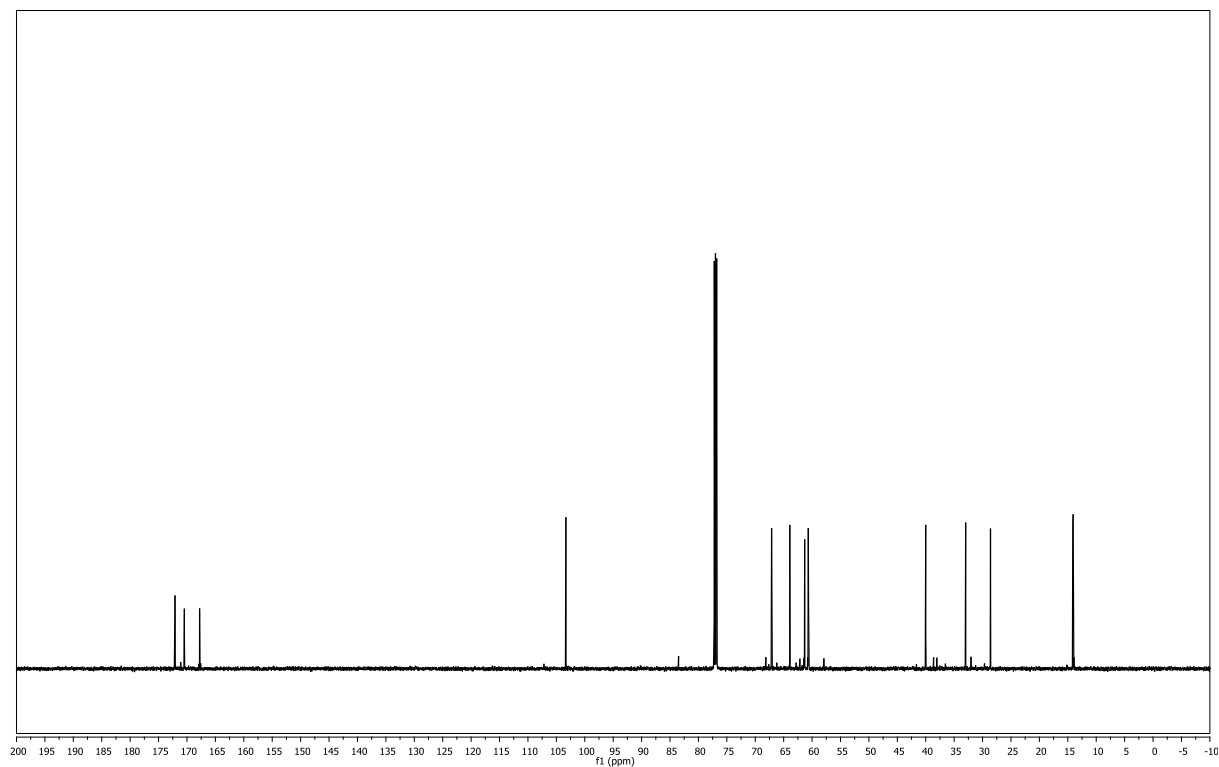
(CDCl₃, 151 MHz)



ethyl-2-(2-(2-(2-ethoxy-2-oxoethoxy)-5-oxotetrahydrofuran-3-yl)ethoxy)acetate
(175) Isomer 2 **(CDCl₃, 600 MHz)**



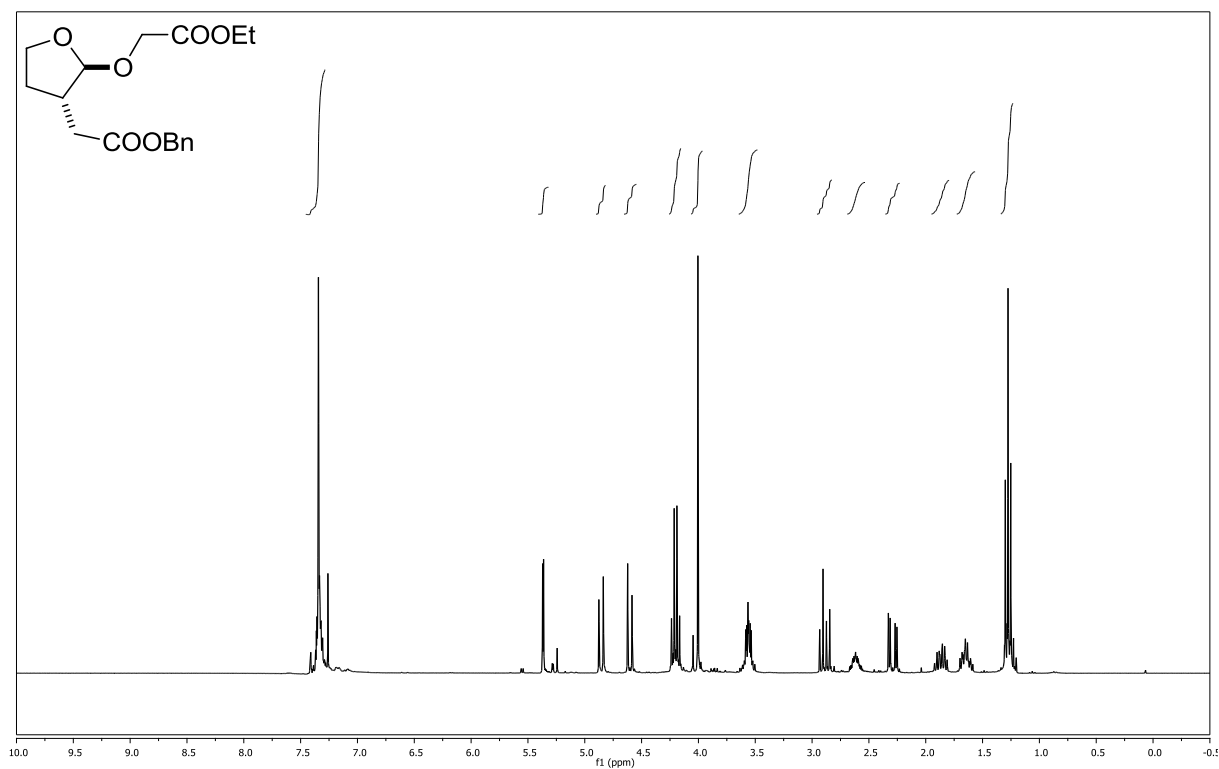
(CDCl₃, 151 MHz)



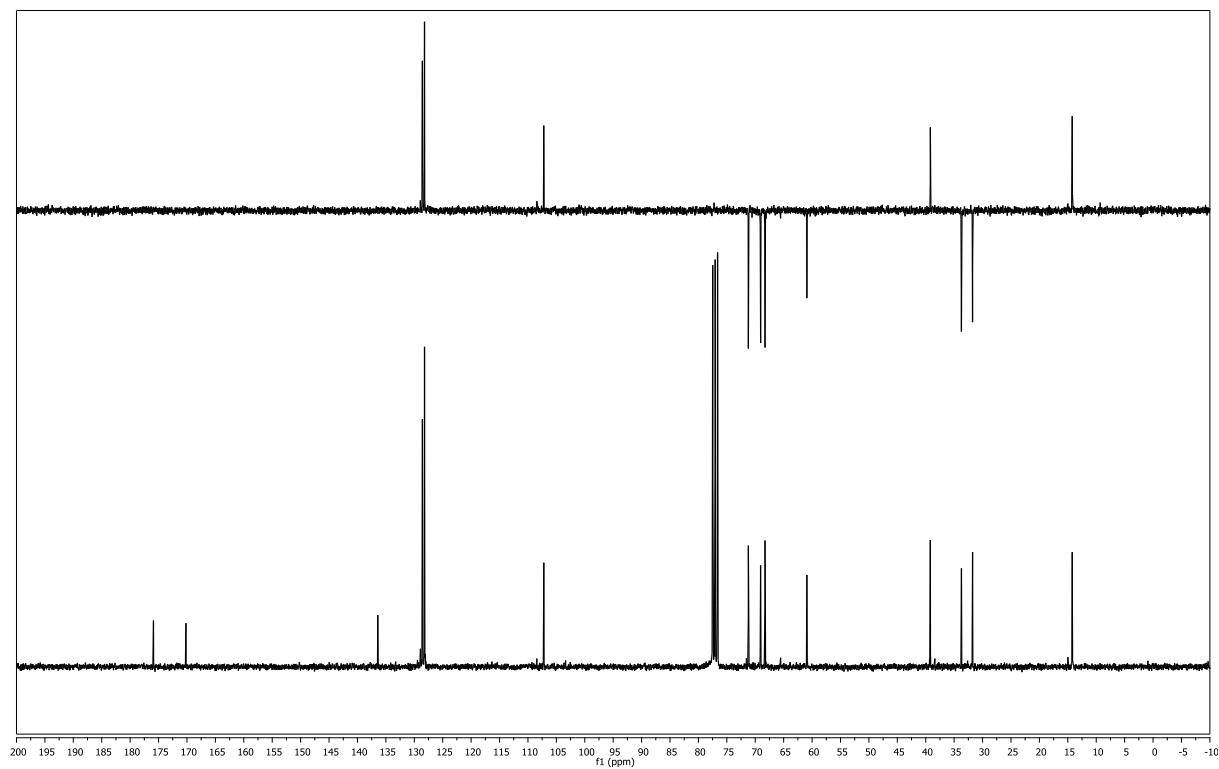
benzyl 2-(2-(2-ethoxy-2-oxoethoxy)tetrahydrofuran-3-yl)acetate (176)

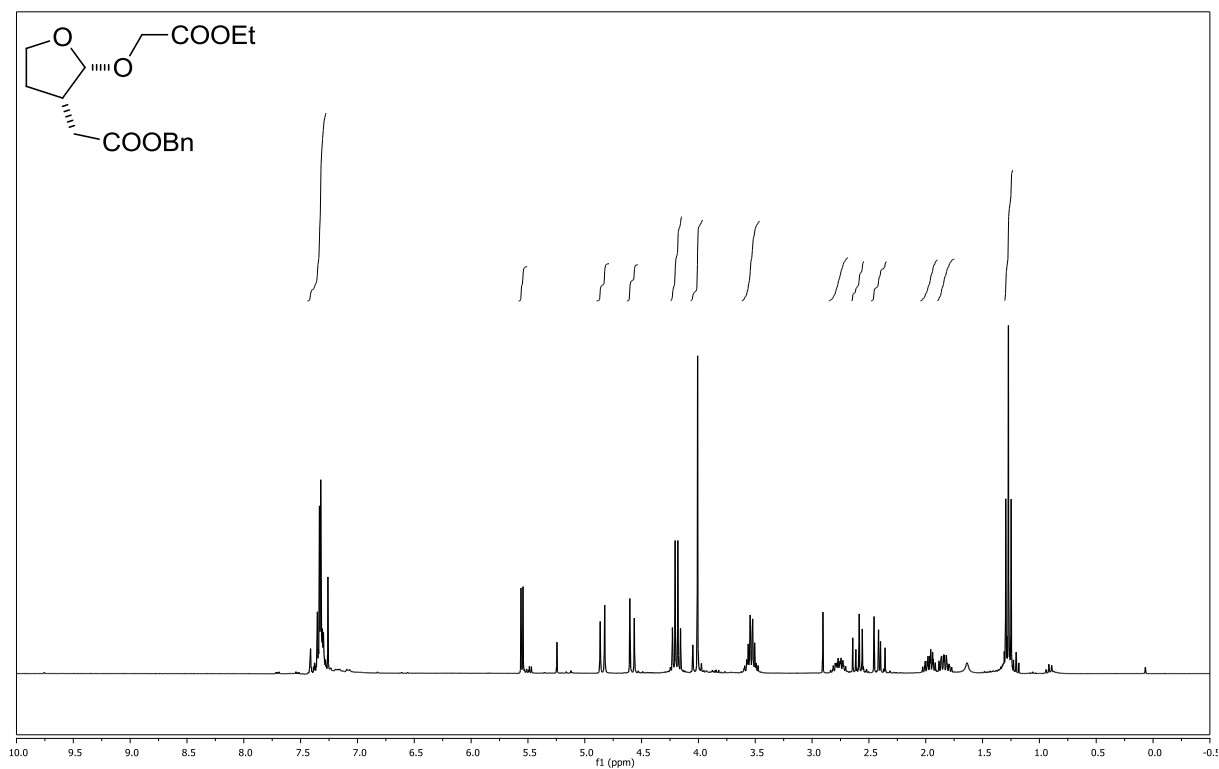
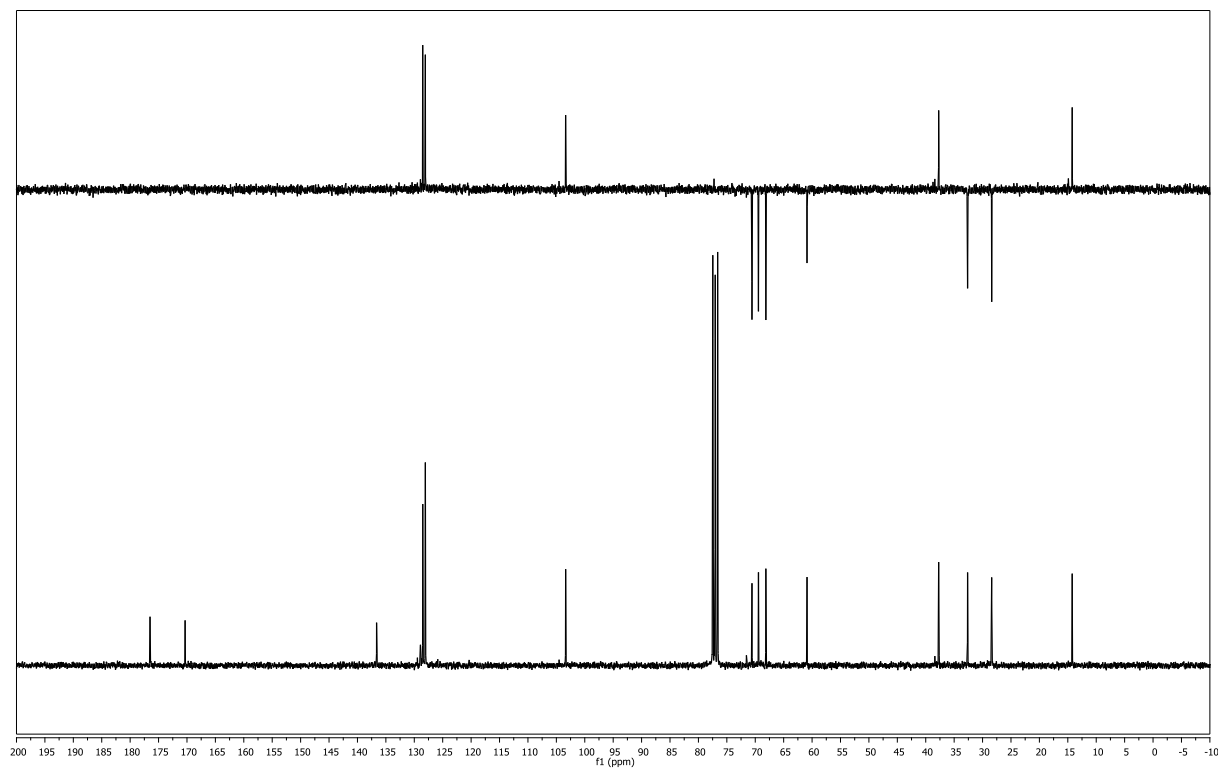
***anti*-isomer**

(CDCl₃, 300 MHz)



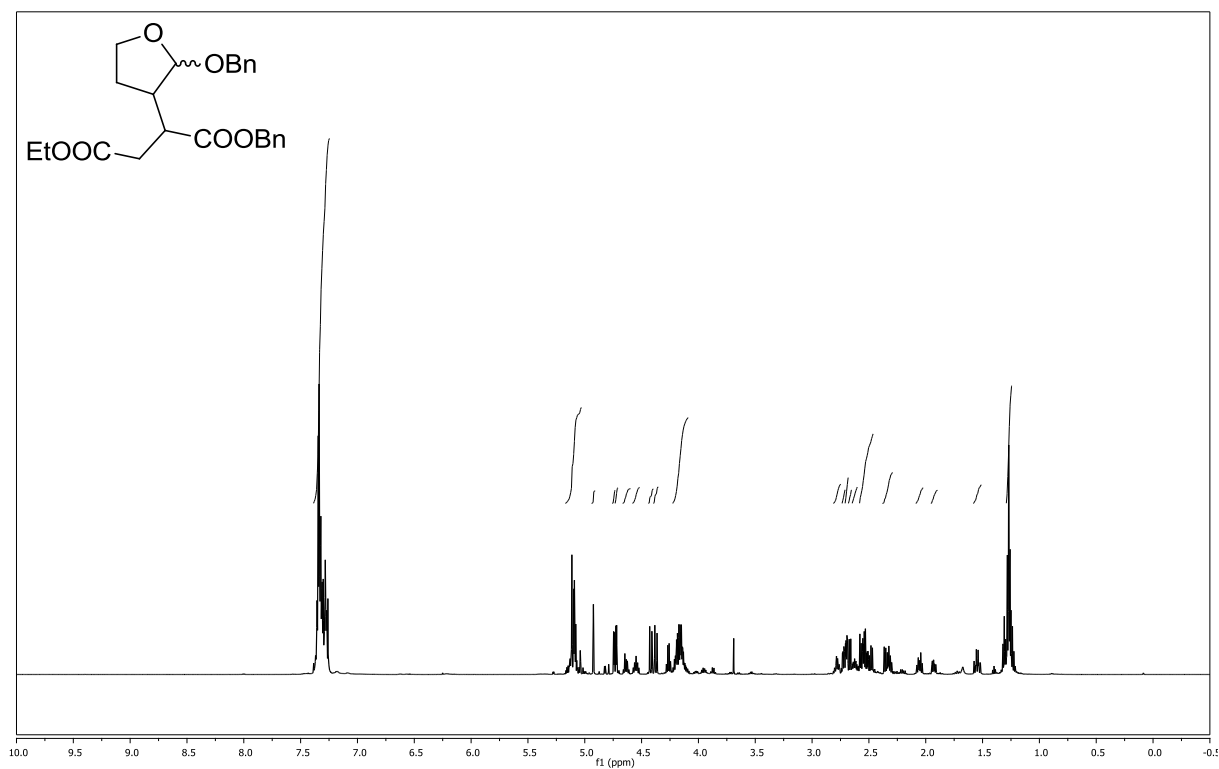
(CDCl₃, 75 MHz)



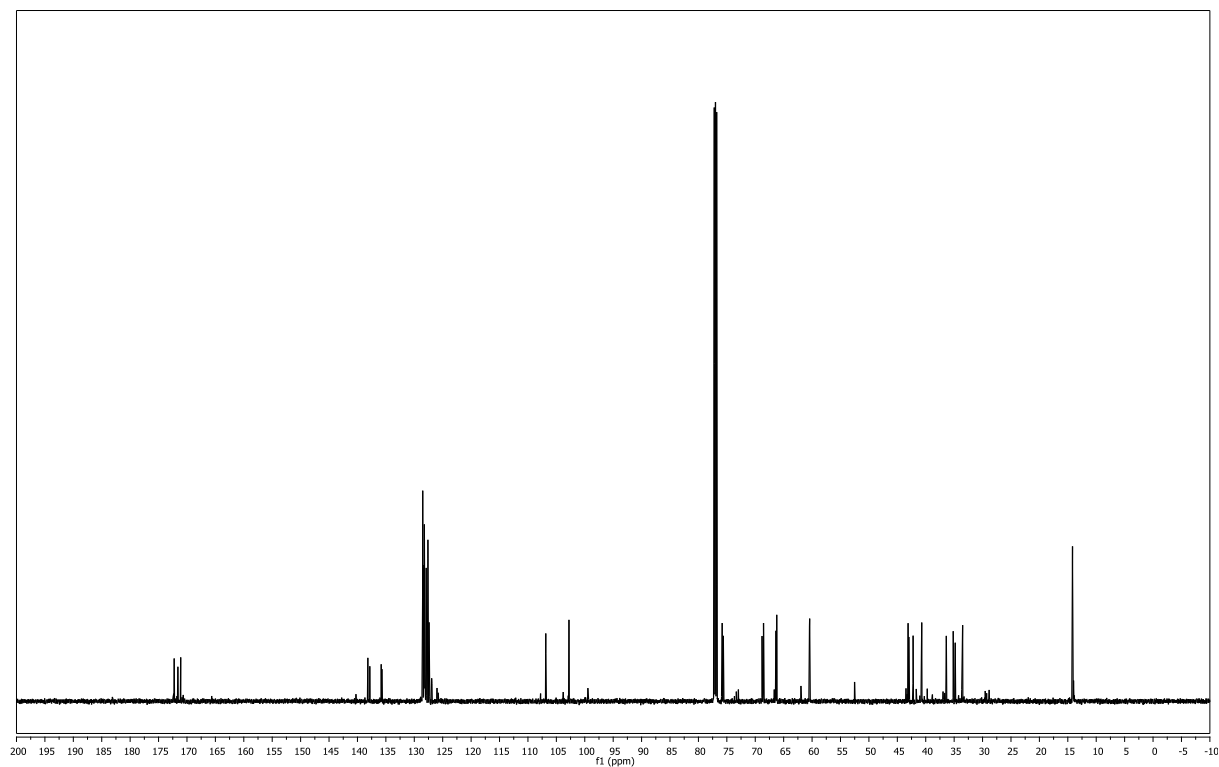
benzyl 2-(2-(2-ethoxy-2-oxoethoxy)tetrahydrofuran-3-yl)acetate (176)***syn*-isomer****(CDCl₃, 300 MHz)****(CDCl₃, 75 MHz)**

1-benzyl 4-ethyl 2-(2-(benzyloxy)tetrahydrofuran-3-yl)succinate (177)

(CDCl₃, 600 MHz)

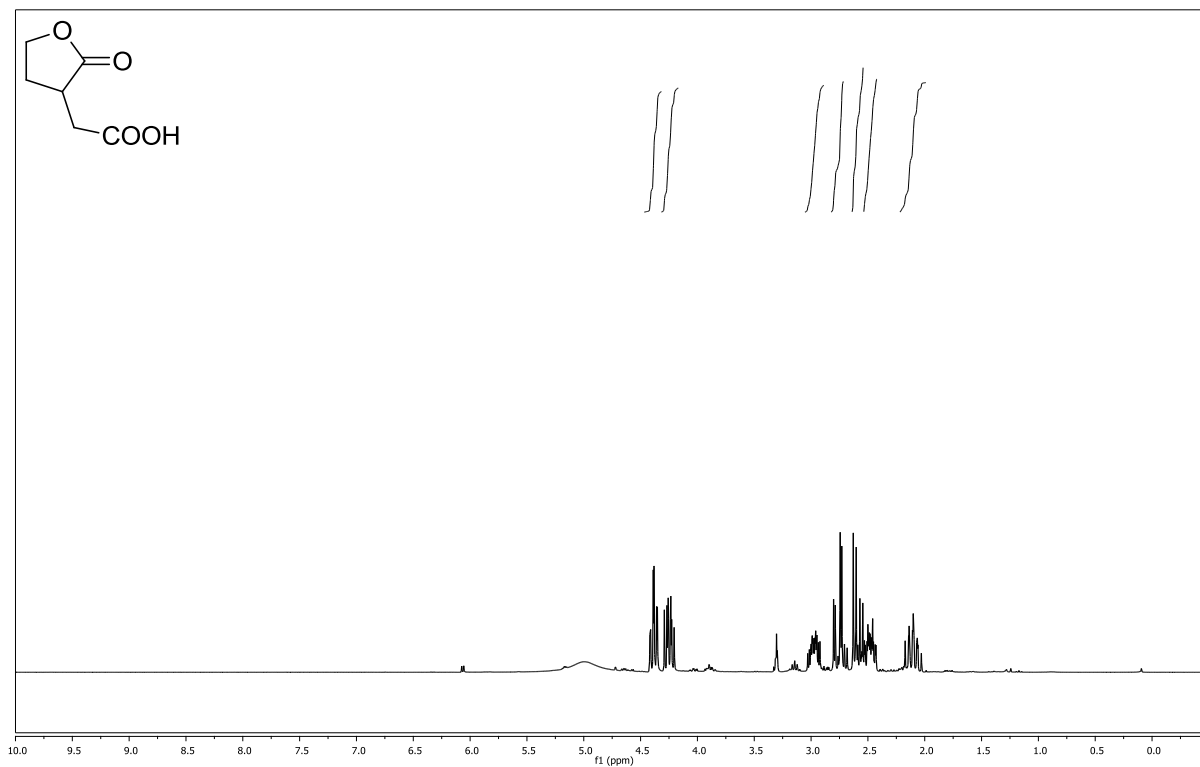


(CDCl₃, 151 MHz)

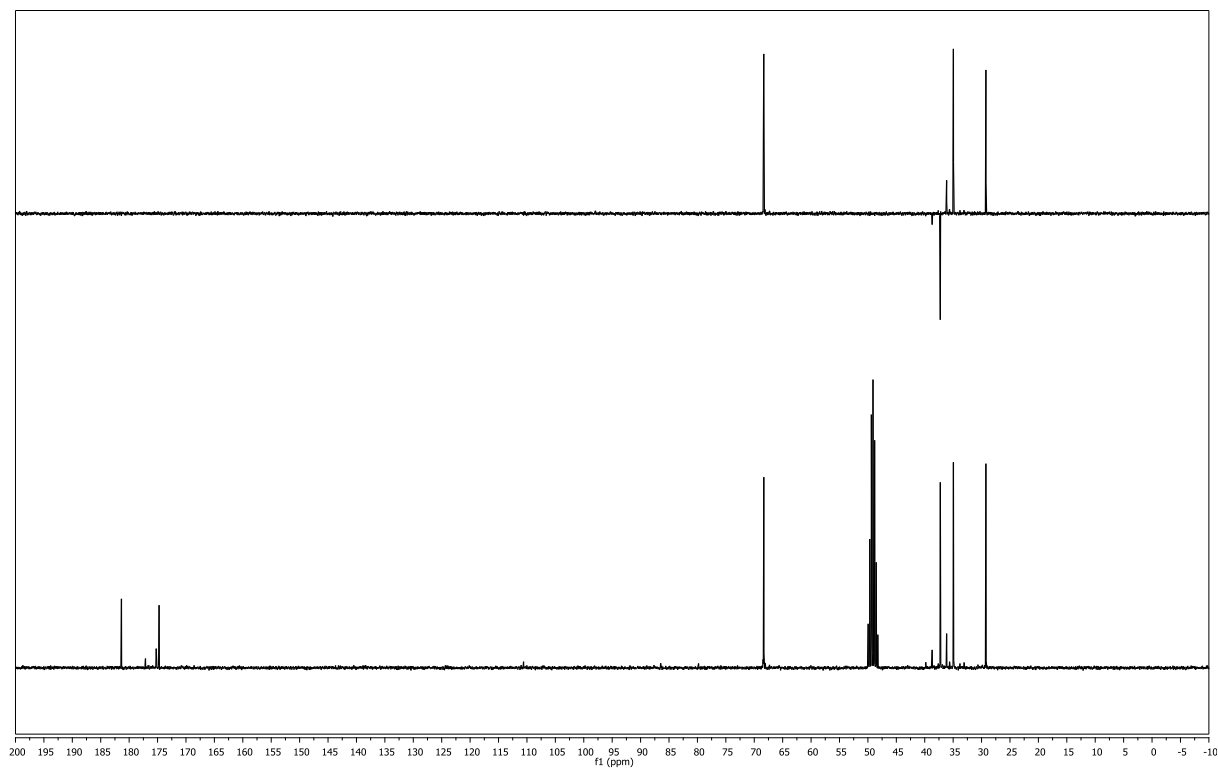


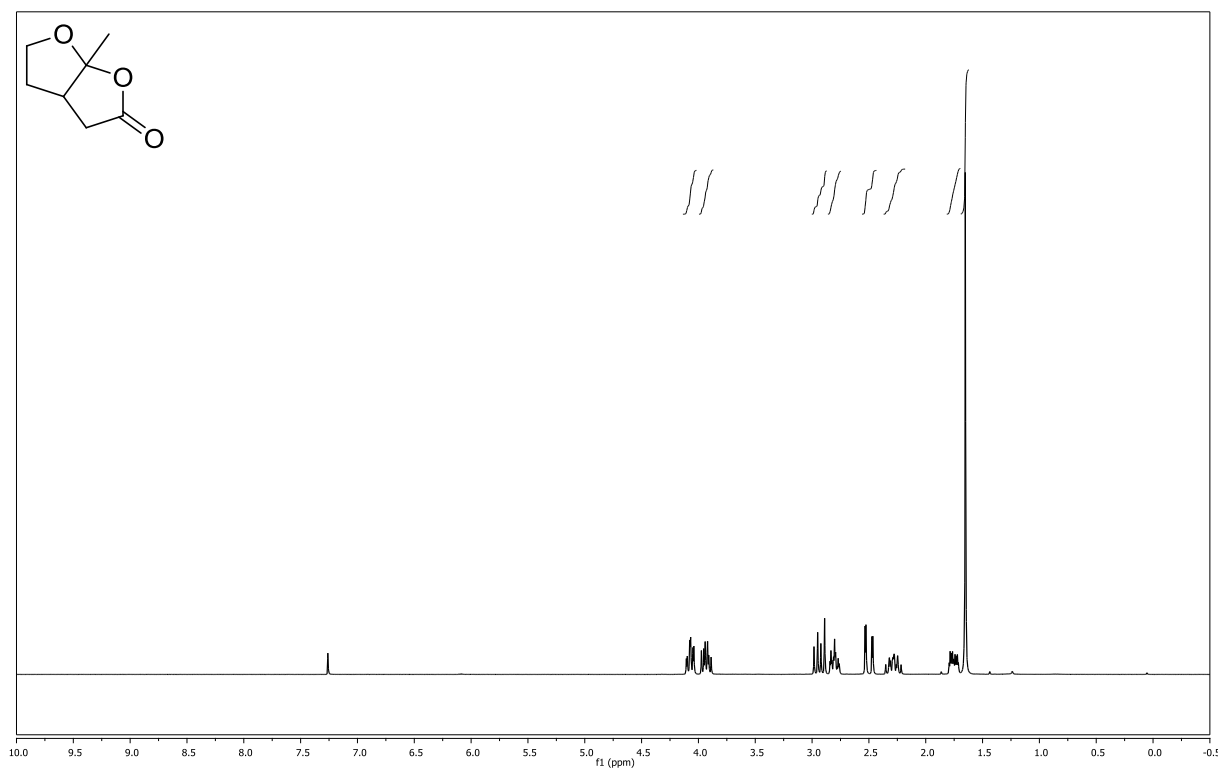
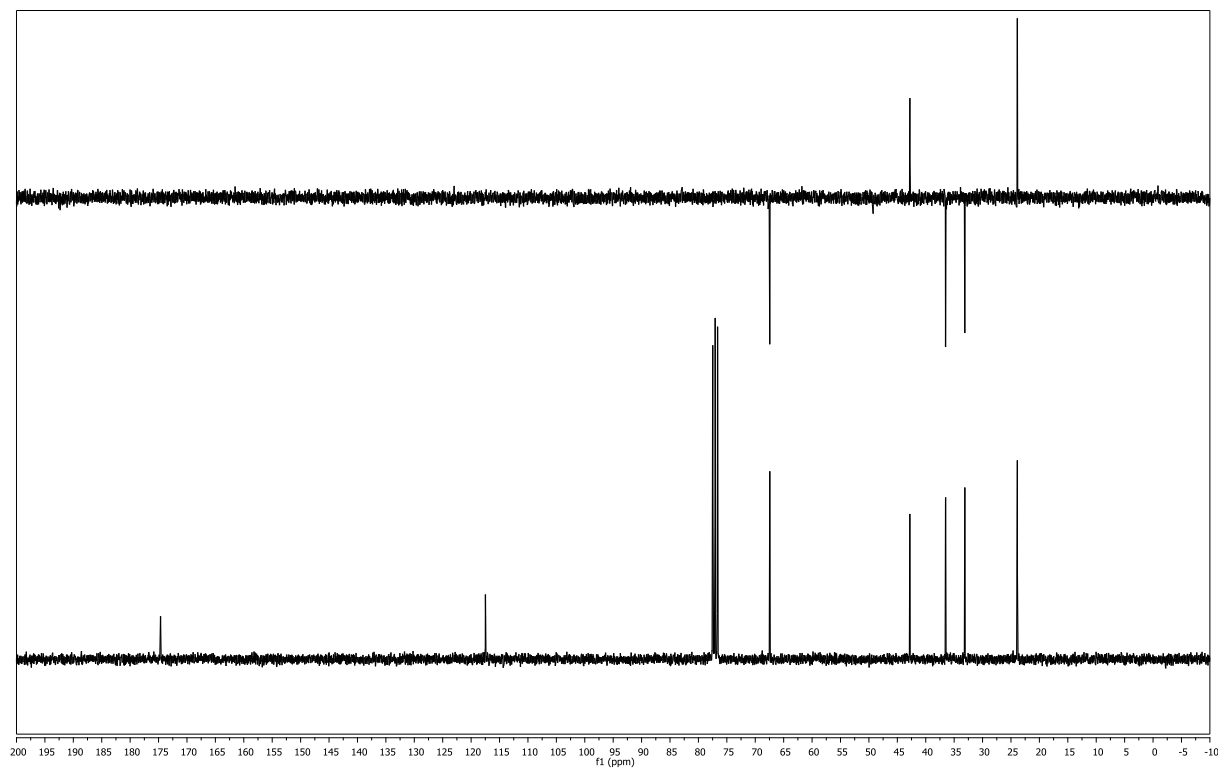
2-(2-oxotetrahydrofuran-3-yl)acetic acid (183)

(methanol-d₄, 300 MHz)



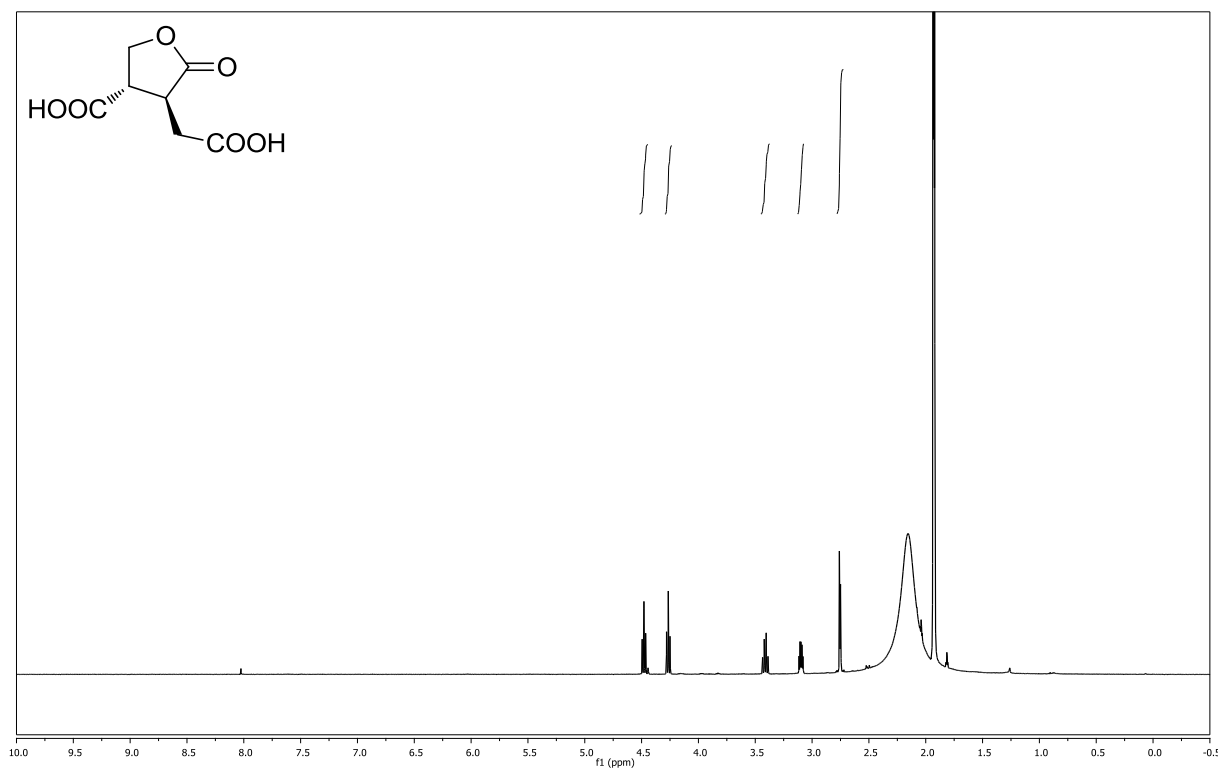
(methanol-d₄, 75 MHz)



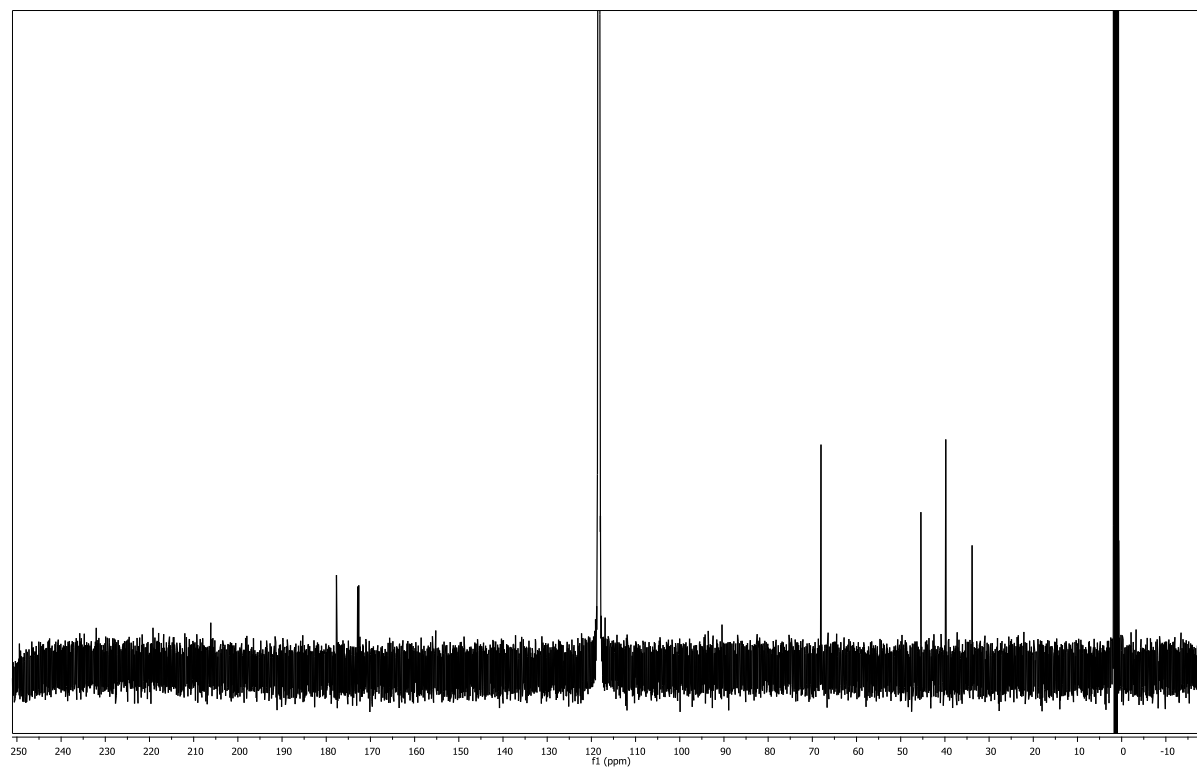
6a-methyltetrahydrofuro[2,3-*b*]furan-2(6aH)-one (185)**(CDCl₃, 300 MHz)****(CDCl₃, 75 MHz)**

(3*S*,4*S*)-4-(carboxymethyl)-5-oxotetrahydrofuran-3-carboxylic acid (186)

(acetone-d₆, 600 MHz)

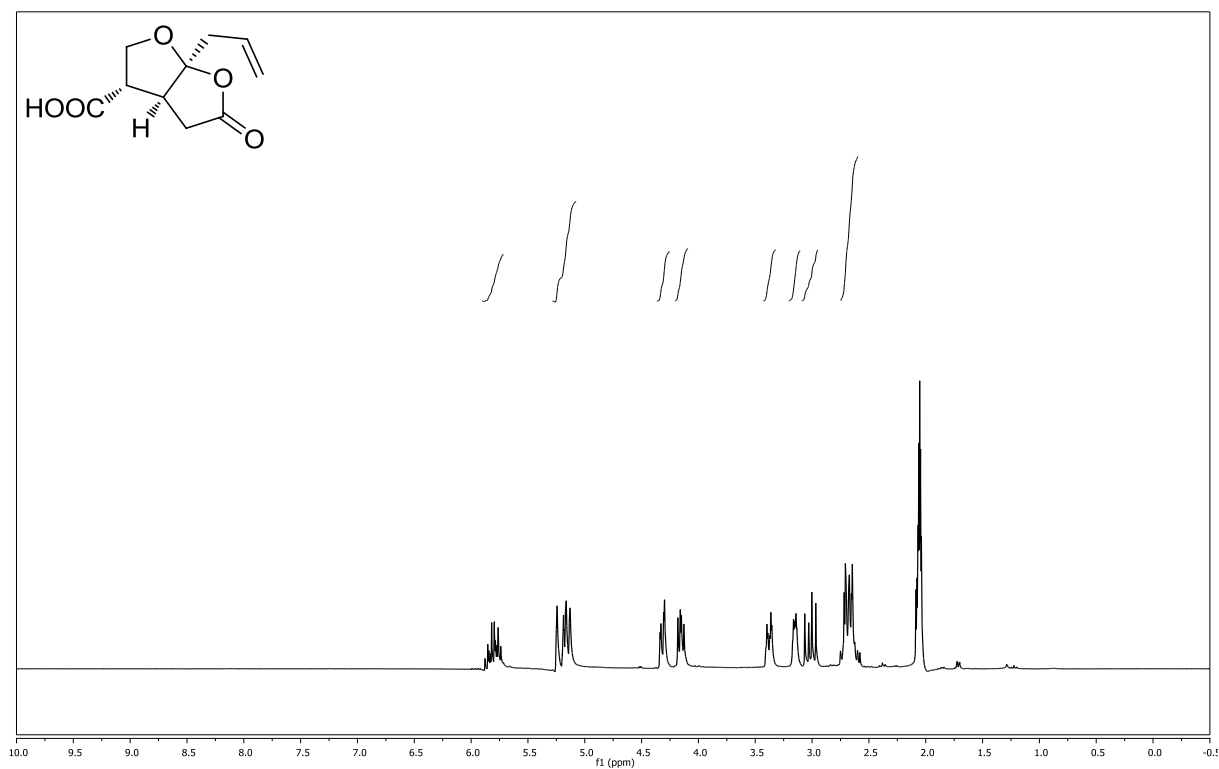


(acetone-d₆, 151 MHz)

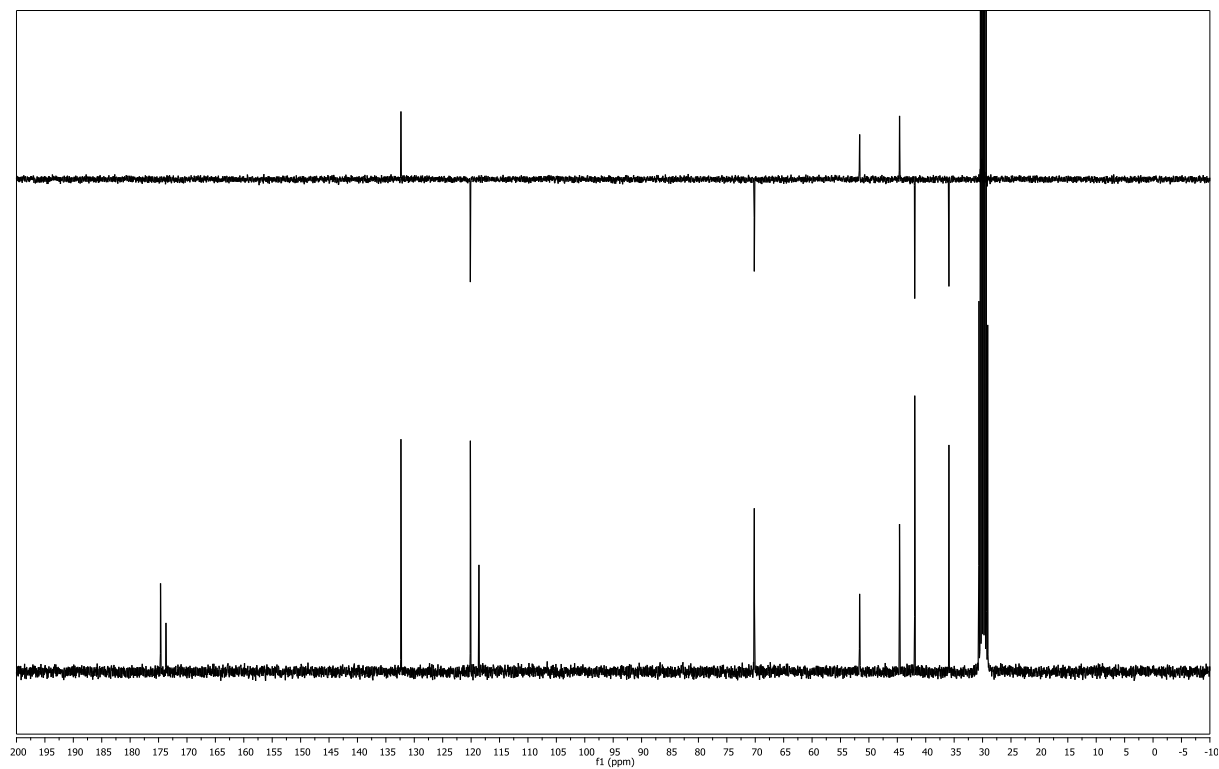


(3*S*,3*aS*,6*aS*)-6*a*-allyl-5-oxohexahydrofuro[2,3-*b*]furan-3-carboxylic acid (187)

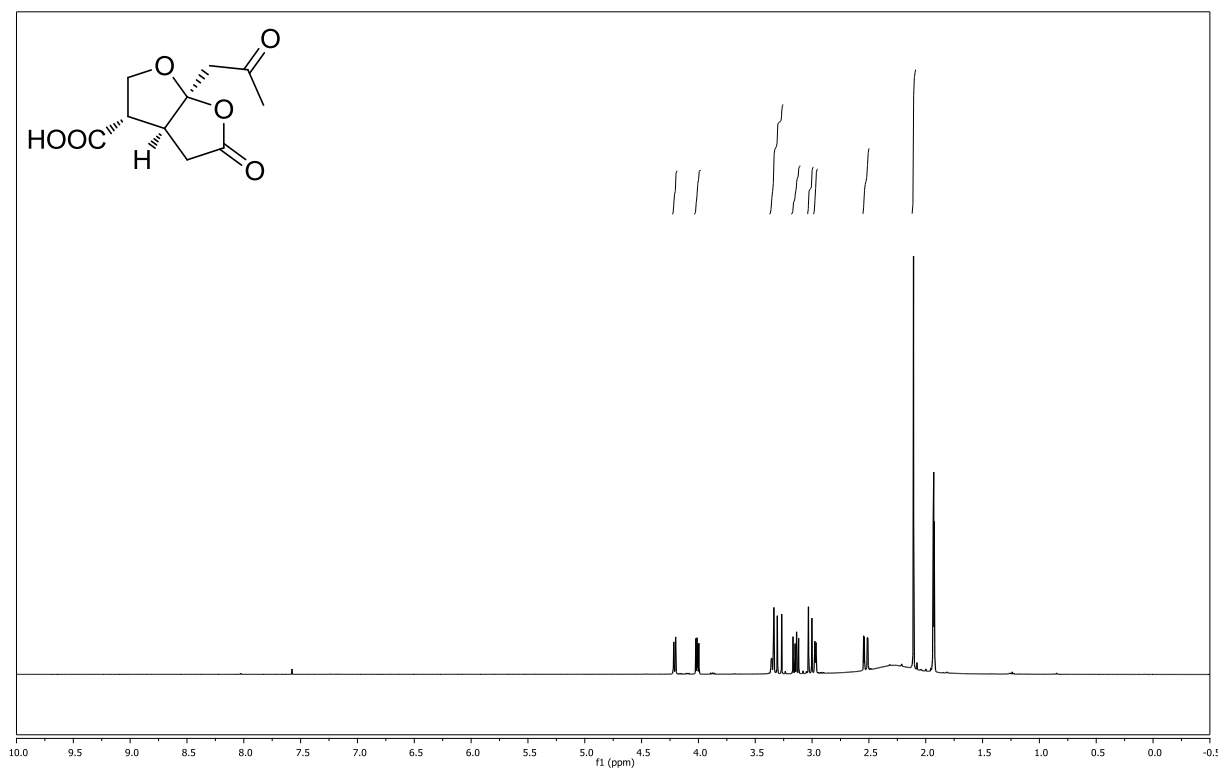
(acetone-*d*₆, 300 MHz)



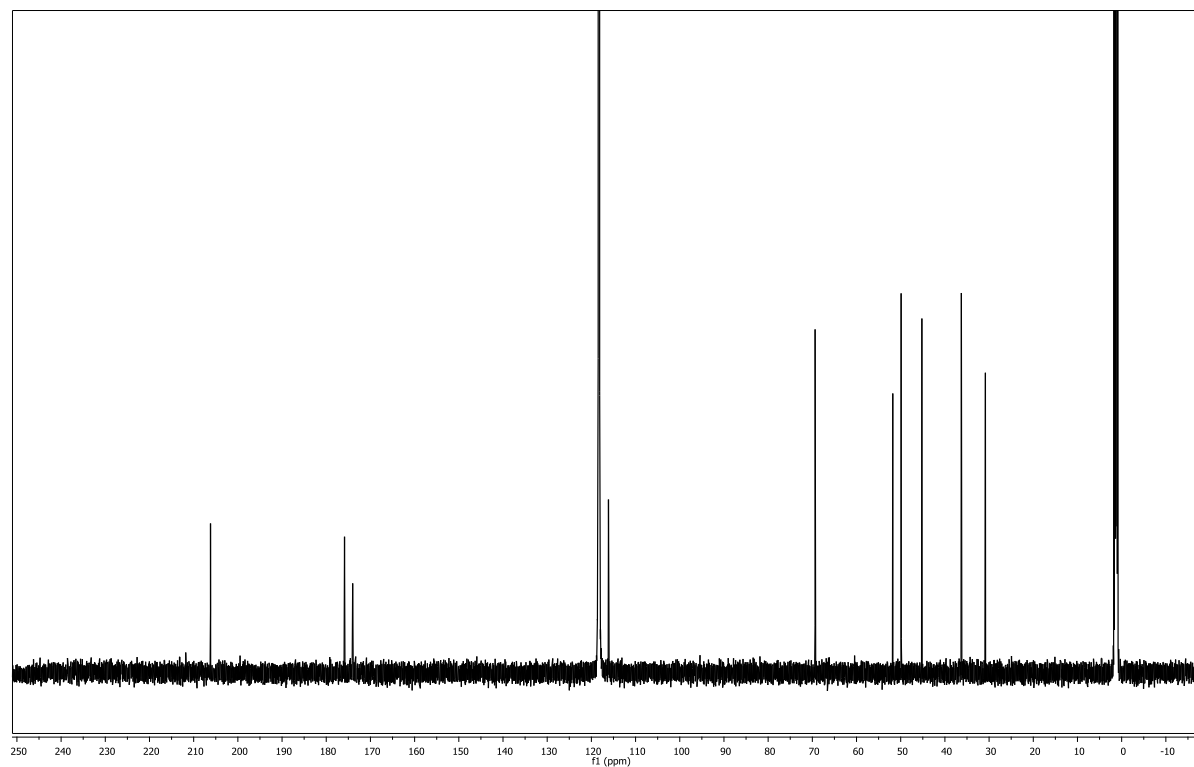
(acetone-*d*₆, 75 MHz)



(3*S*,3*aS*,6*aS*)-5-oxo-6*a*-(2-oxopropyl)hexahydrofuro[2,3-*b*]furan-3-carboxylic acid (189)
(acetonitrile-*d*₃, 600 MHz)

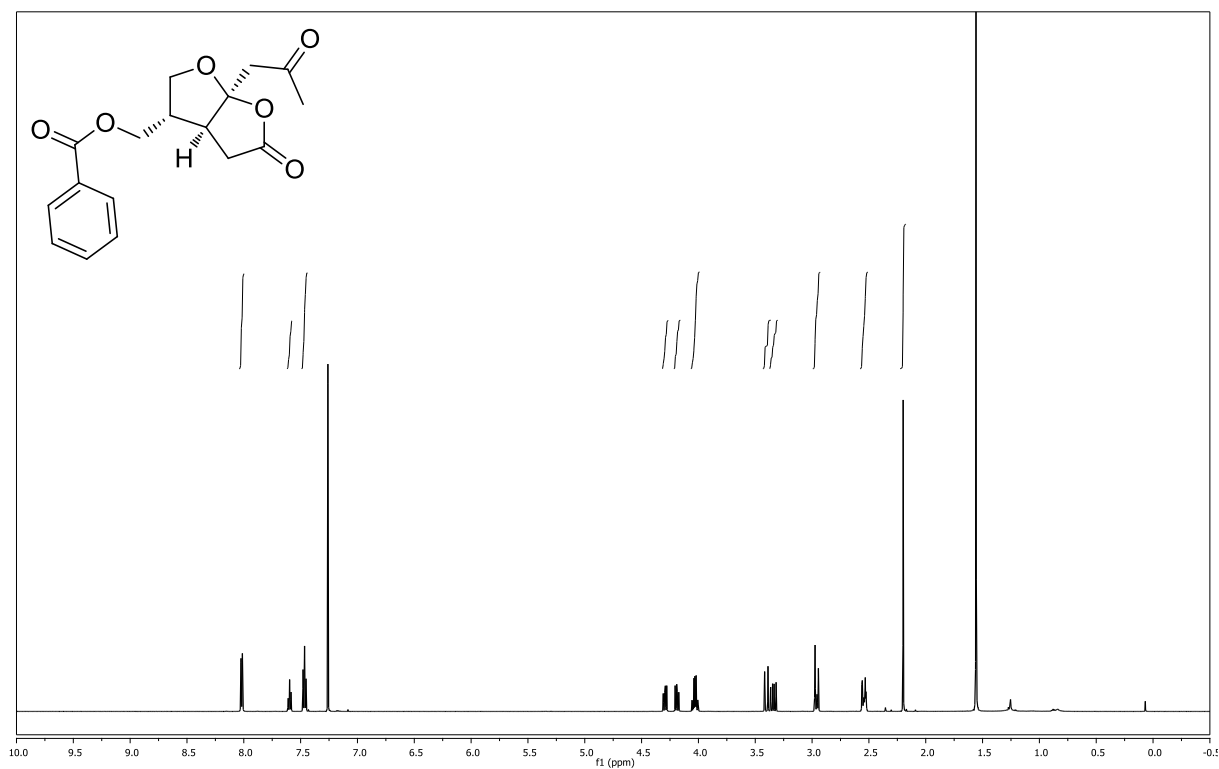


(acetonitrile-*d*₃, 151 MHz)

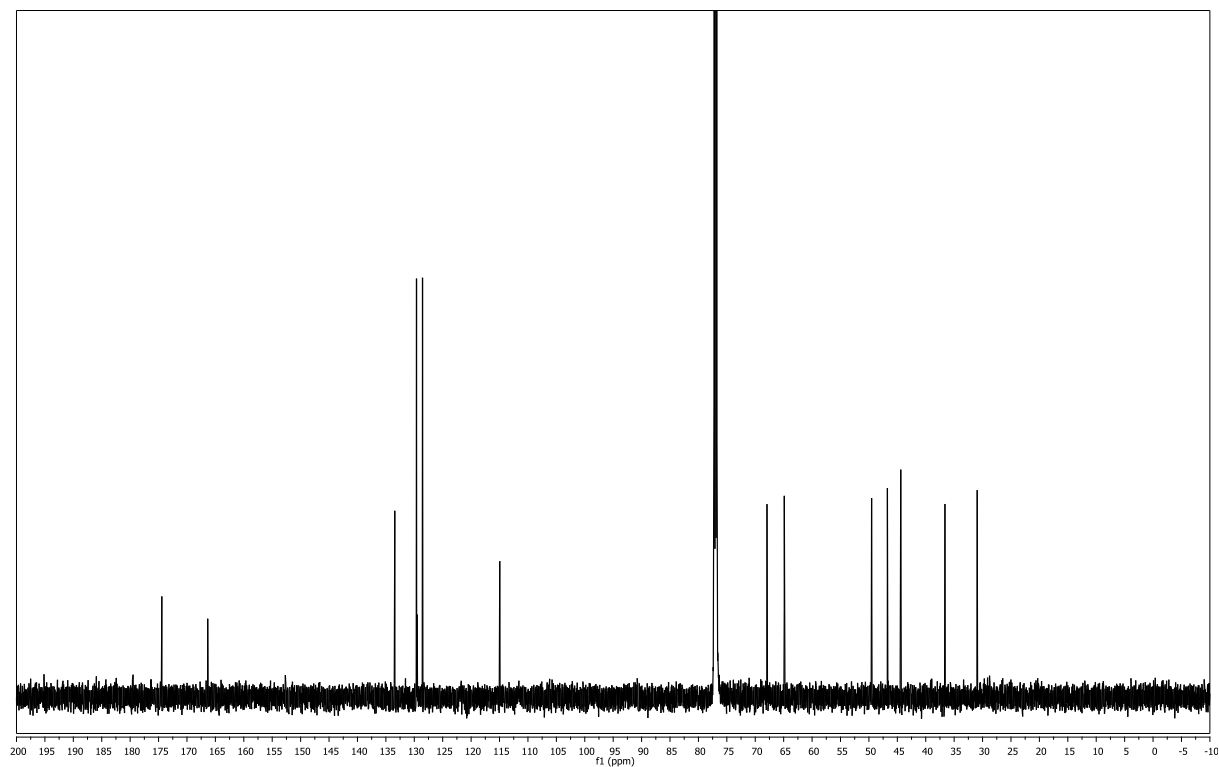


((3*S*,3*aS*,6*aS*)-5-oxo-6*a*-(2-oxopropyl)hexahydrofuro[2,3-*b*]furan-3-yl)methyl benzoate (5) (-)-Paeonilide

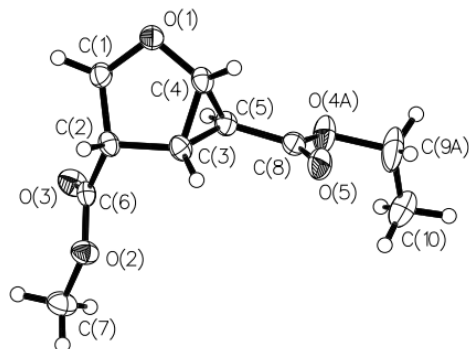
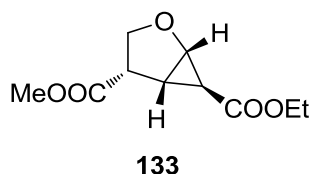
(CDCl₃, 600 MHz)



(CDCl₃, 151 MHz)



2. X-ray crystallography data

(1*S*,4*S*,5*S*,6*S*)-6-ethyl 4-methyl 2-oxabicyclo[3.1.0]hexane-4,6-dicarboxylate (133)**Table 1:** Crystal data and structure refinement for **133**.

Crystal Data	
Empirical formula	C ₁₀ H ₁₄ O ₅
Formula weight	214.21
Crystal size	0.1790 x 0.1140 x 0.1089 mm
Crystal description	stick
Crystal colour	colourless
Crystal system	Orthorhombic
Space group	P 21 21 21
Unit cell dimensions	a = 5.2775(1) Å alpha = 90 deg. b = 7.4363(1) Å beta = 90 deg. c = 26.0428(4) Å gamma = 90 deg.
Volume	1022.05(3) Å ³
Z, Calculated density	4, 1.392 Mg/m ³
Absorption coefficient	0.950 mm ⁻¹
F(000)	456
Data Collection	
Measurement device type	SuperNova, Single source at offset, Atlas
Measurement method	ω scans
Temperature	123 K
Wavelength	1.54184 Å
Monochromator	graphite
Theta range for data collection	3.39 to 76.43 deg.
Index ranges	-6 ≤ h ≤ 6, -9 ≤ k ≤ 9, -31 ≤ l ≤ 32
Reflections collected / unique	9985 / 2129 [R(int) = 0.0311]
Reflections greater I > 2σ(I)	2110
Absorption correction	Analytical
Max. and min. transmission	0.926 and 0.868

Refinement	
Refinement method	Full-matrix least-squares on F ²
Hydrogen treatment	:
Data / restraints / parameters	2129 / 0 / 142
Goodness-of-fit on F ²	1.077
Final R indices [$I > 2\sigma(I)$]	R1 = 0.0431, wR2 = 0.1113
R indices (all data)	R1 = 0.0434, wR2 = 0.1117
Absolute structure parameter	-0.1(3)
Largest diff. peak and hole	0.411 and -0.367 e.Å ⁻³

Table 2: Atomic coordinates ($\times 10^4$) and equivalent isotropic displacement parameters ($\text{\AA}^2 \times 10^3$) for **133**. U(eq) is defined as one third of the trace of the orthogonalized Uij tensor.

Atom	x	y	z	U(eq)
O(1)	1993(3)	9251(2)	2282(1)	30(1)
O(2)	7794(3)	5360(2)	1483(1)	29(1)
O(3)	4026(3)	4302(2)	1729(1)	32(1)
O(4A)	-292(4)	9433(2)	605(1)	41(1)
O(5)	3268(3)	11057(2)	709(1)	40(1)
C(1)	2890(4)	7415(3)	2307(1)	27(1)
C(2)	5219(4)	7326(2)	1960(1)	23(1)
C(3)	4753(4)	8817(2)	1571(1)	25(1)
C(4)	2771(4)	9952(2)	1808(1)	26(1)
C(5)	2129(4)	8841(2)	1327(1)	24(1)
C(6)	5565(4)	5488(2)	1719(1)	22(1)
C(7)	8349(5)	3631(3)	1252(1)	35(1)
C(8)	1843(4)	9895(3)	851(1)	28(1)
C(9A)	-897(8)	10393(4)	134(1)	63(1)
C(10)	-392(14)	9278(8)	-309(2)	48(1)
C(9)	-897(8)	10393(4)	134(1)	63(1)
C(11)	-1700(20)	9331(14)	-267(3)	48(1)
O(4)	-292(4)	9433(2)	605(1)	41(1)

Table 3: Bond lengths [\AA] and angles [deg] for **133**.

O(1)-C(1)	1.447(3)	O(2)-C(6)-O(3)	123.73(16)
O(1)-C(4)	1.403(2)	O(2)-C(6)-C(2)	111.22(15)
O(2)-C(6)	1.331(3)	O(3)-C(6)-C(2)	125.04(19)
O(2)-C(7)	1.450(3)	O(4A)-C(8)-C(5)	110.62(18)
O(3)-C(6)	1.199(2)	O(5)-C(8)-C(5)	125.14(19)
O(4)-C(8)	1.341(3)	O(4A)-C(8)-O(5)	124.19(18)
O(4)-C(9)	1.455(3)	O(4)-C(8)-C(5)	110.62(18)
O(4A)-C(8)	1.341(3)	O(4)-C(8)-O(5)	124.19(18)
O(4A)-C(9A)	1.455(3)	O(4)-C(9)-C(11)	115.2(5)
O(5)-C(8)	1.204(3)	O(4A)-C(9A)-C(10)	110.5(3)
C(1)-C(2)	1.527(3)	O(1)-C(1)-H(1A)	110.00

E. Appendix

C(2)-C(6)	1.514(2)	O(1)-C(1)-H(1B)	111.00
C(2)-C(3)	1.521(2)	C(2)-C(1)-H(1A)	110.00
C(3)-C(5)	1.523(3)	C(2)-C(1)-H(1B)	111.00
C(3)-C(4)	1.479(3)	H(1A)-C(1)-H(1B)	109.00
C(4)-C(5)	1.537(2)	C(1)-C(2)-H(2)	109.00
C(5)-C(8)	1.475(3)	C(3)-C(2)-H(2)	109.00
C(9)-C(11)	1.376(9)	C(6)-C(2)-H(2)	109.00
C(9A)-C(10)	1.445(6)	C(2)-C(3)-H(3)	120.00
C(1)-H(1A)	0.9900	C(4)-C(3)-H(3)	120.00
C(1)-H(1B)	0.9900	C(5)-C(3)-H(3)	120.00
C(2)-H(2)	10.000	O(1)-C(4)-H(4)	118.00
C(3)-H(3)	10.000	C(3)-C(4)-H(4)	118.00
C(4)-H(4)	10.000	C(5)-C(4)-H(4)	118.00
C(5)-H(5)	10.000	C(3)-C(5)-H(5)	118.00
C(7)-H(7A)	0.9800	C(4)-C(5)-H(5)	118.00
C(7)-H(7B)	0.9800	C(8)-C(5)-H(5)	118.00
C(7)-H(7C)	0.9800	O(2)-C(7)-H(7A)	109.00
C(9)-H(9D)	0.9900	O(2)-C(7)-H(7B)	109.00
C(9)-H(9C)	0.9900	O(2)-C(7)-H(7C)	109.00
C(9A)-H(9B)	0.9900	H(7A)-C(7)-H(7B)	109.00
C(9A)-H(9A)	0.9900	H(7A)-C(7)-H(7C)	109.00
C(10)-H(10C)	0.9800	H(7B)-C(7)-H(7C)	110.00
C(10)-H(10A)	0.9800	H(9C)-C(9)-H(9D)	107.00
C(10)-H(10B)	0.9800	O(4)-C(9)-H(9C)	108.00
C(11)-H(11A)	0.9800	O(4)-C(9)-H(9D)	108.00
C(11)-H(11B)	0.9800	C(11)-C(9)-H(9C)	109.00
C(11)-H(11C)	0.9800	C(11)-C(9)-H(9D)	108.00
C(1)-O(1)-C(4)	107.11(13)	C(10)-C(9A)-H(9A)	109.00
C(6)-O(2)-C(7)	115.70(16)	C(10)-C(9A)-H(9B)	110.00
C(8)-O(4)-C(9)	117.5(2)	O(4A)-C(9A)-H(9B)	110.00
C(8)-O(4A)-C(9A)	117.5(2)	O(4A)-C(9A)-H(9A)	110.00
O(1)-C(1)-C(2)	106.14(15)	H(9A)-C(9A)-H(9B)	108.00
C(1)-C(2)-C(6)	112.38(16)	H(10A)-C(10)-H(10C)	109.00
C(3)-C(2)-C(6)	113.73(15)	H(10B)-C(10)-H(10C)	110.00
C(1)-C(2)-C(3)	103.43(16)	C(9A)-C(10)-H(10A)	109.00
C(2)-C(3)-C(5)	115.64(15)	C(9A)-C(10)-H(10B)	109.00
C(4)-C(3)-C(5)	61.57(13)	C(9A)-C(10)-H(10C)	109.00
C(2)-C(3)-C(4)	104.67(16)	H(10A)-C(10)-H(10B)	109.00
O(1)-C(4)-C(5)	116.92(14)	C(9)-C(11)-H(11A)	110.00
C(3)-C(4)-C(5)	60.65(13)	C(9)-C(11)-H(11B)	110.00
O(1)-C(4)-C(3)	111.23(14)	C(9)-C(11)-H(11C)	110.00
C(3)-C(5)-C(4)	57.78(12)	H(11A)-C(11)-H(11B)	110.00
C(3)-C(5)-C(8)	116.72(17)	H(11A)-C(11)-H(11C)	109.00
C(4)-C(5)-C(8)	114.92(14)	H(11B)-C(11)-H(11C)	109.00

Table 4: Anisotropic displacement parameters ($\text{\AA}^2 \times 10^3$) for **133**. The anisotropic displacement factor exponent takes the form: $-2 \pi^2 [h^2 a^{*2} U_{11} + \dots + 2 h k a^* b^* U_{12}]$.

Atom	U11	U22	U33	U23	U13	U12
O(1)	43(1)	25(1)	23(1)	-4(1)	-2(1)	9(1)
O(2)	30(1)	23(1)	35(1)	-3(1)	5(1)	0(1)
O(3)	31(1)	21(1)	45(1)	-4(1)	2(1)	-4(1)
O(4A)	59(1)	34(1)	30(1)	6(1)	-18(1)	-3(1)
O(5)	46(1)	31(1)	42(1)	15(1)	4(1)	1(1)
C(1)	36(1)	22(1)	23(1)	0(1)	-2(1)	4(1)
C(2)	26(1)	18(1)	26(1)	-1(1)	-4(1)	1(1)
C(3)	27(1)	17(1)	32(1)	2(1)	-1(1)	-1(1)
C(4)	33(1)	18(1)	26(1)	-2(1)	-5(1)	2(1)
C(5)	29(1)	19(1)	25(1)	-1(1)	-2(1)	0(1)
C(6)	26(1)	18(1)	23(1)	4(1)	-4(1)	1(1)
C(7)	38(1)	29(1)	39(1)	-7(1)	5(1)	5(1)
C(8)	38(1)	21(1)	25(1)	-2(1)	1(1)	6(1)
C(9A)	105(3)	50(2)	33(1)	10(1)	-29(2)	8(2)
C(10)	62(3)	53(2)	28(1)	8(1)	-5(2)	-7(3)
C(9)	105(3)	50(2)	33(1)	10(1)	-29(2)	8(2)
C(11)	62(3)	53(2)	28(1)	8(1)	-5(2)	-7(3)
O(4)	59(1)	34(1)	30(1)	6(1)	-18(1)	-3(1)

Table 5: Hydrogen coordinates ($\times 10^4$) and isotropic displacement parameters ($\text{\AA}^2 \times 10^3$) for **133**.

Atom	x	y	z	U(eq)
H(2)	6760	7627	2166	28
H(3)	6215	9389	1390	30
H(5)	1035	7755	1372	29
H(7A)	7062	3353	993	53
H(4)	2914	11286	1772	31
H(7C)	10022	3674	1089	53
H(9A)	-2707	10742	136	76
H(9B)	132	11504	113	76
H(10A)	1438	9081	-340	72
H(10B)	-1019	9879	-619	72
H(10C)	-1251	8119	-268	72
H(7B)	8339	2698	1518	53
H(1A)	1566	6575	2184	32
H(1B)	3345	7091	2664	32
H(9C)	-2235	11287	210	76
H(9D)	627	11063	22	76
H(11A)	-649	8249	-286	72
H(11B)	-1564	10004	-590	72
H(11C)	-3475	8984	-212	72

Table 6: Torsion angles [deg] for **133**.

C(4)-O(1)-C(1)-C(2)	26.33(19)	C(3)-C(2)-C(6)-O(3)	-106.2(2)
C(1)-O(1)-C(4)-C(3)	-15.5(2)	C(1)-C(2)-C(3)-C(4)	17.06(19)
C(1)-O(1)-C(4)-C(5)	51.4(2)	C(4)-C(3)-C(5)-C(8)	103.91(17)
C(7)-O(2)-C(6)-O(3)	-3.1(3)	C(2)-C(3)-C(4)-O(1)	-1.7(2)
C(7)-O(2)-C(6)-C(2)	178.28(16)	C(2)-C(3)-C(4)-C(5)	-111.52(15)
C(8)-O(4A)-C(9A)-C(10)	104.8(4)	C(5)-C(3)-C(4)-O(1)	109.80(16)
C(9A)-O(4A)-C(8)-O(5)	0.6(3)	C(2)-C(3)-C(5)-C(4)	93.41(17)
C(9A)-O(4A)-C(8)-C(5)	178.1(2)	C(2)-C(3)-C(5)-C(8)	-162.68(16)
O(1)-C(1)-C(2)-C(3)	-26.66(18)	O(1)-C(4)-C(5)-C(8)	152.56(17)
O(1)-C(1)-C(2)-C(6)	-149.74(15)	C(3)-C(4)-C(5)-C(8)	-107.05(19)
C(3)-C(2)-C(6)-O(2)	72.4(2)	O(1)-C(4)-C(5)-C(3)	-100.39(18)
C(1)-C(2)-C(3)-C(5)	-48.08(19)	C(4)-C(5)-C(8)-O(4A)	-131.63(19)
C(6)-C(2)-C(3)-C(4)	139.25(17)	C(4)-C(5)-C(8)-O(5)	45.9(3)
C(6)-C(2)-C(3)-C(5)	74.1(2)	C(3)-C(5)-C(8)-O(4A)	163.48(16)
C(1)-C(2)-C(6)-O(2)	-170.52(15)	C(3)-C(5)-C(8)-O(5)	-19.0(3)
C(1)-C(2)-C(6)-O(3)	10.9(3)		

Table 7: Hydrogen-bonds for **133** [Å and deg.].

D-H...A	d(D-H)	d(H...A)	d(D...A)	<(DHA)
C(1)-H(1A)...O(3)	0.9900	24.400	2.826(3)	103.00
C(4)-H(4)...O(3)#1	10.000	23.200	3.308(2)	169.00
C(5)-H(5)...O(2)#2	10.000	24.900	3.478(2)	172.00
C(9A)-H(9B)...O(5)	0.9900	22.900	2.706(4)	104.00

(1*S*,5*R*,6*S*)-6-*tert*-butyl 4-methyl 2-oxabicyclo[3.1.0]hex-3-ene-4,6-dicarboxylate (118)

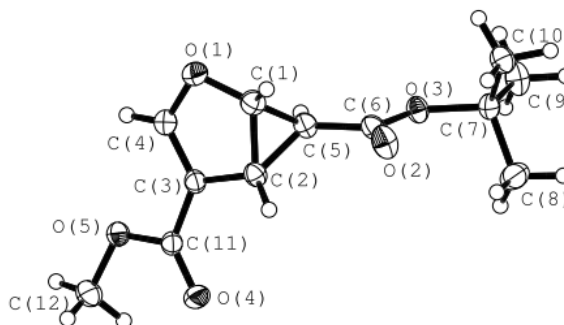
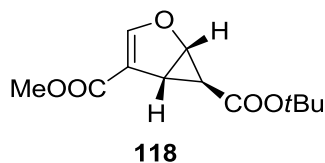


Table 1: Crystal data and structure refinement for **118**.

Crystal Data	
Empirical formula	C ₁₂ H ₁₆ O ₅
Formula weight	240.25
Crystal size	0.7024 x 0.0514 x 0.0399 mm
Crystal description	stick
Crystal colour	translucent colourless
Crystal system	Orthorhombic
Space group	P 2 ₁ 2 ₁ 2 ₁
Unit cell dimensions	a = 5.54365(8) Å alpha = 90 deg. b = 23.9596(4) Å beta = 90 deg. c = 28.0869(4) Å gamma = 90 deg.
Volume	3730.61(10) Å ³
Z, Calculated density	12, 1.283 Mg/m ³
Absorption coefficient	0.839 mm ⁻¹
F(000)	1536
Data Collection	
Measurement device type	SuperNova, Single source at offset, Atlas
Measurement method	\w scans
Temperature	123 K
Wavelength	1.54184 Å
Monochromator	graphite
Theta range for data collection	3.15 to 74.07 deg.
Index ranges	-6 ≤ h ≤ 6, -29 ≤ k ≤ 24, -34 ≤ l ≤ 33
Reflections collected / unique	26433 / 7472 [R(int) = 0.0277]
Reflections greater I > 2σ(I)	7005
Absorption correction	Analytical
Max. and min. transmission	0.974 and 0.785

Refinement	
Refinement method	Full-matrix least-squares on F ²
Hydrogen treatment	:
Data / restraints / parameters	7472 / 0 / 472
Goodness-of-fit on F ²	1.037
Final R indices [$I > 2\sigma(I)$]	R1 = 0.0290, wR2 = 0.0760
R indices (all data)	R1 = 0.0314, wR2 = 0.0778
Absolute structure parameter	-0.03(8)
Largest diff. peak and hole	0.151 and -0.165 e.Å ⁻³

Table 2: Atomic coordinates ($\times 10^4$) and equivalent isotropic displacement parameters ($\text{\AA}^2 \times 10^3$) for **118**. U(eq) is defined as one third of the trace of the orthogonalized Uij tensor.

Atom	x	y	z	U(eq)
O(1)	-4200(2)	2228(1)	6214(1)	33(1)
O(2)	-9861(2)	3336(1)	6638(1)	34(1)
O(3)	-6875(1)	3984(1)	6620(1)	24(1)
O(4)	-4295(2)	2115(1)	7856(1)	33(1)
O(5)	-1040(2)	1773(1)	7479(1)	26(1)
C(1)	-6253(2)	2528(1)	6383(1)	27(1)
C(2)	-6247(2)	2512(1)	6918(1)	23(1)
C(3)	-4014(2)	2192(1)	7019(1)	22(1)
C(4)	-2954(2)	2063(1)	6606(1)	28(1)
C(5)	-5743(2)	3058(1)	6652(1)	24(1)
C(6)	-7754(2)	3468(1)	6639(1)	24(1)
C(7)	-8468(2)	4479(1)	6600(1)	24(1)
C(8)	-9827(3)	4529(1)	7067(1)	36(1)
C(9)	-6669(2)	4951(1)	6537(1)	34(1)
C(10)	-10152(2)	4445(1)	6173(1)	29(1)
C(11)	-3175(2)	2033(1)	7493(1)	22(1)
C(12)	-166(2)	1565(1)	7929(1)	32(1)
O(6)	469(2)	3156(1)	7831(1)	35(1)
O(7)	-5065(2)	4316(1)	8208(1)	36(1)
O(8)	-2026(1)	4946(1)	8259(1)	24(1)
O(9)	615(2)	3154(1)	9477(1)	36(1)
O(10)	3777(2)	2770(1)	9099(1)	31(1)
C(13)	-1543(2)	3470(1)	7996(1)	29(1)
C(14)	-1499(2)	3475(1)	8530(1)	25(1)
C(15)	729(2)	3155(1)	8635(1)	26(1)
C(16)	1746(2)	3003(1)	8223(1)	31(1)
C(17)	-988(2)	4012(1)	8245(1)	25(1)
C(18)	-2951(2)	4430(1)	8234(1)	26(1)
C(19)	-3595(2)	5442(1)	8281(1)	24(1)
C(20)	-5127(3)	5423(1)	8727(1)	35(1)
C(21)	-1764(2)	5912(1)	8310(1)	31(1)
C(22)	-5093(3)	5492(1)	7830(1)	33(1)

C(23)	1642(2)	3035(1)	9111(1)	25(1)
C(24)	4771(3)	2613(1)	9556(1)	35(1)
O(11)	5396(2)	4191(1)	9454(1)	32(1)
O(12)	-347(2)	5278(1)	9864(1)	37(1)
O(13)	2595(1)	5924(1)	9974(1)	24(1)
O(14)	5321(2)	4037(1)	11094(1)	36(1)
O(15)	8658(2)	3750(1)	10716(1)	31(1)
C(25)	3311(2)	4473(1)	9627(1)	27(1)
C(26)	3304(2)	4437(1)	10160(1)	25(1)
C(27)	5567(2)	4127(1)	10257(1)	25(1)
C(28)	6653(2)	4019(1)	9841(1)	28(1)
C(29)	3758(2)	5000(1)	9908(1)	23(1)
C(30)	1752(2)	5405(1)	9910(1)	25(1)
C(31)	944(2)	6406(1)	10010(1)	25(1)
C(32)	-754(2)	6334(1)	10429(1)	33(1)
C(33)	2685(3)	6884(1)	10095(1)	40(1)
C(34)	-400(3)	6485(1)	9545(1)	33(1)
C(35)	6443(2)	3973(1)	10730(1)	25(1)
C(36)	9618(2)	3570(1)	11169(1)	34(1)

Table 3: Bond lengths [Å] and angles [deg] for **118**.

O(1)-C(1)	1.4279(15)	C(2)-C(5)-H(5)	118.00
O(1)-C(4)	1.3591(14)	C(7)-C(8)-H(8B)	110.00
O(2)-C(6)	1.2095(14)	H(8A)-C(8)-H(8B)	109.00
O(3)-C(6)	1.3318(14)	H(8A)-C(8)-H(8C)	109.00
O(3)-C(7)	1.4789(14)	C(7)-C(8)-H(8A)	109.00
O(4)-C(11)	1.2085(14)	H(8B)-C(8)-H(8C)	109.00
O(5)-C(11)	1.3382(14)	C(7)-C(8)-H(8C)	109.00
O(5)-C(12)	1.4443(14)	C(7)-C(9)-H(9C)	110.00
O(6)-C(13)	1.4229(15)	C(7)-C(9)-H(9B)	109.00
O(6)-C(16)	1.3593(16)	H(9A)-C(9)-H(9B)	110.00
O(7)-C(18)	1.2057(14)	H(9A)-C(9)-H(9C)	109.00
O(8)-C(19)	1.4736(14)	C(7)-C(9)-H(9A)	109.00
O(8)-C(18)	1.3409(14)	H(9B)-C(9)-H(9C)	109.00
O(9)-C(23)	1.2101(14)	H(10A)-C(10)-H(10B)	109.00
O(10)-C(24)	1.4460(17)	H(10A)-C(10)-H(10C)	109.00
O(10)-C(23)	1.3436(15)	C(7)-C(10)-H(10C)	109.00
O(11)-C(28)	1.3557(14)	C(7)-C(10)-H(10A)	110.00
O(11)-C(25)	1.4238(15)	H(10B)-C(10)-H(10C)	109.00
O(12)-C(30)	1.2091(14)	C(7)-C(10)-H(10B)	110.00
O(13)-C(30)	1.3400(14)	H(12A)-C(12)-H(12C)	109.00
O(13)-C(31)	1.4784(14)	H(12B)-C(12)-H(12C)	110.00
O(14)-C(35)	1.2082(14)	O(5)-C(12)-H(12A)	109.00
O(15)-C(36)	1.4459(16)	O(5)-C(12)-H(12B)	109.00
O(15)-C(35)	1.3397(14)	H(12A)-C(12)-H(12B)	110.00
C(1)-C(5)	1.5048(17)	O(5)-C(12)-H(12C)	109.00

E. Appendix

C(1)-C(2)	1.5015(16)	C(14)-C(13)-C(17)	61.67(8)
C(2)-C(5)	1.5332(17)	O(6)-C(13)-C(14)	108.53(9)
C(2)-C(3)	1.4837(16)	O(6)-C(13)-C(17)	116.55(9)
C(3)-C(11)	1.4607(16)	C(13)-C(14)-C(15)	102.08(9)
C(3)-C(4)	1.3373(16)	C(13)-C(14)-C(17)	59.45(8)
C(5)-C(6)	1.4855(16)	C(15)-C(14)-C(17)	112.48(9)
C(7)-C(9)	1.5177(16)	C(14)-C(15)-C(16)	108.56(10)
C(7)-C(8)	1.5183(18)	C(14)-C(15)-C(23)	125.10(10)
C(7)-C(10)	1.5202(16)	C(16)-C(15)-C(23)	126.34(11)
C(1)-H(1)	10.000	O(6)-C(16)-C(15)	114.07(10)
C(2)-H(2)	10.000	C(13)-C(17)-C(14)	58.89(8)
C(4)-H(4)	0.9500	C(13)-C(17)-C(18)	115.08(9)
C(5)-H(5)	10.000	C(14)-C(17)-C(18)	116.18(9)
C(8)-H(8C)	0.9800	O(7)-C(18)-O(8)	125.82(11)
C(8)-H(8A)	0.9800	O(8)-C(18)-C(17)	110.02(9)
C(8)-H(8B)	0.9800	O(7)-C(18)-C(17)	124.16(11)
C(9)-H(9C)	0.9800	O(8)-C(19)-C(22)	110.60(9)
C(9)-H(9B)	0.9800	O(8)-C(19)-C(21)	101.86(8)
C(9)-H(9A)	0.9800	C(21)-C(19)-C(22)	110.72(10)
C(10)-H(10B)	0.9800	C(20)-C(19)-C(21)	110.60(10)
C(10)-H(10A)	0.9800	C(20)-C(19)-C(22)	112.69(11)
C(10)-H(10C)	0.9800	O(8)-C(19)-C(20)	109.86(10)
C(12)-H(12A)	0.9800	O(10)-C(23)-C(15)	112.19(10)
C(12)-H(12B)	0.9800	O(9)-C(23)-O(10)	123.16(11)
C(12)-H(12C)	0.9800	O(9)-C(23)-C(15)	124.65(11)
C(13)-C(17)	1.5069(17)	O(6)-C(13)-H(13)	119.00
C(13)-C(14)	1.4981(16)	C(14)-C(13)-H(13)	119.00
C(14)-C(17)	1.5402(17)	C(17)-C(13)-H(13)	119.00
C(14)-C(15)	1.4839(16)	C(13)-C(14)-H(14)	122.00
C(15)-C(23)	1.4568(16)	C(17)-C(14)-H(14)	122.00
C(15)-C(16)	1.3384(18)	C(15)-C(14)-H(14)	122.00
C(17)-C(18)	1.4798(16)	O(6)-C(16)-H(16)	123.00
C(19)-C(20)	1.5155(19)	C(15)-C(16)-H(16)	123.00
C(19)-C(22)	1.5181(19)	C(14)-C(17)-H(17)	118.00
C(19)-C(21)	1.5185(16)	C(13)-C(17)-H(17)	118.00
C(13)-H(13)	10.000	C(18)-C(17)-H(17)	118.00
C(14)-H(14)	10.000	C(19)-C(20)-H(20A)	109.00
C(16)-H(16)	0.9500	C(19)-C(20)-H(20B)	109.00
C(17)-H(17)	10.000	H(20B)-C(20)-H(20C)	109.00
C(20)-H(20A)	0.9800	C(19)-C(20)-H(20C)	110.00
C(20)-H(20B)	0.9800	H(20A)-C(20)-H(20B)	110.00
C(20)-H(20C)	0.9800	H(20A)-C(20)-H(20C)	109.00
C(21)-H(21A)	0.9800	C(19)-C(21)-H(21A)	109.00
C(21)-H(21C)	0.9800	C(19)-C(21)-H(21B)	109.00
C(21)-H(21B)	0.9800	C(19)-C(21)-H(21C)	109.00
C(22)-H(22B)	0.9800	H(21B)-C(21)-H(21C)	109.00
C(22)-H(22C)	0.9800	H(21A)-C(21)-H(21B)	109.00

E. Appendix

C(22)-H(22A)	0.9800	H(21A)-C(21)-H(21C)	109.00
C(24)-H(24B)	0.9800	C(19)-C(22)-H(22B)	109.00
C(24)-H(24C)	0.9800	H(22A)-C(22)-H(22C)	110.00
C(24)-H(24A)	0.9800	C(19)-C(22)-H(22C)	109.00
C(25)-C(26)	1.4984(16)	H(22A)-C(22)-H(22B)	109.00
C(25)-C(29)	1.5097(17)	C(19)-C(22)-H(22A)	109.00
C(26)-C(27)	1.4829(16)	H(22B)-C(22)-H(22C)	110.00
C(26)-C(29)	1.5440(17)	O(10)-C(24)-H(24C)	110.00
C(27)-C(28)	1.3403(16)	H(24A)-C(24)-H(24C)	109.00
C(27)-C(35)	1.4607(16)	H(24B)-C(24)-H(24C)	109.00
C(29)-C(30)	1.4754(16)	H(24A)-C(24)-H(24B)	110.00
C(31)-C(32)	1.5170(16)	O(10)-C(24)-H(24A)	109.00
C(31)-C(33)	1.5163(19)	O(10)-C(24)-H(24B)	109.00
C(31)-C(34)	1.5171(18)	O(11)-C(25)-C(26)	108.39(9)
C(25)-H(25)	10.000	O(11)-C(25)-C(29)	116.21(9)
C(26)-H(26)	10.000	C(26)-C(25)-C(29)	61.76(8)
C(28)-H(28)	0.9500	C(25)-C(26)-C(27)	102.18(9)
C(29)-H(29)	10.000	C(25)-C(26)-C(29)	59.48(8)
C(32)-H(32A)	0.9800	C(27)-C(26)-C(29)	112.57(9)
C(32)-H(32B)	0.9800	C(26)-C(27)-C(28)	108.42(10)
C(32)-H(32C)	0.9800	C(26)-C(27)-C(35)	125.13(10)
C(33)-H(33A)	0.9800	C(28)-C(27)-C(35)	126.45(11)
C(33)-H(33B)	0.9800	O(11)-C(28)-C(27)	114.15(10)
C(33)-H(33C)	0.9800	C(25)-C(29)-C(26)	58.76(7)
C(34)-H(34A)	0.9800	C(25)-C(29)-C(30)	115.34(10)
C(34)-H(34B)	0.9800	C(26)-C(29)-C(30)	116.73(9)
C(34)-H(34C)	0.9800	O(12)-C(30)-O(13)	125.58(11)
C(36)-H(36A)	0.9800	O(12)-C(30)-C(29)	124.08(11)
C(36)-H(36B)	0.9800	O(13)-C(30)-C(29)	110.34(9)
C(36)-H(36C)	0.9800	O(13)-C(31)-C(32)	110.40(10)
C(1)-O(1)-C(4)	106.31(9)	O(13)-C(31)-C(33)	101.99(9)
C(6)-O(3)-C(7)	121.86(9)	O(13)-C(31)-C(34)	109.95(10)
C(11)-O(5)-C(12)	115.47(9)	C(32)-C(31)-C(33)	111.12(11)
C(13)-O(6)-C(16)	106.66(9)	C(32)-C(31)-C(34)	112.23(10)
C(18)-O(8)-C(19)	121.32(9)	C(33)-C(31)-C(34)	110.69(11)
C(23)-O(10)-C(24)	115.93(10)	O(14)-C(35)-O(15)	123.22(11)
C(25)-O(11)-C(28)	106.75(9)	O(14)-C(35)-C(27)	124.51(11)
C(30)-O(13)-C(31)	121.28(9)	O(15)-C(35)-C(27)	112.27(10)
C(35)-O(15)-C(36)	115.50(9)	O(11)-C(25)-H(25)	119.00
C(2)-C(1)-C(5)	61.33(8)	C(26)-C(25)-H(25)	119.00
O(1)-C(1)-C(2)	108.60(9)	C(29)-C(25)-H(25)	119.00
O(1)-C(1)-C(5)	116.26(9)	C(25)-C(26)-H(26)	122.00
C(3)-C(2)-C(5)	112.51(9)	C(27)-C(26)-H(26)	122.00
C(1)-C(2)-C(5)	59.44(8)	C(29)-C(26)-H(26)	122.00
C(1)-C(2)-C(3)	101.96(9)	O(11)-C(28)-H(28)	123.00
C(2)-C(3)-C(4)	108.61(10)	C(27)-C(28)-H(28)	123.00
C(4)-C(3)-C(11)	126.23(11)	C(25)-C(29)-H(29)	118.00

C(2)-C(3)-C(11)	125.14(10)	C(26)-C(29)-H(29)	118.00
O(1)-C(4)-C(3)	114.41(10)	C(30)-C(29)-H(29)	118.00
C(2)-C(5)-C(6)	116.02(9)	C(31)-C(32)-H(32A)	109.00
C(1)-C(5)-C(6)	113.91(9)	C(31)-C(32)-H(32B)	109.00
C(1)-C(5)-C(2)	59.23(8)	C(31)-C(32)-H(32C)	109.00
O(2)-C(6)-O(3)	126.52(11)	H(32A)-C(32)-H(32B)	109.00
O(2)-C(6)-C(5)	123.57(11)	H(32A)-C(32)-H(32C)	110.00
O(3)-C(6)-C(5)	109.90(9)	H(32B)-C(32)-H(32C)	109.00
C(8)-C(7)-C(9)	111.53(11)	C(31)-C(33)-H(33A)	109.00
C(8)-C(7)-C(10)	112.35(10)	C(31)-C(33)-H(33B)	110.00
C(9)-C(7)-C(10)	110.65(10)	C(31)-C(33)-H(33C)	109.00
O(3)-C(7)-C(10)	110.76(9)	H(33A)-C(33)-H(33B)	109.00
O(3)-C(7)-C(9)	102.05(8)	H(33A)-C(33)-H(33C)	110.00
O(3)-C(7)-C(8)	109.02(10)	H(33B)-C(33)-H(33C)	109.00
O(4)-C(11)-C(3)	124.20(11)	C(31)-C(34)-H(34A)	109.00
O(5)-C(11)-C(3)	112.03(10)	C(31)-C(34)-H(34B)	109.00
O(4)-C(11)-O(5)	123.76(11)	C(31)-C(34)-H(34C)	109.00
C(5)-C(1)-H(1)	119.00	H(34A)-C(34)-H(34B)	110.00
C(2)-C(1)-H(1)	119.00	H(34A)-C(34)-H(34C)	109.00
O(1)-C(1)-H(1)	119.00	H(34B)-C(34)-H(34C)	110.00
C(1)-C(2)-H(2)	122.00	O(15)-C(36)-H(36A)	109.00
C(5)-C(2)-H(2)	122.00	O(15)-C(36)-H(36B)	109.00
C(3)-C(2)-H(2)	122.00	O(15)-C(36)-H(36C)	109.00
C(3)-C(4)-H(4)	123.00	H(36A)-C(36)-H(36B)	110.00
O(1)-C(4)-H(4)	123.00	H(36A)-C(36)-H(36C)	109.00
C(1)-C(5)-H(5)	118.00	H(36B)-C(36)-H(36C)	110.00
C(6)-C(5)-H(5)	118.00		

Table 4: Anisotropic displacement parameters ($\text{\AA}^2 \times 10^3$) for **118** The anisotropic displacement factor exponent takes the form: $-2 \pi^2 [h^2 a^{*2} U_{11} + \dots + 2 h k a^* b^* U_{12}]$.

Atom	U11	U22	U33	U23	U13	U12
O(1)	41(1)	35(1)	22(1)	-1(1)	1(1)	10(1)
O(2)	20(1)	30(1)	51(1)	8(1)	-3(1)	-1(1)
O(3)	20(1)	22(1)	31(1)	2(1)	-2(1)	1(1)
O(4)	33(1)	42(1)	25(1)	3(1)	7(1)	13(1)
O(5)	24(1)	29(1)	25(1)	3(1)	1(1)	7(1)
C(1)	30(1)	27(1)	26(1)	0(1)	-1(1)	1(1)
C(2)	22(1)	22(1)	26(1)	3(1)	0(1)	-1(1)
C(3)	23(1)	19(1)	25(1)	2(1)	2(1)	1(1)
C(4)	30(1)	25(1)	27(1)	1(1)	2(1)	6(1)
C(5)	20(1)	23(1)	29(1)	4(1)	1(1)	0(1)
C(6)	21(1)	24(1)	27(1)	4(1)	-1(1)	-1(1)
C(7)	22(1)	22(1)	29(1)	0(1)	0(1)	3(1)
C(8)	38(1)	41(1)	30(1)	-5(1)	5(1)	4(1)
C(9)	29(1)	24(1)	50(1)	1(1)	-4(1)	1(1)
C(10)	28(1)	30(1)	30(1)	3(1)	-5(1)	4(1)

C(11)	23(1)	19(1)	25(1)	1(1)	2(1)	1(1)
C(12)	30(1)	37(1)	28(1)	5(1)	-4(1)	8(1)
O(6)	45(1)	32(1)	29(1)	-2(1)	5(1)	12(1)
O(7)	21(1)	25(1)	63(1)	2(1)	-2(1)	-2(1)
O(8)	19(1)	19(1)	34(1)	1(1)	1(1)	0(1)
O(9)	37(1)	42(1)	30(1)	0(1)	9(1)	12(1)
O(10)	28(1)	31(1)	33(1)	4(1)	5(1)	8(1)
C(13)	31(1)	25(1)	32(1)	-1(1)	2(1)	3(1)
C(14)	24(1)	20(1)	31(1)	2(1)	4(1)	1(1)
C(15)	25(1)	19(1)	32(1)	2(1)	7(1)	2(1)
C(16)	35(1)	24(1)	33(1)	1(1)	7(1)	7(1)
C(17)	22(1)	21(1)	32(1)	2(1)	3(1)	1(1)
C(18)	23(1)	22(1)	32(1)	2(1)	1(1)	-1(1)
C(19)	24(1)	21(1)	27(1)	1(1)	1(1)	3(1)
C(20)	35(1)	34(1)	35(1)	1(1)	11(1)	4(1)
C(21)	30(1)	22(1)	42(1)	-1(1)	-1(1)	-1(1)
C(22)	36(1)	29(1)	34(1)	1(1)	-8(1)	5(1)
C(23)	25(1)	19(1)	32(1)	2(1)	6(1)	1(1)
C(24)	33(1)	35(1)	37(1)	3(1)	-5(1)	3(1)
O(11)	40(1)	29(1)	26(1)	-3(1)	5(1)	5(1)
O(12)	19(1)	29(1)	63(1)	0(1)	-1(1)	-3(1)
O(13)	20(1)	21(1)	29(1)	-1(1)	2(1)	1(1)
O(14)	39(1)	39(1)	30(1)	4(1)	11(1)	9(1)
O(15)	27(1)	36(1)	32(1)	6(1)	5(1)	5(1)
C(25)	29(1)	24(1)	29(1)	-2(1)	1(1)	-1(1)
C(26)	25(1)	22(1)	29(1)	2(1)	6(1)	0(1)
C(27)	25(1)	20(1)	31(1)	1(1)	6(1)	0(1)
C(28)	32(1)	21(1)	31(1)	0(1)	5(1)	3(1)
C(29)	21(1)	21(1)	28(1)	1(1)	3(1)	0(1)
C(30)	23(1)	24(1)	27(1)	2(1)	3(1)	-2(1)
C(31)	24(1)	23(1)	27(1)	-1(1)	0(1)	3(1)
C(32)	30(1)	42(1)	26(1)	-1(1)	4(1)	9(1)
C(33)	31(1)	26(1)	62(1)	-9(1)	-1(1)	2(1)
C(34)	39(1)	33(1)	28(1)	4(1)	-2(1)	7(1)
C(35)	27(1)	18(1)	29(1)	2(1)	5(1)	-1(1)
C(36)	32(1)	34(1)	34(1)	6(1)	-2(1)	0(1)

Table 5. Hydrogen coordinates ($\times 10^4$) and isotropic displacement parameters ($\text{\AA}^2 \times 10^3$) for **118**.

Atom	x	y	z	U(eq)
H(1)	-7822	2489	6210	33
H(2)	-7761	2454	7105	28
H(4)	-1455	1872	6588	33
H(5)	-4054	3205	6651	29
H(8A)	-10663	4889	7079	44
H(8B)	-8686	4504	7333	44

E. Appendix

H(8C)	-11009	4226	7091	44
H(9A)	-5519	4947	6802	41
H(9B)	-7528	5308	6533	41
H(9C)	-5798	4902	6237	41
H(10A)	-11386	4161	6232	35
H(10B)	-10930	4808	6124	35
H(10C)	-9225	4345	5889	35
H(12A)	-283	1861	8170	38
H(12B)	-1144	1245	8028	38
H(12C)	1521	1450	7896	38
H(13)	-3127	3428	7830	35
H(14)	-3002	3429	8723	30
H(16)	3229	2805	8206	37
H(17)	712	4151	8235	30
H(20A)	-5875	5788	8779	42
H(20B)	-4108	5328	9001	42
H(20C)	-6387	5139	8691	42
H(21A)	-754	5861	8593	37
H(21B)	-2610	6271	8332	37
H(21C)	-747	5909	8025	37
H(22A)	-6303	5193	7824	40
H(22B)	-5905	5855	7825	40
H(22C)	-4039	5458	7552	40
H(24A)	4639	2928	9777	42
H(24B)	3875	2293	9683	42
H(24C)	6472	2511	9518	42
H(25)	1753	4431	9451	33
H(26)	1791	4363	10343	30
H(28)	8171	3837	9819	34
H(29)	5438	5151	9913	28
H(32A)	-1575	6688	10494	39
H(32B)	169	6220	10711	39
H(32C)	-1953	6046	10354	39
H(33A)	3582	6818	10390	48
H(33B)	1783	7235	10121	48
H(33C)	3817	6909	9827	48
H(34A)	-1537	6176	9500	40
H(34B)	-1286	6839	9553	40
H(34C)	756	6490	9281	40
H(36A)	9480	3875	11400	40
H(36B)	8706	3246	11283	40
H(36C)	11319	3468	11131	40

Table 6: Torsion angles [deg] for **118**.

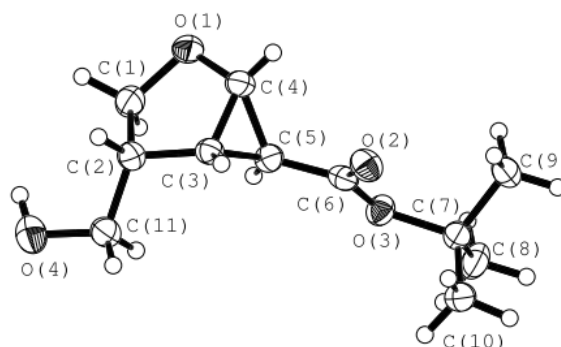
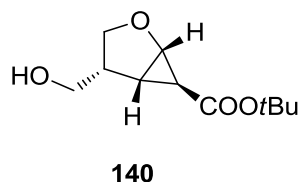
C(4)-O(1)-C(1)-C(2)	-2.75(12)	C(2)-C(5)-C(6)-O(3)	149.92(10)
C(4)-O(1)-C(1)-C(5)	63.78(12)	C(2)-C(5)-C(6)-O(2)	-31.37(17)
C(1)-O(1)-C(4)-C(3)	3.55(14)	C(1)-C(5)-C(6)-O(2)	34.66(16)
C(7)-O(3)-C(6)-C(5)	179.41(9)	C(14)-C(13)-C(17)-C(18)	-106.65(11)
C(7)-O(3)-C(6)-O(2)	0.75(18)	O(6)-C(13)-C(14)-C(15)	1.66(12)
C(6)-O(3)-C(7)-C(10)	-57.27(13)	O(6)-C(13)-C(17)-C(18)	155.64(10)
C(6)-O(3)-C(7)-C(9)	-175.08(10)	C(17)-C(13)-C(14)-C(15)	-109.13(10)
C(6)-O(3)-C(7)-C(8)	66.86(13)	O(6)-C(13)-C(14)-C(17)	110.79(10)
C(12)-O(5)-C(11)-O(4)	2.87(16)	O(6)-C(13)-C(17)-C(14)	-97.71(11)
C(12)-O(5)-C(11)-C(3)	-175.61(10)	C(13)-C(14)-C(15)-C(23)	179.89(11)
C(16)-O(6)-C(13)-C(17)	63.83(12)	C(17)-C(14)-C(15)-C(16)	-61.32(13)
C(13)-O(6)-C(16)-C(15)	3.53(14)	C(15)-C(14)-C(17)-C(13)	91.07(10)
C(16)-O(6)-C(13)-C(14)	-3.09(12)	C(13)-C(14)-C(15)-C(16)	0.38(13)
C(18)-O(8)-C(19)-C(22)	-62.85(13)	C(13)-C(14)-C(17)-C(18)	104.77(11)
C(18)-O(8)-C(19)-C(20)	62.17(13)	C(17)-C(14)-C(15)-C(23)	118.19(12)
C(18)-O(8)-C(19)-C(21)	179.44(10)	C(15)-C(14)-C(17)-C(18)	-164.16(10)
C(19)-O(8)-C(18)-C(17)	-176.72(9)	C(23)-C(15)-C(16)-O(6)	178.03(11)
C(19)-O(8)-C(18)-O(7)	2.95(18)	C(16)-C(15)-C(23)-O(10)	3.57(17)
C(24)-O(10)-C(23)-C(15)	-177.54(10)	C(14)-C(15)-C(23)-O(10)	-175.85(11)
C(24)-O(10)-C(23)-O(9)	2.13(17)	C(16)-C(15)-C(23)-O(9)	-176.10(12)
C(28)-O(11)-C(25)-C(26)	-2.84(12)	C(14)-C(15)-C(16)-O(6)	-2.48(14)
C(25)-O(11)-C(28)-C(27)	3.53(14)	C(14)-C(15)-C(23)-O(9)	4.5(2)
C(28)-O(11)-C(25)-C(29)	64.07(12)	C(13)-C(17)-C(18)-O(7)	28.09(17)
C(30)-O(13)-C(31)-C(33)	178.15(11)	C(14)-C(17)-C(18)-O(8)	141.70(10)
C(30)-O(13)-C(31)-C(32)	59.99(13)	C(14)-C(17)-C(18)-O(7)	-37.98(17)
C(31)-O(13)-C(30)-O(12)	2.18(18)	C(13)-C(17)-C(18)-O(8)	-152.23(10)
C(30)-O(13)-C(31)-C(34)	-64.38(13)	O(11)-C(25)-C(26)-C(29)	110.47(10)
C(31)-O(13)-C(30)-C(29)	-177.35(9)	C(29)-C(25)-C(26)-C(27)	-109.18(10)
C(36)-O(15)-C(35)-O(14)	1.94(17)	O(11)-C(25)-C(29)-C(26)	-97.75(11)
C(36)-O(15)-C(35)-C(27)	-178.13(10)	O(11)-C(25)-C(26)-C(27)	1.30(12)
O(1)-C(1)-C(2)-C(5)	110.37(10)	C(26)-C(25)-C(29)-C(30)	-107.15(11)
O(1)-C(1)-C(2)-C(3)	1.14(12)	O(11)-C(25)-C(29)-C(30)	155.11(10)
C(2)-C(1)-C(5)-C(6)	-107.12(11)	C(25)-C(26)-C(27)-C(35)	-179.61(11)
C(5)-C(1)-C(2)-C(3)	-109.23(10)	C(29)-C(26)-C(27)-C(28)	-61.04(13)
O(1)-C(1)-C(5)-C(2)	-97.79(11)	C(25)-C(26)-C(27)-C(28)	0.73(13)
O(1)-C(1)-C(5)-C(6)	155.09(10)	C(29)-C(26)-C(27)-C(35)	118.62(12)
C(1)-C(2)-C(3)-C(11)	-177.41(11)	C(25)-C(26)-C(29)-C(30)	104.78(11)
C(5)-C(2)-C(3)-C(4)	-60.75(13)	C(27)-C(26)-C(29)-C(30)	-164.06(10)
C(1)-C(2)-C(5)-C(6)	103.55(11)	C(27)-C(26)-C(29)-C(25)	91.16(10)
C(3)-C(2)-C(5)-C(1)	90.91(10)	C(26)-C(27)-C(35)-O(15)	-173.17(11)
C(1)-C(2)-C(3)-C(4)	0.91(13)	C(26)-C(27)-C(28)-O(11)	-2.71(14)
C(3)-C(2)-C(5)-C(6)	-165.54(10)	C(35)-C(27)-C(28)-O(11)	177.64(11)
C(5)-C(2)-C(3)-C(11)	120.93(12)	C(28)-C(27)-C(35)-O(14)	-173.64(12)
C(2)-C(3)-C(4)-O(1)	-2.86(14)	C(28)-C(27)-C(35)-O(15)	6.43(18)
C(11)-C(3)-C(4)-O(1)	175.44(11)	C(26)-C(27)-C(35)-O(14)	6.8(2)
C(2)-C(3)-C(11)-O(4)	4.94(19)	C(25)-C(29)-C(30)-O(12)	27.64(17)

E. Appendix

C(2)-C(3)-C(11)-O(5)	-176.58(10)	C(25)-C(29)-C(30)-O(13)	-152.82(10)
C(4)-C(3)-C(11)-O(4)	-173.08(12)	C(26)-C(29)-C(30)-O(12)	-38.53(17)
C(4)-C(3)-C(11)-O(5)	5.39(17)	C(26)-C(29)-C(30)-O(13)	141.00(10)
C(1)-C(5)-C(6)-O(3)	-144.05(10)		

Table 7: Hydrogen-bonds for **118** [Å and deg.].

D-H...A	d(D-H)	d(H...A)	d(D...A)	<(DHA)
C(5)-H(5)...O(2)#1	10.000	23.500	3.3286(14)	167.00
C(8)-H(8C)...O(2)	0.9800	25.600	3.1007(17)	115.00
C(9)-H(9B)...O(14)#2	0.9800	25.300	3.3948(15)	148.00
C(10)-H(10A)...O(2)	0.9800	24.300	2.9643(15)	114.00
C(16)-H(16)...O(4)#1	0.9500	23.600	3.2267(15)	151.00
C(17)-H(17)...O(7)#1	10.000	23.800	3.3650(14)	170.00
C(20)-H(20C)...O(7)	0.9800	25.000	3.0280(17)	113.00
C(22)-H(22A)...O(7)	0.9800	24.600	3.0107(16)	115.00
C(26)-H(26)...O(15)#3	10.000	25.000	3.4325(14)	154.00
C(28)-H(28)...O(9)#1	0.9500	23.300	3.1870(15)	150.00
C(29)-H(29)...O(12)#1	10.000	23.600	3.3379(14)	166.00
C(32)-H(32C)...O(12)	0.9800	24.600	2.9941(17)	114.00
C(34)-H(34A)...O(12)	0.9800	24.700	3.0273(17)	116.00

(1*S*,4*R*,5*S*,6*S*)-*tert*-butyl 4-(hydroxymethyl)-2-oxabicyclo[3.1.0]hexane-6-carboxylate (140)**Table 1:** Crystal data and structure refinement for **140**.

Crystal Data	
Empirical formula	C ₁₁ H ₁₈ O ₄
Formula weight	214.25
Crystal size	0.2203 x 0.0587 x 0.0207 mm
Crystal description	stick
Crystal colour	colourless
Crystal system	Triclinic
Space group	P 1
Unit cell dimensions	a = 5.6783(3) Å alpha = 91.884(4) deg. b = 9.1467(5) Å beta = 92.675(4) deg. c = 22.1094(11) Å gamma = 91.532(4) deg.
Volume	1145.98(10) Å ³
Z, Calculated density	4, 1.242 Mg/m ³
Absorption coefficient	0.774 mm ⁻¹
F(000)	464
Data Collection	
Measurement device type	SuperNova, Single source at offset, Atlas
Measurement method	\w scans
Temperature	123 K
Wavelength	1.54184 Å
Monochromator	graphite
Theta range for data collection	4.01 to 75.40 deg.
Index ranges	-7 ≤ h ≤ 6 -11 ≤ k ≤ 11 -21 ≤ l ≤ 27
Reflections collected / unique	7732 / 5280 [R(int) = 0.0338]
Reflections greater I > 2σ(I)	4987
Absorption correction	Analytical
Max. and min. transmission	0.984 and 0.922

Refinement	
Refinement method	Full-matrix least-squares on F^2
Hydrogen treatment	:
Data / restraints / parameters	5280 / 3 / 542
Goodness-of-fit on F^2	1.030
Final R indices [$I > 2\sigma(I)$]	$R1 = 0.0554$, $wR2 = 0.1472$
R indices (all data)	$R1 = 0.0579$, $wR2 = 0.1518$
Absolute structure parameter	0.2(2)
Largest diff. peak and hole	0.330 and -0.313 e. \AA^{-3}

Table 2: Atomic coordinates ($\times 10^4$) and equivalent isotropic displacement parameters ($\text{\AA}^2 \times 10^3$) for **140**. $U(\text{eq})$ is defined as one third of the trace of the orthogonalized U_{ij} tensor.

Atom	x	y	z	$U(\text{eq})$
O(1)	9415(5)	3089(3)	-2071(1)	43(1)
O(2)	7308(5)	-1462(3)	-1910(1)	35(1)
O(3)	4243(4)	-783(3)	-2522(1)	32(1)
O(4)	4678(5)	4803(3)	-689(1)	42(1)
C(1)	7856(7)	3963(4)	-1717(2)	38(1)
C(2)	7304(6)	3065(4)	-1161(2)	31(1)
C(3)	7663(6)	1505(4)	-1381(1)	28(1)
C(4)	8984(6)	1626(4)	-1942(2)	33(1)
C(5)	6419(6)	1049(4)	-1993(1)	28(1)
C(6)	6071(6)	-535(4)	-2128(2)	29(1)
C(7)	3507(6)	-2285(4)	-2742(2)	32(1)
C(8)	1546(7)	-1951(4)	-3210(2)	41(1)
C(9)	5511(7)	-3031(4)	-3050(2)	39(1)
C(10)	2590(7)	-3147(4)	-2233(2)	39(1)
C(11)	4894(6)	3355(4)	-920(2)	34(1)
O(5)	7819(4)	4535(3)	381(1)	29(1)
O(6)	13057(4)	1215(3)	336(1)	33(1)
O(7)	10021(4)	-263(2)	-36(1)	26(1)
O(8)	7770(4)	1621(3)	2128(1)	31(1)
C(12)	6309(6)	4244(4)	871(2)	28(1)
C(13)	7809(6)	3499(3)	1361(1)	26(1)
C(14)	9806(5)	2886(3)	1014(1)	24(1)
C(15)	9714(6)	3575(3)	417(1)	26(1)
C(16)	9111(5)	1942(3)	444(1)	25(1)
C(17)	10960(6)	939(3)	247(1)	25(1)
C(18)	11543(6)	-1471(3)	-236(2)	27(1)
C(19)	9739(7)	-2591(4)	-505(2)	37(1)
C(20)	12853(8)	-2069(4)	311(2)	42(1)
C(21)	13165(7)	-954(4)	-714(2)	36(1)
C(22)	6366(5)	2383(3)	1690(1)	26(1)
O(9)	3928(4)	-4480(3)	2240(1)	31(1)
O(10)	9350(4)	-2677(3)	3455(1)	38(1)

O(11)	6498(4)	-2516(3)	4136(1)	28(1)
O(12)	591(5)	-562(3)	1731(1)	41(1)
C(23)	2372(6)	-3342(4)	2039(2)	28(1)
C(24)	3852(6)	-1925(4)	2047(2)	30(1)
C(25)	5915(6)	-2210(4)	2488(2)	30(1)
C(26)	5849(6)	-3803(4)	2573(2)	29(1)
C(27)	5329(5)	-2797(3)	3112(1)	26(1)
C(28)	7297(6)	-2635(4)	3581(2)	28(1)
C(29)	8160(6)	-2334(4)	4674(2)	31(1)
C(30)	9568(8)	-3707(4)	4753(2)	41(1)
C(31)	6472(8)	-2134(6)	5184(2)	52(1)
C(32)	9746(7)	-991(4)	4621(2)	40(1)
C(33)	2401(6)	-618(4)	2193(2)	33(1)
O(13)	6131(5)	-8447(3)	4054(1)	41(1)
O(14)	3798(4)	-5847(3)	5575(1)	33(1)
O(15)	971(4)	-7649(3)	5567(1)	28(1)
O(16)	1053(5)	-6605(3)	2724(1)	38(1)
C(34)	4518(7)	-8206(4)	3549(2)	36(1)
C(35)	3774(6)	-6611(4)	3609(2)	30(1)
C(36)	4141(6)	-6276(3)	4284(2)	27(1)
C(37)	5619(6)	-7456(4)	4521(2)	32(1)
C(38)	3042(6)	-7381(3)	4696(2)	28(1)
C(39)	2676(6)	-6848(3)	5323(2)	27(1)
C(40)	339(6)	-7386(4)	6201(1)	28(1)
C(41)	2434(6)	-7614(4)	6632(2)	34(1)
C(42)	-1587(6)	-8558(4)	6269(2)	34(1)
C(43)	-639(6)	-5873(4)	6279(2)	36(1)
C(44)	1288(7)	-6330(4)	3363(2)	33(1)

Table 3: Bond lengths [Å] and angles [deg] for **140**.

O(1)-C(1)	1.449(5)	H(10B)-C(10)-H(10C)	109.00
O(1)-C(4)	1.395(5)	H(10A)-C(10)-H(10B)	110.00
O(2)-C(6)	1.213(4)	H(10A)-C(10)-H(10C)	109.00
O(3)-C(6)	1.334(4)	C(7)-C(10)-H(10B)	109.00
O(3)-C(7)	1.485(5)	C(7)-C(10)-H(10C)	109.00
O(4)-C(11)	1.414(5)	C(7)-C(10)-H(10A)	109.00
O(4)-H(4O)	0.8400	C(2)-C(11)-H(11B)	109.00
O(5)-C(15)	1.408(4)	H(11A)-C(11)-H(11B)	108.00
O(5)-C(12)	1.441(4)	O(4)-C(11)-H(11B)	109.00
O(6)-C(17)	1.216(4)	O(4)-C(11)-H(11A)	109.00
O(7)-C(17)	1.333(4)	C(2)-C(11)-H(11A)	109.00
O(7)-C(18)	1.489(4)	O(5)-C(12)-C(13)	107.1(3)
O(8)-C(22)	1.435(4)	C(12)-C(13)-C(22)	111.7(3)
O(8)-H(8O)	0.8400	C(14)-C(13)-C(22)	115.3(2)
O(9)-C(23)	1.450(4)	C(12)-C(13)-C(14)	103.1(2)
O(9)-C(26)	1.405(4)	C(13)-C(14)-C(15)	106.7(2)
O(10)-C(28)	1.213(4)	C(15)-C(14)-C(16)	60.85(19)

E. Appendix

O(11)-C(28)	1.330(4)	C(13)-C(14)-C(16)	116.5(2)
O(11)-C(29)	1.486(4)	O(5)-C(15)-C(16)	117.3(3)
O(12)-C(33)	1.418(5)	C(14)-C(15)-C(16)	61.33(19)
O(12)-H(12O)	0.8400	O(5)-C(15)-C(14)	109.9(3)
O(13)-C(37)	1.397(4)	C(14)-C(16)-C(15)	57.83(19)
O(13)-C(34)	1.437(5)	C(14)-C(16)-C(17)	114.5(2)
O(14)-C(39)	1.207(4)	C(15)-C(16)-C(17)	115.9(3)
O(15)-C(39)	1.343(4)	O(6)-C(17)-C(16)	122.9(3)
O(15)-C(40)	1.478(4)	O(7)-C(17)-C(16)	111.5(3)
O(16)-C(44)	1.426(4)	O(6)-C(17)-O(7)	125.7(3)
O(16)-H(16O)	0.8400	O(7)-C(18)-C(20)	109.4(3)
C(1)-C(2)	1.540(5)	C(19)-C(18)-C(21)	110.7(3)
C(2)-C(11)	1.518(5)	C(19)-C(18)-C(20)	110.6(3)
C(2)-C(3)	1.515(5)	O(7)-C(18)-C(19)	102.0(3)
C(3)-C(5)	1.537(5)	O(7)-C(18)-C(21)	110.5(2)
C(3)-C(4)	1.485(5)	C(20)-C(18)-C(21)	113.1(3)
C(4)-C(5)	1.534(5)	O(8)-C(22)-C(13)	112.3(2)
C(5)-C(6)	1.476(5)	O(5)-C(12)-H(12B)	110.00
C(7)-C(9)	1.519(5)	C(13)-C(12)-H(12B)	110.00
C(7)-C(10)	1.501(6)	O(5)-C(12)-H(12A)	110.00
C(7)-C(8)	1.528(5)	C(13)-C(12)-H(12A)	110.00
C(1)-H(1A)	0.9900	H(12A)-C(12)-H(12B)	109.00
C(1)-H(1B)	0.9900	C(12)-C(13)-H(13)	109.00
C(2)-H(2)	10.000	C(22)-C(13)-H(13)	109.00
C(3)-H(3)	10.000	C(14)-C(13)-H(13)	109.00
C(4)-H(4)	10.000	C(16)-C(14)-H(14)	119.00
C(5)-H(5)	10.000	C(13)-C(14)-H(14)	119.00
C(8)-H(8B)	0.9800	C(15)-C(14)-H(14)	119.00
C(8)-H(8A)	0.9800	C(16)-C(15)-H(15)	118.00
C(8)-H(8C)	0.9800	O(5)-C(15)-H(15)	118.00
C(9)-H(9C)	0.9800	C(14)-C(15)-H(15)	118.00
C(9)-H(9B)	0.9800	C(17)-C(16)-H(16)	118.00
C(9)-H(9A)	0.9800	C(14)-C(16)-H(16)	118.00
C(10)-H(10A)	0.9800	C(15)-C(16)-H(16)	118.00
C(10)-H(10B)	0.9800	C(18)-C(19)-H(19A)	109.00
C(10)-H(10C)	0.9800	C(18)-C(19)-H(19C)	109.00
C(11)-H(11A)	0.9900	C(18)-C(19)-H(19B)	109.00
C(11)-H(11B)	0.9900	H(19A)-C(19)-H(19B)	109.00
C(12)-C(13)	1.536(5)	H(19A)-C(19)-H(19C)	109.00
C(13)-C(22)	1.517(4)	H(19B)-C(19)-H(19C)	109.00
C(13)-C(14)	1.509(4)	C(18)-C(20)-H(20B)	109.00
C(14)-C(16)	1.534(4)	C(18)-C(20)-H(20A)	109.00
C(14)-C(15)	1.480(4)	H(20A)-C(20)-H(20C)	110.00
C(15)-C(16)	1.527(4)	H(20A)-C(20)-H(20B)	109.00
C(16)-C(17)	1.484(4)	C(18)-C(20)-H(20C)	109.00
C(18)-C(19)	1.517(5)	H(20B)-C(20)-H(20C)	109.00
C(18)-C(21)	1.514(5)	C(18)-C(21)-H(21C)	109.00

E. Appendix

C(18)-C(20)	1.515(5)	H(21A)-C(21)-H(21B)	110.00
C(12)-H(12A)	0.9900	C(18)-C(21)-H(21B)	110.00
C(12)-H(12B)	0.9900	H(21B)-C(21)-H(21C)	109.00
C(13)-H(13)	10.000	H(21A)-C(21)-H(21C)	109.00
C(14)-H(14)	10.000	C(18)-C(21)-H(21A)	109.00
C(15)-H(15)	10.000	H(22A)-C(22)-H(22B)	108.00
C(16)-H(16)	10.000	O(8)-C(22)-H(22B)	109.00
C(19)-H(19C)	0.9800	C(13)-C(22)-H(22B)	109.00
C(19)-H(19B)	0.9800	C(13)-C(22)-H(22A)	109.00
C(19)-H(19A)	0.9800	O(8)-C(22)-H(22A)	109.00
C(20)-H(20C)	0.9800	O(9)-C(23)-C(24)	106.9(3)
C(20)-H(20B)	0.9800	C(25)-C(24)-C(33)	116.5(3)
C(20)-H(20A)	0.9800	C(23)-C(24)-C(25)	103.6(3)
C(21)-H(21B)	0.9800	C(23)-C(24)-C(33)	111.4(3)
C(21)-H(21A)	0.9800	C(26)-C(25)-C(27)	60.7(2)
C(21)-H(21C)	0.9800	C(24)-C(25)-C(27)	117.3(3)
C(22)-H(22A)	0.9900	C(24)-C(25)-C(26)	105.6(3)
C(22)-H(22B)	0.9900	O(9)-C(26)-C(25)	110.9(3)
C(23)-C(24)	1.525(5)	O(9)-C(26)-C(27)	118.0(3)
C(24)-C(33)	1.505(5)	C(25)-C(26)-C(27)	61.9(2)
C(24)-C(25)	1.523(5)	C(25)-C(27)-C(26)	57.4(2)
C(25)-C(27)	1.544(5)	C(25)-C(27)-C(28)	114.5(3)
C(25)-C(26)	1.475(5)	C(26)-C(27)-C(28)	114.2(3)
C(26)-C(27)	1.526(5)	O(10)-C(28)-C(27)	122.3(3)
C(27)-C(28)	1.491(4)	O(11)-C(28)-C(27)	111.6(3)
C(29)-C(31)	1.522(6)	O(10)-C(28)-O(11)	126.1(3)
C(29)-C(30)	1.517(5)	O(11)-C(29)-C(31)	101.6(3)
C(29)-C(32)	1.515(5)	C(31)-C(29)-C(32)	111.4(3)
C(23)-H(23B)	0.9900	C(30)-C(29)-C(32)	111.8(3)
C(23)-H(23A)	0.9900	C(30)-C(29)-C(31)	111.0(3)
C(24)-H(24)	10.000	O(11)-C(29)-C(30)	110.1(3)
C(25)-H(25)	10.000	O(11)-C(29)-C(32)	110.5(3)
C(26)-H(26)	10.000	O(12)-C(33)-C(24)	107.1(3)
C(27)-H(27)	10.000	O(9)-C(23)-H(23B)	110.00
C(30)-H(30C)	0.9800	H(23A)-C(23)-H(23B)	109.00
C(30)-H(30B)	0.9800	C(24)-C(23)-H(23A)	110.00
C(30)-H(30A)	0.9800	O(9)-C(23)-H(23A)	110.00
C(31)-H(31A)	0.9800	C(24)-C(23)-H(23B)	110.00
C(31)-H(31B)	0.9800	C(25)-C(24)-H(24)	108.00
C(31)-H(31C)	0.9800	C(33)-C(24)-H(24)	108.00
C(32)-H(32B)	0.9800	C(23)-C(24)-H(24)	108.00
C(32)-H(32C)	0.9800	C(24)-C(25)-H(25)	119.00
C(32)-H(32A)	0.9800	C(27)-C(25)-H(25)	119.00
C(33)-H(33B)	0.9900	C(26)-C(25)-H(25)	119.00
C(33)-H(33A)	0.9900	C(27)-C(26)-H(26)	118.00
C(34)-C(35)	1.533(5)	O(9)-C(26)-H(26)	118.00
C(35)-C(36)	1.517(5)	C(25)-C(26)-H(26)	118.00

E. Appendix

C(35)-C(44)	1.521(5)	C(25)-C(27)-H(27)	119.00
C(36)-C(38)	1.524(4)	C(26)-C(27)-H(27)	119.00
C(36)-C(37)	1.479(5)	C(28)-C(27)-H(27)	119.00
C(37)-C(38)	1.534(5)	C(29)-C(30)-H(30A)	109.00
C(38)-C(39)	1.479(5)	H(30A)-C(30)-H(30C)	110.00
C(40)-C(42)	1.527(5)	H(30B)-C(30)-H(30C)	109.00
C(40)-C(43)	1.512(5)	H(30A)-C(30)-H(30B)	109.00
C(40)-C(41)	1.512(5)	C(29)-C(30)-H(30C)	109.00
C(34)-H(34A)	0.9900	C(29)-C(30)-H(30B)	109.00
C(34)-H(34B)	0.9900	C(29)-C(31)-H(31A)	109.00
C(35)-H(35)	10.000	C(29)-C(31)-H(31B)	110.00
C(36)-H(36)	10.000	H(31B)-C(31)-H(31C)	109.00
C(37)-H(37)	10.000	H(31A)-C(31)-H(31B)	110.00
C(38)-H(38)	10.000	C(29)-C(31)-H(31C)	109.00
C(41)-H(41A)	0.9800	H(31A)-C(31)-H(31C)	109.00
C(41)-H(41B)	0.9800	C(29)-C(32)-H(32A)	109.00
C(41)-H(41C)	0.9800	C(29)-C(32)-H(32B)	109.00
C(42)-H(42A)	0.9800	C(29)-C(32)-H(32C)	110.00
C(42)-H(42B)	0.9800	H(32A)-C(32)-H(32B)	109.00
C(42)-H(42C)	0.9800	H(32A)-C(32)-H(32C)	109.00
C(43)-H(43A)	0.9800	H(32B)-C(32)-H(32C)	110.00
C(43)-H(43B)	0.9800	O(12)-C(33)-H(33B)	110.00
C(43)-H(43C)	0.9800	H(33A)-C(33)-H(33B)	109.00
C(44)-H(44A)	0.9900	C(24)-C(33)-H(33A)	110.00
C(44)-H(44B)	0.9900	C(24)-C(33)-H(33B)	110.00
C(1)-O(1)-C(4)	107.5(3)	O(12)-C(33)-H(33A)	110.00
C(6)-O(3)-C(7)	121.9(3)	O(13)-C(34)-C(35)	106.7(3)
C(11)-O(4)-H(4O)	109.00	C(34)-C(35)-C(44)	114.9(3)
C(12)-O(5)-C(15)	108.2(3)	C(36)-C(35)-C(44)	113.5(3)
C(17)-O(7)-C(18)	120.8(2)	C(34)-C(35)-C(36)	102.6(3)
C(22)-O(8)-H(8O)	109.00	C(35)-C(36)-C(37)	105.7(3)
C(23)-O(9)-C(26)	107.8(3)	C(37)-C(36)-C(38)	61.4(2)
C(28)-O(11)-C(29)	120.7(3)	C(35)-C(36)-C(38)	115.8(3)
C(33)-O(12)-H(12O)	109.00	O(13)-C(37)-C(36)	110.5(3)
C(34)-O(13)-C(37)	107.6(3)	C(36)-C(37)-C(38)	60.7(2)
C(39)-O(15)-C(40)	121.3(3)	O(13)-C(37)-C(38)	117.4(3)
C(44)-O(16)-H(16O)	110.00	C(36)-C(38)-C(39)	115.9(2)
O(1)-C(1)-C(2)	106.2(3)	C(37)-C(38)-C(39)	115.7(3)
C(3)-C(2)-C(11)	115.2(3)	C(36)-C(38)-C(37)	57.9(2)
C(1)-C(2)-C(11)	113.4(3)	O(14)-C(39)-C(38)	124.0(3)
C(1)-C(2)-C(3)	103.1(3)	O(15)-C(39)-C(38)	110.4(3)
C(4)-C(3)-C(5)	61.0(2)	O(14)-C(39)-O(15)	125.6(3)
C(2)-C(3)-C(5)	115.8(3)	O(15)-C(40)-C(42)	101.9(3)
C(2)-C(3)-C(4)	105.5(3)	O(15)-C(40)-C(43)	109.9(3)
O(1)-C(4)-C(3)	110.9(3)	C(41)-C(40)-C(42)	111.1(3)
O(1)-C(4)-C(5)	117.7(3)	C(41)-C(40)-C(43)	112.1(3)
C(3)-C(4)-C(5)	61.2(2)	C(42)-C(40)-C(43)	110.7(3)

E. Appendix

C(4)-C(5)-C(6)	116.1(3)	O(15)-C(40)-C(41)	110.7(3)
C(3)-C(5)-C(4)	57.8(2)	O(16)-C(44)-C(35)	111.5(3)
C(3)-C(5)-C(6)	116.9(3)	O(13)-C(34)-H(34A)	110.00
O(3)-C(6)-C(5)	110.4(3)	O(13)-C(34)-H(34B)	110.00
O(2)-C(6)-C(5)	123.9(3)	C(35)-C(34)-H(34A)	110.00
O(2)-C(6)-O(3)	125.7(3)	C(35)-C(34)-H(34B)	110.00
C(8)-C(7)-C(10)	111.8(3)	H(34A)-C(34)-H(34B)	109.00
C(8)-C(7)-C(9)	110.1(3)	C(34)-C(35)-H(35)	108.00
O(3)-C(7)-C(9)	110.7(3)	C(36)-C(35)-H(35)	109.00
C(9)-C(7)-C(10)	112.6(3)	C(44)-C(35)-H(35)	109.00
O(3)-C(7)-C(10)	110.3(3)	C(35)-C(36)-H(36)	120.00
O(3)-C(7)-C(8)	100.8(3)	C(37)-C(36)-H(36)	120.00
O(4)-C(11)-C(2)	113.3(3)	C(38)-C(36)-H(36)	120.00
O(1)-C(1)-H(1B)	111.00	O(13)-C(37)-H(37)	118.00
C(2)-C(1)-H(1B)	110.00	C(36)-C(37)-H(37)	118.00
O(1)-C(1)-H(1A)	110.00	C(38)-C(37)-H(37)	118.00
H(1A)-C(1)-H(1B)	109.00	C(36)-C(38)-H(38)	118.00
C(2)-C(1)-H(1A)	111.00	C(37)-C(38)-H(38)	118.00
C(11)-C(2)-H(2)	108.00	C(39)-C(38)-H(38)	118.00
C(3)-C(2)-H(2)	108.00	C(40)-C(41)-H(41A)	109.00
C(1)-C(2)-H(2)	108.00	C(40)-C(41)-H(41B)	109.00
C(5)-C(3)-H(3)	120.00	C(40)-C(41)-H(41C)	109.00
C(2)-C(3)-H(3)	120.00	H(41A)-C(41)-H(41B)	110.00
C(4)-C(3)-H(3)	120.00	H(41A)-C(41)-H(41C)	109.00
O(1)-C(4)-H(4)	118.00	H(41B)-C(41)-H(41C)	109.00
C(3)-C(4)-H(4)	118.00	C(40)-C(42)-H(42A)	109.00
C(5)-C(4)-H(4)	118.00	C(40)-C(42)-H(42B)	109.00
C(6)-C(5)-H(5)	117.00	C(40)-C(42)-H(42C)	109.00
C(4)-C(5)-H(5)	118.00	H(42A)-C(42)-H(42B)	110.00
C(3)-C(5)-H(5)	118.00	H(42A)-C(42)-H(42C)	109.00
C(7)-C(8)-H(8B)	109.00	H(42B)-C(42)-H(42C)	109.00
C(7)-C(8)-H(8C)	109.00	C(40)-C(43)-H(43A)	109.00
H(8A)-C(8)-H(8C)	110.00	C(40)-C(43)-H(43B)	109.00
H(8A)-C(8)-H(8B)	109.00	C(40)-C(43)-H(43C)	109.00
H(8B)-C(8)-H(8C)	109.00	H(43A)-C(43)-H(43B)	109.00
C(7)-C(8)-H(8A)	109.00	H(43A)-C(43)-H(43C)	109.00
C(7)-C(9)-H(9B)	109.00	H(43B)-C(43)-H(43C)	110.00
C(7)-C(9)-H(9C)	109.00	O(16)-C(44)-H(44A)	109.00
H(9A)-C(9)-H(9C)	109.00	O(16)-C(44)-H(44B)	109.00
H(9A)-C(9)-H(9B)	110.00	C(35)-C(44)-H(44A)	109.00
H(9B)-C(9)-H(9C)	109.00	C(35)-C(44)-H(44B)	109.00
C(7)-C(9)-H(9A)	110.00	H(44A)-C(44)-H(44B)	108.00

Table 4: Anisotropic displacement parameters ($\text{\AA}^2 \times 10^3$) for **140**. The anisotropic displacement factor exponent takes the form: $-2 \pi^2 [h^2 a^{*2} U_{11} + \dots + 2 h k a^* b^* U_{12}]$.

Atom	U11	U22	U33	U23	U13	U12
O(1)	50(2)	43(1)	35(1)	-5(1)	19(1)	-16(1)
O(2)	33(1)	38(1)	36(1)	1(1)	1(1)	9(1)
O(3)	27(1)	29(1)	39(1)	-2(1)	-3(1)	0(1)
O(4)	45(2)	39(1)	43(2)	-6(1)	-1(1)	8(1)
C(1)	46(2)	35(2)	34(2)	-3(1)	8(2)	-9(2)
C(2)	31(2)	34(2)	27(2)	-3(1)	3(1)	-2(1)
C(3)	25(2)	35(2)	24(2)	-1(1)	2(1)	-3(1)
C(4)	28(2)	41(2)	29(2)	-5(1)	7(1)	-6(1)
C(5)	28(2)	31(2)	25(1)	2(1)	0(1)	-2(1)
C(6)	24(2)	35(2)	27(2)	0(1)	7(1)	2(1)
C(7)	26(2)	28(2)	41(2)	-5(1)	3(1)	0(1)
C(8)	36(2)	31(2)	55(2)	-9(2)	-7(2)	-4(1)
C(9)	34(2)	43(2)	39(2)	-12(2)	7(1)	3(1)
C(10)	33(2)	32(2)	53(2)	-3(2)	11(2)	-1(1)
C(11)	31(2)	38(2)	34(2)	-3(1)	4(1)	2(1)
O(5)	30(1)	31(1)	27(1)	5(1)	4(1)	3(1)
O(6)	20(1)	39(1)	40(1)	-8(1)	5(1)	-1(1)
O(7)	23(1)	27(1)	28(1)	-3(1)	3(1)	1(1)
O(8)	31(1)	33(1)	30(1)	5(1)	-1(1)	1(1)
C(12)	26(2)	28(1)	31(2)	2(1)	5(1)	6(1)
C(13)	24(2)	28(1)	25(1)	-4(1)	1(1)	3(1)
C(14)	21(1)	28(1)	23(1)	0(1)	1(1)	1(1)
C(15)	24(2)	30(2)	25(2)	3(1)	2(1)	1(1)
C(16)	17(1)	30(2)	29(1)	-4(1)	2(1)	0(1)
C(17)	23(2)	30(1)	24(1)	0(1)	7(1)	2(1)
C(18)	30(2)	25(1)	27(1)	-2(1)	6(1)	5(1)
C(19)	41(2)	31(2)	39(2)	-3(1)	3(1)	1(1)
C(20)	53(2)	38(2)	35(2)	1(1)	-3(2)	12(2)
C(21)	35(2)	38(2)	37(2)	-5(1)	15(1)	3(1)
C(22)	22(2)	30(2)	27(1)	0(1)	2(1)	3(1)
O(9)	30(1)	31(1)	30(1)	1(1)	3(1)	1(1)
O(10)	24(1)	58(2)	33(1)	7(1)	3(1)	5(1)
O(11)	25(1)	35(1)	26(1)	2(1)	3(1)	2(1)
O(12)	39(2)	42(1)	43(1)	2(1)	-6(1)	7(1)
C(23)	27(2)	30(2)	28(2)	3(1)	1(1)	2(1)
C(24)	28(2)	34(2)	28(2)	6(1)	6(1)	2(1)
C(25)	25(2)	34(2)	33(2)	5(1)	5(1)	-1(1)
C(26)	22(2)	38(2)	28(2)	3(1)	6(1)	2(1)
C(27)	20(1)	29(1)	29(2)	3(1)	3(1)	-1(1)
C(28)	20(2)	32(2)	30(2)	6(1)	2(1)	2(1)
C(29)	30(2)	34(2)	29(2)	-1(1)	3(1)	0(1)
C(30)	47(2)	37(2)	39(2)	8(2)	-14(2)	-2(2)
C(31)	42(2)	83(3)	31(2)	-11(2)	6(2)	-11(2)
C(32)	37(2)	33(2)	48(2)	0(2)	-6(2)	2(1)

C(33)	30(2)	32(2)	38(2)	4(1)	4(1)	-1(1)
O(13)	43(2)	48(1)	32(1)	5(1)	7(1)	16(1)
O(14)	33(1)	36(1)	28(1)	0(1)	0(1)	-6(1)
O(15)	28(1)	33(1)	25(1)	0(1)	5(1)	-1(1)
O(16)	43(2)	46(1)	24(1)	5(1)	-3(1)	-10(1)
C(34)	41(2)	40(2)	29(2)	0(1)	8(1)	1(2)
C(35)	31(2)	34(2)	24(1)	4(1)	3(1)	-1(1)
C(36)	25(2)	29(1)	27(2)	3(1)	2(1)	-3(1)
C(37)	30(2)	38(2)	28(2)	3(1)	3(1)	6(1)
C(38)	30(2)	27(1)	27(2)	3(1)	2(1)	-3(1)
C(39)	24(2)	29(2)	28(2)	4(1)	1(1)	2(1)
C(40)	21(2)	40(2)	24(1)	1(1)	6(1)	1(1)
C(41)	26(2)	48(2)	28(2)	6(1)	7(1)	3(1)
C(42)	27(2)	45(2)	32(2)	4(1)	7(1)	-1(1)
C(43)	30(2)	43(2)	36(2)	-6(1)	1(1)	8(1)
C(44)	37(2)	36(2)	25(2)	2(1)	-1(1)	-1(1)

Table 5: Hydrogen coordinates ($\times 10^4$) and isotropic displacement parameters ($\text{\AA}^2 \times 10^3$) for **140**.

Atom	x	y	z	U(eq)
H(1A)	6388	4156	-1957	46
H(1B)	8634	4912	-1588	46
H(2)	8526	3321	-831	37
H(3)	8088	744	-1084	33
H(4)	10259	916	-2013	39
H(4O)	5509	5375	-885	51
H(5)	5201	1713	-2162	33
H(8A)	2171	-1300	-3511	50
H(8B)	260	-1474	-3007	50
H(8C)	949	-2866	-3412	50
H(9A)	4920	-3947	-3252	46
H(9B)	6757	-3242	-2746	46
H(9C)	6150	-2384	-3351	46
H(10A)	1395	-2587	-2029	47
H(10B)	3893	-3342	-1943	47
H(10C)	1884	-4077	-2395	47
H(11A)	3677	3159	-1250	41
H(11B)	4588	2667	-595	41
H(8O)	8631	2226	2337	37
H(12A)	4961	3595	727	34
H(12B)	5686	5168	1036	34
H(13)	8463	4263	1662	31
H(14)	11369	2750	1229	29
H(15)	11234	3879	241	31
H(16)	7423	1613	376	30
H(19A)	10543	-3473	-637	45

E. Appendix

H(19B)	8891	-2180	-854	45
H(19C)	8616	-2844	-199	45
H(20A)	11725	-2327	615	50
H(20B)	13985	-1324	484	50
H(20C)	13696	-2942	187	50
H(21A)	14012	-1788	-877	43
H(21B)	14301	-221	-533	43
H(21C)	12231	-518	-1042	43
H(22A)	5093	2886	1898	31
H(22B)	5619	1665	1391	31
H(12O)	-70	-1392	1678	49
H(23A)	1057	-3241	2315	34
H(23B)	1704	-3582	1625	34
H(24)	4476	-1809	1635	36
H(25)	7465	-1693	2440	36
H(26)	7381	-4317	2585	35
H(27)	3670	-2747	3242	31
H(30A)	10493	-3631	5138	50
H(30B)	10633	-3815	4419	50
H(30C)	8489	-4561	4751	50
H(31A)	5384	-2984	5185	63
H(31B)	5574	-1247	5122	63
H(31C)	7373	-2043	5573	63
H(32A)	10768	-854	4989	47
H(32B)	8777	-129	4570	47
H(32C)	10720	-1120	4270	47
H(33A)	1709	-718	2593	40
H(33B)	3396	289	2204	40
H(16O)	1705	-5916	2546	46
H(34A)	3125	-8878	3557	44
H(34B)	5295	-8380	3162	44
H(35)	4907	-5986	3391	36
H(36)	4454	-5243	4435	32
H(37)	6887	-7192	4837	38
H(38)	1888	-8128	4508	34
H(41A)	1926	-7577	7050	41
H(41B)	3634	-6843	6583	41
H(41C)	3099	-8571	6543	41
H(42A)	-961	-9525	6180	41
H(42B)	-2924	-8383	5987	41
H(42C)	-2113	-8517	6685	41
H(43A)	-1154	-5732	6693	43
H(43B)	-1985	-5771	5991	43
H(43C)	588	-5137	6202	43
H(44A)	153	-6969	3565	39
H(44B)	902	-5301	3457	39

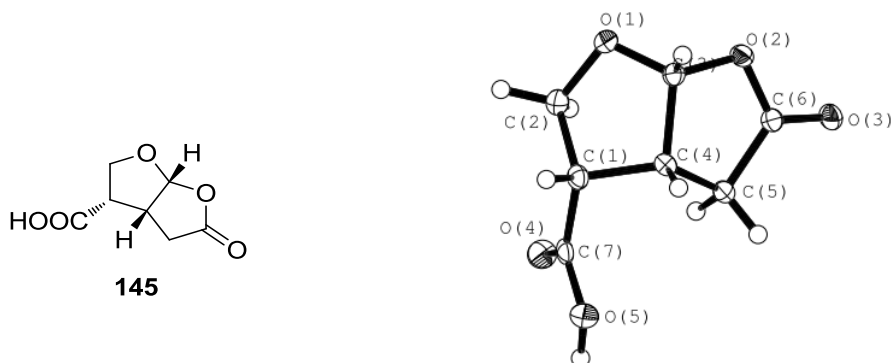
Table 6: Torsion angles [deg] for **140**.

C(4)-O(1)-C(1)-C(2)	25.9(4)	C(12)-C(13)-C(14)-C(15)	13.3(3)
C(1)-O(1)-C(4)-C(5)	51.3(4)	C(12)-C(13)-C(14)-C(16)	-51.9(3)
C(1)-O(1)-C(4)-C(3)	-16.2(4)	C(12)-C(13)-C(22)-O(8)	176.9(2)
C(7)-O(3)-C(6)-C(5)	179.5(3)	C(13)-C(14)-C(15)-O(5)	-0.5(3)
C(6)-O(3)-C(7)-C(8)	-175.3(3)	C(13)-C(14)-C(16)-C(15)	95.1(3)
C(7)-O(3)-C(6)-O(2)	0.2(5)	C(13)-C(14)-C(16)-C(17)	-158.6(2)
C(6)-O(3)-C(7)-C(10)	66.5(4)	C(16)-C(14)-C(15)-O(5)	111.0(3)
C(6)-O(3)-C(7)-C(9)	-58.8(4)	C(15)-C(14)-C(16)-C(17)	106.3(3)
C(12)-O(5)-C(15)-C(16)	53.4(3)	C(13)-C(14)-C(15)-C(16)	-111.5(3)
C(15)-O(5)-C(12)-C(13)	22.3(3)	O(5)-C(15)-C(16)-C(17)	157.3(3)
C(12)-O(5)-C(15)-C(14)	-13.8(3)	O(5)-C(15)-C(16)-C(14)	-98.8(3)
C(17)-O(7)-C(18)-C(21)	-64.3(4)	C(14)-C(15)-C(16)-C(17)	-103.8(3)
C(17)-O(7)-C(18)-C(20)	60.9(4)	C(15)-C(16)-C(17)-O(7)	-144.9(3)
C(18)-O(7)-C(17)-C(16)	-175.8(2)	C(14)-C(16)-C(17)-O(6)	-30.0(4)
C(17)-O(7)-C(18)-C(19)	178.1(3)	C(14)-C(16)-C(17)-O(7)	150.5(2)
C(18)-O(7)-C(17)-O(6)	4.7(5)	C(15)-C(16)-C(17)-O(6)	34.6(4)
C(23)-O(9)-C(26)-C(25)	-12.9(4)	O(9)-C(23)-C(24)-C(25)	-22.2(3)
C(23)-O(9)-C(26)-C(27)	55.4(4)	O(9)-C(23)-C(24)-C(33)	-148.2(3)
C(26)-O(9)-C(23)-C(24)	22.1(3)	C(33)-C(24)-C(25)-C(27)	72.3(4)
C(28)-O(11)-C(29)-C(31)	175.9(3)	C(23)-C(24)-C(25)-C(26)	14.3(3)
C(28)-O(11)-C(29)-C(32)	57.6(4)	C(25)-C(24)-C(33)-O(12)	-179.7(3)
C(29)-O(11)-C(28)-O(10)	3.5(6)	C(23)-C(24)-C(25)-C(27)	-50.4(4)
C(29)-O(11)-C(28)-C(27)	-179.6(3)	C(33)-C(24)-C(25)-C(26)	137.0(3)
C(28)-O(11)-C(29)-C(30)	-66.4(4)	C(23)-C(24)-C(33)-O(12)	-61.2(4)
C(34)-O(13)-C(37)-C(38)	50.8(4)	C(27)-C(25)-C(26)-O(9)	111.5(3)
C(37)-O(13)-C(34)-C(35)	25.8(4)	C(24)-C(25)-C(27)-C(26)	93.3(3)
C(34)-O(13)-C(37)-C(36)	-16.0(4)	C(24)-C(25)-C(26)-O(9)	-1.5(4)
C(40)-O(15)-C(39)-C(38)	177.1(3)	C(26)-C(25)-C(27)-C(28)	104.1(3)
C(40)-O(15)-C(39)-O(14)	-1.8(5)	C(24)-C(25)-C(27)-C(28)	-162.6(3)
C(39)-O(15)-C(40)-C(42)	-178.7(3)	C(24)-C(25)-C(26)-C(27)	-112.9(3)
C(39)-O(15)-C(40)-C(43)	63.9(4)	O(9)-C(26)-C(27)-C(25)	-100.0(3)
C(39)-O(15)-C(40)-C(41)	-60.5(4)	O(9)-C(26)-C(27)-C(28)	155.4(3)
O(1)-C(1)-C(2)-C(3)	-25.2(4)	C(25)-C(26)-C(27)-C(28)	-104.6(3)
O(1)-C(1)-C(2)-C(11)	-150.3(3)	C(26)-C(27)-C(28)-O(11)	-144.6(3)
C(1)-C(2)-C(11)-O(4)	-64.8(4)	C(26)-C(27)-C(28)-O(10)	32.5(5)
C(1)-C(2)-C(3)-C(4)	15.4(3)	C(25)-C(27)-C(28)-O(11)	151.8(3)
C(1)-C(2)-C(3)-C(5)	-49.5(4)	C(25)-C(27)-C(28)-O(10)	-31.2(5)
C(3)-C(2)-C(11)-O(4)	176.8(3)	O(13)-C(34)-C(35)-C(36)	-25.1(4)
C(11)-C(2)-C(3)-C(4)	139.4(3)	O(13)-C(34)-C(35)-C(44)	-148.8(3)
C(11)-C(2)-C(3)-C(5)	74.5(4)	C(34)-C(35)-C(44)-O(16)	-64.6(4)
C(2)-C(3)-C(4)-O(1)	-0.3(4)	C(34)-C(35)-C(36)-C(38)	-50.1(4)
C(2)-C(3)-C(5)-C(6)	-160.7(3)	C(44)-C(35)-C(36)-C(37)	139.9(3)
C(5)-C(3)-C(4)-O(1)	110.9(3)	C(34)-C(35)-C(36)-C(37)	15.3(3)
C(4)-C(3)-C(5)-C(6)	105.3(3)	C(36)-C(35)-C(44)-O(16)	177.7(3)
C(2)-C(3)-C(5)-C(4)	94.1(3)	C(44)-C(35)-C(36)-C(38)	74.5(4)
C(2)-C(3)-C(4)-C(5)	-111.3(3)	C(37)-C(36)-C(38)-C(39)	105.4(3)

O(1)-C(4)-C(5)-C(6)	153.5(3)	C(35)-C(36)-C(37)-O(13)	-0.5(4)
C(3)-C(4)-C(5)-C(6)	-106.7(3)	C(35)-C(36)-C(37)-C(38)	-111.2(3)
O(1)-C(4)-C(5)-C(3)	-99.8(3)	C(38)-C(36)-C(37)-O(13)	110.7(3)
C(3)-C(5)-C(6)-O(2)	-25.8(5)	C(35)-C(36)-C(38)-C(37)	94.6(3)
C(4)-C(5)-C(6)-O(3)	-139.6(3)	C(35)-C(36)-C(38)-C(39)	-160.1(3)
C(3)-C(5)-C(6)-O(3)	155.0(3)	O(13)-C(37)-C(38)-C(39)	155.1(3)
C(4)-C(5)-C(6)-O(2)	39.6(5)	C(36)-C(37)-C(38)-C(39)	-105.6(3)
O(5)-C(12)-C(13)-C(22)	-146.0(3)	O(13)-C(37)-C(38)-C(36)	-99.3(3)
O(5)-C(12)-C(13)-C(14)	-21.7(3)	C(37)-C(38)-C(39)-O(14)	40.5(4)
C(22)-C(13)-C(14)-C(16)	70.0(3)	C(37)-C(38)-C(39)-O(15)	-138.4(3)
C(14)-C(13)-C(22)-O(8)	59.7(3)	C(36)-C(38)-C(39)-O(14)	-24.5(5)
C(22)-C(13)-C(14)-C(15)	135.2(3)	C(36)-C(38)-C(39)-O(15)	156.7(3)

Table 7: Hydrogen-bonds for **140** [Å and deg.].

D-H...A	d(D-H)	d(H...A)	d(D...A)	<(DHA)
O(8)-H(8O)...O(16)#1	0.8400	18.800	2.704(4)	168.00
O(16)-H(16O)...O(9)	0.8400	19.600	2.779(4)	166.00
C(9)-H(9B)...O(2)	0.9800	24.300	2.982(5)	116.00
C(10)-H(10A)...O(2)#2	0.9800	25.800	3.501(5)	156.00
C(10)-H(10B)...O(2)	0.9800	25.500	3.097(5)	115.00
C(12)-H(12A)...O(6)#2	0.9900	25.100	3.434(4)	155.00
C(16)-H(16)...O(6)#2	10.000	24.900	3.480(4)	169.00
C(19)-H(19B)...O(2)	0.9800	25.800	3.537(5)	167.00
C(20)-H(20B)...O(6)	0.9800	24.200	3.002(5)	117.00
C(21)-H(21B)...O(6)	0.9800	24.300	3.007(5)	117.00
C(27)-H(27)...O(10)#2	10.000	25.200	3.517(4)	174.00
C(30)-H(30B)...O(10)	0.9800	24.900	3.047(5)	116.00
C(32)-H(32B)...O(13)#3	0.9800	24.500	3.378(5)	158.00
C(32)-H(32C)...O(10)	0.9800	23.500	2.956(5)	119.00
C(41)-H(41A)...O(1)#4	0.9800	25.300	3.459(5)	158.00
C(41)-H(41B)...O(14)	0.9800	24.400	3.004(4)	116.00
C(43)-H(43B)...O(14)#2	0.9800	25.200	3.456(4)	159.00
C(43)-H(43C)...O(14)	0.9800	24.300	3.022(4)	118.00
C(44)-H(44B)...O(10)#2	0.9900	25.800	3.548(5)	166.00

(3*S*,3*aR*,6*aR*)-5-oxohexahydrofuro[2,3-*b*]furan-3-carboxylic acid (145)**Table 1:** Crystal data and structure refinement for **145**.

Crystal Data	
Empirical formula	C ₇ H ₈ O ₅
Formula weight	172.13
Crystal size	0.1337 x 0.0766 x 0.0487 mm
Crystal description	prism
Crystal colour	colourless
Crystal system	Monoclinic
Space group	P 2 ₁ /n
Unit cell dimensions	a = 5.39904(17) Å alpha = 90 deg. b = 14.8577(4) Å beta = 103.704(3) deg. c = 8.6593(3) Å gamma = 90 deg.
Volume	674.85(4) Å ³
Z, Calculated density	4, 1.694 Mg/m ³
Absorption coefficient	1.277 mm ⁻¹
F(000)	360
Data Collection	
Measurement device type	SuperNova, Single source at offset, Atlas
Measurement method	\w scans
Temperature	123 K
Wavelength	1.54184 Å
Monochromator	graphite
Theta range for data collection	5.96 to 75.77 deg.
Index ranges	-5<=h<=6 -18<=k<=18 -9<=l<=10
Reflections collected / unique	2478 / 1379 [R(int) = 0.0260]
Reflections greater I>2s(I)	1247
Absorption correction	Analytical
Max. and min. transmission	0.946 and 0.910

Refinement	
Refinement method	Full-matrix least-squares on F ²
Hydrogen treatment	:
Data / restraints / parameters	1379 / 0 / 112
Goodness-of-fit on F ²	1.045
Final R indices [$I > 2\sigma(I)$]	R1 = 0.0444, wR2 = 0.1187
R indices (all data)	R1 = 0.0487, wR2 = 0.1250
Absolute structure parameter	.
Largest diff. peak and hole	0.313 and -0.282 e.Å ⁻³

Table 2: Atomic coordinates ($\times 10^4$) and equivalent isotropic displacement parameters ($\text{\AA}^2 \times 10^3$) for **145**. U(eq) is defined as one third of the trace of the orthogonalized Uij tensor.

Atom	x	y	z	U(eq)
O(1)	4366(2)	2897(1)	3804(1)	19(1)
O(2)	4524(2)	2787(1)	1131(1)	17(1)
O(3)	4550(2)	3613(1)	-1004(1)	21(1)
O(4)	968(2)	5427(1)	3470(1)	24(1)
O(5)	-2719(2)	4782(1)	2260(1)	21(1)
C(1)	681(3)	3805(1)	3370(2)	16(1)
C(2)	3466(3)	3746(1)	4281(2)	20(1)
C(3)	2972(3)	2663(1)	2292(2)	16(1)
C(4)	683(3)	3304(1)	1807(2)	15(1)
C(5)	1324(3)	3883(1)	493(2)	16(1)
C(6)	3587(3)	3436(1)	91(2)	16(1)
C(7)	-291(3)	4758(1)	3073(2)	16(1)

Table 3: Bond lengths [\AA] and angles [deg] for **145**.

O(1)-C(2)	1.448(2)	O(1)-C(3)-O(2)	110.16(13)
O(1)-C(3)	1.3909(19)	C(1)-C(4)-C(5)	115.37(13)
O(2)-C(3)	1.4649(19)	C(3)-C(4)-C(5)	104.04(13)
O(2)-C(6)	1.3343(19)	C(1)-C(4)-C(3)	103.09(12)
O(3)-C(6)	1.214(2)	C(4)-C(5)-C(6)	105.29(13)
O(4)-C(7)	1.2079(19)	O(2)-C(6)-C(5)	111.23(13)
O(5)-C(7)	1.333(2)	O(3)-C(6)-C(5)	127.41(14)
O(5)-H(5O)	0.91(3)	O(2)-C(6)-O(3)	121.36(15)
C(1)-C(4)	1.545(2)	O(4)-C(7)-C(1)	125.01(15)
C(1)-C(7)	1.510(2)	O(5)-C(7)-C(1)	111.95(13)
C(1)-C(2)	1.526(2)	O(4)-C(7)-O(5)	123.01(14)
C(3)-C(4)	1.538(2)	C(2)-C(1)-H(1)	109.00
C(4)-C(5)	1.529(2)	C(4)-C(1)-H(1)	109.00
C(5)-C(6)	1.502(2)	C(7)-C(1)-H(1)	109.00
C(1)-H(1)	10.000	O(1)-C(2)-H(2A)	111.00
C(2)-H(2A)	0.9900	O(1)-C(2)-H(2B)	111.00
C(2)-H(2B)	0.9900	C(1)-C(2)-H(2A)	111.00

C(3)-H(3)	10.000	C(1)-C(2)-H(2B)	111.00
C(4)-H(4)	10.000	H(2A)-C(2)-H(2B)	109.00
C(5)-H(5A)	0.9900	O(1)-C(3)-H(3)	110.00
C(5)-H(5B)	0.9900	O(2)-C(3)-H(3)	110.00
C(2)-O(1)-C(3)	110.09(12)	C(4)-C(3)-H(3)	110.00
C(3)-O(2)-C(6)	111.54(12)	C(1)-C(4)-H(4)	111.00
C(7)-O(5)-H(5O)	108.2(17)	C(3)-C(4)-H(4)	111.00
C(2)-C(1)-C(4)	102.72(13)	C(5)-C(4)-H(4)	111.00
C(2)-C(1)-C(7)	113.71(13)	C(4)-C(5)-H(5A)	111.00
C(4)-C(1)-C(7)	111.97(12)	C(4)-C(5)-H(5B)	111.00
O(1)-C(2)-C(1)	104.99(12)	C(6)-C(5)-H(5A)	111.00
O(1)-C(3)-C(4)	108.83(12)	C(6)-C(5)-H(5B)	111.00
O(2)-C(3)-C(4)	106.72(12)	H(5A)-C(5)-H(5B)	109.00

Table 4: Anisotropic displacement parameters ($\text{\AA}^2 \times 10^3$) for **145**. The anisotropic displacement factor exponent takes the form: $-2 \pi^2 [h^2 a^{*2} U_{11} + \dots + 2 h k a^* b^* U_{12}]$.

Atom	U11	U22	U33	U23	U13	U12
O(1)	21(1)	20(1)	16(1)	1(1)	2(1)	5(1)
O(2)	16(1)	18(1)	18(1)	2(1)	7(1)	3(1)
O(3)	23(1)	24(1)	19(1)	4(1)	11(1)	5(1)
O(4)	27(1)	18(1)	25(1)	-1(1)	4(1)	-2(1)
O(5)	20(1)	19(1)	24(1)	1(1)	5(1)	2(1)
C(1)	19(1)	17(1)	15(1)	1(1)	7(1)	0(1)
C(2)	22(1)	20(1)	16(1)	-2(1)	3(1)	1(1)
C(3)	16(1)	17(1)	15(1)	1(1)	5(1)	0(1)
C(4)	15(1)	14(1)	17(1)	-1(1)	5(1)	1(1)
C(5)	18(1)	16(1)	16(1)	0(1)	6(1)	3(1)
C(6)	17(1)	16(1)	15(1)	-2(1)	3(1)	1(1)
C(7)	21(1)	18(1)	12(1)	0(1)	9(1)	1(1)

Table 5: Hydrogen coordinates ($\times 10^4$) and isotropic displacement parameters ($\text{\AA}^2 \times 10^3$) for **145**.

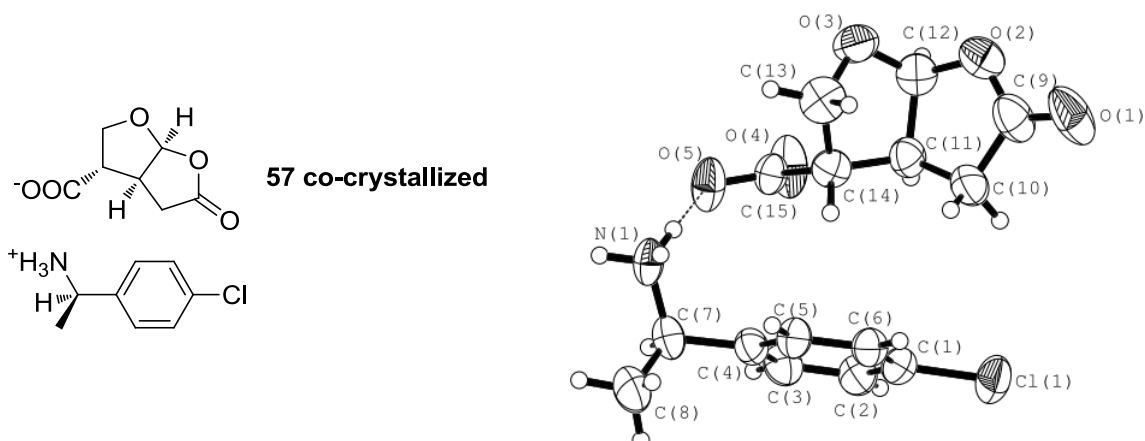
Atom	x	y	z	U(eq)
H(1)	-406	3470	3963	19
H(2A)	4462	4254	3997	23
H(2B)	3609	3758	5442	23
H(3)	2375	2025	2280	19
H(4)	-941	2964	1409	18
H(5A)	-133	3902	-448	20
H(5B)	1748	4505	873	20
H(5O)	-3150(50)	5365(18)	2020(30)	25

Table 6: Torsion angles [deg] for **145**.

C(3)-O(1)-C(2)-C(1)	27.00(16)	C(2)-C(1)-C(7)-O(4)	1.4(2)
C(2)-O(1)-C(3)-O(2)	106.70(13)	C(2)-C(1)-C(7)-O(5)	179.30(12)
C(2)-O(1)-C(3)-C(4)	-9.98(16)	C(4)-C(1)-C(7)-O(4)	-114.45(17)
C(6)-O(2)-C(3)-C(4)	3.47(16)	C(4)-C(1)-C(7)-O(5)	63.42(17)
C(3)-O(2)-C(6)-O(3)	-176.95(14)	O(1)-C(3)-C(4)-C(1)	-10.77(16)
C(3)-O(2)-C(6)-C(5)	3.76(17)	O(2)-C(3)-C(4)-C(5)	-8.85(15)
C(6)-O(2)-C(3)-O(1)	-114.52(14)	O(1)-C(3)-C(4)-C(5)	110.00(13)
C(4)-C(1)-C(2)-O(1)	-32.22(15)	O(2)-C(3)-C(4)-C(1)	-129.62(12)
C(7)-C(1)-C(2)-O(1)	-153.42(12)	C(1)-C(4)-C(5)-C(6)	122.83(14)
C(2)-C(1)-C(4)-C(3)	25.72(15)	C(3)-C(4)-C(5)-C(6)	10.69(15)
C(2)-C(1)-C(4)-C(5)	-86.98(16)	C(4)-C(5)-C(6)-O(3)	171.37(16)
C(7)-C(1)-C(4)-C(3)	148.10(13)	C(4)-C(5)-C(6)-O(2)	-9.39(17)
C(7)-C(1)-C(4)-C(5)	35.40(19)		

Table 7: Hydrogen-bonds for **145** [\AA and deg.].

D-H...A	d(D-H)	d(H...A)	d(D...A)	<(DHA)
O(5)-H(5O)...O(3)#1	0.91(3)	1.83(3)	2.7086(18)	163(2)
C(2)-H(2A)...O(5)#2	0.9900	25.100	3.374(2)	146.00
C(3)-H(3)...O(3)#3	10.000	25.500	3.237(2)	126.00
C(4)-H(4)...O(2)#4	10.000	24.200	3.327(2)	151.00

(R)-1-(4-chlorophenyl)ethanaminium (3S,3aS,6aS)-5-oxohexahydrofuro[2,3-b]furan-3-carboxylate (57)**Table 1:** Crystal data and structure refinement for **57**.

Crystal Data	
Empirical formula	C ₈ H ₁₁ Cl N, C ₇ H ₇ O ₅
Formula weight	327.75
Crystal size	0.5084 x 0.0431 x 0.0264 mm
Crystal description	stick
Crystal colour	colourless
Crystal system	Orthorhombic
Space group	P 2 ₁ 2 ₁ 2 ₁
Unit cell dimensions	a = 6.6331(4) Å alpha = 90 deg. b = 15.380(1) Å beta = 90 deg. c = 15.6364(10) Å gamma = 90 deg.
Volume	1595.18(17) Å ³
Z, Calculated density	4, 1.365 Mg/m ³
Absorption coefficient	2.330 mm ⁻¹
F(000)	688
Data Collection	
Measurement device type	SuperNova, Single source at offset, Atlas
Measurement method	\w scans
Temperature	123 K
Wavelength	1.54184 Å
Monochromator	graphite
Theta range for data collection	4.03 to 75.50 deg.
Index ranges	-8<=h<=8 -19<=k<=19 -19<=l<=19
Reflections collected / unique	11839 / 3283 [R(int) = 0.0618]
Reflections greater I>2s(I)	2637
Absorption correction	Analytical
Max. and min. transmission	0.943 and 0.589

Refinement	
Refinement method	Full-matrix least-squares on F ²
Hydrogen treatment	:
Data / restraints / parameters	3283 / 0 / 201
Goodness-of-fit on F ²	1.089
Final R indices [$I > 2\sigma(I)$]	R1 = 0.0738, wR2 = 0.2097
R indices (all data)	R1 = 0.0868, wR2 = 0.2274
Absolute structure parameter	-0.04(4)
Largest diff. peak and hole	0.507 and -0.305 e.Å ⁻³

Table 2: Atomic coordinates ($\times 10^4$) and equivalent isotropic displacement parameters ($\text{\AA}^2 \times 10^3$) for **57**. U(eq) is defined as one third of the trace of the orthogonalized Uij tensor.

Atom	x	y	z	U(eq)
Cl(1)	5443(2)	1615(1)	2341(1)	71(1)
N(1)	8548(5)	-1868(2)	4550(3)	49(1)
C(1)	6248(7)	609(3)	2725(3)	50(1)
C(2)	4995(7)	-91(3)	2635(3)	54(1)
C(3)	5650(8)	-887(3)	2933(3)	53(1)
C(4)	7539(7)	-968(3)	3310(3)	45(1)
C(5)	8742(6)	-256(3)	3389(3)	46(1)
C(6)	8114(7)	556(3)	3098(3)	48(1)
C(7)	8192(8)	-1865(3)	3612(3)	55(2)
C(8)	10098(14)	-2183(4)	3182(5)	96(3)
O(1)	4274(8)	3086(3)	5187(4)	97(2)
O(2)	3213(6)	1989(3)	5980(2)	66(1)
O(3)	3863(6)	575(3)	6426(2)	66(1)
O(4)	1760(5)	-854(2)	5021(3)	75(2)
O(5)	4752(5)	-1465(2)	5129(3)	67(1)
C(9)	3916(9)	2323(3)	5254(4)	70(2)
C(10)	4045(11)	1629(3)	4568(4)	69(2)
C(11)	3177(8)	823(3)	4968(3)	53(1)
C(12)	2720(8)	1082(3)	5889(3)	57(2)
C(13)	5566(8)	262(4)	5927(4)	64(2)
C(14)	4637(7)	62(3)	5067(3)	50(1)
C(15)	3618(6)	-829(3)	5067(3)	45(1)

Table 3: Bond lengths [\AA] and angles [deg] for **57**.

Cl(1)-C(1)	1.743(5)	C(1)-C(6)-C(5)	117.5(4)
O(1)-C(9)	1.202(7)	N(1)-C(7)-C(4)	110.8(4)
O(2)-C(12)	1.440(7)	C(4)-C(7)-C(8)	113.2(4)
O(2)-C(9)	1.330(7)	N(1)-C(7)-C(8)	107.8(5)
O(3)-C(12)	1.374(6)	C(3)-C(2)-H(2)	121.00
O(3)-C(13)	1.455(7)	C(1)-C(2)-H(2)	121.00
O(4)-C(15)	1.235(5)	C(4)-C(3)-H(3)	120.00

E. Appendix

O(5)-C(15)	1.238(5)	C(2)-C(3)-H(3)	120.00
N(1)-C(7)	1.486(7)	C(6)-C(5)-H(5)	119.00
N(1)-H(1O)	0.9100	C(4)-C(5)-H(5)	119.00
N(1)-H(1P)	0.9100	C(1)-C(6)-H(6)	121.00
N(1)-H(1N)	0.9100	C(5)-C(6)-H(6)	121.00
C(1)-C(2)	1.367(7)	C(4)-C(7)-H(7)	108.00
C(1)-C(6)	1.371(7)	N(1)-C(7)-H(7)	108.00
C(2)-C(3)	1.380(7)	C(8)-C(7)-H(7)	108.00
C(3)-C(4)	1.390(7)	C(7)-C(8)-H(8B)	109.00
C(4)-C(5)	1.361(6)	C(7)-C(8)-H(8C)	109.00
C(4)-C(7)	1.521(7)	H(8A)-C(8)-H(8C)	110.00
C(5)-C(6)	1.393(7)	H(8B)-C(8)-H(8C)	110.00
C(7)-C(8)	1.513(10)	H(8A)-C(8)-H(8B)	109.00
C(2)-H(2)	0.9500	C(7)-C(8)-H(8A)	109.00
C(3)-H(3)	0.9500	O(1)-C(9)-O(2)	121.4(6)
C(5)-H(5)	0.9500	O(1)-C(9)-C(10)	127.9(6)
C(6)-H(6)	0.9500	O(2)-C(9)-C(10)	110.6(4)
C(7)-H(7)	10.000	C(9)-C(10)-C(11)	105.4(5)
C(8)-H(8A)	0.9800	C(10)-C(11)-C(12)	104.7(4)
C(8)-H(8B)	0.9800	C(10)-C(11)-C(14)	115.6(5)
C(8)-H(8C)	0.9800	C(12)-C(11)-C(14)	103.3(4)
C(9)-C(10)	1.516(8)	O(2)-C(12)-O(3)	111.4(4)
C(10)-C(11)	1.503(7)	O(2)-C(12)-C(11)	107.5(4)
C(11)-C(12)	1.525(7)	O(3)-C(12)-C(11)	108.6(4)
C(11)-C(14)	1.527(7)	O(3)-C(13)-C(14)	103.2(4)
C(13)-C(14)	1.511(8)	C(11)-C(14)-C(13)	101.1(4)
C(14)-C(15)	1.528(6)	C(11)-C(14)-C(15)	114.0(4)
C(10)-H(10A)	0.9900	C(13)-C(14)-C(15)	111.3(4)
C(10)-H(10B)	0.9900	O(4)-C(15)-O(5)	125.9(4)
C(11)-H(11)	10.000	O(4)-C(15)-C(14)	118.0(4)
C(12)-H(12)	10.000	O(5)-C(15)-C(14)	116.1(4)
C(13)-H(13A)	0.9900	C(9)-C(10)-H(10A)	111.00
C(13)-H(13B)	0.9900	C(9)-C(10)-H(10B)	111.00
C(14)-H(14)	10.000	C(11)-C(10)-H(10A)	111.00
C(9)-O(2)-C(12)	111.7(4)	C(11)-C(10)-H(10B)	111.00
C(12)-O(3)-C(13)	106.8(4)	H(10A)-C(10)-H(10B)	109.00
H(1N)-N(1)-H(1O)	110.00	C(10)-C(11)-H(11)	111.00
C(7)-N(1)-H(1P)	109.00	C(12)-C(11)-H(11)	111.00
C(7)-N(1)-H(1O)	109.00	C(14)-C(11)-H(11)	111.00
H(1N)-N(1)-H(1P)	110.00	O(2)-C(12)-H(12)	110.00
H(1O)-N(1)-H(1P)	109.00	O(3)-C(12)-H(12)	110.00
C(7)-N(1)-H(1N)	109.00	C(11)-C(12)-H(12)	110.00
Cl(1)-C(1)-C(2)	118.5(4)	O(3)-C(13)-H(13A)	111.00
Cl(1)-C(1)-C(6)	118.4(4)	O(3)-C(13)-H(13B)	111.00
C(2)-C(1)-C(6)	123.1(4)	C(14)-C(13)-H(13A)	111.00
C(1)-C(2)-C(3)	118.2(4)	C(14)-C(13)-H(13B)	111.00
C(2)-C(3)-C(4)	120.4(4)	H(13A)-C(13)-H(13B)	109.00

E. Appendix

C(3)-C(4)-C(7)	118.0(4)	C(11)-C(14)-H(14)	110.00
C(5)-C(4)-C(7)	122.3(4)	C(13)-C(14)-H(14)	110.00
C(3)-C(4)-C(5)	119.7(4)	C(15)-C(14)-H(14)	110.00
C(4)-C(5)-C(6)	121.1(4)		

Table 4: Anisotropic displacement parameters ($\text{\AA}^2 \times 10^3$) for **57**. The anisotropic displacement factor exponent takes the form: $-2 \pi^2 [h^2 a^{*2} U_{11} + \dots + 2 h k a^* b^* U_{12}]$.

Atom	U11	U22	U33	U23	U13	U12
Cl(1)	80(1)	58(1)	75(1)	17(1)	-11(1)	15(1)
N(1)	35(2)	35(2)	76(2)	14(2)	0(2)	-1(1)
C(1)	55(2)	51(2)	45(2)	4(2)	-5(2)	9(2)
C(2)	49(2)	56(2)	56(2)	-3(2)	-12(2)	5(2)
C(3)	52(2)	48(2)	60(3)	-8(2)	-10(2)	-6(2)
C(4)	50(2)	38(2)	48(2)	-3(2)	-3(2)	0(2)
C(5)	36(2)	45(2)	56(2)	4(2)	-5(2)	1(2)
C(6)	46(2)	45(2)	52(2)	1(2)	0(2)	-3(2)
C(7)	63(3)	34(2)	68(3)	-3(2)	-1(2)	2(2)
C(8)	136(7)	63(4)	89(4)	8(3)	37(5)	40(4)
O(1)	92(3)	48(2)	152(5)	-24(2)	53(3)	-17(2)
O(2)	67(2)	65(2)	67(2)	-15(2)	2(2)	-4(2)
O(3)	67(2)	83(3)	49(2)	5(2)	3(2)	9(2)
O(4)	40(2)	52(2)	134(4)	7(2)	-22(2)	-2(1)
O(5)	44(2)	50(2)	106(3)	25(2)	14(2)	7(1)
C(9)	68(3)	49(3)	93(4)	-12(3)	17(3)	-9(2)
C(10)	96(4)	45(2)	66(3)	-3(2)	20(3)	1(3)
C(11)	59(2)	43(2)	57(2)	-1(2)	-2(2)	-4(2)
C(12)	51(2)	59(3)	62(3)	1(2)	2(2)	-2(2)
C(13)	42(2)	77(3)	74(3)	0(3)	-8(2)	-6(2)
C(14)	45(2)	53(2)	53(2)	1(2)	4(2)	-5(2)
C(15)	39(2)	41(2)	56(2)	8(2)	-3(2)	-2(2)

Table 5: Hydrogen coordinates ($\times 10^4$) and isotropic displacement parameters ($\text{\AA}^2 \times 10^3$) for **57**.

Atom	x	y	z	U(eq)
H(1N)	8728	-2425	4732	73
H(1O)	7466	-1631	4821	73
H(1P)	9670	-1550	4670	73
H(2)	3708	-31	2375	65
H(3)	4804	-1382	2881	64
H(5)	10032	-314	3647	55
H(6)	8948	1054	3157	57
H(7)	7084	-2286	3482	66
H(8A)	9868	-2234	2565	144
H(8B)	11191	-1767	3287	144
H(8C)	10470	-2752	3416	144

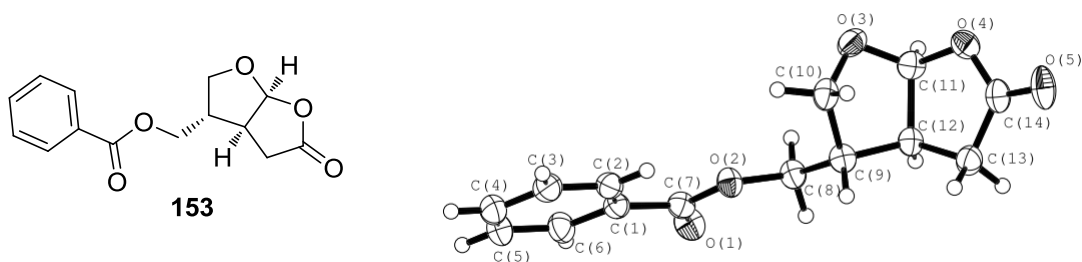
H(10A)	3257	1800	4058	83
H(10B)	5463	1531	4396	83
H(11)	1922	637	4665	64
H(12)	1256	990	6012	69
H(13A)	6158	-266	6188	77
H(13B)	6623	713	5877	77
H(14)	5691	86	4610	60

Table 6: Torsion angles [deg] for **57**.

C(12)-O(2)-C(9)-C(10)	-2.1(6)	C(4)-C(5)-C(6)-C(1)	-0.4(7)
C(9)-O(2)-C(12)-C(11)	-0.4(6)	O(2)-C(9)-C(10)-C(11)	3.7(7)
C(9)-O(2)-C(12)-O(3)	118.5(5)	O(1)-C(9)-C(10)-C(11)	-172.7(6)
C(12)-O(2)-C(9)-O(1)	174.6(6)	C(9)-C(10)-C(11)-C(14)	-116.6(5)
C(13)-O(3)-C(12)-O(2)	-95.9(5)	C(9)-C(10)-C(11)-C(12)	-3.7(6)
C(12)-O(3)-C(13)-C(14)	-39.5(5)	C(10)-C(11)-C(12)-O(2)	2.7(6)
C(13)-O(3)-C(12)-C(11)	22.3(5)	C(12)-C(11)-C(14)-C(13)	-26.1(5)
C(6)-C(1)-C(2)-C(3)	-0.2(7)	C(12)-C(11)-C(14)-C(15)	93.4(5)
C(2)-C(1)-C(6)-C(5)	0.5(7)	C(10)-C(11)-C(12)-O(3)	-118.0(5)
Cl(1)-C(1)-C(2)-C(3)	179.4(4)	C(14)-C(11)-C(12)-O(2)	124.0(4)
Cl(1)-C(1)-C(6)-C(5)	-179.1(4)	C(14)-C(11)-C(12)-O(3)	3.4(5)
C(1)-C(2)-C(3)-C(4)	-0.3(7)	C(10)-C(11)-C(14)-C(13)	87.6(5)
C(2)-C(3)-C(4)-C(5)	0.4(7)	C(10)-C(11)-C(14)-C(15)	-152.9(4)
C(2)-C(3)-C(4)-C(7)	-179.0(4)	O(3)-C(13)-C(14)-C(11)	39.6(5)
C(5)-C(4)-C(7)-N(1)	62.1(6)	O(3)-C(13)-C(14)-C(15)	-81.8(5)
C(3)-C(4)-C(5)-C(6)	0.0(7)	C(11)-C(14)-C(15)-O(4)	-2.6(6)
C(5)-C(4)-C(7)-C(8)	-59.0(7)	C(11)-C(14)-C(15)-O(5)	178.6(4)
C(3)-C(4)-C(7)-C(8)	120.3(6)	C(13)-C(14)-C(15)-O(4)	111.0(5)
C(7)-C(4)-C(5)-C(6)	179.3(4)	C(13)-C(14)-C(15)-O(5)	-67.8(6)
C(3)-C(4)-C(7)-N(1)	-118.6(5)		

Table 7: Hydrogen-bonds for **57** [Å and deg.].

D-H...A	d(D-H)	d(H...A)	d(D...A)	<(DHA)
N(1)-H(1N)...O(5)#1	0.9100	18.500	2.732(4)	162.00
N(1)-H(1O)...O(5)	0.9100	18.800	2.747(5)	158.00
N(1)-H(1P)...O(4)#2	0.9100	18.400	2.741(5)	173.00
C(2)-H(2)...O(3)#3	0.9500	24.100	3.268(6)	150.00
C(5)-H(5)...O(4)#2	0.9500	25.700	3.371(6)	142.00
C(7)-H(7)...Cl(1)#4	10.000	27.100	3.674(5)	163.00
C(11)-H(11)...O(4)	10.000	23.600	2.746(6)	102.00

((3*S*,3*aS*,6*aS*)-5-oxohexahydrofuro[2,3-*b*]furan-3-yl)methyl benzoate (153)**Table 1:** Crystal data and structure refinement for **153**.

Crystal Data	
Empirical formula	C ₁₄ H ₁₄ O ₅
Formula weight	262.25
Crystal size	0.2101 x 0.0992 x 0.0510 mm
Crystal description	plate
Crystal colour	colourless
Crystal system	Orthorhombic
Space group	P 2 ₁ 2 ₁ 2 ₁
Unit cell dimensions	a = 6.55267(18) Å alpha = 90 deg. b = 8.8207(3) Å beta = 90 deg. c = 21.7464(7) Å gamma = 90 deg.
Volume	1256.92(7) Å ³
Z, Calculated density	4, 1.386 Mg/m ³
Absorption coefficient	0.887 mm ⁻¹
F(000)	552
Data Collection	
Measurement device type	SuperNova, Single source at offset, Atlas
Measurement method	\w scans
Temperature	123 K
Wavelength	1.54184 Å
Monochromator	graphite
Theta range for data collection	4.07 to 76.33 deg.
Index ranges	-7 ≤ h ≤ 7 -10 ≤ k ≤ 10 -26 ≤ l ≤ 27
Reflections collected / unique	4694 / 2540 [R(int) = 0.0322]
Reflections greater I > 2σ(I)	2394
Absorption correction	Analytical
Max. and min. transmission	0.959 and 0.907

Refinement	
Refinement method	Full-matrix least-squares on F ²
Hydrogen treatment	:
Data / restraints / parameters	2540 / 0 / 172
Goodness-of-fit on F ²	1.042
Final R indices [$I > 2\sigma(I)$]	R1 = 0.0459, wR2 = 0.1243
R indices (all data)	R1 = 0.0481, wR2 = 0.1275
Absolute structure parameter	0.2(2)
Largest diff. peak and hole	0.211 and -0.233 e.Å ⁻³

Table 2: Atomic coordinates ($\times 10^4$) and equivalent isotropic displacement parameters ($\text{\AA}^2 \times 10^3$) for **153**. U(eq) is defined as one third of the trace of the orthogonalized Uij tensor.

Atom	x	y	z	U(eq)
O(1)	-7618(2)	-3000(2)	-8373(1)	38(1)
O(2)	-4434(2)	-2337(2)	-8634(1)	30(1)
O(3)	-1673(3)	-3483(2)	-10081(1)	38(1)
O(4)	707(2)	-5381(2)	-10253(1)	35(1)
O(5)	3597(2)	-6343(2)	-9900(1)	48(1)
C(1)	-6515(3)	-452(2)	-8214(1)	30(1)
C(2)	-4925(3)	596(2)	-8254(1)	32(1)
C(3)	-5239(4)	2078(3)	-8059(1)	37(1)
C(4)	-7111(4)	2515(3)	-7824(1)	41(1)
C(5)	-8687(4)	1490(3)	-7785(1)	43(1)
C(6)	-8409(4)	2(3)	-7982(1)	38(1)
C(7)	-6285(3)	-2056(2)	-8413(1)	30(1)
C(8)	-4150(3)	-3837(2)	-8892(1)	31(1)
C(9)	-1888(3)	-4001(2)	-9026(1)	30(1)
C(10)	-1145(3)	-2840(2)	-9491(1)	34(1)
C(11)	-1351(3)	-5032(2)	-10046(1)	32(1)
C(12)	-1468(3)	-5508(2)	-9364(1)	29(1)
C(13)	631(4)	-6187(2)	-9228(1)	36(1)
C(14)	1845(3)	-6011(2)	-9810(1)	33(1)

Table 3: Bond lengths [\AA] and angles [deg] for **153**.

O(1)-C(7)	1.210(2)	O(2)-C(8)-C(9)	106.67(15)
O(2)-C(7)	1.329(2)	C(8)-C(9)-C(10)	112.13(16)
O(2)-C(8)	1.448(2)	C(8)-C(9)-C(12)	110.35(15)
O(3)-C(10)	1.444(3)	C(10)-C(9)-C(12)	101.89(16)
O(3)-C(11)	1.385(2)	O(3)-C(10)-C(9)	104.48(15)
O(4)-C(11)	1.455(2)	O(3)-C(11)-O(4)	109.44(16)
O(4)-C(14)	1.339(3)	O(3)-C(11)-C(12)	108.30(15)
O(5)-C(14)	1.201(2)	O(4)-C(11)-C(12)	106.62(15)
C(1)-C(2)	1.396(3)	C(9)-C(12)-C(11)	103.42(15)
C(1)-C(6)	1.398(3)	C(9)-C(12)-C(13)	113.97(16)
C(1)-C(7)	1.487(3)	C(11)-C(12)-C(13)	104.29(16)

C(2)-C(3)	1.390(3)	C(12)-C(13)-C(14)	105.90(17)
C(3)-C(4)	1.384(4)	O(4)-C(14)-O(5)	121.1(2)
C(4)-C(5)	1.375(4)	O(4)-C(14)-C(13)	110.70(17)
C(5)-C(6)	1.393(4)	O(5)-C(14)-C(13)	128.2(2)
C(8)-C(9)	1.518(3)	C(1)-C(2)-H(2)	120.00
C(9)-C(10)	1.520(3)	C(3)-C(2)-H(2)	120.00
C(9)-C(12)	1.544(3)	C(2)-C(3)-H(3)	120.00
C(11)-C(12)	1.543(3)	C(4)-C(3)-H(3)	120.00
C(12)-C(13)	1.529(3)	C(3)-C(4)-H(4)	120.00
C(13)-C(14)	1.502(3)	C(5)-C(4)-H(4)	120.00
C(2)-H(2)	0.9500	C(4)-C(5)-H(5)	120.00
C(3)-H(3)	0.9500	C(6)-C(5)-H(5)	120.00
C(4)-H(4)	0.9500	C(1)-C(6)-H(6)	120.00
C(5)-H(5)	0.9500	C(5)-C(6)-H(6)	120.00
C(6)-H(6)	0.9500	O(2)-C(8)-H(8A)	110.00
C(8)-H(8A)	0.9900	O(2)-C(8)-H(8B)	110.00
C(8)-H(8B)	0.9900	C(9)-C(8)-H(8A)	110.00
C(9)-H(9)	10.000	C(9)-C(8)-H(8B)	110.00
C(10)-H(10A)	0.9900	H(8A)-C(8)-H(8B)	109.00
C(10)-H(10B)	0.9900	C(8)-C(9)-H(9)	111.00
C(11)-H(11)	10.000	C(10)-C(9)-H(9)	111.00
C(12)-H(12)	10.000	C(12)-C(9)-H(9)	111.00
C(13)-H(13A)	0.9900	O(3)-C(10)-H(10A)	111.00
C(13)-H(13B)	0.9900	O(3)-C(10)-H(10B)	111.00
C(7)-O(2)-C(8)	115.34(15)	C(9)-C(10)-H(10A)	111.00
C(10)-O(3)-C(11)	107.57(15)	C(9)-C(10)-H(10B)	111.00
C(11)-O(4)-C(14)	112.42(15)	H(10A)-C(10)-H(10B)	109.00
C(2)-C(1)-C(6)	119.70(18)	O(3)-C(11)-H(11)	111.00
C(2)-C(1)-C(7)	122.44(17)	O(4)-C(11)-H(11)	111.00
C(6)-C(1)-C(7)	117.86(18)	C(12)-C(11)-H(11)	111.00
C(1)-C(2)-C(3)	119.58(19)	C(9)-C(12)-H(12)	112.00
C(2)-C(3)-C(4)	120.4(2)	C(11)-C(12)-H(12)	112.00
C(3)-C(4)-C(5)	120.4(2)	C(13)-C(12)-H(12)	112.00
C(4)-C(5)-C(6)	120.1(2)	C(12)-C(13)-H(13A)	111.00
C(1)-C(6)-C(5)	119.8(2)	C(12)-C(13)-H(13B)	111.00
O(1)-C(7)-O(2)	123.80(17)	C(14)-C(13)-H(13A)	111.00
O(1)-C(7)-C(1)	124.13(18)	C(14)-C(13)-H(13B)	111.00
O(2)-C(7)-C(1)	112.06(16)	H(13A)-C(13)-H(13B)	109.00

Table 4: Anisotropic displacement parameters ($\text{\AA}^2 \times 10^3$) for **153**. The anisotropic displacement factor exponent takes the form: $-2 \pi^2 [h^2 a^{*2} U_{11} + \dots + 2 h k a^* b^* U_{12}]$.

Atom	U11	U22	U33	U23	U13	U12
O(1)	29(1)	40(1)	45(1)	-5(1)	5(1)	-8(1)
O(2)	25(1)	29(1)	38(1)	-3(1)	5(1)	-2(1)
O(3)	34(1)	39(1)	40(1)	11(1)	0(1)	6(1)
O(4)	31(1)	40(1)	34(1)	-2(1)	4(1)	-1(1)
O(5)	26(1)	42(1)	74(1)	-18(1)	2(1)	6(1)

C(1)	29(1)	32(1)	28(1)	1(1)	0(1)	2(1)
C(2)	31(1)	34(1)	29(1)	0(1)	1(1)	1(1)
C(3)	42(1)	33(1)	35(1)	-1(1)	-4(1)	-1(1)
C(4)	50(1)	39(1)	35(1)	-5(1)	-2(1)	12(1)
C(5)	41(1)	45(1)	42(1)	-3(1)	8(1)	13(1)
C(6)	33(1)	38(1)	42(1)	0(1)	8(1)	3(1)
C(7)	27(1)	33(1)	31(1)	1(1)	2(1)	-2(1)
C(8)	30(1)	26(1)	37(1)	-2(1)	4(1)	-4(1)
C(9)	26(1)	29(1)	36(1)	-2(1)	2(1)	-4(1)
C(10)	27(1)	27(1)	48(1)	2(1)	8(1)	0(1)
C(11)	25(1)	37(1)	34(1)	0(1)	-2(1)	-2(1)
C(12)	24(1)	28(1)	35(1)	-1(1)	1(1)	-1(1)
C(13)	37(1)	35(1)	36(1)	-3(1)	-5(1)	7(1)
C(14)	27(1)	28(1)	44(1)	-9(1)	-2(1)	-1(1)

Table 5: Hydrogen coordinates ($\times 10^4$) and isotropic displacement parameters ($\text{\AA}^2 \times 10^3$) for **153**.

Atom	x	y	z	U(eq)
H(2)	-3636	298	-8413	38
H(3)	-4163	2796	-8088	44
H(4)	-7309	3529	-7689	50
H(5)	-9968	1797	-7623	51
H(6)	-9503	-702	-7960	45
H(8A)	-4954	-3950	-9274	37
H(8B)	-4598	-4621	-8595	37
H(9)	-1073	-3939	-8638	36
H(10A)	-1835	-1853	-9429	41
H(10B)	348	-2691	-9457	41
H(11)	-2385	-5593	-10296	38
H(12)	-2584	-6262	-9292	35
H(13A)	1296	-5641	-8885	43
H(13B)	505	-7271	-9116	43

Table 6: Torsion angles [deg] for **153**.

C(7)-O(2)-C(8)-C(9)	-171.59(16)	C(2)-C(3)-C(4)-C(5)	-0.5(3)
C(8)-O(2)-C(7)-O(1)	6.2(3)	C(3)-C(4)-C(5)-C(6)	-0.1(4)
C(8)-O(2)-C(7)-C(1)	-174.38(16)	C(4)-C(5)-C(6)-C(1)	0.8(3)
C(11)-O(3)-C(10)-C(9)	-37.9(2)	O(2)-C(8)-C(9)-C(10)	-61.4(2)
C(10)-O(3)-C(11)-O(4)	-92.25(18)	O(2)-C(8)-C(9)-C(12)	-174.21(16)
C(10)-O(3)-C(11)-C(12)	23.6(2)	C(8)-C(9)-C(10)-O(3)	-82.31(19)
C(14)-O(4)-C(11)-O(3)	117.86(17)	C(12)-C(9)-C(10)-O(3)	35.68(19)
C(11)-O(4)-C(14)-C(13)	0.7(2)	C(8)-C(9)-C(12)-C(11)	97.99(18)
C(14)-O(4)-C(11)-C(12)	0.9(2)	C(8)-C(9)-C(12)-C(13)	-149.45(17)
C(11)-O(4)-C(14)-O(5)	-178.55(18)	C(10)-C(9)-C(12)-C(11)	-21.27(19)
C(6)-C(1)-C(2)-C(3)	0.4(3)	C(10)-C(9)-C(12)-C(13)	91.30(19)

C(7)-C(1)-C(2)-C(3)	-179.88(19)	O(3)-C(11)-C(12)-C(9)	-0.3(2)
C(2)-C(1)-C(6)-C(5)	-0.9(3)	O(4)-C(11)-C(12)-C(13)	-2.08(18)
C(7)-C(1)-C(6)-C(5)	179.4(2)	O(3)-C(11)-C(12)-C(13)	-119.77(17)
C(2)-C(1)-C(7)-O(1)	178.5(2)	O(4)-C(11)-C(12)-C(9)	117.37(16)
C(6)-C(1)-C(7)-O(1)	-1.8(3)	C(9)-C(12)-C(13)-C(14)	-109.61(18)
C(6)-C(1)-C(7)-O(2)	178.79(17)	C(11)-C(12)-C(13)-C(14)	2.43(19)
C(2)-C(1)-C(7)-O(2)	-0.9(3)	C(12)-C(13)-C(14)-O(5)	177.2(2)
C(1)-C(2)-C(3)-C(4)	0.3(3)	C(12)-C(13)-C(14)-O(4)	-2.0(2)

Table 7: Hydrogen-bonds for **153** [Å and deg.].

D-H...A	d(D-H)	d(H...A)	d(D...A)	<(DHA)
C(9)-H(9)...O(1)#1	10.000	24.800	3.259(2)	135.00
C(10)-H(10A)...O(2)	0.9900	24.600	2.883(2)	105.00
C(10)-H(10B)...O(3)#2	0.9900	24.300	3.289(3)	145.00

((3*S*,3*aS*,6*aS*)-5-oxo-6*a*-(2-oxopropyl)hexahydrofuro[2,3-*b*]furan-3-yl)methyl benzoate (5)

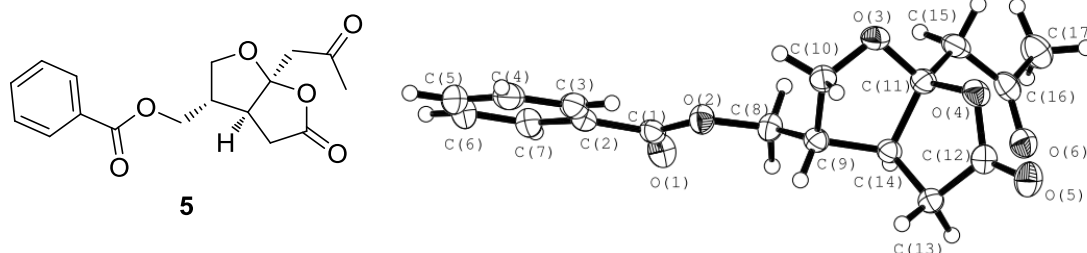


Table 1: Crystal data and structure refinement for **5**.

Crystal Data	
Empirical formula	C ₁₇ H ₁₈ O ₆
Formula weight	318.31
Crystal size	0.2041 x 0.0467 x 0.0293 mm
Crystal description	stick
Crystal colour	colourless
Crystal system	Monoclinic
Space group	P 2 ₁
Unit cell dimensions	a = 9.9890(2) Å α = 90 deg. b = 6.47394(13) Å β = 99.014(2) deg. c = 12.1110(3) Å γ = 90 deg.
Volume	773.52(3) Å ³
Z, Calculated density	2, 1.367 Mg/m ³
Absorption coefficient	0.870 mm ⁻¹
F(000)	336
Data Collection	
Measurement device type	SuperNova, Single source at offset, Atlas
Measurement method	ω scans
Temperature	123 K
Wavelength	1.54184 Å
Monochromator	graphite
Theta range for data collection	3.70 to 72.89 deg.
Index ranges	-12 ≤ h ≤ 8 -7 ≤ k ≤ 7 -14 ≤ l ≤ 14
Reflections collected / unique	5084 / 2940 [R(int) = 0.0335]
Reflections greater I > 2σ(I)	2830
Absorption correction	Analytical
Max. and min. transmission	0.975 and 0.884

Refinement	
Refinement method	Full-matrix least-squares on F ²
Hydrogen treatment	:
Data / restraints / parameters	2940 / 1 / 208
Goodness-of-fit on F ²	1.036
Final R indices [$I > 2\sigma(I)$]	R1 = 0.0438, wR2 = 0.1160
R indices (all data)	R1 = 0.0452, wR2 = 0.1190
Absolute structure parameter	0.13(18)
Largest diff. peak and hole	0.346 and -0.297 e.Å ⁻³

Table 2: Atomic coordinates ($\times 10^4$) and equivalent isotropic displacement parameters ($\text{\AA}^2 \times 10^3$) for **5**. U(eq) is defined as one third of the trace of the orthogonalized Uij tensor.

Atom	x	y	z	U(eq)
O(1)	3884(2)	4619(2)	4672(1)	35(1)
O(2)	2911(1)	1556(2)	4191(1)	31(1)
O(3)	357(1)	-1675(2)	5619(1)	31(1)
O(4)	855(1)	-4031(2)	7068(1)	31(1)
O(5)	2166(2)	-6608(2)	7829(1)	39(1)
O(6)	1779(2)	-1494(2)	9061(1)	35(1)
C(1)	3479(2)	3351(3)	3973(2)	28(1)
C(2)	3562(2)	3603(3)	2758(2)	29(1)
C(3)	3242(2)	2012(4)	1990(2)	35(1)
C(4)	3362(2)	2339(5)	872(2)	42(1)
C(5)	3779(2)	4236(5)	533(2)	47(1)
C(6)	4082(3)	5826(5)	1287(2)	47(1)
C(7)	3980(2)	5518(4)	2409(2)	37(1)
C(8)	2750(2)	1233(3)	5345(2)	28(1)
C(9)	2657(2)	-1073(3)	5533(2)	26(1)
C(10)	1368(2)	-2015(3)	4902(2)	30(1)
C(11)	981(2)	-1885(3)	6720(2)	28(1)
C(12)	2067(2)	-4895(3)	7434(2)	29(1)
C(13)	3200(2)	-3483(3)	7248(2)	28(1)
C(14)	2525(2)	-1498(3)	6764(2)	25(1)
C(15)	221(2)	-563(3)	7441(2)	32(1)
C(16)	793(2)	-503(3)	8663(2)	32(1)
C(17)	58(3)	891(4)	9352(2)	43(1)

Table 3: Bond lengths [\AA] and angles [deg] for **5**.

O(1)-C(1)	1.204(2)	O(3)-C(10)-C(9)	104.67(15)
O(2)-C(1)	1.338(2)	O(3)-C(11)-O(4)	108.93(15)
O(2)-C(8)	1.447(2)	O(3)-C(11)-C(14)	108.08(15)
O(3)-C(10)	1.448(2)	O(3)-C(11)-C(15)	108.05(16)
O(3)-C(11)	1.387(2)	O(4)-C(11)-C(14)	105.82(15)
O(4)-C(11)	1.463(2)	O(4)-C(11)-C(15)	107.35(15)

E. Appendix

O(4)-C(12)	1.344(2)	C(14)-C(11)-C(15)	118.33(16)
O(5)-C(12)	1.206(2)	O(4)-C(12)-O(5)	121.79(19)
O(6)-C(16)	1.211(2)	O(4)-C(12)-C(13)	111.05(16)
C(1)-C(2)	1.496(3)	O(5)-C(12)-C(13)	127.14(19)
C(2)-C(3)	1.390(3)	C(12)-C(13)-C(14)	105.80(15)
C(2)-C(7)	1.394(3)	C(9)-C(14)-C(11)	103.33(15)
C(3)-C(4)	1.395(3)	C(9)-C(14)-C(13)	114.99(16)
C(4)-C(5)	1.380(4)	C(11)-C(14)-C(13)	104.72(15)
C(5)-C(6)	1.378(4)	C(11)-C(15)-C(16)	115.91(17)
C(6)-C(7)	1.393(3)	O(6)-C(16)-C(15)	122.59(18)
C(8)-C(9)	1.515(3)	O(6)-C(16)-C(17)	122.5(2)
C(9)-C(10)	1.518(3)	C(15)-C(16)-C(17)	114.89(18)
C(9)-C(14)	1.542(3)	C(2)-C(3)-H(3)	120.00
C(11)-C(14)	1.555(3)	C(4)-C(3)-H(3)	120.00
C(11)-C(15)	1.509(3)	C(3)-C(4)-H(4)	120.00
C(12)-C(13)	1.499(3)	C(5)-C(4)-H(4)	120.00
C(13)-C(14)	1.526(3)	C(4)-C(5)-H(5)	120.00
C(15)-C(16)	1.502(3)	C(6)-C(5)-H(5)	120.00
C(16)-C(17)	1.497(3)	C(5)-C(6)-H(6)	120.00
C(3)-H(3)	0.9500	C(7)-C(6)-H(6)	120.00
C(4)-H(4)	0.9500	C(2)-C(7)-H(7)	120.00
C(5)-H(5)	0.9500	C(6)-C(7)-H(7)	120.00
C(6)-H(6)	0.9500	O(2)-C(8)-H(8A)	110.00
C(7)-H(7)	0.9500	O(2)-C(8)-H(8B)	110.00
C(8)-H(8A)	0.9900	C(9)-C(8)-H(8A)	110.00
C(8)-H(8B)	0.9900	C(9)-C(8)-H(8B)	110.00
C(9)-H(9)	10.000	H(8A)-C(8)-H(8B)	108.00
C(10)-H(10A)	0.9900	C(8)-C(9)-H(9)	110.00
C(10)-H(10B)	0.9900	C(10)-C(9)-H(9)	110.00
C(13)-H(13A)	0.9900	C(14)-C(9)-H(9)	110.00
C(13)-H(13B)	0.9900	O(3)-C(10)-H(10A)	111.00
C(14)-H(14)	10.000	O(3)-C(10)-H(10B)	111.00
C(15)-H(15A)	0.9900	C(9)-C(10)-H(10A)	111.00
C(15)-H(15B)	0.9900	C(9)-C(10)-H(10B)	111.00
C(17)-H(17A)	0.9800	H(10A)-C(10)-H(10B)	109.00
C(17)-H(17B)	0.9800	C(12)-C(13)-H(13A)	111.00
C(17)-H(17C)	0.9800	C(12)-C(13)-H(13B)	111.00
C(1)-O(2)-C(8)	115.54(15)	C(14)-C(13)-H(13A)	111.00
C(10)-O(3)-C(11)	108.14(14)	C(14)-C(13)-H(13B)	111.00
C(11)-O(4)-C(12)	112.12(15)	H(13A)-C(13)-H(13B)	109.00
O(1)-C(1)-O(2)	124.03(19)	C(9)-C(14)-H(14)	111.00
O(1)-C(1)-C(2)	123.66(18)	C(11)-C(14)-H(14)	111.00
O(2)-C(1)-C(2)	112.31(17)	C(13)-C(14)-H(14)	111.00
C(1)-C(2)-C(3)	122.29(18)	C(11)-C(15)-H(15A)	108.00
C(1)-C(2)-C(7)	117.38(18)	C(11)-C(15)-H(15B)	108.00
C(3)-C(2)-C(7)	120.3(2)	C(16)-C(15)-H(15A)	108.00
C(2)-C(3)-C(4)	119.4(2)	C(16)-C(15)-H(15B)	108.00

C(3)-C(4)-C(5)	120.0(3)	H(15A)-C(15)-H(15B)	107.00
C(4)-C(5)-C(6)	120.9(2)	C(16)-C(17)-H(17A)	109.00
C(5)-C(6)-C(7)	119.8(3)	C(16)-C(17)-H(17B)	109.00
C(2)-C(7)-C(6)	119.6(2)	C(16)-C(17)-H(17C)	109.00
O(2)-C(8)-C(9)	107.83(15)	H(17A)-C(17)-H(17B)	110.00
C(8)-C(9)-C(10)	112.80(16)	H(17A)-C(17)-H(17C)	110.00
C(8)-C(9)-C(14)	109.73(15)	H(17B)-C(17)-H(17C)	109.00
C(10)-C(9)-C(14)	102.74(15)		

Table 4: Anisotropic displacement parameters ($\text{\AA}^2 \times 10^3$) for **5**. The anisotropic displacement factor exponent takes the form: $-2 \pi^2 [h^2 a^{*2} U_{11} + \dots + 2 h k a^* b^* U_{12}]$.

Atom	U11	U22	U33	U23	U13	U12
O(1)	44(1)	29(1)	36(1)	-4(1)	13(1)	-4(1)
O(2)	35(1)	30(1)	28(1)	2(1)	5(1)	-6(1)
O(3)	22(1)	37(1)	32(1)	0(1)	0(1)	-2(1)
O(4)	28(1)	27(1)	38(1)	1(1)	5(1)	-6(1)
O(5)	51(1)	25(1)	43(1)	5(1)	10(1)	-2(1)
O(6)	36(1)	38(1)	31(1)	1(1)	8(1)	2(1)
C(1)	23(1)	28(1)	34(1)	2(1)	8(1)	3(1)
C(2)	21(1)	37(1)	31(1)	4(1)	6(1)	4(1)
C(3)	27(1)	44(1)	33(1)	-1(1)	6(1)	4(1)
C(4)	30(1)	64(2)	32(1)	-3(1)	4(1)	5(1)
C(5)	36(1)	73(2)	32(1)	14(1)	10(1)	8(1)
C(6)	41(1)	60(2)	43(1)	18(1)	15(1)	0(1)
C(7)	33(1)	39(1)	40(1)	9(1)	8(1)	0(1)
C(8)	32(1)	26(1)	26(1)	1(1)	4(1)	-3(1)
C(9)	24(1)	26(1)	28(1)	2(1)	4(1)	-1(1)
C(10)	29(1)	32(1)	28(1)	-1(1)	2(1)	-4(1)
C(11)	24(1)	27(1)	31(1)	2(1)	2(1)	-4(1)
C(12)	34(1)	25(1)	28(1)	-1(1)	7(1)	-1(1)
C(13)	26(1)	27(1)	30(1)	4(1)	5(1)	2(1)
C(14)	22(1)	24(1)	27(1)	0(1)	3(1)	-2(1)
C(15)	21(1)	33(1)	42(1)	2(1)	8(1)	0(1)
C(16)	30(1)	28(1)	40(1)	0(1)	13(1)	-5(1)
C(17)	43(1)	41(1)	47(1)	-5(1)	19(1)	2(1)

Table 5: Hydrogen coordinates ($\times 10^4$) and isotropic displacement parameters ($\text{\AA}^2 \times 10^3$) for **5**.

Atom	x	y	z	U(eq)
H(3)	2944	714	2226	41
H(4)	3156	1256	344	50
H(5)	3859	4448	-230	56
H(6)	4359	7129	1042	56
H(7)	4195	6605	2934	44
H(8A)	1916	1925	5502	34
H(8B)	3534	1816	5850	34

H(9)	3472	-1790	5331	31
H(10A)	1104	-1326	4170	36
H(10B)	1490	-3509	4775	36
H(13A)	3745	-4109	6719	33
H(13B)	3802	-3199	7962	33
H(14)	2833	-283	7247	29
H(15A)	190	868	7149	38
H(15B)	-724	-1069	7361	38
H(17A)	680	1958	9702	64
H(17B)	-282	81	9933	64
H(17C)	-705	1545	8871	64

Table 6: Torsion angles [deg] for **5**.

C(8)-O(2)-C(1)-O(1)	2.5(3)	O(2)-C(8)-C(9)-C(10)	-67.7(2)
C(8)-O(2)-C(1)-C(2)	-177.82(15)	O(2)-C(8)-C(9)-C(14)	178.40(15)
C(1)-O(2)-C(8)-C(9)	-157.17(16)	C(8)-C(9)-C(10)-O(3)	-84.02(18)
C(11)-O(3)-C(10)-C(9)	-36.31(18)	C(14)-C(9)-C(10)-O(3)	34.04(18)
C(10)-O(3)-C(11)-O(4)	-91.71(17)	C(8)-C(9)-C(14)-C(11)	100.04(17)
C(10)-O(3)-C(11)-C(14)	22.81(19)	C(8)-C(9)-C(14)-C(13)	-146.47(16)
C(10)-O(3)-C(11)-C(15)	151.97(15)	C(10)-C(9)-C(14)-C(11)	-20.16(18)
C(12)-O(4)-C(11)-O(3)	123.27(16)	C(10)-C(9)-C(14)-C(13)	93.33(18)
C(12)-O(4)-C(11)-C(14)	7.3(2)	O(3)-C(11)-C(14)-C(9)	-0.62(19)
C(12)-O(4)-C(11)-C(15)	-119.96(17)	O(3)-C(11)-C(14)-C(13)	-121.35(16)
C(11)-O(4)-C(12)-O(5)	174.76(18)	O(4)-C(11)-C(14)-C(9)	115.95(16)
C(11)-O(4)-C(12)-C(13)	-6.8(2)	O(4)-C(11)-C(14)-C(13)	-4.79(18)
O(1)-C(1)-C(2)-C(3)	171.9(2)	C(15)-C(11)-C(14)-C(9)	-123.74(18)
O(1)-C(1)-C(2)-C(7)	-8.1(3)	C(15)-C(11)-C(14)-C(13)	115.53(18)
O(2)-C(1)-C(2)-C(3)	-7.8(3)	O(3)-C(11)-C(15)-C(16)	-176.97(16)
O(2)-C(1)-C(2)-C(7)	172.24(17)	O(4)-C(11)-C(15)-C(16)	65.7(2)
C(1)-C(2)-C(3)-C(4)	-178.97(19)	C(14)-C(11)-C(15)-C(16)	-53.8(2)
C(7)-C(2)-C(3)-C(4)	1.0(3)	O(4)-C(12)-C(13)-C(14)	3.3(2)
C(1)-C(2)-C(7)-C(6)	179.6(2)	O(5)-C(12)-C(13)-C(14)	-178.35(19)
C(3)-C(2)-C(7)-C(6)	-0.3(3)	C(12)-C(13)-C(14)-C(9)	-111.52(17)
C(2)-C(3)-C(4)-C(5)	-0.8(3)	C(12)-C(13)-C(14)-C(11)	1.15(19)
C(3)-C(4)-C(5)-C(6)	0.0(3)	C(11)-C(15)-C(16)-O(6)	-2.0(3)
C(4)-C(5)-C(6)-C(7)	0.6(4)	C(11)-C(15)-C(16)-C(17)	177.43(18)
C(5)-C(6)-C(7)-C(2)	-0.5(4)		

Table 7: Hydrogen-bonds for **5** [Å and deg.].

D-H...A	d(D-H)	d(H...A)	d(D...A)	<(DHA)
C(9)-H(9)...O(1)#1	10.000	25.100	3.281(2)	133.00
C(10)-H(10A)...O(2)	0.9900	25.900	2.980(2)	103.00
C(14)-H(14)...O(5)#2	10.000	26.000	3.458(2)	144.00
C(15)-H(15A)...O(5)#2	0.9900	25.900	3.204(2)	120.00

3. List of publications

Enantioselective Synthesis of (-)-Paeonilide

Klaus Harrar, Oliver Reiser

Manuscript in preparation

4. Poster presentations and scientific meetings

Model Study towards Crassalactone D

Klaus Harrar, Oliver Reiser

ESF-COST High-Level Research Conference on Natural Products Chemistry,
Biology and Medicine II, Acquafredda di Maratea, Italy, **2009**

Towards the Stereoselective Synthesis of Paeonilide

Klaus Harrar, Oliver Reiser

3rd EuCheMS Chemistry Congress, Nürnberg, Germany, **2010**

5. Curriculum vitae

Personal Data

Name: Klaus Harrar

Date of birth: 23.10.1982

Marital status: Married

Nationality: German

Education

10/2007-12/2011 **PhD thesis** at the University of Regensburg under supervision of Prof. Dr. Oliver Reiser
“Enantioselective Synthesis of (-)-Paeonilide”

09/2007 **Graduation:** Diplom Chemiker (diploma in chemistry, Master of Science equivalent)

01/2007-09/2007 **Diploma thesis** at the University of Regensburg under supervision of Prof. Dr. Oliver Reiser
“Studien zur asymmetrischen Synthese von Paeonilid”

10/2002-09/2007 **Studies in Chemistry**, University of Regensburg, Germany

09/1993-06/2002 **Abitur** (A-level)
Ludwigsgymnasium Straubing, Germany
(High school Certificate equivalent)

09/1989-08-1993 Primary school Rain, Germany

Languages

German (native)

English (fluently)

Professional References

Prof. Dr.Oliver Reiser

Institute für Organische Chemie

Universität Regensburg

Universitätsstr. 31

93053 Regensburg

Phone: +49-941-9434631

E-mail: oliver.reiser@chemie.uni-regensburg.de

F. References

1. Xue, T. H.; Roy, R., *Science* **2003**, 300, 740.
2. Oka, H.; Yamamoto, S.; Kuroki, T.; Harihara, S.; Marumo, T.; Kim, S. R.; Monna, T.; Kobayashi, K.; Tango, T., *Cancer* **1995**, 76, 743.
3. Sheehan, M. P.; Rustin, M. H. A.; Atherton, D. J.; Buckley, C.; Harris, D. J.; Brostoff, J.; Ostlere, L.; Dawson, A., *Lancet* **1992**, 340, 13.
4. Normile, D., *Science* **2003**, 299, 188.
5. Kimura, M.; Kimura, I.; Nojima, H.; Takahashi, K.; Hayashi, T.; Shimizu, M.; Morita, N., *Jpn J Pharmacol* **1984**, 35, 61.
6. Chen, L.; Wang, D.; Wu, J.; Yu, B.; Zhu, D., *J Pharm Biomed Anal* **2009**, 49, 267.
7. Hatakeyama, S.; Kawamura, M.; Shimanuki, E.; Takano, S., *Tet Lett* **1992**, 33, 333.
8. Hayashi, T.; Shinbo, T.; Shimizu, M.; Arisawa, M.; Morita, N.; Kimura, M.; Matsuda, S.; Kikuchi, T., *Tet Lett* **1985**, 26, 3699.
9. Shimizu, M.; Hayashi, T.; Morita, N.; Kimura, I.; Kimura, M.; Kiuchi, F.; Noguchi, H.; Iitaka, Y.; Sankawa, U., *Tet Lett* **1981**, 22, 3069.
10. Morita, N. *The report of the results of studies on muscle relaxants from Paeony root*, 1983, p 24, supported by a Grant-in-Aid for Scientific Research from the Ministry of Education, Science, and Culture of Japan.
11. Liu, J. K.; Ma, Y. B.; Wu, D. G.; Lu, Y.; Shen, Z. Q.; Zheng, Q. T.; Chen, Z. H., *Biosci Biotechnol Biochem* **2000**, 64, 1511.
12. http://www.giftpflanzen.com/paeonia_delavayi.html (accessed 07.09.2011).
13. Good, W. <http://www.paeonia.ch/weltd/einfd6.htm> (accessed 05.09.2011).
14. Nakanishi, K.; Jaracz, S.; Stromgaard, K., *J Org Chem* **2002**, 67, 4623.
15. Schmid, W., *Nature* **1997**, 386, 755.
16. Jagel, A. http://www.ruhr-uni-bochum.de/boga/html/Ginkgo_biloba_Foto.html (accessed 06.09.2011).
17. DeFeudis, F. Y., *Ginkgo biloba extract (EGB 761): Pharmacological Activities and Clinical Application*. Elsevier: Paris, 1991; p 97.
18. Kleijnen, J.; Knipschild, P., *Lancet* **1992**, 340, 1136.
19. Le Bars, P. L.; Katz, M. M.; Berman, N.; Itil, T. M.; Freedman, A. M.; Schatzberg, A. F., *J Am Med Assoc* **1997**, 278, 1327.

20. Braquet, P.; Hosford, D., *J Ethnopharmacol* **1991**, 32, 135.
21. Sugimoto, T.; Tsuchimochi, H.; McGregor, C. G. A.; Mutoh, H.; Shimizu, T.; Kurachi, Y., *Biochem Bioph Res Co* **1992**, 189, 617.
22. Plow, E. F.; Marguerie, G.; Ginsberg, M., *Biochem Pharmacol* **1987**, 36, 4035.
23. Fuster, V.; Badimon, L.; Badimon, J. J.; Chesebro, J. H., *N Engl J Med* **1992**, 326, 310.
24. Wang, C.; Liu, J.; Ji, Y.; Zhao, J.; Li, L.; Zhang, H., *Org Lett* **2006**, 8, 2479.
25. Du, Y.; Liu, J.; Linhardt, R. J., *J Org Chem* **2007**, 72, 3952.
26. Wang, C.; Zhang, H.; Liu, J.; Ji, Y.; Shao, Z.; Li, L., *Synlett* **2006**, 1051.
27. Rubottom, G. M.; Gruber, J. M., *J Org Chem* **1978**, 43, 1599.
28. Weisser, R.; Yue, W.; Reiser, O., *Org Lett* **2005**, 7, 5353.
29. Bubert, C.; Cabrele, C.; Reiser, O., *Synlett* **1997**, 1997, 827.
30. Salaün, J., Cyclopropane Derivatives and their Diverse Biological Activities, Small Ring Compounds in Organic Synthesis VI. de Meijere, A., Ed. Springer Berlin / Heidelberg: 2000; Vol. 207, pp 1.
31. Faust, R., *Angew Chem Int Ed* **2001**, 40, 2251.
32. Gnad, F.; Reiser, O., *Chem Rev* **2003**, 103, 1603.
33. Koglin, N.; Zorn, C.; Beumer, R.; Cabrele, C.; Bubert, C.; Sewald, N.; Reiser, O.; Beck-Sickinger, A. G., *Angew Chem Int Ed* **2003**, 42, 202.
34. Patai, S.; Rappoport, Z., *Biochemistry of the Cyclopropyl Group*. Wiley: Chichester, New York, Brisbane, Toronto, Singapore, 1987, Chapter 16.
35. Saltykova, L. E.; Vasil'vitskii, A. E.; Shostakovskii, V. M.; Nefedov, O. M., *Russ Chem B+* **1988**, 37, 2557.
36. Wenkert, E.; Guo, M.; Lavilla, R.; Porter, B.; Ramachandran, K.; Sheu, J. H., *J Org Chem* **1990**, 55, 6203.
37. Nosse, B.; Chhor, R. B.; Jeong, W. B.; Böhm, C.; Reiser, O., *Org Lett* **2003**, 5, 941.
38. Jezek, E.; Schall, A.; Kreitmeier, P.; Reiser, O., *Synlett* **2005**, 2005, 0915.
39. Kalidindi, S.; Jeong, W. B.; Schall, A.; Bandichhor, R.; Nosse, B.; Reiser, O., *Angew Chem Int Ed* **2007**, 46, 6361.
40. Chhor, R. B.; Nosse, B.; Sörgel, S.; Böhm, C.; Seitz, M.; Reiser, O., *Chem Eur J* **2003**, 9, 260.
41. Böhm, C.; Reiser, O., *Org Lett* **2001**, 3, 1315.

42. Noels, A. F.; Demonceau, A.; Petiniot, N.; Hubert, A. J.; Teyssié, P., *Tetrahedron* **1982**, *38*, 2733.
43. Divald, S.; Chun, M. C.; Joullie, M. M., *J Org Chem* **1976**, *41*, 2835.
44. Schinnerl, M.; Seitz, M.; Kaiser, A.; Reiser, O., *Org Lett* **2001**, *3*, 4259.
45. Evans, D. A.; Woerpel, K. A.; Nosse, B.; Schall, A.; Shinde, Y.; Jezek, E.; Haque, M. M.; Chhor, R. B.; Reiser, O., *Org Synth* **2006**, *11*, 821.
46. Diez-Barra, E.; De, I. H. A.; Moreno, A.; Sanchez-Verdu, P., *J Chem Soc Perkin Trans 1* **1991**, 2589.
47. Aggarwal, V. K.; Bell, L.; Coogan, M. P.; Jubault, P., *J. Chem. Soc., Perkin Trans. 1* **1998**, 2037.
48. Regitz, M., *Angew Chem Int Edit* **1967**, *6*, 733.
49. Nicewicz, D. A.; Breteche, G.; Johnson, J. S., *Org Synth* **2008**, *85*, 278.
50. Warner, P.; Sutherland, R., *J Org Chem* **1992**, *57*, 6294.
51. Silberrad, O.; Roy, C. S., *J Chem Soc Transact* **1906**, *89*, 179.
52. Davies, H. M. L., *Tetrahedron* **1993**, *49*, 5203.
53. Mann, J., *Tetrahedron* **1986**, *42*, 4611.
54. Piers, E., *In Comprehensive Organic Synthesis*. Trost, B. M. ed.; Pergamon Press: Oxford, 1991, Vol. 5, p 971; Vol. 5.
55. Hudlicky, T.; Fan, R.; Reed, J. W.; Gadamasetti, K. G., Divinylcyclopropane-Cycloheptadiene Rearrangement. In *Organic Reactions*, John Wiley & Sons, Inc.: 2004.
56. Hudlicky, T.; Reed, J. W., *In Comprehensive Organic Synthesis*. Trost, B. M., Fleming, I. ed.; Pergamon Press: Oxford, 1991, Vol. 5, p 899; Vol. 5, p 899.
57. Goldschmidt, Z.; Crammer, B., *Chem Soc Rev* **1988**, *17*, 229.
58. Hudlický, T.; Kutchan, T. M.; Naqvi, S. M., The Vinylcyclopropane–Cyclopentene Rearrangement. In *Organic Reactions*, John Wiley & Sons, Inc.: 2004.
59. Nonhebel, D. C., *Chem Soc Rev* **1993**, *22*, 347.
60. Baird, M.; Reißig, H. U.; Salaün, J.; Reißig, H.-U., Donor-acceptor-substituted cyclopropanes: Versatile building blocks in organic synthesis, Small ring compounds in organic synthesis III. Springer Berlin / Heidelberg: 1988; Vol. 144, pp 73.

61. Baird, M.; Reißig, H. U.; Salaün, J.; Salaün, J., Synthesis and synthetic applications of 1-donor substituted cyclopropanes with ethynyl, vinyl and carbonyl groups, *Small ring compounds in organic synthesis III*. Springer Berlin / Heidelberg: 1988; Vol. 144, pp 1.
62. Wong, H. N. C.; Hon, M. Y.; Tse, C. W.; Yip, Y. C.; Tanko, J.; Hudlicky, T., *Chem Rev* **1989**, 89, 165.
63. Reissig, H.-U.; Zimmer, R., *Chem Rev* **2003**, 103, 1151.
64. Wenkert, E., *Acc Chem Res* **1980**, 13, 27.
65. Wenkert, E., *Heterocycles* **1980**, 14, 1703.
66. Fraile, J. M.; García, J. I.; Martínez-Merino, V.; Mayoral, J. A.; Salvatella, L., *J Am Chem Soc* **2001**, 123, 7616.
67. Rasmussen, T.; Jensen, J. F.; Østergaard, N.; Tanner, D.; Ziegler, T.; Norrby, P.-O., *Chem Eur J* **2002**, 8, 177.
68. Lebel, H.; Marcoux, J. F.; Molinaro, C.; Charette, A. B., *Chem Rev* **2003**, 103, 977.
69. Salomon, R. G.; Kochi, J. K., *J Am Chem Soc* **1973**, 95, 3300.
70. Moser, W. R., *J Am Chem Soc* **1969**, 91, 1135.
71. Doyle, M. P.; Protopopova, M. N.; Brandes, B. D.; Davies, H. M. L.; Huby, N. J. S.; Whitesell, J. K., *Synlett* **1993**, 1993, 151.
72. Doyle, M. P.; Dorow, R. L.; Terpstra, J. W.; Rodenhouse, R. A., *J Org Chem* **1985**, 50, 1663.
73. Haddad, N.; Galili, N., *Tet Asym* **1997**, 8, 3367.
74. Fritschi, H.; Leutenegger, U.; Pfaltz, A., *Helv Chim Acta* **1988**, 71, 1553.
75. Temme, O.; Taj, S.-A.; Andersson, P. G., *J Org Chem* **1998**, 63, 6007.
76. Reiser, O.; Schinnerl, M.; Böhm, C.; Seitz, M., *Tet Asym* **2003**, 14, 765.
77. Kim, C.; Brady, T.; Kim, S. H.; Theodorakis, E. A., *Synth Commun* **2004**, 34, 1951.
78. Morizawa, Y.; Hiyama, T.; Nozaki, H., *Tet Lett* **1981**, 22, 2297.
79. Patnode, W.; Schmidt, F., *J Am Chem Soc* **1945**, 67, 2272.
80. Kantlehner, W.; Haug, E.; Mergen, W. W., *Synthesis* **1980**, 460.
81. Sommer, L. H.; Kerr, G. T.; Whitmore, F. C., *J Am Chem Soc* **1948**, 70, 445.
82. Bodensteiner, J.; Buschauer, A.; Reiser, O., New tetrahydrofurane based compounds as potential histamine H3 and H4 receptor ligands. In *5th Summerschool "Medicinal Chemistry" GRK 760, 2010*, Regensburg, 2010.

83. Zhang, M.; Zhu, L.; Ma, X.; Dai, M.; Lowe, D., *Org Lett* **2003**, 5, 1587.
84. Weisser, R. Darstellung von asymmetrisch substituierten Tetrahydrofuranen als Bausteine in der Naturstoffsynthese. PhD Thesis, Universität Regensburg, Regensburg, 2006.
85. Ung, A. T.; Pyne, S. G.; Batenburg-Nguyen, U.; Davis, A. S.; Sherif, A.; Bischoff, F.; Lesage, A. S. J., *Tetrahedron* **2005**, 61, 1803.
86. Hudlicky, T.; Sinai-Zingde, G.; Natchus, M. G., *Tet Lett* **1987**, 28, 5287.
87. Peschko, C.; Winklhofer, C.; Steglich, W., *Chem Eur J* **2000**, 6, 1147.
88. Müller, P.; Siegfried, B., *Helv Chim Acta* **1974**, 57, 987.
89. Crawforth, J. M.; Fawcett, J.; Rawlings, B. J., *J Chem Soc Perk Trans 1* **1998**, 1721.
90. Theodorakis, E. A.; Brady, T. P.; Kim, S. H.; Wen, K.; Kim, C., *Chem-Eur J* **2005**, 11, 7175.
91. von E. Doering, W.; Buttery, R. G.; Laughlin, R. G.; Chaudhuri, N., *J Am Chem Soc* **1956**, 78, 3224.
92. Arndtsen, B. A.; Bergman, R. G.; Mobley, T. A.; Peterson, T. H., *Acc Chem Res* **1995**, 28, 154.
93. Dyker, G., *Angew Chem Int Ed* **1999**, 38, 1698.
94. Guari, Y.; Sabo-Etienne, S.; Chaudret, B., *Eur J Inorg Chem* **1999**, 1999, 1047.
95. Caballero, A.; Diaz-Requejo, M. M.; Belderrain, T. R.; Nicasio, M. C.; Trofimenko, S.; Perez, P. J., *Organometallics* **2003**, 22, 4145.
96. Doyle, M. P., In *Comprehensive Organometallic Chemistry II*, Pergamon Press: Oxford, U.K.: 1995; Vol. 12, p 421.
97. Doyle, M. P.; McKervey, M. A.; Ye, T., *Modern Catalytic Methods for Organic Synthesis with Diazo Compounds*. John Wiley & Sons: New York, 1998.
98. Scott, L. T.; DeCicco, G. J., *J Am Chem Soc* **1974**, 96, 322.
99. Wulfman, D. S.; McDaniel Jr, R. S.; Peace, B. W., *Tetrahedron* **1976**, 32, 1241.
100. Demonceau, A.; Noels, A. F.; Hubert, A. J.; Teyssie, P., *J Chem Soc, Chem Commun* **1981**, 688.
101. Demonceau, A.; Noels, A. F.; Hubert, A. J.; Teyssie, P., *B Soc Chim Belg* **1984**, 93, 945.

102. Demonceau, A.; Noels, A. F.; Teyssie, P.; Hubert, A. J., *J Mol Catal* **1988**, *49*, L13.
103. Demonceau, A.; Noels, A. F.; Hubert, A. J., *J Mol Catal* **1989**, *57*, 149.
104. Demonceau, A.; Noels, A. F.; Costa, J. L.; Hubert, A. J., *J Mol Catal* **1990**, *58*, 21.
105. Doyle, M. P., In *Comprehensive Organometallic Chemistry II*, Pergamon Press: Oxford, U.K.: 1995; Vol. 12, p 115.
106. Blanksby, S. J.; Ellison, G. B., *Acc Chem Res* **2003**, *36*, 255.
107. Greuter, F.; Kalvoda, J.; Jeger, O., *Proc Chem Soc* **1958**, 349.
108. Burke, S. D.; Grieco, P. A., *Org. React.* **1979**, *26*, 361.
109. Padwa, A.; Austin, D. J., *Angew Chem Int Ed Engl* **1994**, *33*, 1797.
110. Fraile, J. M.; Garcia, J. I.; Mayoral, J. A.; Roldan, M., *Org Lett* **2007**, *9*, 731.
111. Davies, H. M. L.; Hansen, T.; Churchill, M. R., *J Am Chem Soc* **2000**, *122*, 3063.
112. Diaz-Requejo, M. M.; Belderrain, T. R.; Nicasio, M. C.; Trofimenko, S.; Perez, P. J., *J Am Chem Soc* **2002**, *124*, 896.
113. Adams, J.; Poupart, M.-A.; Grenier, L.; Schaller, C.; Ouimet, N.; Frenette, R., *Tet Lett* **1989**, *30*, 1749.
114. Stork, G.; Kazuhiko, N., *Tet Lett* **1988**, *29*, 2283.
115. Kraus, G. A.; Landgrebe, K., *Tetrahedron* **1985**, *41*, 4039.
116. Juffermans, J. P. H.; Habraken, C. L., *J Org Chem* **1986**, *51*, 4656.
117. Rheingold, A. L.; Liable-Sands, L. M.; Incarvito, C. L.; Trofimenko, S., *J Chem Soc, Dalton Trans* **2002**, 2297.
118. Caballero, A.; Díaz-Requejo, M. M.; Belderrain, T. R.; Nicasio, M. C.; Trofimenko, S.; Pérez, P. J., *J Am Chem Soc* **2003**, *125*, 1446.
119. Elschenbroich, C., *Organometallics*. 3rd, completely rev. and extended ed.; Wiley-VCH: Weinheim, 2006, p 610; p xiv.
120. Matsuda, S.; Yamanoi, T.; Watanabe, M., *Tetrahedron* **2008**, *64*, 8082.
121. Taft, R. W.; Bordwell, F. G., *Acc Chem Res* **1988**, *21*, 463.
122. Kende, A. S.; Fludzinski, P., *Org Synth* **1986**, *64*, 104.
123. Elsnér, P.; Jetter, P.; Brodner, K.; Helmchen, G., *Eur J Org Chem* **2008**, 2551.
124. Narasimhan, S.; Madhavan, S.; Prasad, K. G., *J Org Chem* **1995**, *60*, 5314.
125. Crimmins, M. T.; Ellis, J. M.; Emmitte, K. A.; Haile, P. A.; McDougall, P. J.; Parrish, J. D.; Zuccarello, J. L., *Chem-Eur J* **2009**, *15*, 9223.

126. Smidt, J.; Hafner, W.; Jira, R.; Sedlmeier, J.; Sieber, R.; Rüttinger, R.; Kojer, H., *Angew Chem* **1959**, 71, 176.
127. Jacques, M., *Tetrahedron* **2007**, 63, 7505.
128. Takacs, J. M.; Jiang, X. T., *Curr Org Chem* **2003**, 7, 369.
129. Tsuji, J., *Synthesis* **1984**, 369.
130. Sharma, G. V. M.; Krishna, P. R., *Curr Org Chem* **2004**, 8, 1187.
131. Han, J. S.; Lowary, T. L., *J Org Chem* **2003**, 68, 4116.
132. Mitsudome, T.; Umetani, T.; Nosaka, N.; Mori, K.; Mizugaki, T.; Ebitani, K.; Kaneda, K., *Angew Chem Int Edit* **2006**, 45, 481.
133. Shao, H. W.; Ekthawatchai, S.; Chen, C. S.; Wu, S. H.; Zou, W., *J Org Chem* **2005**, 70, 4726.
134. Rogers, H. R.; McDermott, J. X.; Whitesides, G. M., *J Org Chem* **1975**, 40, 3577.
135. Kitching, W., *Organomet Chem Rev A* **1968**, 3, 61.
136. Zou, W.; Bhasin, M.; Vembaiyan, K.; Williams, D. T., *Carbohydr Res* **2009**, 344, 1024.
137. Tomioka, H.; Oshima, K.; Nozaki, H., *Tet Lett* **1982**, 23, 539.
138. Rydberg, D. B.; Meinwald, J., *Tet Lett* **1996**, 37, 1129.
139. Stevens, R. V.; Chapman, K. T.; Stubbs, C. A.; Tam, W. W.; Albizati, K. F., *Tet Lett* **1982**, 23, 4647.
140. Corey, E. J.; Ishiguro, M., *Tet Lett* **1979**, 2745.
141. Stevens, R. V.; Chapman, K. T.; Weller, H. N., *J Org Chem* **1980**, 45, 2030.
142. Schlessinger, R. H.; Lopes, A., *J Org Chem* **1981**, 46, 5252.
143. Dess, D. B.; Martin, J. C., *J Org Chem* **1983**, 48, 4155.
144. Horeau, A., *Tet Lett* **1969**, 3121.
145. Evans, D. A.; Peterson, G. S.; Johnson, J. S.; Barnes, D. M.; Campos, K. R.; Woerpel, K. A., *J Org Chem* **1998**, 63, 4541.
146. Glos, M.; Reiser, O., *Org Lett* **2000**, 2, 2045.
147. Eisenbraun, E. J., *Org Synth* **1973**, 5, 310.

G. Acknowledgement

Bei Prof. Dr. Oliver Reiser möchte ich mich herzlichst für die interessante Themenstellung und für die Unterstützung während der gesamten Arbeit bedanken.

Bedanken möchte ich mich auch bei der Firma Schwabe GmbH & Co. KG für das Durchführen der biologischen Testungen.

Priv. Doz. Dr. Kirsten Zeitler danke ich für die zahlreichen Diskussionen und die Hilfe bei vielen fachlichen Fragestellungen.

Herzlich bedanke ich mich auch bei Dr. Peter Kreitmeier, für seine ständige Hilfe bei allen Problemen, mit denen man im Laboralltag zu kämpfen hat.

Ganz besonderer Dank gilt meinen Laborkollegen, Dr. Markus Hager, Ludwig Pils, Dr. Woraluk Mansawat, Dr. Ramesh Rasappan, Dr. Gang Xu und Simon Lindner für die kollegiale und hilfsbereite Atmosphäre in den letzten Jahren. Dabei möchte ich im besonderen Markus und Ludwig für ihre Freundschaft danken!

Dank auch an alle derzeitigen und ehemaligen Mitarbeitern am Lehrstuhl, für die Hilfe bei der Arbeit, eine angenehme Atmosphäre und natürlich auch für alle Aktivitäten neben dem Labor wie Grillabende, Wanderungen, BBV, Public Viewing und vieles mehr. Dabei möchte ich besonders folgenden Kollegen danken: Ludwig Pils, Dr. Markus Hager, Sebastian Wittmann, Andreas Kreuzer, Kathrin Ulbrich, Paul Kohls, Dr. Alexander Schätz, Dr. Florian Sahr, Dr. Michael Kuhn, Michael Schwarz, Julian Bodensteiner, Roland Linhardt, Quirin Kainz, Dr. Tobias Olbrich, Dr. Hans Zwicknagel und Dr. Alexander Tereshchenko.

Für ihre Ausdauer beim Korrekturlesen der Arbeit danke ich Dr. Alexander Schätz, Dr. Markus Hager, Ludwig Pils, Sebastian Wittmann, Andreas Kreuzer und Agnes.

Darüber hinaus danke ich Georg Adolin, Klaus Döring, Andrea Roithmeier, Helena Konkel und Robert Tomahogh für kleinere und größere Arbeiten am Lehrstuhl, die den Arbeitsalltag deutlich erleichtert haben. Das Selbe gilt auch für unsere Sekretärinnen Young Rotermund und Hedwig Ohli.

Nicht weniger möchte ich mich bei meinen Freunden außerhalb des Lehrstuhls bedanken: Dr. Matthias Stich, Rebecca Schreib, Dr. Anna Hezinger, Benjamin Gruber, Bernadette Streifinger, Judith Hager, August Breu, Dr. Nikola Pluym, Dr. Stefanie und Dr. Tobias Gärtner, Dr. Tobias Birnkammer, Tobias Negele, Inka Chia, Andreas Mandl, Robert Rolle und alle, die ich hier noch vergessen haben sollte.

Ich danke auch allen Mitarbeitern der Zentralen Analytik, deren unermüdliche Arbeit zum Gelingen dieser Dissertation maßgeblich beigetragen hat.

Letztendlich gilt mein größter Dank jedoch meiner Frau Agnes und meiner Familie, die immer hinter mir standen, mich gehalten und unterstützt haben. Ohne sie wären die letzten Jahre, das Studium und die Promotion, so nicht möglich gewesen.

Declaration

Herewith I declare that I have made this existing work single-handed. I have only used the stated utilities.

Regensburg, 19th December 2011

Klaus Harrar